

**Dissertation zur Erlangung des Doktorgrades
der Fakultät für Chemie und Pharmazie
der Ludwig-Maximilians-Universität München**

**Down-modulation of the apoptosis receptor Fas and the EGF receptor
by the adenovirus E3/10.4-14.5K proteins requires the concerted action of two
distinct transport signals**

**vorgelegt von
Annette Hilgendorf
aus
Ludwigshafen am Rhein**

Juni 2003

Erklärung

Diese Dissertation wurde im Sinne von §13 Abs. 3 bzw. 4 der Promotionsordnung vom 29. Januar 1998 von Prof. Dr. Rudolf Grosschedl betreut.

Ehrenwörtliche Versicherung

Diese Dissertation wurde selbständig, ohne unerlaubte Hilfe erarbeitet.

München, den 4. Juni 2003

Annette Hilgendorf

Dissertation eingereicht am 5. Juni 2003

1. Gutachter: Prof. Dr. Rudolf Grosschedl
2. Gutachter: PD Dr. Stefan Weiß

Mündliche Prüfung am 15. Juli 2003

Danksagung

An erster Stelle danke ich PD Dr. Hans-Gerhard Burgert für die Möglichkeit, diese Doktorarbeit in seiner Arbeitsgruppe am Max-von-Pettenkofer Institut und dem Genzentrum der LMU München anzufertigen, und für die Betreuung und Unterstützung während dieser Zeit. Prof. Dr. Rudolf Grosschedl gilt mein besonderer Dank, da er meine Dissertation vor der Fakultät für Chemie und Pharmazie der LMU München vertritt. Den weiteren Mitgliedern der Promotionskommission danke ich für ihr Interesse am Inhalt meiner Dissertation und ihre Bereitschaft als Gutachter und Prüfer zu fungieren.

Prof. Dr.med. Ulrich Koszinowski möchte ich insbesondere dafür danken, dass er nach dem Institutswechsel von PD Dr. H.-G. Burgert mir die Fortführung des Projektes ermöglicht und die Finanzierung übernommen hat. Unverzichtbar für diese Arbeit waren alle Wissenschaftler am Genzentrum und in der Virologieabteilung des Max-von-Pettenkofer Instituts, die für eine angenehme Arbeitsatmosphäre gesorgt und den wissenschaftlichen Gedankenaustausch gefördert haben. Namentlich hervorheben möchte ich PD Dr. H.-G. Burgert, Dr. Mark Windheim und Dr. Zsolt Ruzsics, die durch besonders ertragreiche Diskussionen und praktische Hinweise zum Gelingen dieser Arbeit beigetragen haben. Für hervorragende technische Assistenz danke ich Elke Maas. Christian Kuenzel danke ich für die Immunisierung von Kaninchen zur Antikörpergewinnung. Bei Dr. Walter Muranyi bedanke ich mich für die Unterweisung in der Nutzung des konfokalen Laserfluoreszenzmikroskops.

Dr. Stefan Höning an der Universität Göttingen danke ich für die Durchführung einer Surface Plasmon Resonance-Analyse, sowie Andreas Elsing, Susanne Obermeier, Johan Lindberg und Madelaine Löfqvist für ihre Vorarbeiten zum Thema dieser Dissertation.

Für meine Eltern

Table of Contents

Summary	1
Introduction.....	3
1.1 Adenoviridae: classification and pathogenicity	3
1.2 Adenovirus particle	4
1.3 Viral life cycle.....	5
1.3.1 Infection.....	5
1.3.2 Genome organization	7
1.3.3 Viral transcriptional program and replication cycle	8
1.4 Host immune response to adenovirus infection	11
1.5 Adenovirus genes counteracting host defense mechanisms:.....	11
1.5.1 Evasion of the innate immune response	11
1.5.2 Evasion of the adaptive immune response	14
1.6 Immune evasive functions encoded by the E3 region.....	15
1.7 Adenovirus E3/10.4-14.5K	20
1.7.1 Biochemical characteristics of 10.4K and 14.5K encoded by subgroup C Ads	20
1.7.2 10.4-14.5K-mediated down-regulation of cell surface receptors	22
1.8 The cellular protein sorting machinery	26
1.8.1 Principles of membrane protein transport.....	26
1.8.2 Clathrin-coated vesicle formation: Adaptor complexes and sorting signals.....	29
1.8.3 Sorting within endosomes for return to the TGN or transport to lysosomes	33
1.9 Putative transport motifs within Ad2 10.4-14.5K.....	34
1.10 Aims of this study	36
Materials and Methods.....	37
2.1 Materials.....	37
2.2 Methods	46

2.2.1	Bacterial cultures.....	46
2.2.2	DNA techniques.....	48
2.2.3	Generation of recombinant Ads.....	54
2.2.4	Cell culture.....	59
2.2.5	Protein techniques.....	65
	Results	71
3.	Relevance of strictly conserved amino acids for Ad2 10.4-14.5K function.....	71
3.1	Identification of strictly conserved amino acids within 10.4K and 14.5K.....	71
3.2	Functional relevance of strictly conserved amino acids in 14.5K.....	73
3.3	Surface expression levels of mutant FLAG-14.5K.....	77
3.4	Complex formation of 10.4K with 14.5K mutants.....	78
3.5	Functional relevance of dileucine type sequence elements within 10.4K.....	81
3.6	Influence of mutations in 10.4K on FLAG-14.5K surface expression.....	83
3.7	Complex formation of mutant 10.4K with 14.5K.....	84
3.8	The cellular adaptor proteins AP-1 and AP-2 bind to 10.4K and 14.5K cytoplasmic tail peptides in a motif-dependent fashion.....	86
4	Importance of the 10.4K dileucine and 14.5K Y ¹²² XXΦ motifs for intracellular trafficking of 10.4-14.5K.....	88
4.1.	Establishment of an efficient heterologous expression system for 10.4-14.5K suitable for analysis of intracellular localization by immunofluorescence.....	88
4.2.	Functional activity of 10.4 and 14.5K proteins encoded by single expression vectors..	92
4.3.	Analysis of intracellular trafficking of 10.4K and FLAG-14.5K coexpressed upon transfection of separate expression vectors.....	96
4.4.	Mutations of 10.4LL and 14.5Y122 induce missorting of 10.4-14.5K.....	98
4.5.	Enhanced transport of 10.4-14.5 to late endosomes/lysosomes in the absence of the 10.4K dileucine motif.....	101
5.	Characterization of 10.4-14.5K loss of function mutants in infected cells.....	103
5.1.	BAC technology for manipulation of Ad2 genomic DNA.....	103
5.2.	Generation of recombinant Ad mutants by ET cloning:.....	103

5.2.1.	Generation of 10.4LL-F14.5 and F14.5Y74A mutant alleles by PCR	103
5.2.2.	ET recombination strategy	104
5.2.3.	ET cloning strategy for the generation of 10.4K and 14.5K single knock-out viruses	106
5.2.4.	Analysis of minitransposon-containing mutant pAd2-BACs	107
5.2.5.	Transposon removal.....	108
5.3.	Recombinant Ads expressing 10.4-14.5 mutants are defective in receptor down-modulation.....	111
5.4.	Complex formation of mutant 10.4-14.5K in infected cells	116
5.5.	Immunofluorescence of infected primary cells.....	117
5.6.	10.4-14.5K and Fas do not profoundly colocalize in Ad2-infected cells	121
6.	Analysis of homologous E3/10.4-14.5K proteins of adenovirus 4 (subgenus E)	123
6.1.	Down-regulation of cell surface receptors following infection with Ad4	123
6.2.	Generation of recombinant Ad2 viruses encoding Ad4 homologues of 10.4K and 14.5K	123
6.3.	Expression of Ad4 10.4K and Ad4 14.5K proteins in cells infected with Ad2/Ad4 chimeric viruses.....	128
	Discussion	132
7.1.	Importance of strictly conserved amino acids for the function of Ad2 10.4-14.5K.....	132
7.2.	Functional relevance of putative transport motifs within 10.4-14.5K for receptor down-modulation	133
7.3.	Importance of putative transport motifs for down-regulation of TRAIL-receptors DR4 and DR5	138
7.4.	Transport processes underlying the mechanism of down-modulation of plasma membrane receptors by 10.4-14.5K	141
7.5.	Differential requirements for expression of Ad4 10.4-14.5K proteins.....	151
	References	157
	Abbreviations	176
	Annexe	179
	CURRICULUM VITAE	185

Summary

Human adenoviruses (Ads) have evolved elaborate mechanisms to counteract the host's antiviral immune response. The early transcription unit 3 (E3) of the virus is not essential for virus replication *in vitro*, but is known to encode proteins with immunomodulatory functions. The Ad2 E3/10.4-14.5K proteins are both integral membrane proteins, which form a physical complex and function together to modulate cell surface expression of the EGFR and selective members of the TNF/NGF receptor superfamily, namely Fas/CD95 and TRAIL-R1, whereas TRAIL-R2 modulation additionally requires E3/6.7K. In a process referred to as receptor down-regulation, 10.4-14.5K relocates receptor targets from the cell surface to lysosomes for degradation. The aim of this study was to characterize functional determinants within the Ad2 10.4-14.5K proteins, that are required for down-regulation of plasma membrane receptors. In particular, I focussed on the characterization of potential transport motifs present in the cytoplasmic tail of both proteins: The Ad2 14.5K tail contains three YXX Φ sequence motifs (Y denotes tyrosine, X any amino acid and Φ a bulky, hydrophobic residue) while the Ad2 10.4K sequence displays two consensus elements of the second large class of transport signals, the dileucine motifs. Both types of motifs are recognized by cellular adaptor proteins which select cargo for directed transport in clathrin-coated vesicles. FACS analysis of stable E3-transfectants expressing 10.4-14.5K mutant proteins revealed that residues contained within these putative transport motifs were essential for down-regulation of Fas and the EGFR *in vivo*. Receptor expression was restored when either the dileucine pair (LL^{87,88}) of 10.4K or 14.5K Y74 or Y122 were replaced by alanine. Whereas loss of function of the 14.5K mutant Y74 can be explained by its inability to interact with 10.4K, several lines of evidence suggest that the 10.4K dileucine pair and 14.5 Y¹²²XX Φ motif function as transport signals: (i) Surface plasmon resonance spectroscopy showed that mutation of the two motifs prevents binding of 10.4K and 14.5K cytoplasmic tail peptides to purified adaptor protein complexes AP-1 and AP-2 *in vitro*. (ii) FACS analysis demonstrated that mutation of these motifs strongly affects FLAG-14.5K cell surface expression. (iii) In line with the FACS data, immunofluorescence microscopy revealed that mutant 14.5Y¹²²A accumulates together with 10.4K at the cell surface, suggesting that the Y¹²²FNL motif normally directs internalization of 10.4-14.5K. (iv) Substitution of the 10.4K dileucine pair increased the transport of 10.4-14.5K into lysosomes, resulting in enhanced degradation of both 10.4K and 14.5K without significantly disrupting complex formation. (v) The accumulation of mutant 10.4-14.5K at the cell surface upon coexpression of 10.4LL/AA and 14.5Y¹²²A suggests that the dileucine motif acts downstream of Y122 and fulfills a sorting function subsequent to endocytosis. Transfer of the mutations into Ad2 and infection of primary

fibroblasts revealed a similar defect in trafficking of 10.4LL/AA and 14.5 Y¹²²A mutant proteins. Moreover, in infected cells substitution of the 10.4K dileucine pair and 14.5K Y122 impaired down-regulation of Fas, EGFR and both TRAIL-R1 and TRAIL-R2, implying a general role of these sorting signals for the mechanism of receptor down-regulation. Thus, two distinct transport signals present in the different subunits of the 10.4-14.5K complex seem to act in concert to establish efficient down-regulation of receptor targets.

Alanine replacement mutagenesis of several other strictly conserved amino acids in 14.5K and FACS analysis of stable E3-transfectants revealed that those mutants which exhibited an altered FLAG-14.5K surface expression had defects in Fas and EGFR down-modulation. Surprisingly, Ad4 was unable to modulate Fas and EGFR expression, even though the Ad4 14.5K protein contained all the strictly conserved amino acids. As a first step to identify structural features that determine target specificity of 10.4-14.5K, I chose to replace the 10.4-14.5K ORFs in Ad2 by their Ad4 homologues. Although the Ad4 10.4-14.5K proteins could be detected in Ad4-infected cells, their expression level was drastically reduced when encoded by the Ad2 E3 region. This indicated that expression of Ad4 10.4-14.5K is differently regulated as compared to Ad2, possibly due to altered splicing. Further exploration of this system will require a detailed analysis of splicing within the Ad4 E3 region.

Introduction

1.1 Adenoviridae: classification and pathogenicity

Adenoviruses (Ads) were first described in the early 1950s as infectious agents isolated from explanted human tonsillar tissue (adenoids) (Shenk, 2001). The different adenovirus types characterized to date have been classified into two genera, according to their host range, genome organization and serological criteria: Mastadenovirus infecting mammals and Aviaadenovirus infecting solely birds. The natural host range of most adenoviruses is confined to one species or to closely related species, allowing to distinguish human adenoviruses and different classes of animal viruses. So far, 51 different human adenovirus serotypes have been identified, which are divided into six subgroups A-F (Table 1) based on serum neutralization of hemagglutination, polypeptide composition of the virions and oncogenicity in rodents. Overall DNA homology within one subgroup is higher than 50%, but below 20% between different subgenera (Shenk, 2001).

Table 1 Classification scheme of human adenoviruses

Subgenus	Serotypes
A	12, 18, 31
B	3, 7, 11, 14, 16, 21, 34, 35, 50
C	1, 2, 5, 6
D	8, 9, 10, 13, 15, 17, 19, 20, 22-30, 32, 33, 36-39, 42-49, 51
E	4
F	40, 41

Although each Ad subtype can infect a broad variety of post-mitotic and highly differentiated cells of the human body, a distinct disease pattern is observed for Ads belonging to different subgroups. Symptoms are often mild and infections are self-limiting, but can be severe or even fatal in immunocompromised patients, e.g. during AIDS or in allogeneic bone marrow recipients (Horwitz, 2001a). Adenovirus type 2 (Ad2) and Ad5 of subgenus C are the most common serotypes to which adults have been exposed (Shenk, 2001). The occurrence of Ad-specific antibodies in the human population is very high worldwide, e.g. more than 85% of adults carry antibodies against subgenus C Ads in their blood. Thus, the host immune response is insufficient to prevent spread of the virus among individuals. The most prevalent serotypes of subgenus B/C mainly cause acute respiratory disease, pertussis-like syndrome or pneumonia (see Table 2). Those of subgenus A and F cause gastrointestinal infections, primarily in infants and young children. Adenovirus type 4 (Ad4), the only member of subgenus E adenovirus, is known to cause epidemic outbreaks of an acute respiratory disease in military recruits (Barraza et al., 1999). Subgenus D is by far the largest subgenus, containing 31 serotypes, which tend to cause eye

Table 2 Diseases associated with human adenovirus infections (according to (Lukashok and Horwitz, 1998))

Disease	Individuals at high risk	Principal serotypes
acute febrile pharyngitis	infants, young children	1, 2, 3, 5, 6, 7
pneumonia	infants, young children	1, 2, 3, 7
pertussis-like syndrome	infants, young children	40, 41
gastroenteritis		
pharyngoconjunctival fever	school-age children	3, 7, 14
acute respiratory disease	military recruits	3, 4, 7, 14, 21
pneumonia	military recruits	4, 7
epidemic keratoconjunctivitis	any age group	8, (11), 19a, 37
acute hemorrhagic cystitis	young children	11, 21
meningoencephalitis	children and immuno-compromised hosts	7, 12, 32
hepatitis	infants and children with liver transplants	1, 2, 5
persistence of virus in the urinary tract	bone marrow transplant recipients, patients with acquired immunodeficiency or other immunosuppression	9, 11, 19, 20, 22, 23, 26, 27, 34, 35, 43, 44, 45, 48, 49

diseases. Specifically Ad8, Ad19a and Ad37 have been found to be associated with a severe and extremely contagious form of eye infection involving both the cornea and the conjunctiva, termed epidemic keratoconjunctivitis (EKC) (Lukashok and Horwitz, 1998).

Following the acute phase of infection, adenoviruses may persist in the host for several months or even years (Horwitz, 2001a). During persistent infection the virus seems to be constantly produced, with intermittent shedding and excretion, thus facilitating virus spread. For subgroup C viruses which are considered to be endemic a low level of continuous Ad production in lymphoid cells has been reported (Mahr and Gooding, 1999). In the lungs of patients with COPD, chronic obstructive pulmonary disease, a truly latent state of adenovirus induces a heightened inflammatory response to air contaminants (Hayashi, 2002). As evidenced by the establishment of persistent infection, adenovirus can withstand attack by the host immune response. Intricate interactions between viral and cellular gene products result in a complex balance between the virus and the host immune system.

1.2 Adenovirus particle

Adenoviridae contain a linear double-stranded (ds) DNA genome, which is encapsulated in a non-enveloped protein shell of approximately 70-100 nm in diameter (Kay et al., 2001). Genome length varies between 26-45 kbp. The viral DNA is framed by inverted terminal repeats of 40-160 bp and a virus-encoded terminal protein (TP) is covalently attached to the 5'-end of each strand (Shenk, 2001). The viral DNA covered with the highly basic protein VII, a small peptide

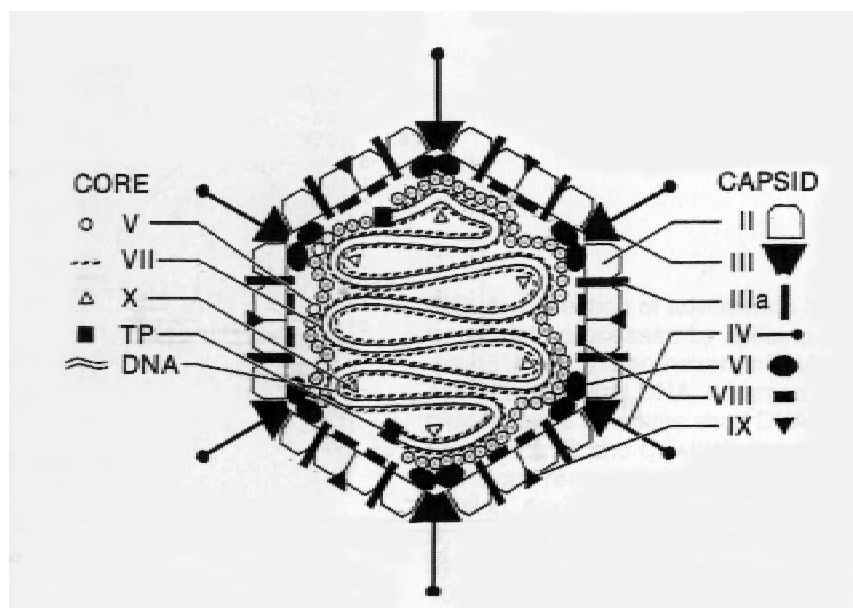


Fig. 1 Composition of the adenovirus particle

Schematic drawing of the adenovirus particle, adapted from (Shenk, 2001). Protein components of the virion are designated with numbers (II-X), except for the terminal protein (TP).

termed μ (X) and protein V form the core structure (Fig. 1). Interaction of protein V with protein VI seems to link the core to the capsid. The icosahedral capsid is composed of 252 subunits, of which 240 are hexon (trimer of protein II) and 12 penton capsomeres. Each penton capsomere contains a base (five copies of protein III), which forms part of the capsid surface and a protruding fiber (three copies of polypeptide IV) folding into a terminal knob. Proteins named VI, VIII, IX, IIIa and IVa2 are minor capsid components (Fig. 1, (Russell, 2000; Shenk, 2001).

1.3 Viral life cycle

The viral life cycle can be divided into two temporally distinct phases: infection and replication. Infection covers the entry of the virus into the host cell and passage of the virus genome to the nucleus. In the nucleus the viral transcription program is initiated which leads to selective transcription and translation of early genes. These early events modulate the functions of the cell to facilitate the replication of viral DNA and expression of late genes. In the late phase structural proteins are expressed and assembly of new infectious viral particles occurs.

1.3.1 Infection

Adenovirus infection starts with the adsorption of the virions to the host cell. The Ad fiber proteins except for those from subgenus B Ads (Roelvink et al., 1998), mediate attachment by binding with high affinity to a 46 kD cell surface molecule called coxsackie/adenovirus receptor (CAR) (Roelvink et al., 1998; Tomko et al., 1997; Wang and Bergelson, 1999), which is expressed

in variable amounts in most tissues (Nemerow, 2000). Critical for CAR binding are extended loops on the lateral surface of the fiber knob (Bewley et al., 1999; Roelvink et al., 1999).

Adenoviruses readily infect the epithelium of the lung. But, contrary to expectations the CAR protein is not found on the exposed apical surface of these sheets of epithelial cells, but rather on the basolateral membrane. It functions in allowing epithelial cells to stick to one another and to form a continuous sheet. Recently, it was discovered that binding of the adenovirus fiber protein to CAR can disrupt these cell-to-cell contacts. In productive infection of epithelial cells surplus fiber protein is produced, which is released along with viral progeny to the basolateral surface and can bind to CAR, thereby opening up holes in the sheet of epithelial cells, through which the virus can escape into the lungs (Walters et al., 2002). Besides CAR other receptors involved in adenovirus entry have been proposed (Nemerow, 2000), such as the class I major histocompatibility complex (MHC) α_2 domain as a receptor for the Ad5 fiber knob (Hong et al., 1997). Some members of subgenus D, namely the EKC causing Ads Ad8, Ad19a and Ad37 seem to utilize $\alpha(2\rightarrow3)$ -linked sialic acid instead of CAR (Nemerow, 2000). As these attachment receptors are widely expressed they cannot sufficiently explain the differences in tissue tropism and distinct pathogenesis of Ads from different subgenera. It rather seems that viral tropism additionally depends on postattachment processes, e.g. internalisation, and the differential countermeasures against the host immune response. After initial receptor binding an exposed RGD motif of the penton base interacts with cellular $\alpha_v\beta_3$ or $\alpha_v\beta_5$ integrins (Nemerow and Stewart, 1999) triggering rapid endocytosis of the virions via clathrin-coated pits. Virus entry also requires activation of PI3K (phosphoinositide-3-OH kinase) and Rho guanosine triphosphatases which cause reorganization of the actin cytoskeleton (Russell, 2000). After internalisation, the virion, which is very stable outside the cell, is dismantled by an ordered elimination of structural proteins, in order to deliver its DNA to the nucleus. Penton base and fiber proteins are degraded and the capsid is partially disassembled by proteolytic activity of the viral cysteine protease p23 (Russell, 2000). Ads escape from the endosomal/lysosomal compartment by inducing acid-enhanced lysis of the endosomal membrane. The Ad particles migrate along microtubules to the nuclear pore complex driven by dynein (Russell, 2000). Penetration of the nuclear pore (40nm diameter) requires complete disassembly of the Ad capsid. Histon H1 and the H1 import factors Imp β and Imp7 facilitate injection of the viral DNA-protein complex into nucleus (Trotman et al., 2001). The viral DNA attaches to the nuclear matrix via interaction of the terminal protein (TP) with cellular factors and nuclear matrix association is required for efficient activation of transcription (Russell, 2000).

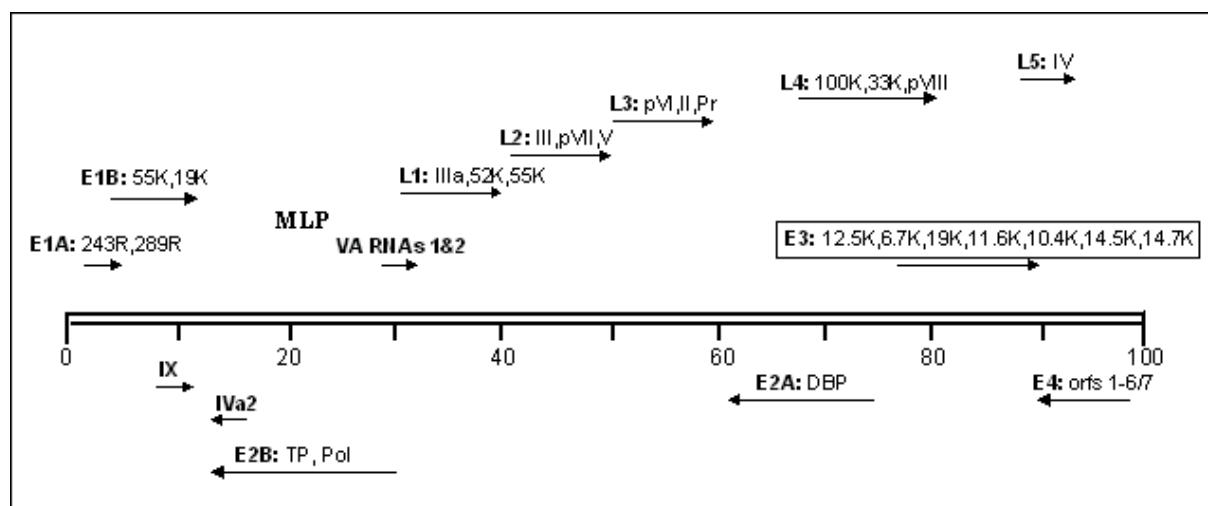


Fig. 2 Organization of the adenovirus genome (subgenus C)

Transcription units are designated E (boldface) for early and L for late expression. The proteins encoded by each transcription unit are listed on top of an arrow, which describes their position in the genome map (Map units 0-100). Most late mRNAs originate from the major late promoter (MLP). Proteins of the E3 transcription unit are boxed. For details see text.

1.3.2 Genome organization

Adenovirus encodes about 40 polypeptides, one third being structural proteins. Genes become expressed in a defined, temporarily regulated manner, controlled by transcription initiation and post-transcriptional RNA processing (reviewed in (Imperiale et al., 1995)). In this respect, subgroup C adenoviruses type 2 and 5 (Ad2 and Ad5) genomes, which are completely sequenced, have been studied in greatest detail (Fig. 2). Host RNA polymerase II (RNA Pol II) transcribes both DNA strands to generate transcripts belonging to five early transcription units (E1A, E1B, E2, E3, E4), two delayed early units (IVa2, IX) and one major late unit. Each unit encodes multiple mRNAs which are differentiated by alternative splicing and the use of different polyadenylation sites. The late unit is processed to generate five families of late mRNAs (L1 to L5). In fact, analysis of adenovirus mRNA structure led to the discovery of splicing (Padgett et al., 1984). All RNA Pol II transcripts become capped and polyadenylated by cellular factors. Two non-coding highly structured virus-associated (VA) RNAs are transcribed by host RNA Pol III and act as antagonists of the antiviral interferon- α and - β response by inhibiting activation of cellular PKR, a double-stranded RNA-dependent protein kinase (reviewed in (Burgert et al., 2002; Mahr and Gooding, 1999)). Many of the individual adenovirus transcription units encode a series of polypeptides with related functions. The grouping into units that are defined by a single transcriptional control element allows coordinated expression of multiple polypeptides which are needed simultaneously to execute a certain function, such as DNA replication which is controlled

by E2. Moreover, it might be useful to closely group the coding regions of products that interact physically or functionally to reduce the frequency with which they could be separated by recombination.

1.3.3 Viral transcriptional program and replication cycle

E1A genes are the first to be transcribed and E1A proteins transactivate the promoters of early transcription units E1B, E2, E3 and E4 (Shenk, 2001). Ad infection of quiescent cells induces transition from G1 or G0 into S-phase of the cell cycle and cellular proliferation by transcriptional activation of a set of growth-promoting cellular genes (Cress and Nevins, 1996), which provide optimal conditions for viral replication. Adenovirus E1A, E1B and E4 gene products contribute to cell cycle deregulation. A huge panoply of functions has been attributed to E1A based mainly on *in vitro* studies ((Gallimore and Turnell, 2001; Russell, 2000) and references therein) and E1A expression is essential for both Ad-induced transformation and a productive Ad infection. The E1A region of human adenoviruses gives rise to two major alternatively spliced mRNAs of 12S and 13S. The corresponding gene products are nuclear phosphoproteins termed 289R and 243R, based on the number of amino acid residues. Between different serotypes three conserved regions (CR1-3) have been identified, CR3 being unique to the 13S product. These regions are important in defining interactions with a number of cellular proteins. CR3 is essential for transactivation of both early viral and cellular promoters (Jones, 1995), as it binds transcription factors such as ATF-2, transcriptional mediators hSur2 and the basal transcriptional machinery TATA-box binding protein (TBP) directly (Gallimore and Turnell, 2001). Ad E1A binds the retinoblastoma protein Rb and Rb-related proteins p107, p130 through interactions with CR1 and CR2. These interactions liberate the transcription factor E2F that stimulates expression of gene products involved in DNA synthesis, including adenovirus E2 gene products. E1A also binds p21 and related CDK (cyclin-dependent kinase) inhibitors thereby stimulating cell division and growth (Russell, 2000). Moreover the N-terminus of AdE1A can bind to the p300/CBP (CBP, *CRE*-binding protein; *CRE*, *cAMP responsive element*) family of transcription transactivators that play a key role in regulating the transcription of many components of the cell cycle (Russell, 2000). However, these E1A-induced changes also provoke the intrinsic cellular death program. Transcription factors E2F and ETF, released from Rb, trigger apoptosis by promoting the synthesis and stability of p53 (Hale and Braithwaite, 1999). They induce transcription of p53 itself, but also upregulate mouse p19^{ARF} (or human p14^{ARF}), which can interact with Mdm2 and block the ubiquitin ligase activity of Mdm2, that normally mediates p53 proteolysis via the ubiquitin pathway (Ashcroft and Vousden, 1999). Furthermore, E1A proteins sensitize cells to induction of

apoptosis by external stimuli, such as TNF- α (abbreviated as TNF), Fas ligand (FasL) and TRAIL (Duerksen-Hughes et al., 1989; Routes et al., 2000; White, 2001). TNF-susceptibility is induced by E1A binding to either p300/CBP or Rb (Shisler et al., 1996), and can also occur in p53-null cells (Putzer et al., 2000). E1A may sensitize to TNF-induced apoptosis by eliminating synthesis of prosurvival factors, such as Bcl-2 family members or IAPs (inhibitor of apoptosis proteins), through indirect inhibition of TNF-induced nuclear factor- κ B (NF- κ B) activation. E1A interferes with IKK-mediated I κ B phosphorylation, and consequently, may inhibit NF- κ B release to the nucleus (Shao et al., 1999). Recently, it was reported that E1A can inhibit TNF-dependent induction of cFLIPs (cellular FLICE inhibitory proteins), thereby promoting activation of caspase 8 at the death-inducing signaling complex (Perez and White, 2003; White, 2001). E1A also has an important immune evasive function, namely to block interferon-induced signal transduction in infected cells (Burgert et al., 2002; Mahr and Gooding, 1999).

Two gene products of the E1B region, E1B-19K and E1B-55K counteract the apoptosis program initiated by E1A proteins. E1B-55K interacts directly with promoter-associated p53 inhibiting p53-dependent transcription (Martin and Berk, 1998). Together with E4orf6 E1B-55K can accelerate degradation of p53 (Tauber and Dobner, 2001), and such increased turnover overcomes the E1A-induced increase in p53. Thus, in productive viral infection E1A seems to induce apoptosis mostly in a p53-independent manner. E1B-19K blocks apoptosis induced by E1A via both p53-dependent (oncogenic transformation) and p53-independent (viral infection) mechanisms, and may interfere with death signals emanating from death receptors Fas, TNFR or TRAIL: E1B-19K is a viral homologue of the cellular Bcl-2 gene product, and seems to interrupt the mitochondrial pathway of apoptosis mainly by inhibiting proapoptotic members of the Bax and Bak family (Desagher and Martinou, 2000; White, 2001). Bax and Bak have been identified as central mediators of E1A-induced apoptosis during infection, which is efficiently counteracted by E1B-19K. In infection with virus mutants lacking E1B-19K, Bax/Bak-mediated apoptosis reduces the efficiency of virus replication, indicating that the apoptotic response of the cell to infection has indeed evolved as an antiviral response (Cuconati et al., 2002)(Lomonosova et al., 2002).

The Ad E2 gene products are subdivided into E2A (DNA binding protein, DBP) and E2B (TP and Pol), which in conjunction with cellular factors provide the machinery for replication of virus DNA and the ensuing transcription of late genes.

Products of E3 genes are dispensable for replication of the virus in tissue culture and *in vivo* in cotton rat lungs (Ginsberg et al., 1989), but are thought to play a key role in regulating the interaction of Ads with the immune system of the host (Burgert, 1996; Burgert and Blusch, 2000;

Mahr and Gooding, 1999; Wold et al., 1995). Incorporation of E3 functions into a recombinant adenoviral vector attenuated antiviral humoral and cellular immune response and allowed long-term gene expression in an animal model (Ilan et al., 1997). Several E3 proteins have been shown to counteract host defense mechanisms, such as antigen presentation, apoptosis and the inflammatory response (see also chapter 1.6). One of the E3 proteins (E3/11.6K) has been termed the adenovirus death protein (ADP), since it appears to facilitate late cytolysis and release of virus progeny at late stages of infection (Tollefson et al., 1996b). Although it is encoded within the E3 transcription unit 11.6K is synthesized only in small amounts from the E3 promoter at early times after infection, but abundantly from the major late promoter during late stages of infection.

E4 proteins termed orf 1-6/7 regulate virus mRNA metabolism, promote virus replication and shut-off of host protein DNA synthesis (Leppard, 1997). E4orf6 and E1B-55K facilitate nuclear export and cytoplasmic accumulation of late viral mRNAs and concomitantly inhibit export of cellular mRNAs (Gonzalez and Flint, 2002). E4orf6 and E4orf3 both interact with E1B-55K, thereby influencing the activity of p53 (Konig et al., 1999). E4orf6/7 can functionally replace E1A in induction of E2F (O'Connor and Hearing, 2000). Proapoptotic E4orf4 seems to be involved in E1A-induced p53-independent apoptosis and the killing of infected cells at the end of the infection cycle (Lavoie et al., 1998).

The late phase of virus infection starts with the onset of viral replication. DNA replication begins from two replication origins, one is present in each terminal repeat. The terminal protein (TP), viral polymerase and cellular factors are involved in initiating replication by a protein priming mechanism and the DNA binding protein (DBP) facilitates strand-displacement during elongation. Replication ensues transcription of the Major Late Transcription Unit. The major late promoter controls synthesis of a large polycistronic primary transcript that is processed by differential usage of polyadenylation sites and splicing to generate mRNA families L1-L5 (Fig. 2). During transcription of early E1A, E1B, E2, E3 and E4 genes the major late promoter is attenuated to a low basal level of transcription. After the onset of viral replication the IVa2 and IX genes are expressed at high levels and specifically activate transcription via the MLP (Lutz and Kedinger, 1996), whereas early gene expression is repressed (Fessler and Young, 1998). From the late transcripts structural components of the virus and assembly proteins are expressed, leading to encapsidation and maturation of virus particles in the nucleus. Despite massive production of Ad particles cells do not lyse and remain intact for several days. Finally, the virus is set free from the nucleus by active disintegration of the nuclear envelope by the adenovirus death protein (Tollefson et al., 1996a).

1.4 Host immune response to adenovirus infection

The host immune response elicited by adenovirus has received increasing attention especially with the use of adenoviral vectors for gene therapy. Most of the knowledge has been gained following administration of replication-defective Ad vectors carrying deletions in the viral genome and possible insertions of transgenes into rodent models (rarely in humans). Very often these vectors lack the E3 region of the viral genome, which encodes immunomodulatory functions (see chapter 1.6), and therefore the outcome may differ from that of an infection with wt Ads.

Ad vectors induce both humoral and cellular immune responses against the vector-derived proteins as well as those derived from the inserted transgenes (Dai et al., 1995) (Kaplan et al., 1997; Yang et al., 1996). Potent host immune response against viral proteins and the capsid result in transient transgene expression and an inability to readminister vectors of the same serotype to previously immunized subjects (Zoltick et al., 2001). In the absence of all viral transcription the adenoviral capsid is also immunogenic, capable of inducing chemokines, the interferon response and adenovirus-specific cytotoxic T lymphocytes (Kafri et al., 1998; Muruve et al., 1999; Reich et al., 1988). Concomitantly with virus entry Ad infection stimulates the Raf/MAPK (mitogen-activated protein kinase) signaling pathway, possibly by interaction of the penton base with cellular integrins, which leads to the production of multiple chemokines, such as IL-8 (Bruder and Kovesdi, 1997). Chemokines recruit neutrophils, macrophages and natural killer cells to the site of infection and invoke an immediate inflammatory response (Muruve et al., 1999). Innate defense mechanisms have been proposed to play a significant role in the clearance of (partial E1- and E3-deficient) Ad-vector-transduced cells *in vivo*, especially in the respiratory tract (Worgall et al., 1997a; Worgall et al., 1997b). A major mediator of the elimination of Ad-transduced cells from the mouse liver are Fas-FasL interactions (Chirmule et al., 1999) and the granzyme/perforin pathway (Yang et al., 1995). In addition, Ad E1A activation of p53 triggers proapoptotic stimuli in the infected cells. As described above the intrinsic apoptosis program is counteracted by E1B products, whereas Ad E3 proteins (chapter 1.6) seem to have evolved to decapitate death receptor-mediated apoptosis pathways and cytolysis by cytotoxic T lymphocytes.

1.5 Adenovirus genes counteracting host defense mechanisms: Viral immune evasion

1.5.1 Evasion of the innate immune response

Infected cells secrete a number of cytokines which elicit an immediate inflammatory response mediated predominantly by neutrophils, macrophages and NK cells (Muruve et al., 1999; Worgall et al., 1997b). The Ad E1A protein induces susceptibility to NK cell lysis of transformed

cells, whereas cells infected with Ad2 or Ad5 exhibit no increased sensitivity. This indicates an effective countermeasure of the virus, but the adenoviral gene products involved remain unknown (Routes and Cook, 1995). Ad E1A also sensitizes cells to TNF- α , FasL and TRAIL-induced apoptosis (White, 2001). TNF- α is a major inflammatory cytokine secreted by activated macrophages and monocytes and is thought to play a central role in the elimination of virally transduced cells (Elkon et al., 1997; Sparer et al., 1996; Zhang et al., 1998a).

TNF- α (abbreviated as TNF) mediates its activity by binding to two receptors, TNFR1 (p55) and TNFR2 (p75). Whereas TNFR1 is constitutively expressed in nearly all tissues, TNFR2 expression is more restricted, e.g. to lymphoid tissue. While sharing structural similarities in their extracellular domain, the two TNFRs differ in their intracellular domain and consequently their signal transduction (Hehlgans and Mannel, 2002). TNFR2 has no death domain and its prominent interaction is the direct recruitment of TRAF2 and the activation of the NF- κ B pathway. TNF-induced NF- κ B upregulates transcription of a number of genes of the pro-survival Bcl-2 and inhibitors of apoptosis (IAPs) families (Barkett and Gilmore, 1999; Pahl, 1999; Wang et al., 1998). Ligation of TNFR1 may lead to cell death by recruitment of death domain-containing proteins and initiation of a cascade of caspase activation or promote cell survival by activation of two major transcription factors, NF- κ B and AP-1, which culminates in a proinflammatory and anti-apoptotic response (Ashkenazi and Dixit, 1998; Karin and Lin, 2002; Shaulian and Karin, 2002). Additionally, TNF-induced expression and activation of cytosolic phospholipase A₂ (cPLA₂) leads to the production of inflammatory mediators (Wallach et al., 1999).

The TNF-induced production of proinflammatory cytokines, mediates the initiation of the innate immune response to Ad infection (Borgland et al., 2000). TNF-induced cytolysis and inflammation is counteracted by E1B-19K, E3/14.7K and a complex of E3/10.4K and E3/14.5K (E3/10.4-14.5K) (Fig. 3, (Gooding et al., 1991a; Krajcsi et al., 1996; White et al., 1992). Of benefit to the virus, TNF-induced NF- κ B also binds to NF- κ B sites within the E3 promoter and thereby upregulates the expression of Ad E3 immunomodulatory functions (Fig. 3, (Deryckere et al., 1995; Korner et al., 1992). Moreover, Ad E1A can inhibit NF- κ B activation (Shao et al., 1999).

Ad infection also elicits interferon (IFN) production, and thus stimulates transcription of IFN-stimulated genes (ISG) whose products exhibit potent antiviral, immunomodulatory and antiproliferative activities (Stark et al., 1998). Most cell types produce type I interferons (IFN- α/β) and IL-12 upon infection, which enhance NK cell cytotoxicity and stimulate NK cells to produce IFN- γ (Type II interferon) (Biron and Brossay, 2001). Interferons signal via activation of the janus kinase/signal transducers and activators of transcription pathway (JAK/STAT), which transduce

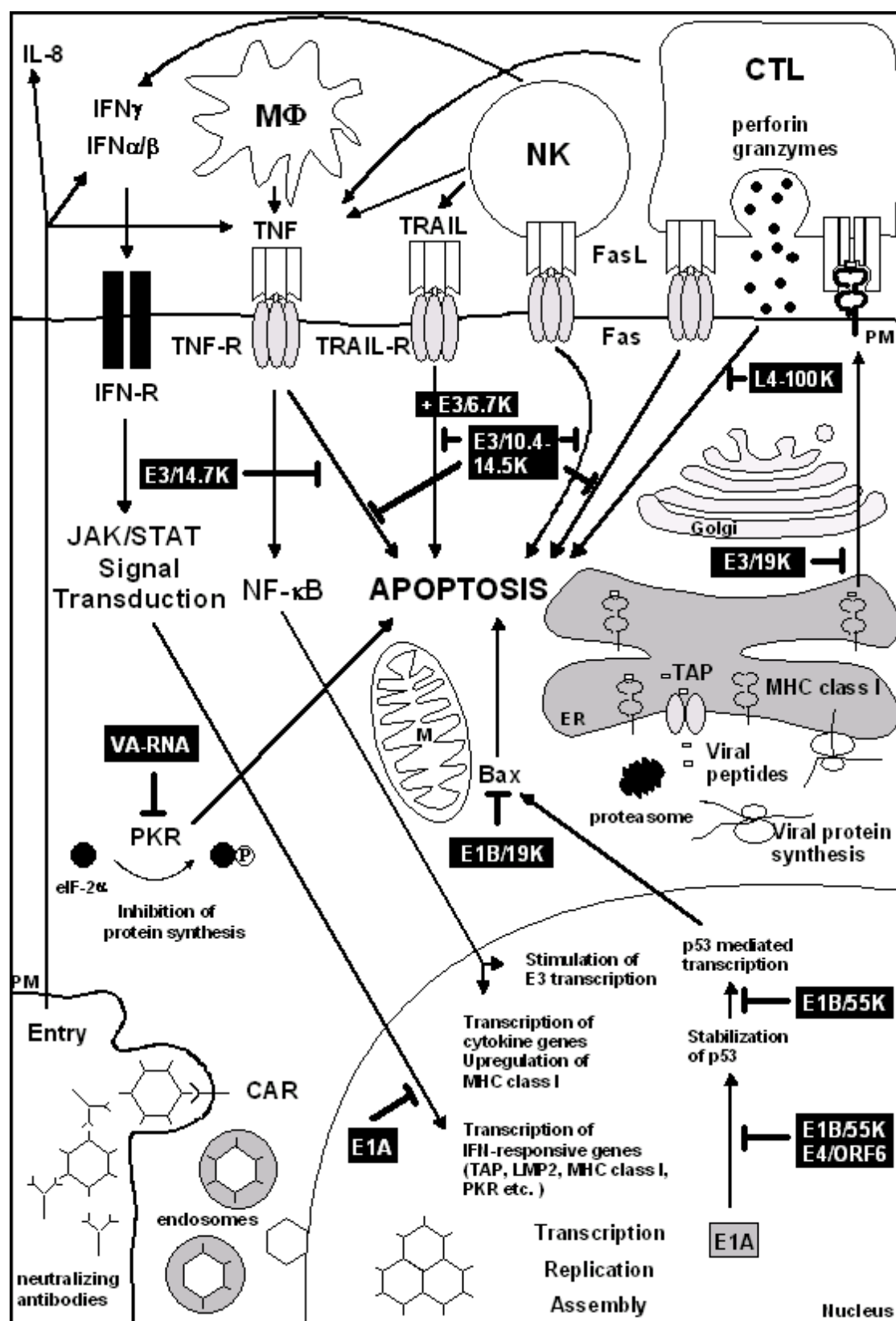


Fig. 3 Adenovirus encoded immune evasive functions (adapted from (Burgert et al., 2002))

A cartoon (not to scale) illustrating some of the sites of action of adenovirus gene products counteracting host defense pathways. Viral gene products (proteins and VA RNAs) are highlighted with black shading. See text for details. Abbreviations not explained in the text: MΦ, macrophage; PM, plasma membrane; M, mitochondrium; ER, endoplasmic reticulum; TAP, transporter associated with antigen processing.

signals to the nucleus (O'Shea et al., 2002; Stark et al., 1998). Ad E1A interferes with interferon signaling (Fig. 3) by decreasing levels of p48 and STAT1, which act as transactivators of IFN- α - and IFN- γ -responsive promoters. Secondly, E1A sequesters the transcriptional coactivator p300/CBP and thereby imposes a block on transcription of IFN-regulated genes (Juang et al., 1998). Potent antiviral products of IFN-induced genes are the double-stranded RNA-induced Ser/Thr protein kinase PKR which arrests protein translation by phosphorylating elongation-initiation factor 2 α (eIF2 α), 2' \rightarrow 5' oligoadenylate synthetase which upregulates RNaseL to degrade RNA, and MHC class I/II molecules which present viral antigens on the cell surface (Goodbourn et al., 2000). In the late phase of infection Ad VA RNAs are transcribed that act as competitive inhibitors of PKR (Fig. 3) to preserve viral translation (Shenk, 2001).

1.5.2 Evasion of the adaptive immune response

Ad vector administration in human patients stimulates a CD4⁺ T cell response and the proliferation of B cells which generate antibodies directed against capsid components, like fiber, penton, hexon and core protein V (Molnar-Kimber et al., 1998). Thus, in a second encounter of the immune system with viral antigens neutralizing antibodies bind to viral particles, block the ability of virions to infect cells and mediate phagocytosis of free virus and virus-infected cells.

Viral protein expression and turnover in the infected cells rapidly generates peptides that can be presented by MHC class I antigens on the cell surface. CD8⁺ cytotoxic T lymphocytes (CTLs) recognize peptide-loaded MHC class I complexes on the surface of infected cells and release their granular content, including granzymes, perforin and proapoptotic factors to promote lysis and elimination of the infected cell (Trapani et al., 2000). Alternatively, apoptosis can be triggered by interaction of FasL on the surface of CTLs with the death receptor Fas on the target cell surface (Harty et al., 2000). A well-understood protective countermeasure of the virus against lytic attack by CTL is the E3/19K-mediated subversion of antigen presentation (Fig. 3, for a recent review refer to (Burgert et al., 2002)). In transformed cells Ad12 E1A can exert transcriptional repression on MHC molecules and several components of the antigen processing machinery, such as transporter subunits TAP1 and TAP2 or components of the immune proteasome, e.g. LMP2 (Fig. 3) (Gallimore and Turnell, 2001). Recently, the Ad assembly protein L4-100K was shown to inhibit granzyme B-induced apoptosis (Fig. 3, (Andrade et al., 2001). FasL- or TRAIL-induced apoptosis of several infected human epithelial cell lines and primary cells can be efficiently inhibited by a complex of E3/10.4K and E3/14.5K proteins (Fig. 3, (Benedict et al., 2001; Elsing and Burgert, 1998; Shisler et al., 1997; Tollefson et al., 1998). E3/10.4-14.5K has also been reported

to protect some cultured human B and T lymphocytes from Fas-induced apoptosis, which might contribute to Ad persistence in lymphocytes (McNees et al., 2002). Ad E3 functions will be discussed in detail in the following chapter.

1.6 Immune evasive functions encoded by the E3 region

The E3 proteins of subgenus C viruses, which are encoded by homologous ORFs in Ads from all other subgroups (Fig. 4), have been attributed an immunomodulatory function (Burgert et al., 2002; Burgert and Blusch, 2000; Horwitz, 2001b; Mahr and Gooding, 1999; Wold et al., 1995). The Ad2 E3/19K protein forms a complex with nascent MHC class I molecules in the endoplasmic reticulum (ER) and blocks their translocation to the cell surface (Fig. 3, (Andersson et al., 1985; Burgert and Kvist, 1985; Paabo et al., 1987)(Burgert, 1996). This results in a diminished lytic response *in vitro* if cells expressing gp19K are exposed to class I specific cytotoxic T cells (Burgert et al., 1987). Additionally, E3/19K can associate with TAP (transporter associated with antigen processing) and might block the interaction between MHC class I antigens and TAP (Bennett et al., 1999).

In a murine pneumonia model E3/14.7K counteracted the antiviral and inflammatory effects of TNF- α (Tufariello et al., 1994). E3/14.7K prevents TNF-induced cytolysis of adenovirus-infected C3HA mouse fibroblasts (Gooding et al., 1988; Gooding et al., 1990; Horton et al., 1991) independent of other Ad proteins. The mechanism of 14.7K action remains incompletely understood, but it has been shown that the 14.7K protein does not affect the number of TNF receptors or its affinity towards ligand (Gooding et al., 1990). Instead, 14.7K seems to inhibit the TNF-induced activation of cytoplasmic phospholipase A2 (cPLA₂) and thereby prevent arachidonic acid release (Krajcsi et al., 1996). cPLA₂ can cleave arachidonic acid (AA) from membrane phospholipids and provide it to cyclo- and lipoxygenases which catalyze its conversion to prostaglandins and leukotrienes (Balsinde et al., 1999; Leslie, 1997). cPLA₂, which becomes activated by MAP kinases and possibly caspases, also seems to be involved in TNF-induced cell death (Krajcsi and Wold, 1998; Wissing et al., 1997). Maximal cPLA₂ activation requires increased intracellular Ca²⁺ concentrations (micromolar amounts), which induce translocation of cPLA₂ to cellular membranes, where it can release AA. The involvement of cPLA₂ in release of AA and cytolysis upon infection with mutant viruses lacking E3/14.7K was confirmed by using specific cPLA₂ inhibitors and antisense oligonucleotides (Thorne et al., 1996). Thus, 14.7K interferes with the function of cPLA₂ which is thought to be required, but is not sufficient for TNF-induced cytolysis (Wallach et al., 1999; Wold et al., 1995).

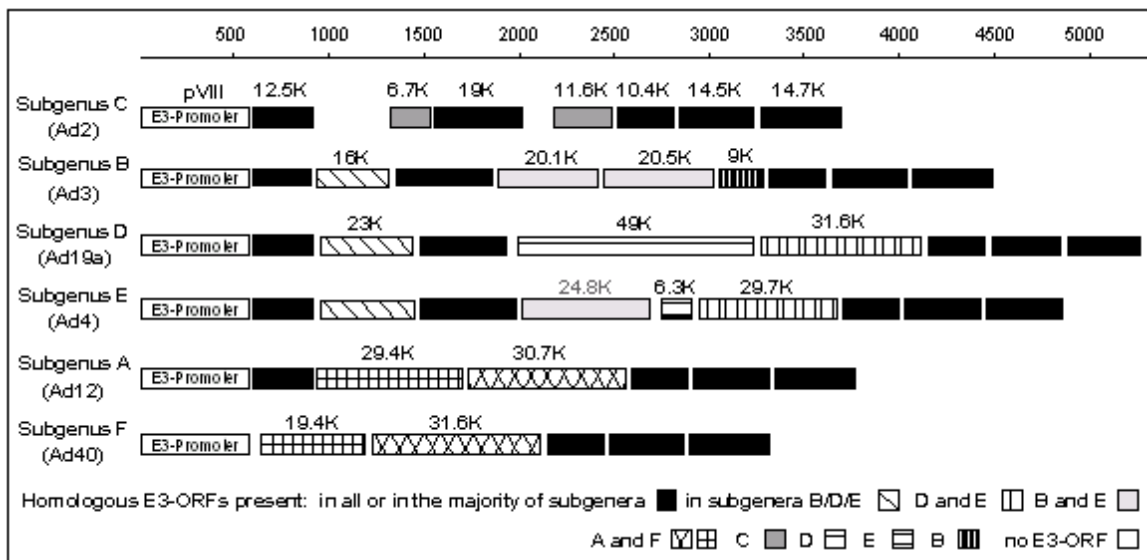


Fig. 4 Organization of the E3 region in different adenovirus subgenera (adapted from (Burgert and Blusch, 2000))

The line on top denotes the size in bp. Open reading frames (ORFs) are indicated as bars and drawn to scale. Significant overall homology (similarity $\geq 25\%$) is illustrated by identical shading. Homology to a portion of a protein was neglected. The shading code is depicted at the bottom of the figure. For each subgroup one representative member is shown, as designated on the left. The size/name of related ORFs is given only once. For sequence data used refer to (Burgert and Blusch, 2000). pVIII is not an E3 protein, but part of its sequence overlaps with the E3 promoter.

By overexpression of FasL, FADD, or caspase 8 via Ad vectors it was shown that Ad5 14.7K protein could bind to caspase 8 (FLICE) and prevent it from triggering the downstream caspase cascade, suggesting that 14.7K can interfere with execution of the cell death signal (Chen et al., 1998). As a CPP32-type caspase implicated in TNF-induced cell death signaling has been reported to cleave and thereby activate cPLA₂ (Wissing et al., 1997), this activity could explain the activity of 14.7K to inhibit cPLA₂. However, human cells infected with an Ad2 virus mutant lacking expression of all E3 proteins except for 12.5K and 14.7K remained sensitive to Fas-mediated cell death (Elsing and Burgert, 1998), and thus during the normal course of Ad infection 14.7K cannot profoundly inhibit FLICE (Horwitz, 2001b).

Yeast-2-hybrid studies revealed interactions of 14.7K with several cellular proteins, which were named 14.7K interacting proteins (FIPs) FIP-1, FIP-2 and FIP-3 (Li et al., 1997; Li et al., 1998a; Li et al., 1999), but the importance of these interactions during adenovirus infection still awaits to be elucidated. FIP-3 is identical with IKK γ (NEMO), which forms part of the I κ B-kinase complex (IKK) (Li et al., 1999). IKK γ was also shown to interact with RIP, a protein recruited to the cytoplasmic domains of Fas and TNFR (Li et al., 1999) and essential for the activation of NF- κ B by TNFR1. FIP-2, a protein containing two leucine zipper domains, was found to reverse the protective effect of 14.7K on cell death induced by overexpression of RIP or the TNFR

intracellular domain (Li et al., 1998a). FIP-1 is identical to the small GTPase RagA and acts in bridging E3/14.7K to TCTEL1, which is a component of the microtubule motor protein dynein (Lukashok et al., 2000). The functional significance of this ternary complex is still unknown.

Several mouse cell lines infected with Ad mutants lacking E3/14.7K remained resistant to TNF-induced cytolysis, despite expression of E1A. In 11 of 15 tested mouse cell lines protection from TNF-cytolysis was conferred by E3/10.4-14.5K (Gooding et al., 1991b). Interestingly, the adenovirus-infected mouse C3HA fibroblast cell line, which had been shown to be efficiently protected by E3/14.7K (Gooding et al., 1988), cannot be protected against TNF by 10.4-14.5K. This differential effect in different cell lines might be due to a difference in expression and/or the mechanism of action of these two sets of proteins. It has been proposed that E3/14.7K and E3/10.4-14.5K function independently in Ad-infected mouse cells to inhibit both TNF-induced apoptosis as well as TNF-induced release of arachidonic acid (Krajcsi et al., 1996). In human cells (but not mouse cells) also E1B/19K can inhibit TNF cytolysis (Gooding et al., 1991a) and in its absence E3 proteins (either 10.4-14.5K or 14.7K) confer protection (Fig. 3). In human A549 cells it could be demonstrated that 10.4-14.5K inhibit TNF-induced translocation of cPLA₂ to membranes and the subsequent arachidonic acid release without interfering with cPLA₂ phosphorylation. E3/14.7K and E1B/19K were not required for this effect (Dimitrov et al., 1997). 10.4-14.5K do not appear to modulate cell surface expression of murine and human TNFR (Benedict et al., 2001; Shisler et al., 1997).

Interestingly, E3/10.4-14.5K specifically down-regulate cell surface expression of other members of the TNF/NGF (tumor necrosis factor/nerve growth factor) receptor superfamily. TNFR superfamily members are type I transmembrane proteins characterized by two to five copies of cysteine-rich extracellular repeats, which are typically defined by three intrachain disulfide bridges formed between strictly conserved cysteines. Death receptors share an intracellular amino acid stretch within the carboxy-terminus of the receptor, called the death domain (DD) (Locksley et al., 2001). When death receptors TNFR1, Fas (CD95/APO-1), DR3/WSL (the receptor for APO-3L), and the TNF-related apoptosis-inducing ligand (TRAIL/APO-2L) receptors DR4 and DR5 are bound by ligand apoptosis can occur as a consequence. Ligand engagement typically causes homotypic interaction of the receptor's DD with adaptors such as FAS-associated DD protein (FADD) or TNFR-associated DD protein (TRADD) that may ultimately lead to caspase activation and cell death (reviewed in (Ashkenazi and Dixit, 1998).

In Ad-infected and E3-transfected cells 10.4-14.5K induce down-modulation of the apoptosis receptor Fas from the cell surface and its degradation in lysosomes (Elsing and Burgert, 1998; Shisler et al., 1997; Tollefson et al., 1998). Thereby, E3/10.4-14.5K prevent apoptosis

triggered by FasL or agonist Fas antibodies (Fig. 3). Whereas Fas is constitutively expressed in a wide variety of tissues, Fas ligand (FasL) is largely restricted to cells of the immune system, such as macrophages, NK cells and activated T cells (Nagata, 1999). Expression of the CD95 gene is enhanced by interferon- γ and TNF and by activation of lymphocytes (Walczak and Krammer, 2000). Besides being important for immune cell homeostasis and for down-regulation of an immune response (Rathmell and Thompson, 2002), Fas-FasL interactions permit CTL and NK cells to induce apoptosis in target cells. The contribution of Fas-mediated cytotoxicity *in vivo* to clearance of virus infections largely depends on the type of virus (Harty et al., 2000; Trapani et al., 2000). As many viruses encode antiapoptotic proteins viral interference with apoptosis seems to be a prerequisite for effective reproduction of viruses and possibly also for establishing viral persistence (O'Brien, 1998; Teodoro and Branton, 1997).

Recently, it has been discovered that E3/10.4-14.5K in conjunction with E3/6.7K act to block TRAIL-induced apoptosis (Fig. 3), by down-regulation of the two death-signaling receptors for TRAIL, TRAIL-R1 (DR4) and TRAIL-R2 (DR5) (Benedict et al., 2001). Another study using different experimental conditions suggested that E3-6.7K is not required for the down-regulation of DR4 by 10.4-14.5K (Tollefson et al., 2001), yet it may still be required by 10.4-14.5K in down-regulating DR5. E3/6.7K has been described as an Asn-linked integral membrane glycoprotein localized in the ER (Wilson-Rawls and Wold, 1993). In correlation with its localization to the ER, E3/6.7K appears to function also independently of 10.4-14.5K in maintaining calcium homeostasis, blocking thapsigargin (inhibitor of ER-associated calcium ATPase)-induced apoptosis, reducing death receptor-induced apoptosis and TNF-induced release of arachidonic acid (Moise et al., 2002). TRAIL is known to induce apoptosis selectively in tumor cells, but not in normal cells (Walczak and Krammer, 2000). TRAIL has been found to be expressed and involved in apoptosis induction by IFN- γ -stimulated monocytes (Griffith et al., 1999), IFN- α and IFN- β or TCR-stimulated T cells (Kayagaki et al., 1999a; Musgrave et al., 1999), non-stimulated CD4⁺ T cells (Kayagaki et al., 1999b), natural killer (NK) cells (Kashii et al., 1999; Kayagaki et al., 1999c), and IFN- α and IFN- γ -stimulated DCs (Fanger et al., 1999). Interestingly, functional surface expression of TRAIL is often associated with stimulation by interferons, suggesting that TRAIL may contribute to the antiviral effects of IFNs and recent reports indicate an involvement of the TRAIL system in overcoming viral infections. Human cytomegalovirus (HCMV) infection of primary fibroblasts increased expression of TRAIL-R1, TRAIL-R2 and TRAIL. IFN- γ and TNF potentiated these effects, permitting selective killing of virus-infected cells by down-regulation of TRAIL receptors on the uninfected cells (Sedger et al., 1999). Reovirus-induced apoptosis is

mediated by TRAIL (Clarke et al., 2000). Measles virus (MV) infection of dendritic cells is accompanied by production of functional TRAIL (possibly induced via interferon production), which permits MV-infected DCs to induce apoptosis of activated T lymphocytes and might explain immunosuppression observed in MV infection (Vidalain et al., 2000). Increased expression of FasL and/or TRAIL on HIV-infected T cells, HCMV and measles-virus-infected DCs has been suggested to be another viral immune evasion tactic (counter-attack) aimed at killing infiltrating host CTLs and DCs (Xu et al., 2001). The presence of Ad functions which interfere with death receptor signaling at the earliest time point possible (the encounter of the receptor with its cognate ligand) indicates that FasL/Fas and TRAIL/TRAIL-R interactions are important effector mechanisms of the host immune response to adenovirus infection. The loss of death receptors may function to protect infected cells from cytolysis by CTLs and NK cells which express FasL and TRAIL upon activation ((Benedict et al., 2002).

In addition to Fas and the TRAIL-receptors involved in apoptosis control, E3/10.4-14.5K also down-regulate cell surface expression of the epidermal growth factor receptor (EGFR/erbB1) (Carlin et al., 1989; Tollefson et al., 1991) and to a lesser extent some other structurally related receptor tyrosine kinases (RTK): Infection with virus mutants overexpressing both viral proteins has been reported to cause down-regulation of the insulin receptor and insulin-like growth factor 1 receptor, as well as p185c-neu/erbB2, which is a RTK closely related to the EGFR (Kuivinen et al., 1993). The purpose of EGFR down-regulation early during infection is unknown. One possibility is that it induces constitutively the EGFR mitogenic signal and thereby stimulates cellular metabolism and provides a cell environment that facilitates viral replication. This is conceivable, in view of primary targets of group C Ad infection *in vivo* being primary epithelial cells of the respiratory tract. Such a function might not be needed in rapidly proliferating cultured cells, but might increase virulence *in vivo*. A mitogenic potential has been proposed for a class of poxvirus proteins, which have EGF-like activities (Yarden and Sliwkowski, 2001). But, in contrast to 10.4-14.5K function, these virus-encoded EGF-like ligands cause only limited receptor down-regulation, thereby their mitogenic potency is enhanced relative to their mammalian counterpart. Moreover, 10.4-14.5K-mediated down-regulation occurs independently from intrinsic tyrosine kinase activity of the EGFR suggesting that the mechanism differs from ligand-induced down-regulation of the activated receptor (Hoffman and Carlin, 1994). Down-regulation of the EGFR early after virus infection might be important to limit inflammation. EGF binding to the EGFR stimulates AA release through the phosphorylation of cPLA₂ mediated by MAPK ERK and p38 pathways and also regulates cPLA₂ gene expression (Chepenik et al., 1994). Recently, it has been described that EGF induces gene and protein expression of a cPLA₂ antagonist, known as p11, which can

suppress AA release at later time points after induction (Huang et al., 2002). Thus, EGFR ligation is implicated in the regulation of cPLA₂ activity and AA release.

In summary, many Ad E3 proteins seem to have evolved to inhibit apoptosis and allow viral replication even when infected cells are under immune attack.

1.7 Adenovirus E3/10.4-14.5K

In the struggle between virus and host control over the cell's death machinery is crucial for survival. The E3/10.4-14.5K proteins of subgroup C viruses have been reported to selectively down-regulate plasma membrane receptors involved in apoptosis signaling and growth control. The term down-regulation has originally been invented to describe the process of ligand-induced internalization of activated receptors via coated pits, which involves sorting of receptor-ligand complexes in endosomes followed by receptor degradation in lysosomes (Sorkin and Waters, 1993). This process serves as an important determinant of the intensity and duration of ligand-induced signaling. Therefore, 10.4-14.5K function might be interpreted as a surrogate receptor-ligand interaction aimed at blocking signaling of cell surface receptors by causing their removal from the cell surface and their degradation. In the following structural features of 10.4-14.5K proteins and the characteristics of the process of down-modulation of different types of receptor targets will be summarized.

1.7.1 Biochemical characteristics of 10.4K and 14.5K encoded by subgroup C Ads

Adenovirus E3/10.4K and 14.5K are both integral membrane proteins which associate non-covalently with each other and localize as a complex to the plasma membrane (Fig. 5), (Hoffman et al., 1992b; Stewart et al., 1995). Ad2 10.4K exists as two different isoforms that are visualized as two distinct bands on SDS-PAGE (Tollefson et al., 1990b). One isoform is processed by cleavage of a signal sequence for membrane insertion between Ala-22 and Ala-23 (Krajcsi et al., 1992a). The other isoform represents the uncleaved full-length protein, resulting in a protein with two membrane-spanning regions. Both forms are type 1 transmembrane proteins that are linked by a disulfide-bond formed between cysteine residues (Cys-31) in the extracellular domain (Fig. 5), (Hoffman et al., 1992b; Krajcsi et al., 1992a). The faster migrating isoform seems to be a cleavage product of the long form which retains the second membrane anchor. In wt Ads, processing of the long isoform continues until both bands are equal in abundance, suggesting that they exist as an equimolar complex (Krajcsi et al., 1992a). Formation of a stable complex might also explain, why the cleavage reaction remains incomplete and occurs at a rate much slower than cotranslational signal peptidase cleavage reactions. These properties are inherent to the 10.4K sequence as

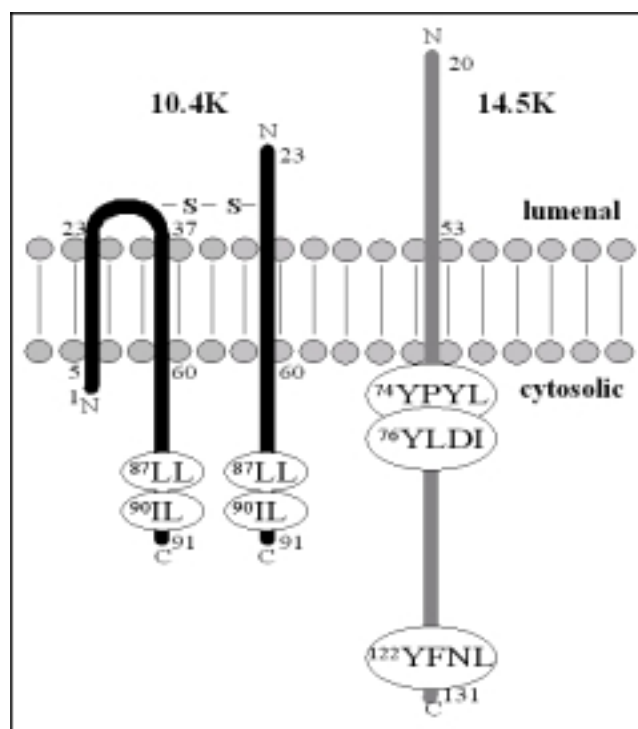


Fig. 5 A model depicting predicted secondary structure and orientation of the Ad2 10.4K and 14.5K proteins in the lipid bilayer

10.4K is shown with both isoforms that are covalently linked by a disulfide bond. Amino acid numbers of the predicted full-length sequences are used to indicate lumenal, transmembrane and cytoplasmic domains. N- and C-termini are designated with N and C, respectively. S-S indicates the proposed disulfide bond formed between strictly conserved cysteine residues at position 31 in the 10.4K sequence. Sequence elements that correspond to the consensus of putative transport motifs are shown in circles. Their sequence is described in single letter amino acid code and the position of the starting residue in the Ad2 10.4-14.5K protein sequences is given.

membrane insertion and the described stoichiometric proteolytic cleavage is reproduced *in vitro* in cell-free translation systems in the presence of microsomes (Krajcsi et al., 1992a). Homologous 10.4K ORFs are found in all subgroups of human adenoviruses and sequence homology is relatively high (35%-72%, average 47.5%, (Burgert et al., 2002)). The predicted amino acid sequences share a length of 91 amino acids, with the exception of subgenus F homologs (Ad40 and Ad41) that have 90 amino acids (see Fig. 8). A putative N-terminal signal sequence and 30-residue transmembrane domain has been predicted for all these homologs (Burgert et al., 2002; Burgert and Blusch, 2000).

The 14.5K protein is a type one transmembrane protein (Fig. 5), (Krajcsi et al., 1992b), with an N-terminal signal sequence for membrane insertion. From infection studies with an Ad2 mutant virus overexpressing the Ad2 version of 10.4K and Ad5 14.5K it was concluded that Ad5 14.5K has mucin-type O-linked oligosacchrides (Krajcsi et al., 1992c) attached to its lumenal domain, but is not N-glycosylated. Whereas 10.4K is not phosphorylated, 14.5K is phosphorylated

on one or two serines in the cytoplasmic domain (Krajcsi and Wold, 1992). Following transient transfection of Ad5 10.4K and 14.5K expression plasmids 14.5K could be shown to be phosphorylated on one site, Ser116, which gave rise to two separate bands of phosphorylated 14.5K (Lichtenstein et al., 2002). Interestingly, in the absence of 10.4K phosphothreonine could additionally be detected in 14.5K (Krajcsi and Wold, 1992), which is reflected by a more pronounced heterogeneity of the banding pattern (Krajcsi et al., 1992c; Tollefson et al., 1990a). The 10.4K protein is not required for O-glycosylation of 14.5K to proceed to a stage where sialic acid is a terminal residue (Krajcsi et al., 1992c). In pulse-chase experiments it could be shown, that with time the fast migrating bands of 14.5K are chased into the top band, which is assumed to represent mainly the fully glycosylated, sialylated and phosphorylated form of 14.5K. (Krajcsi et al., 1992c). The sequence homology between 14.5K proteins of different subgenera is significantly lower (21-50%, average 30%, (Burgert et al., 2002) than that of 10.4K proteins. In addition, the predicted length of the mature 14.5K protein varies from 91 to 127 amino acids (Fig. 8). 10.4K usually coimmunoprecipitates with 14.5K implying that both proteins exist as a complex in infected cells (Tollefson et al., 1991). Moreover, in subgroup C viruses 10.4K and 14.5K have been shown to be translated primarily from the same mRNA, designated mRNA f (Tollefson et al., 1990b; Tollefson et al., 1990a). Both proteins can be synthesized by cell-free translation from this particular mRNA, and 10.4K and 14.5K are over- or underexpressed *in vivo* by the use of virus mutants that over- or underproduce mRNA f, suggesting a direct relationship. Interestingly, the site of signal sequence cleavage in 14.5K varies depending on the presence or absence of 10.4K. In the presence of 10.4K, cleavage occurs predominantly between Cys-18 and Ser-19, whereas with a virus mutant lacking 10.4K it occurred mainly between Phe-17 and Cys-18. In both cases, a minority of molecules was cleaved one or two residues upstream or downstream of the major cleavage site (Krajcsi et al., 1992b). Whereas the Phe-17/Cys-18 site appears disfavored, the Cys-18/Ser-19 cleavage site (compare Fig. 8) is in accord with the (-3,-1) rule for signal sequence cleavage, which states that residues at positions -3 and -1 must be small and neutral for cleavage to occur correctly (Nielsen et al., 1997). By analogy, the closely related Ad2 14.5K protein has been predicted to have a major signal sequence cleavage site at residues Cys-19, Ser-20 (Burgert et al., 2002). The mechanism how 10.4K affects the cleavage site in 14.5K remains unclear.

1.7.2 10.4-14.5K-mediated down-regulation of cell surface receptors

Removal of the epidermal growth factor receptor (EGFR) from the cell surface of infected cells during early infection with subgroup C viruses led to the identification of the 10.4K protein. Its presence was accompanied by endocytosis and degradation of the human EGFR (Carlin et al.,

1989). But initial gene mapping studies did not allow to exclude an additional requirement for 14.5K for this activity, as these were based on virus mutants with deletions within E3 that did not precisely cover individual ORFs and might have caused unpredictable alterations of E3 splicing. In one report using retrovirus-mediated transfer of the 10.4K gene alone, 10.4K was sufficient to reduce EGFR cell surface expression (Hoffman et al., 1990). However, two other groups have clearly demonstrated that in the natural context of adenovirus infection both 10.4K and 14.5K are required to down-regulate the epidermal growth factor receptor (Elsing and Burgert, 1998; Tollefson et al., 1991). These discrepancies are most likely due to the use of different experimental systems and 10.4K may well be overexpressed following retrovirus infection. But the observation that 10.4K alone can induce changes in the trafficking and steady-state localization of the EGFR indicates that there is a direct or indirect association of 10.4K with this receptor. A complex of 10.4K and 14.5K (10.4-14.5K) does not affect the initial synthesis of the EGFR, but reroutes surface EGFR molecules to lysosomes for degradation (Tollefson et al., 1991). Recently, it could be shown by use of a virus mutant overexpressing 10.4K, that 10.4K directly associates with the EGFR in an early endosomal compartment during the process of receptor down-regulation (Crooks et al., 2000). Mechanistic studies demonstrated that adenovirus-induced down-regulation of the EGFR occurs with an internalization rate indistinguishable from the rate of constitutive internalization of unoccupied receptors and independently of EGF binding to the receptor, receptor dimerisation or EGFR tyrosine kinase activity (Hoffman et al., 1992a; Hoffman and Carlin, 1994). Thus, the mechanism of 10.4-14.5K-mediated receptor down-regulation differs in these key characteristics from ligand-induced EGFR down-modulation. Ligand-occupied, kinase-active EGFR dimers are internalized at a rate that is about 10-fold greater than that for receptors unoccupied by ligand (Opresko et al., 1995). Ligand-receptor complexes are rapidly internalized via clathrin-coated pits and subsequently transported to lysosomes for degradation. Cryptic sorting signals in the cytosolic tail of the receptor are unmasked by conformational changes after ligand engagement, receptor activation and autophosphorylation (Chang et al., 1993) (Nesterov et al., 1995a; Nesterov et al., 1995b). But, although the EGFR strongly binds to the μ 2 subunit of the AP-2 complex of clathrin-coated pits via the sequence Y⁹⁷⁴RAL, mutations in this motif which abolish EGFR interaction with AP-2, do not significantly affect internalization of the receptor (Nesterov et al., 1995b; Sorkin et al., 1996) and the EGFR can be internalized in a μ 2-independent manner (Nesterov et al., 1999). Thus, AP-2 binding is not the sole determinant for internalization of the activated EGFR. At present, the molecular mechanism of clathrin-dependent endocytosis of the EGFR is not well-understood. EGFR tyrosine kinase activity is necessary for the initial coated pit recruitment step of endocytosis (Sorkina et al., 2002) and tyrosine phosphorylation of eps15 is

specifically required for ligand-regulated EGFR internalization via clathrin-coated pits (Confalonieri et al., 2000). Several SH2/PTB domain containing proteins, such as c-Cbl, Grb2 and Shc, have been proposed to bind to phosphotyrosines in the cytoplasmic tail of the autophosphorylated EGFR and participate in EGFR endocytosis by recruiting the components of the cellular endocytosis machinery (Jiang et al., 2003; Sakaguchi et al., 2001; Soubeyran et al., 2002; Szymkiewicz et al., 2002) (Wang and Moran, 1996; Waterman et al., 2002). Thus, it appears that multiple redundant mechanisms of EGFR internalization may exist, which are regulated by tyrosine kinase activity of the receptor. Moreover, EGFR signaling leads to activation of the tyrosine kinase Src which may participate in regulation of the EGFR endocytosis by phosphorylation of clathrin (Wilde et al., 1999), dynamin (Ahn et al., 2002), and c-Cbl (Bao et al., 2003; Kassenbrock et al., 2002). The activated EGFR remains phosphorylated and bound to signal transducers Shc, Grb2 and c-Cbl within the endosome suggesting that signaling is not attenuated at the internalization step (Oksvold et al., 2001). Inactivation of the receptor occurs through dissociation of the activating ligand, dephosphorylation of tyrosine residues of the RTK and degradation of both the ligand and the receptor (Gill, 2002). Whereas recycling receptors are confined to the limiting membrane of a late endosomal compartment called multivesicular body (MVB), activated EGFRs accumulate on internal vesicles. When all the recycling receptors have been removed, the mature MVBs fuse directly with the lysosome and EGF-EGFR complexes are rapidly degraded. Tyrosine kinase activity of the EGFR is required for inclusion in internal vesicles (Felder et al., 1990; Futter et al., 2001). EGF-induced accelerated internalization is not sufficient for enhanced degradation of the EGFR, which appears to require distinct sorting signals that mediate endosomal retention (Herbst et al., 1994) or sequestration from the recycling pathway (Opresko et al., 1995). Sequences within the cytoplasmic domain of the EGFR distinct from the kinase domain (Kil et al., 1999; Kil and Carlin, 2000; Kornilova et al., 1996; Opresko et al., 1995) have been shown to enhance degradation of truncated receptors, but these may be inactive in the full-length receptor. So far the importance of potential sorting signals for trafficking of the full-length receptor has only been confirmed for the leucine-based determinant L679L680 (Kil et al., 1999; Kil and Carlin, 2000). Substitution of L679L680 by alanine led to a reduction in ligand-induced receptor degradation due to rapid recycling from early endocytic compartments, but without affecting internalization. How L679L680 may contribute to sequestration of the activated EGFR in late endosomes/lysosomes remains unknown. Recently, c-Cbl an E3 ubiquitin ligase has been shown to catalyze polyubiquitination of the EGFR (Levkowitz et al., 1998; Longva et al., 2002) and thereby regulates lysosomal degradation. Sustained activation of the receptor, to maintain the association with c-Cbl and the ubiquitinated state, is required for directed passage into

MVBs (Longva et al., 2002). At the late endosome TSG101 is involved in sorting ubiquitinated cargo into multivesicular endosomes and *tsg101* mutant cells recycle ligand-bound EGFRs instead of degrading (Babst et al., 2000). Another molecule involved in sorting of EGFRs to lysosomes may be Hrs, which becomes phosphorylated in response to EGF and inhibits lysosomal degradation of the EGFR when overexpressed (Chin et al., 2001; Raiborg et al., 2001). Hrs is recruited to early endosomes through its lipid binding domain FYVE and implicated in MVB formation (Lloyd et al., 2002). It interacts with sorting nexin (SNX)1 in a complex that excludes the EGFR. EGF-induced tyrosine phosphorylation of Hrs may liberate SNX1, which associates with the activated EGFR and enhances the efficiency of lysosomal targeting of the receptor (Kurten et al., 1996). By analogy, 10.4-14.5K may function within endosomes to increase the rate of lysosomal degradation of constitutively internalized EGFR without increasing the rate of receptor internalization.

Several groups have demonstrated that 10.4K and 14.5K are both necessary and sufficient to induce internalization and degradation of the Fas receptor (Shisler et al., 1997) (Elsing and Burgert, 1998; Tollefson et al., 1998). 10.4-14.5K-mediated down-modulation of Fas has been shown to protect cultured cells from Fas-mediated apoptosis independently from other viral functions. Remarkably, down-regulation of Fas also occurs after infection of primary cells (Elsing and Burgert, 1998). The observation that the kinetic of Fas disappearance from the cell surface of infected cells is much more rapid than after inhibition of Fas cell surface transport by Brefeldin A on mock-infected cells, argues in favor of an active rerouting of Fas from the cell surface, rather than a direct transport from the TGN to lysosomes (Elsing and Burgert, 1998). In infected cells the overall levels of Fas are decreased, but this is not due to inhibition of de novo Fas synthesis (Shisler et al., 1997; Tollefson et al., 1998). 10.4-14.5K-induced degradation of Fas can be inhibited by treatment with chloroquine, ammonium chloride or Bafilomycin A₁, which act as inhibitors of lysosomal acidification, and under these conditions Fas accumulates in vesicles staining for lysosome-associated membrane protein 2 (Lamp-2) (Elsing and Burgert, 1998; Tollefson et al., 1998). Recent reports suggest that 10.4-14.5K acts in concert with E3/6.7K to protect infected cells from TRAIL-induced apoptosis (Benedict et al., 2001). 10.4-14.5K is necessary and sufficient to clear TRAIL-R1 from the cell surface and induce degradation of TRAIL-R1 in a Bafilomycin A₁-sensitive late endosomal/lysosomal compartment (Tollefson et al., 2001), but DR5 down-regulation was shown to require E3/6.7K in addition to 10.4-14.5K (Benedict et al., 2001). Interestingly, E3/6.7K is found only in subgroup C viruses (Fig. 4) and therefore, it will be interesting to determine whether serotypes from other subgroups are also capable of down-regulating DR5.

1.8 The cellular protein sorting machinery

Obviously, many immune evasive functions of Ad E3 proteins are based on their capacity to deregulate trafficking of host proteins (Burgert and Blusch, 2000). Interestingly, the E3 region is the only part of the genome that harbors transmembrane proteins, and many of them contain potential sorting motifs in their cytoplasmic tails, which might permit them to exploit the cellular protein sorting machinery to exert their function (Windheim et al., 2003 in press). Examples from other viruses, such as mouse cytomegalovirus glycoproteins gp40 and gp48 (Reusch et al., 1999) (Ziegler et al., 2000) which interfere with the MHC class I pathway of antigen presentation or HIV-1 nef, a versatile adaptor protein that down-regulates CD4 and MHC I surface expression by multiple interactions with the cellular protein sorting machinery ((Blagoveshchenskaya et al., 2002) and references therein), illustrate the importance of the exploitation of the cellular trafficking pathways for virus-host interactions. Therefore, in the following an overview about the principal players involved in intracellular protein trafficking and its regulation is given.

1.8.1 Principles of membrane protein transport

A characteristic feature of eucaryotic cells is their ability to maintain a diverse set of intracellular membrane-bound compartments, which are characterized by distinct protein complements, morphology and lipid composition and carry out specific functions. Although substances can be transported from one membrane-bound compartment to another, their unique identities are not compromised. Apparently, a steady-state is achieved between forward and reverse traffic between donor and acceptor compartments (Mellman and Warren, 2000). For the Golgi compartment and lysosomes also maturation models have been proposed to explain differences between subcompartments, namely between the cis- and trans-Golgi or early and late endosomes, lysosomes.

A fundamental principle of intracellular membrane traffic involves cargo-laden vesicles and their associated regulatory proteins and coat components, which provide the machinery for selection of cargo, membrane deformation and vesicle budding from a donor compartment and fusion with a specific acceptor compartment. The three best understood classes of coated vesicles are: COPII vesicles which mediate ER to ERGIC (ER-Golgi intermediate compartment) traffic, COPI vesicles which direct retrograde traffic from the Golgi to the ERGIC and the ER, as well as anterograde traffic from the ERGIC to Golgi and traffic between Golgi cisternae, and clathrin-coated vesicles, which mediate certain endocytic and post-Golgi vesicular trafficking steps (Barlowe, 2000; Kirchhausen, 2000b), Fig. 6). Membrane proteins are incorporated into transport vesicles upon recognition of intrinsic sorting signals that may either be directly bound by the coat

components (COPI, COPII) or may be recognized by so-called adaptor complexes (AP), which bridge between selected cargo and clathrin. The coats are derived from soluble, cytosolic precursors that are specifically recruited to organelle membranes in a GTP-dependent process. Budding of COPII vesicles at specific ER exit sites requires the small guanosine triphosphatase (GTPase) Sar1p, while COPI is recruited to Golgi membranes by the small GTPase (ADP ribosylation factor) Arf-1 (Barlowe, 2000). Coat assembly leads to deformation of the donor membrane and scission of the budding vesicle. Shortly after formation the coats dissociate from the newly formed transport vesicle freeing the vesicle to fuse with target membrane. Vesicle fusion is accomplished by first tethering the vesicle to a target membrane and subsequent assembly of a tight membrane fusion complex (docking) by pairing of specific SNARE (soluble NSF attachment protein receptors) proteins on the vesicle membrane (v-SNARE) with those on the membrane of the target organelle (t-SNARE) (Chen and Scheller, 2001).

Protein sorting begins early on in the secretory pathway at the level of the ER and may involve recognition of specific ER export signals or retention and retrieval motifs in ER resident proteins which lead to segregation of specific sets of proteins from others. The ER-Golgi-intermediate compartment ERGIC (Fig. 6) seems to be the major site for sorting out proteins for anterograde transport to the Golgi, from those that must be returned to the ER. Trafficking between the ER, ERGIC and the Golgi/TGN complex is mainly accomplished by COPI, COPII coats ((Mellman and Warren, 2000), Fig. 6). Steady-state ERGIC localization of ERGIC-53 appears to be mediated by a C-terminal pair of phenylalanines acting as ER export signal via direct interaction with COPII (Hauri et al., 2000). Sorting motifs implicated in COPI binding and retrograde transport to the ER are C-terminal KKXX and KXXKXX sequences, where K is lysine and X any amino acid (Teasdale and Jackson, 1996). This type of sorting signal is present and functionally active in the cytoplasmic tail of the adenovirus E3/19K protein and contributes to the ER localization of E3/19K (reviewed in Windheim et al., 2003 in press). Specific interaction of E3/19K with MHC class I complexes results in their retention in the ER, whereby the recognition of infected cells by CTLs through MHC class I-mediated presentation of viral peptides is impaired. Additionally, mechanisms related to quality control contribute to ER retention: correct assembly of oligomeric membrane receptors, such as the T cell receptor-CD3 complex is achieved by the presence of single basic or acidic residues within the TMD of individual subunits. Proper pairing of subunits neutralizes charges and allows efficient export (Letourneur and Cosson, 1998). Moreover, chaperones (calnexin, calreticulin) contain ER retrieval or retention motifs and thus trap proteins in the ER until they are correctly folded (Ellgaard et al., 1999).

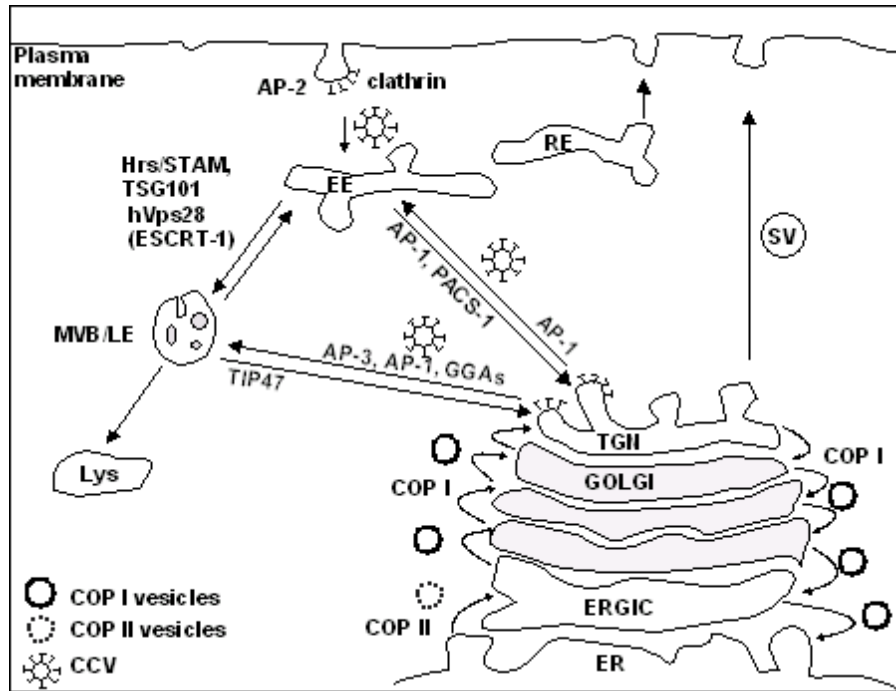


Fig. 6 Overview of the cellular sorting machinery for transport of membrane-associated proteins (non-polarized cells)

Export of membrane proteins out of the ER occurs in COPII vesicles. COPI vesicles are implicated in both anterograde transport from the ERGIC through the Golgi to the TGN and retrograde traffic between the TGN and the ER. From the TGN proteins can reach the plasma-membrane directly in secretory vesicles, or indirectly through late endosomes (LE) and/or early endosomes (EE), presumably by incorporation into clathrin-coated vesicles (CCV) involving the clathrin adaptor complexes AP-1, AP-3 or GGAs. Early endosomes can be reached by endocytosis through clathrin-coated pits, involving AP-2. Proteins may exit EE for transport to the cell surface by two pathways: 1.) by inclusion into recycling endosomes or 2.) recycling to the TGN likely by incorporation into CCV mediated by PACS-1 and AP-1. At the early endosome the formation and segregation of cargo into MVB for transport into lysosomes (Lys) is initiated, a process involving ubiquitin-recognizing proteins, such as Hrs/STAM and an ESCRT-1-like complex. Lysosomal avoidance signals in cargo proteins may be recognized by TIP47 at the late endosome. For abbreviations and more details refer to text.

Transit through the Golgi complex involves passage through 3-5 Golgi stacks (cis, medial, trans). The cisternal maturation model proposes that secretory proteins transit the Golgi in cisternae that mature by the continuous retrograde transport of Golgi resident enzymes in vesicles (Allan and Balch, 1999). Additionally, COPI vesicles may mediate a fast anterograde transport of secretory proteins through Golgi-stacks ((Pelham and Rothman, 2000), Fig. 6). Golgi-resident glycosyltransferases, SNAREs and some viral proteins are sorted within the Golgi by their TMD, which is on average five residues shorter than that of plasma membrane proteins and therefore these proteins are excluded from the sphingolipid, cholesterol-rich membranes (rafts) involved in Golgi protein export (Munro, 1998). At the TGN proteins are sorted into specialized secretory vesicles, either for transport to the plasma membrane or into endosomes/lysosomes. In polarized

cells the TGN is also the sorting station for proteins that are targeted to the apical or basolateral membrane (Keller et al., 2001). In non-polarized cells trafficking to the cell surface is believed to occur by default and coat proteins of secretory vesicles have not been identified yet. Most other trafficking pathways between TGN, endosomes/lysosomes and the plasma membrane are mediated by clathrin-coated vesicles (CCVs) which are also implicated in basolateral transport in polarized cells (Heilker et al., 1999). Coats for apical transport are still unknown.

1.8.2 Clathrin-coated vesicle formation: Adaptor complexes and sorting signals

Clathrin is a heterohexameric complex composed of three heavy chains and three light chains. Heavy chains are joined at their C-termini, which confers the three-legged appearance of a triskelion (Kirchhausen, 2000a). Multimerization of triskelia into polyhedral cages is regulated by a number of clathrin-binding proteins (Dell'Angelica, 2001). Among them the adaptor protein complexes (APs) have been characterized most extensively. APs are heterotetramers with a molecular mass of 250-300 kDa composed of two large subunits ($\gamma, \alpha, \delta, \epsilon$ and $\beta 1-4$) one medium subunit $\mu 1-4$ and a small subunit σ (Boehm and Bonifacino, 2001). For several subunits cell-type specific isoforms have been identified. The different subunits perform different functions. The β subunits are particularly important for clathrin-binding and a five amino acid consensus sequence (clathrin-box) has been identified (Dell'Angelica, 2001; Kirchhausen, 2000a). The α and γ subunits are known to interact with regulatory/accessory proteins involved in clathrin-coated vesicle (CCV) formation (Jarrowse and Kelly, 2000; Owen et al., 1999; Traub et al., 1999). The μ and β subunits have been implicated in cargo selection (see below). Directed transport is achieved by selective association of different adaptors to distinct donor membranes, and specific recognition of cargo proteins by APs mediates sequestration of cargo in a specific type of transport vesicle for delivery to its intermediate or final destination (Fig. 6).

Four APs are distinguished according to their composition (AP-1 $\gamma\sigma 1\beta 1\mu 1$, AP-2 $\alpha\sigma 2\beta 2\mu 2$, AP-3 $\delta\sigma 3\beta 3\mu 3$, AP-4 $\epsilon\sigma 4\beta 4\mu 4$) and localization within the cell ((Boehm and Bonifacino, 2001; Kirchhausen, 1999; Robinson and Bonifacino, 2001), Fig. 6). AP-1 localizes to the TGN and endosomes. AP-1 is implicated in traffic directly from the TGN to endosomes (Heilker et al., 1999), and has been detected in coated buds of the TGN, containing mannose-6-phosphate receptors (MPRs). MPRs act as commuters between the TGN and the endosomal/lysosomal system for delivery of lysosomal hydrolases to endosomes. However, in mammalian cells that lack functional AP-1 MPRs accumulate in early endosomes suggesting a major role of AP-1 in early endosome-Golgi recycling (Black and Pelham, 2001; Meyer et al., 2000;

Meyer et al., 2001). In polarized epithelial cells AP-1 with its μ 1B subunit directs basolateral sorting at the TGN (Folsch et al., 1999). AP-3 is found at the TGN and a peripheral endosomal compartment and has been shown to be involved in the sorting of lysosome-associated membrane proteins (Lamp-1 and Limp-II) directly from the TGN to lysosomes (Dell'Angelica et al., 1999; Le Borgne et al., 1998). AP-2 is the only adaptor known to associate with the plasma membrane and directs endocytosis (Bonifacino and Traub, 2003). AP-2 might also participate in the budding of clathrin-coated vesicles in a retrograde trafficking pathway out of the lysosomal compartment (Arneson et al., 1999). For AP-1 and AP-2 the association with clathrin-coated vesicles has been demonstrated, whereas AP-3 vesicles appear not to require clathrin, and AP-4, which has no clathrin-binding motif in its β 4 subunit, is a component of a non-clathrin coat at the TGN. AP-4 may be implicated in basolateral sorting at the TGN (Bonifacino and Traub, 2003).

At the TGN and within the endosomal/lysosomal system, the membrane association of APs and coat components requires the activity of the small GTP-binding proteins of the ARF family. ARFs themselves also cycle between cytosol and membranes in a process that in turn is regulated by guanine nucleotide exchange factors (GEFs) and GTPase activating proteins (GAPs). Exchange of GTP for GDP in ARFs induces a conformational change that increases ARFs affinity for membranes, whereas activation of GAP triggers vesicle uncoating. The small GTP binding protein Arf-1 is essential for TGN association of AP-1 (Zhu et al., 1999), membrane association of AP-3 (Ooi et al., 1998) and AP-4 (Boehm et al., 2001). AP-2 is an exception in that its association with membranes is not regulated by ARFs, but rather requires synaptotagmin for nucleation of endocytic CCVs (Takei and Haucke, 2001). Additionally, coated vesicle fission at the plasma membrane requires the GTPase dynamin (Marsh and McMahon, 1999).

Another class of small GTP binding proteins, the Rab GTPases, coordinate consecutive stages of transport, such as vesicle formation, vesicle movement along cytoskeletal filaments and tethering of vesicles to their target compartment (reviewed in (Zerial and McBride, 2001)). Rab effectors, such as p115 in the Golgi and EEA1 involved in endosomal fusion, act as so-called tethering factors to confer targeting specificity to the vesicles (Pfeffer, 1999) and regulate the formation of SNARE complexes (Chen and Scheller, 2001). Therefore, Rab proteins are key determinants of compartmental specificity in vesicular membrane transport.

Incorporation of membrane-associated proteins into transport vesicles relies on sorting information contained within short peptide motifs facing the cytosol. Three distinct sorting signals for incorporation into CCVs have been identified: NPXY, YXX Φ (where X is any amino acid and Φ denotes an amino acid with a bulky hydrophobic side-chain (L, F, V, I, M) and

dileucine (LL) (Bonifacino and Traub, 2003). Dileucine (LL) motifs may be constituted by a pair of two leucines, but one of the leucines may also be substituted for by another bulky residue (I, V, M, F). Whereas NPXY signals mediate only rapid internalisation from the plasma membrane, YXX Φ and LL motifs are the most frequent sorting motifs that direct trafficking in the TGN and endosomal/lysosomal system.

YXX Φ motifs binding has been mapped to the μ subunits of AP complexes (Aguilar et al., 2001; Ohno et al., 1998). The crystal structure of a complex formed between the μ 2 subunit and a peptide containing the YXX Φ motifs of TGN38 and the EGFR revealed that Y and Φ are key determinants of the interaction as they fit into two hydrophobic pockets (Owen and Evans, 1998). Recently, the binding site for the FDNPVY motif in the LDL receptor has also been mapped to the μ 2 subunit, but at a site distinct from the YXX Φ binding site (Boll et al., 2002). It is currently controversial whether dileucine motifs are also recognized by the μ subunits (Bremnes et al., 1998) (Rodionov and Bakke, 1998) or the β subunits (Rapoport et al., 1998). Both YXX Φ and LL signals can be recognized by AP-1, AP-2 and AP-3, although sorting by dileucine motifs does not compete with sorting via YXX Φ motifs (Marks et al., 1996). Strikingly, YXX Φ and LL motifs both function in sorting processes at the TGN, in endosomes/lysosomes and basolateral transport. In a single cargo molecule these sorting signals can be found in multiple copies or in combination, e.g. invariant chain Ii (Kongsvik et al., 2002), MPR46 (Tikkanen et al., 2000). Therefore, it remains a puzzling question how APs can distinguish between different YXX Φ and LL motifs for cargo selection. At the TGN for example AP-1 and AP-3 have to recognize a distinct subset of cargo molecules containing YXX Φ and LL motifs for CCV-mediated transport to endosomes/lysosomes, from other YXX Φ or LL containing proteins destined to reach the plasma membrane for subsequent endocytosis via AP-2. An example is the YTRF sorting signal of the transferrin receptor which interacts selectively with μ 2 but not μ 1 (Ohno et al., 1995). By surface plasmon resonance analysis LL motifs of limp-II and tyrosinase have been found to exhibit a higher affinity for purified adaptor protein complex AP-3, than AP-1 or AP-2 (Honing et al., 1998). Some μ chains seem to preferentially bind to selected subsets of YXX Φ signals. By a combinatorial library approach for the interaction of μ 2 with peptides a YXRL consensus emerged (Boll et al., 1996). In a yeast-2-hybrid screen mutations in the SDYQRL of TGN38 were found to differentially affect the interaction with μ 1 and μ 2 subunits, suggesting an implication of amino acids surrounding the critical tyrosine in binding to different types of adaptors (Ohno et al., 1996). Moreover, the relative position of the signal within the cytoplasmic tail is a critical feature that distinguishes lysosomal targeting signals from internalisation signals (Bonifacino and Traub, 2003).

Interestingly, the consensus lysosomal targeting signal (GYXX Φ) of LAMPs (lysosome-associated membrane proteins) appears to depend on the presence of both glycine and tyrosine (Honing and Hunziker, 1995) and a narrowly restricted distance (7 residues) from the lipid bilayer (Rohrer et al., 1996). In a yeast two-hybrid screen using a combinatorial library of XXXYXX Φ peptide sequences a considerable specificity overlap, but also small variations in the sequence requirements for binding to different μ 1-3 and μ 4 subunits were observed (Aguilar et al., 2001; Ohno et al., 1998). This might reflect the situation *in vivo* in that in many cases internalisation signals and basolateral targeting overlap but are not identical (Heilker et al., 1999). Moreover, mutations that impair lysosomal targeting may have minimal effects on internalisation (Rohrer et al., 1996). In good correlation the μ 2 chain recognizes a larger array of tyrosine-based signals than μ 1, μ 3 (Ohno et al., 1998).

For dileucine type motifs characterized to date a consensus sequence was proposed with a negatively charged residue (aspartate (D), glutamate (E) or phosphoserine) at position -4 to -5 ([DE]XXXL[LI]) from the first leucine (Bonifacino and Traub, 2003; Kirchhausen, 1999). An acidic residue in position -4 or -5 (E, D) was required for internalisation of the invariant chain (Pond et al., 1995) and both the DDQRDLI and NEQLPML signals of Ii bind to AP-1 and AP-2, but not detectably to AP-3 (Hofmann et al., 1999). In contrast, the DERAPLI signal of LimpII binds to AP-3 but not to AP-1 or AP-2 (Honing et al., 1998). By surface plasmon resonance it could be shown that a DE pair in position $-4,-5$ from the LI sorting motif in LimpII was required for its interaction with AP-3 (Honing et al., 1998). In good correlation, by immunofluorescence analysis the glutamic acid at position -4 was shown to be necessary for efficient intracellular sorting of LimpII to lysosomes, but dispensable for internalisation (Sandoval et al., 2000). Thus, similarly to YXX Φ signals, the fine specificity of interactions of [DE]XXXL[LI]-type signals may be dictated by the X residues, e.g. proline in -1 favors AP-3 binding (Rodionov et al., 2002). Moreover, recognition of several dileucine type motifs seems to be positively regulated by serine phosphorylation (e.g. CD4 (Shin et al., 1991), CD3 γ (Dietrich et al., 1994). For the function of the phosphorylation-dependent LL motif in CD3 γ a minimum spacing of 7 amino acids between the phosphorylated serine and the transmembrane domain was required, and for the constitutively active, phosphorylation-independent dileucine-type motif a minimal spacing of 6 residues relative to the lipid bilayer was required for function (Geisler et al., 1998). In summary, sequence and positional requirements seem to exist for recognition of YXX Φ - and LL-motifs by different APs.

Recently, a distinct subset of dileucine-based sorting signals, composed of a DXXLL consensus sequence has been identified. The D residue is generally found in the context of a

number of acidic residues, therefore this type of motif has been termed acidic cluster dileucine motif (reviewed in (Bonifacino and Traub, 2003)). Acidic cluster dileucine type motifs are specifically recognized by another type of clathrin-adaptor, the GGA proteins (Golgi-associated, γ -ear-containing, ARF binding proteins). GGAs perform similar functions like the APs, but consist of only a single polypeptide chain. Three GGAs are expressed in mammalian cells and localize to the TGN in an ARF-dependent manner. The crystal structures of VHS domains (identified in VPS27, Hrs, STAM) of GGA1 and GGA3 in complex with peptides containing the acidic cluster sorting sequences have been solved, revealing that both acidic cluster and dileucine form key contacts with the VHS domain, and thus determine the affinity for recognition by GGAs and allow cargo selection for transport ((Kirchhausen, 2002)and references therein). GGAs recognize acidic cluster dileucine motifs within MPRs (mannose-6-phosphate receptors) and sortilin and mediate TGN export (Nielsen et al., 2001; Puertollano et al., 2001; Zhu et al., 2001). It appears that in yeast GGAs and AP-1 are associated with distinct populations of CCVs budding from the TGN (Black and Pelham, 2001; Hirst et al., 2001), and GGAs may be responsible for traffic from the Golgi to late endosomes, but not to early endosomes (Black and Pelham, 2000). In mammalian cells GGAs have been described to assist in packaging MPRs in AP-1 containing vesicles at the TGN (Doray et al., 2002).

1.8.3 Sorting within endosomes for return to the TGN or transport to lysosomes

Lysosomal avoidance and other sorting signals that are implicated in retrieval of proteins from the plasma membrane and endosomes back to the TGN have been identified. TGN localization of furin and the cI-MPR seems to involve a cytosolic protein named PACS-1 (phosphofurin acidic cluster sorting protein 1) (Wan et al., 1998). PACS-1 specifically recognizes acidic clusters on cargo proteins in a casein-kinase II phosphorylation-dependent manner and physically interacts with AP-1 and AP-3, but not with AP-2. Therefore, it has been suggested to selectively connect the cytosolic adaptor to acidic cluster sorting signals in cargo molecules and direct TGN localization of these proteins (Crump et al., 2001). The retrieval of MPR46 from late endosomes to the TGN requires a pair of aromatic amino acids (FW) (Schweizer et al., 1997) that is recognized by TIP47 (tail-interacting protein of 47 kD) and acts as a lysosomal avoidance signal (Diaz and Pfeffer, 1998). TIP47 also specifically binds to the cI-MPR despite the absence of an FW sequence, and the intracellular distribution of TIP47 is compatible with a role in retrieval of MPRs from late endosomes (Bonifacino and Traub, 2003).

Within endosomes proteins destined for degradation in lysosomes are incorporated into the internal vesicles of a late endosomal compartment, which has the appearance of a

multivesicular body (MVB). MVB formation is regulated by lipid partitioning and a protein machinery that controls the process of inward vesiculation (Piper and Luzio, 2001). Studies from yeast suggest that ubiquitin might function as a sorting tag for sequestration of cargo in interior vesicles. In animal cells, transferrin receptors with an in-frame ubiquitin at the N-terminus are not recycled to the surface as efficiently as the wild-type receptor (Raiborg et al., 2002) and cells expressing ubiquitination-defective EGFR display elevated EGFR recycling at the expense of receptor degradation (Waterman et al., 2002). Therefore, it has been suggested that ubiquitin participates in partitioning molecules away from recycling cargo. A high density of UIM (ubiquitin-interacting motif)-bearing endocytic proteins on endosomal structures, as e.g. Hrs (hepatocyte growth factor-regulated tyrosine kinase substrate), can concentrate ubiquitinated cargo at that site (Raiborg et al., 2002). Recently, Hrs, signal-transducing adaptor molecules (STAM) and eps15 have been proposed to form a clathrin-associated multivalent ubiquitin-binding complex on early endosomes that might sequester ubiquitinated membrane proteins ((Bache et al., 2003), Fig. 6) and/or assemble the machinery for inward vesiculation. Hrs might be required to recruit ESCRT-1 (endosomal sorting complex required for transport), composed of Vps23, 28 and 37 to endosomal membranes, a complex which is involved in sorting of ubiquitinated cargo into MVBs in yeast (Katzmann et al., 2001; Raiborg et al., 2002). In the absence of the human ortholog of Vps23, the tumor suppressor gene TSG101, internalized ligand-activated EGFR escapes degradation and is recycled to the plasma membrane (Babst et al., 2000; Bishop et al., 2002).

1.9 Putative transport motifs within Ad2 10.4-14.5K

As 10.4-14.5K are both integral membrane proteins and function to remove important host recognition molecules from the cell surface by rerouting them into lysosomes, the question was addressed whether 10.4-14.5K exploit the cellular protein sorting machinery to bring about down-regulation of plasma membrane receptors. Close inspection of the Ad2 10.4-14.5K sequence revealed that both 10.4 and 14.5K contain sequence elements within their cytoplasmic tails that conform to the consensus of putative transport motifs: a conserved dileucine motif in 10.4K (L⁸⁷, L⁸⁸ in Ad2 10.4K) and 3 YXXΦ motifs in 14.5K (Fig. 5). To evaluate their functional significance *in vivo* the critical tyrosines Y74, Y76 and Y122, and leucines (LL^{87,88}) of these motifs were replaced by alanines (Lindberg, unpublished). Mutations were introduced in plasmids encoding the entire E3 region of Ad2 and stable E3 transfectants of 293 cells were selected with G418. Transfectant clones expressing wt (E3-45) or mutant 10.4-14.5K proteins (designated 10.4LL/AA, 14.5Y⁷⁴A, Y⁷⁶A and Y¹²²A, respectively). with an intracellular E3/19K content (Fig. 7A, white bars) and an HLA reduction (Fig. 7A, black bars) equivalent to E3-45 cells were selected for FACS analysis of

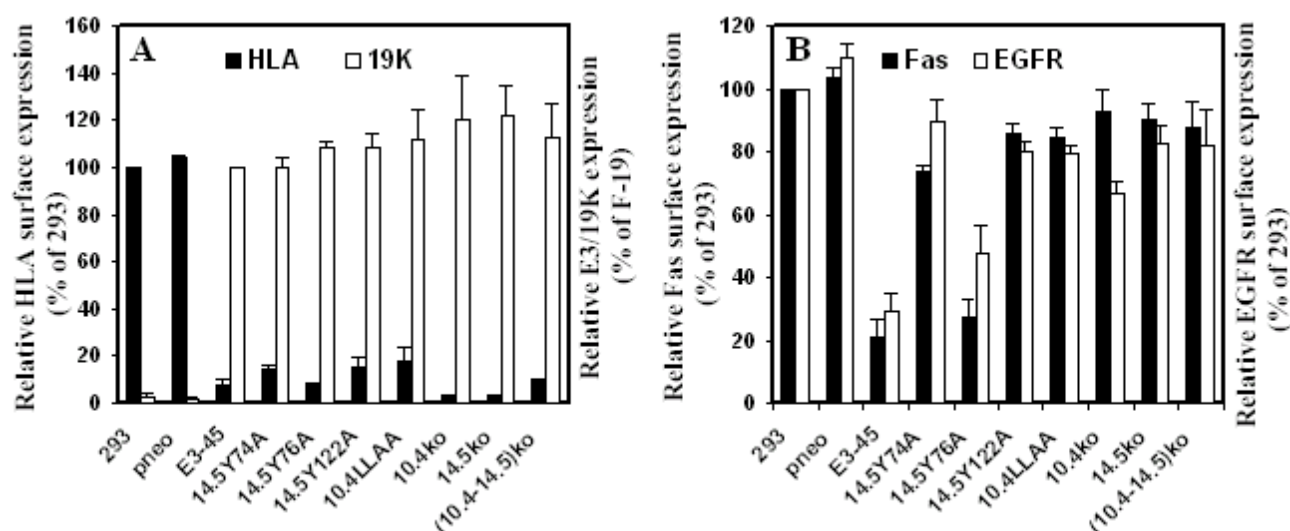


Fig. 7 Fas and EGFR surface expression on E3+ 293 cells is restored when either the 10.4LL motif or YXX Φ motifs in position Y74 or Y122 of Ad2 14.5K are mutated

(A) Relative expression of intracellular E3/19K (in the presence of 0,1% saponin, mAb Tw1.3) and cell surface HLA (mAb W6/32), as detected by FACS analysis of 293 cells and its E3+derivatives. **(B)** Relative cell surface expression of 10.4-14.5 target proteins Fas (mAb B-G27) and EGFR (mAb 528), respectively. FITC-labeled goat anti-mouse IgG (SIGMA, Munich, Germany) was used as secondary antibody. After deduction of the background staining obtained with the secondary antibody alone, the mean value of fluorescence (MVF) for HLA, Fas and the EGFR of each cell clone was related to that of 293 cells, which was set to 100%. The 19K MVFs were related to E3-45 cells, a representative clone of 293 cells expressing wild-type E3 proteins. Bars denote the mean value calculated from at least five measurements with three clones from each transfection. Error bars represent the standard error SEM. pneo designates 293 cells transfected with pSV2-neo^r. 10.4ko (clone 293E3-10.4*-2), 14.5ko (clone 293E3-14.5*8) (Elsing and Burgert, 1998), and 10.4-14.5ko cells are mutant E3 transfectants which do not express either 10.4, 14.5 or both.

Fas and EGFR surface expression (Burgert and Kvist, 1985; Elsing and Burgert, 1998). Wild-type 10.4-14.5K proteins expressed by E3-45 cells reduce Fas and EGFR surface expression by 70-80% relative to 293 cells. This modulating capacity is largely retained in cells expressing the 14.5Y⁷⁶A mutant which exhibit about 10% higher Fas and EGFR levels as compared to E3-45 cells. By contrast, cell surface expression of Fas and the EGFR on 293 E3+ cells is almost completely restored when either the LL motif of 10.4K or starting residues Y74 and Y122 of 14.5K YXX Φ motifs are replaced by alanines. Thus, three mutations severely suppress the function of the 10.4-14.5 complex, resulting in receptor expression levels similar to those seen for 10.4 and 14.5 knock-out cells, which are 293 E3 transfectants that lack expression of either 10.4 (10.4ko), 14.5 (14.5ko) or both ((10.4-14.5)ko). Small differences exist regarding the effectiveness of the different mutations. For example, Fas levels were not fully reconstituted upon mutation of Y74 and 14.5 alone (in 10.4ko) which may indicate some residual activity towards Fas and the EGFR (Elsing and Burgert, 1998). In sum, two tyrosines in 14.5K at position Y122 and Y74 and the dileucine sequence in 10.4K of Ad2 have been shown to be of crucial functional importance *in vivo*, whereas

Y76 does not seem to be critical for 10.4-14.5 function. But it remained unknown how these residues affect the mechanism of receptor down-modulation. As they are part of putative transport motifs it should be explored whether these critical residues modify intracellular trafficking of 10.4-14.5K and constitute transport signals that function to connect 10.4-14.5K with the cellular protein sorting machinery.

1.10 Aims of this study

The above presented data (from J. Lindberg) demonstrated that residues within putative transport motifs in 10.4K and 14.5K are essential for 10.4-14.5K-mediated down-regulation of Fas and the EGFR in stable E3-transfectants. It remained unclear, however, whether they function indeed as transport motifs or have other essential roles. Therefore, the primary aim of this study was to explore whether these critical residues modify intracellular trafficking of 10.4-14.5K and constitute transport signals which can be recognized by adaptor protein complexes. A prerequisite for such an investigation is that transport of 10.4-14.5K can be directly monitored. This should be achieved by tagging the extracellular domain of 14.5K and quantitative measurement of cell surface expression. In addition, a suitable expression system should be developed to compare the intracellular distribution of wt and mutant proteins by immunofluorescence analysis. On the other hand, effects of the mutation on the stability of the proteins or 10.4-14.5K complex formation have to be excluded. Secondly, to complete the picture the role of additional potential transport motifs that have not been examined yet should also be studied by mutational analysis. Third, the functional defects seen in stable transfectants raise the question whether these deficiencies can also be observed in the viral context. Therefore it should be attempted to incorporate the mutations into the viral genome. This would also allow to extend the analysis to infected primary cells. It will be of particular interest to examine whether these mutations also disrupt down-regulation of other 10.4-14.5K target proteins, namely the TRAIL-receptors. Thereby, it should be possible to find out whether the mechanism underlying down-regulation of plasma membrane receptors by the 10.4-14.5K is the same for all target molecules.

A further aim was to investigate the role of strictly conserved amino acids in 14.5K for functional activity. As Ad4 infection does not result in the down-regulation of Fas, EGFR and TRAIL-R2, but solely modulates TRAIL-R1, this differential activity can be exploited to explore the molecular basis of target specificity of 10.4-14.5K proteins. As a first attempt to find out whether or not the Ad4 10.4-14.5K proteins are responsible for the altered target specificity of Ad4, the Ad4 10.4-14.5K genes should be introduced into the Ad2 background which is known to allow full target modulation.

Materials and Methods

2.1 Materials

Chemicals

Acetic Acid	Roth, Karlsruhe, Germany
Acrylamide/Bisacrylamide 29:1 (Protogel)	National Diagnostics, Atlanta, USA
Agar for plates	Invitrogen, Karlsruhe, Germany
Agarose (low melting point, SeaPlaque)	Biozym, Hess. Oldendorf, Germany
Agarose type I	Sigma, Munich, Germany
Ammonium persulfate (APS)	Sigma, Munich, Germany
Ampicillin (Ap)	Roche Diagnostics, Mannheim, Germany
Bacto yeast extract	Invitrogen, Karlsruhe, Germany
Bacto trypton	Difco Lab., Detroit, MI, USA
Bafilomycin A1 (Baf A1)	Sigma, Munich, Germany; Baf A1 was dissolved in DMSO, 100 μ M aliquots were stored at -20°C
Blue Dextran (50 mg/ml)/EDTA (25 mM)	Perkin Elmer, Vaterstetten, Germany
Boric acid	Roth, Karlsruhe, Germany
Bromophenol blue	Serva, Heidelberg, Germany
BSA (bovine serum albumin)	Sigma, Munich, Germany
Chloramphenicol (Cm)	Sigma, Munich, Germany
Coomassie brilliant blue R-250	Bio-Rad, Munich, Germany
Digitonin high purity	Calbiochem, Bad Soden, Germany
Dithiothreitol (DTT)	Roth, Karlsruhe, Germany
dNTPs	Roche Diagnostics, Mannheim, Germany
Dulbecco's modified Eagle's medium (DMEM)	Invitrogen, Karlsruhe, Germany
Ethanol (EtOH)	Riedel-de Haën, Seelze, Germany
Ethidium bromide	Sigma, Munich, Germany
Ethylendiamintetraacetate disodium salt(EDTA)	Roth, Karlsruhe, Germany
Fetal calf serum (FCS)	Roche Diagnostics, Mannheim, Germany
Formamide	Sigma, Munich, Germany
Ficoll (type 400)	Amersham Pharmacia, Freiburg, Germany
Geneticin disulfate salt (G418)	Invitrogen, Karlsruhe, Germany
Glycerol	Roth, Karlsruhe, Germany
Glycine	Serva, Heidelberg, Germany
HEPES	Invitrogen, Karlsruhe, Germany
Histogel mounting medium	Linaris, Wertheim-Bettingen, Germany
Hygromycin B	Calbiochem San Diego, CA, USA
Iodacetamide	Sigma, Munich, Germany
Isopropanol	Riedel-de Haën, Seelze, Germany
Kanamycin(Km)	Serva, Heidelberg, Germany
L-arabinose	Sigma, Munich, Germany
Leupeptin	Sigma, Munich, Germany
L-glutamine	Invitrogen, Karlsruhe, Germany
Paraformaldehyde	J.T.Baker B.V., Deventer, Holland
Penicillin-Streptomycin	Invitrogen, Karlsruhe, Germany
Phenol/chloroform	Roth, Karlsruhe, Germany
Phenylmethylsulfonfluoride (PMSF)	Roche Diagnostics, Mannheim, Germany
Phosphate buffered saline (liquid) Dulbecco's	Invitrogen, Karlsruhe, Germany
Phosphate buffered saline (powder)	Biochrom KG, Berlin, Germany
Ponceau S	Sigma, Munich, Germany

Protein A Sepharose CL-4B	Amersham-Pharmacia, Freiburg, Germany
RPMI1640 w/o Cys/Met	Invitrogen, Karlsruhe, Germany
Saponin	Calbiochem, Bad Soden, Germany
Scintillator cocktail (Aquasafe 300 plus)	Zinsser, Frankfurt, Germany
[35S]-cysteine/methionine (Promix)	Amersham-Pharmacia, Freiburg, Germany
SeaPlaque agarose	FMC bioproducts, Rockland, Maine, USA
Sodium acetate	Riedel-de Haën, Seelze, Germany
Sodium azide	Serva, Heidelberg, Germany
Sodium chloride	Riedel-de Haën, Seelze, Germany
Sodium hydroxid	J.T.Baker B.V., Deventer, Holland
Sucrose	Sigma, Munich, Germany
Tetramethylethyldiamin (TEMED)	Amersham-Pharmacia, Freiburg, Germany
Triton X-100	Serva, Heidelberg, Germany
Trypsin inhibitor	Sigma, Munich, Germany
Urea	Roth, Karlsruhe, Germany
Xylene cyanole FF	Fluka, Seelze, Germany
All other chemicals were purchased from Merck, Darmstadt, Germany	

Additional materials

Autoradiography films BioMaxMR	Eastman-Kodak, Rochester, USA
Cell culture plastic ware	Greiner, Nürtingen, Germany
	Nunc, Wiesbaden, Germany
	Falcon/Becton Dickinson, Heidelberg, Germany
Electroporation cuvettes (2mm, 4mm)	BioRad, Munich, Germany
Glass plates (round, 12 mm Ø)	Roth, Karlsruhe, Germany
Glass slides	Marienfeld, Bad Mergentheim, Germany Hybond
ECL Nitrocellulose membranes	Amersham-Pharmacia, Freiburg, Germany
Sterile filter units	Millipore, Bradford, MA, USA

Cell lines

A549	human lung epithelial carcinoma (American Type Culture Collection (ATCC): CCL-185)
293	human embryonic kidney cell line (ATCC: CRL-1573), established by transformation with Ad5 DNA, expressing Ad5 E1A and E1B genes (Graham et al., 1977).
SeBu	primary foreskin fibroblasts (Elsing and Burgert, 1998)
SV80Fas	human fibroblast cell line transformed with SV40 large T antigen and overexpressing the human Fas receptor (Rensing-Ehl et al., 1995)
293 E3/F14.5+	stable cell lines expressing wt (F-19, F-8, F-16), kindly provided by A. Elsing, University of Munich) or mutant 10.4K and FLAG-14.5K proteins (this study), established by transfection of wt or mutant pBSΔX-E3/F14.5 and pSV2-neo ^r , as described in Materials and Methods. Clone LL-11, a representative clone of pBSΔX-E3/10.4LL-F14.5 transfectants, was kindly provided by M. Löfqvist, University of Munich.
293 E3+	stable cell lines expressing wt (E3-45), kindly provided by A. Elsing, University of Munich) or mutant 10.4LLAA and 14.5K Y74A, Y76A, Y122A proteins (kindly provided by Johan Lindberg, University of Munich), established by transfection of wt or mutant pBSΔX-E3 and pSV2-neo ^r .

10.4ko	293 E3+ mutant cell line lacking expression of 10.4K, (Elsing and Burgert, 1998)
14.5ko	293 E3+ mutant cell line lacking expression of 14.5K, (Elsing and Burgert, 1998)
10.4-14.5ko	293 E3+ mutant cell line, lacking expression of 10.4K and 14.5K, kindly provided by J. Lindberg, University of Munich
pneo	293 cells transfected with pSV2-neo ^r
A549 (10.4 and/or F14.5)+this study	

Viruses

Ad2	ATCC: VR-846
Ad4	strain RI-67, ATCC: VR4
Ad2/F14.5	kindly provided by Zsolt Ruzsics, Max-von-Pettenkofer Institute, Gene Center, Munich, Germany
Ad2/10.4-14.5ko	kindly provided by Zsolt Ruzsics and Susanne Obermaier, Max-von-Pettenkofer Institute, Gene Center, Munich, Germany
Ad2/10.4ko-F14.5	this study
Ad2/14.5ko	this study
Ad2/F14.5Y122	kindly provided by Zsolt Ruzsics, Max-von-Pettenkofer Institute, Gene Center, Munich, Germany
Ad2/F14.5Y74	this study
Ad2/10.4LL-F14.5	this study
Ad2/Ad4-10.4 #12-1	this study
Ad2/Ad4-14.5 #7-1	this study
Ad2/Ad4-14.5 #3-8	this study
Ad2/Ad4-10.4-14.5 #7-4	this study
Ad2/Ad4-10.4-14.5 #16-1	this study

Bacterial strains

DH5 α	Invitrogen, Karlsruhe, Germany
DH10B	Invitrogen, Karlsruhe, Germany
RP-12	DH10B containing pUC19RP12, kindly provided by Zsolt Ruzsics, Max-von-Pettenkofer Institute, Gene Center, Munich, Germany
B53 $\alpha\beta\gamma$	DH10B containing pBAD $\alpha\beta\gamma$ and pAd2-BAC, kindly provided by Zsolt Ruzsics, Max-von-Pettenkofer Institute, Gene Center, Munich, Germany

Plasmids

pA4E3	provided by Zsolt Ruzsics, Max-von-Pettenkofer Institute, Gene Center, Munich, Germany. The E3 region containing <i>Hind</i> III, <i>Bcl</i> I-DNA fragment (map units 71.3-86.9) of Ad4 (strain RI-67, ATCC VR4) was inserted into LITMUS 28 cloning vector (New England Biolabs, Frankfurt, Germany). The Ad4 E3 sequence was determined and submitted to GenBank (AF361223).
pBAD $\alpha\beta\gamma$	(Zhang et al., 1998b)
pBluescriptII (KS+)	Stratagene, Amsterdam, The Netherlands
pBS Δ X-E3	(Elsing and Burgert, 1998); pBS Δ X-E3 was generated using plasmid pBS-E3, a derivative of pBluescript II KS (Stratagene, Amsterdam, The Netherlands) containing the <i>Eco</i> RVc fragment of Ad2, that encompasses the entire E3 region of Ad2 (Korner et al., 1992). pBS-E3

	was cleaved with <i>KpnI</i> and <i>ClaI</i> to eliminate the <i>XhoI</i> site 5' of the <i>EcoRV</i> cloning site, yielding pBSΔX-E3 after Klenow treatment and blunt-end religation (Elsing and Burgert, 1998).
pBSΔX-E310.4*	<i>XhoI</i> cleavage of pBSΔX-E3 within the 10.4K coding sequence, blunting and religation generated a 4 bp frameshift 13 bp downstream of the E3/10.4K start codon (Elsing and Burgert, 1998).
pBSΔX-E3/F14.5	pBSΔX-E3 was utilized for introducing a FLAG-tag downstream of the 14.5K signal sequence using primers FLAG-14.5K gactataaagacgatgatgataaatcccaaacctcagcg and FLAG-14.5K rev atcgtctttatagtcgcaagcacaggttaggg (A. Elsing, University of Munich).
pBSΔX-E3/10.4LL-F14.5	provided by Madelaine Löfqvist, University of Munich
pBSΔX-E3/F14.5Y74	provided by Madelaine Löfqvist, University of Munich
pBSΔX-E3/F14.5 C32	this study
pBSΔX-E3/F14.5 C43	this study
pBSΔX-E3/F14.5 Y44	this study
pBSΔX-E3/F14.5 S121	this study
pBSΔX-E3/F14.5 F123	this study
GPS1.1	New England Biolabs, Frankfurt, Germany.
pMG	InvivoGen, San Diego, USA
pMG-10.4	this study (clone #1)
pMG-10.4+F14.5	this study (clone #1)
pSG5	Stratagene, Amsterdam, The Netherlands
pSG5/10.4	this study (clone #2)
pSG5/10.4LL	this study (clone #4)
pSG5/F14.5	this study (clone #2)
pSG5/F14.5Y122	this study (clone #1)
pSG5/10.4-F14.5	this study (clone #8)
pSG5/10.4LL-F14.5	this study (clone #5)
pSG5/10.4-F14.5Y122	this study (clone #6)
pMG-10.4	this study (clone #1)
pMG-10.4 +F14.5	this study (clone #1)
pST76A	(Posfai et al., 1997)
pST76Tet	(Posfai et al., 1997)
pSV2-neo ^r	(Korner et al., 1992)
pUC19RP12	(Posfai et al., 1999)

Bacterial artificial chromosomes (BAC)

pAd2	kindly provided by Zsolt Ruzsics, Max-von-Pettenkofer Institute, Gene Center, Munich, Germany. F-factor-based BAC vector (Shizuya et al., 1992), containing the complete Ad2 genomic sequence obtained by red $\alpha\beta\gamma$ -mediated homologous recombination of linear genomic Ad2 DNA with the left and right inverted terminal repeats of Ad2 encoded by plasmid pKBS2 (Ruzsics et al., manuscript in preparation).
pAd2-H7	derived from pAd2 by insertion of a Km ^r carrying mTn7 transposon (from plasmid GPS1.1, New England Biolabs, Frankfurt, Germany), in the E3-fiber intergenic region, kindly provided by Zsolt Ruzsics, Max-von-Pettenkofer Institute, Gene Center, Munich, Germany. The mTn sequence was amplified using two primers specific for the left and right transposon ends, respectively, with an appendix of 40 base-pairs with

	homology to the Ad2 sequence 5' and 3' of the site of mTn insertion. The mTn insertion site was located 37 nucleotides downstream from the 14.7K stop codon within the GTCAGC sequence. The TCA triplet was changed to CTA and incorporated in the upstream primer, whereas the downstream primer contained TGA at its 3' end, thus the Tns excision reaction yielded cohesive three nucleotide overhangs. Recircularization of the BAC vector after the Tn excision reaction generated a new <i>NheI</i> recognition site (GCTAGC).
pAd2/F14.5	pAd2-BAC with a FLAG-octapeptide encoding insertion in the 14.5K gene obtained by a gene replacement method. The E3 region encoded by plasmid pBSΔX-E3/F14.5 was modified by insertion of the Km ^r gene sequence into the unique <i>SwaI</i> site within the 19K CDS. The Km ^r -tagged E3 sequence was cut out of this plasmid with <i>EcoRV</i> and used for ET recombination with pAd2. The Cm-resistant BAC clone carrying the FLAG-14.5K sequence was freed from the Km ^r gene by <i>SwaI</i> cleavage (no additional <i>SwaI</i> sites are present in the Ad2 genome or BAC sequence) and religation, reconstituting the wt E3/19K sequence. pAd2/F14.5 was kindly provided by Zsolt Ruzsics, Max-von-Pettenkofer Institute, Gene Center, Munich, Germany.
pAd2-H7/10.4LL-F14.5	this study
pAd2-H7/F14.5Y74	this study
pAd2-H7/10.4ko-F14.5	this study (clone #37, #41)
pAd2-H7/14.5ko	this study
pAd2/10.4LL-F14.5	this study
pAd2/F14.5Y74	this study
pAd2/F14.5Y122	kindly provided by Zsolt Ruzsics, Max-von-Pettenkofer Institute, Gene Center, Munich, Germany.
pAd2/10.4ko-F14.5	this study (clone #43-1, #44-1)
pAd2/14.5ko	this study
pAd2/(10.4-14.5)ko	kindly provided by Zsolt Ruzsics and Susanne Obermaier, Max-von-Pettenkofer Institute, Gene Center, Munich, Germany
pAd2/(10.4Tn)	this study (clone #1B)
pAd2/(14.5Tn)	this study (clone #1A)
pAd2/((10.4-14.5)Tn)	this study (clone #2A)
pAd2/(10.4Tn)(Ad4.14.5)	this study (clone #2)
pAd2/(Ad4-10.4)TAAGC14.5	this study (clone #12-1)
pAd2/10.4TAAGC(Ad4-14.5)	this study (clone #3-8)
pAd2/10.4GC(Ad4-14.5)	this study (clone #7-1)
pAd2/(Ad4-10.4)TAAGC(Ad4-14.5)	this study (clone #7-4)
pAd2/(Ad4-10.4)TT(Ad4-14.5)	this study (clone #16-1)

Oligonucleotides

The oligonucleotides were obtained from metabion (Martinsried, Germany) except for those marked with a * which were purchased from Gibco, Karlsruhe, Germany. Underlining denotes altered nucleotides.

a) Oligonucleotides used for site-directed mutagenesis

Oligonucleotides for generation of alanine replacement mutants are named by the amino acid to be replaced and its position within Ad2 sequences.

template	name	orientation	sequence (5'→3')
pBSΔX-E3 pBSΔX-E3F14.5	10.4s 2395 *	sense	attggacggctgaaacc
pBSΔX-E3 pBSΔX-E3F14.5	14.7as 3468rev *	antisense	gttgaatggaataagatctctaatacc
pBSΔX-E3	14.5*(Elsing and Burgert, 1998)	sense	ctttaattaacgaaacggagtgtc
pBSΔX-E3	14.5*(Elsing and Burgert, 1998)	antisense	ccgtttcgtaattaagaattctg
pBSΔX-E3	14.5Y74As	sense	gcgatcgctccataccttgacattgg
pBSΔX-E3	14.5Y74Aas	antisense	ggagcgcgctagggcaaaaatgg
pBSΔX-E3	14.5Y76As	sense	tatccagcgccttgacattggctgg
pBSΔX-E3	14.5Y76Aas	antisense	gtcaagcgcctggatattatggctagg
pBSΔX-E3 pBSΔX-E3F14.5	14.5Y122As	sense	ctgagattagcgccttaatttgacagg
pBSΔX-E3 pBSΔX-E3F14.5	14.5Y122Aas	antisense	gtcaaataaaggcgctaatctcagt
pBSΔX-E3F14.5	10.4LLAAs	sense	gctgatgctgcagaattcttaattatg
pBSΔX-E3F14.5	10.4LLAAs	antisense	gaattctggcagcatcagctatagtc
pBSΔX-E3F14.5	10.4L1As	sense	agctgatgcactcagaattcttta
pBSΔX-E3F14.5	10.4L1Aas	antisense	ttctgagtgcacatcagctatagtc
pBSΔX-E3F14.5	10.4L2As	sense	tgatcttgcagaattcttaatt
pBSΔX-E3F14.5	10.4L2Aas	antisense	gaattctggcaagatcagctatag
pBSΔX-E3F14.5	10.4ILAAAs	sense	ctcagagctgcctaattatgaacgg
pBSΔX-E3F14.5	10.4ILAAAs	antisense	cataattaggcagctctgagaagatcag
pBSΔX-E3F14.5	14.5S114As	sense	ccccctgctcccaccccca
pBSΔX-E3F14.5	14.5S114Aas	antisense	tgggagcagggggcgagg
pBSΔX-E3F14.5	14.5R111A/S114Aas	antisense	tgggagcagggggcgagg
pBSΔX-E3F14.5	14.5R111As	sense	tcagcctgcccccttctccc
pBSΔX-E3F14.5	14.5R111Aas	antisense	aggggggagcagctgattgattg
pBSΔX-E3F14.5	14.5Y44As	sense	ccagctgcgcaaacaaacagagc
pBSΔX-E3F14.5	14.5Y44Aas	antisense	gttgtttgcgagctgggaatg
pBSΔX-E3F14.5	14.5C32As	sense	catattccgccagattcactca
pBSΔX-E3F14.5	14.5C32Aas	antisense	gaattctggcggaaatattgtct
pBSΔX-E3F14.5	14.5C43As	sense	ttccagcgcctacaacaacag
pBSΔX-E3F14.5	14.5C43Aas	antisense	tgttgaagcgcctgggaatgttc
pBSΔX-E3F14.5	14.5W81As	sense	cattggcgcgaatgcatagatg
pBSΔX-E3F14.5	14.5W81Aas	antisense	atggcattggcgcgaatgtcaag
pBSΔX-E3F14.5	14.5S121As	sense	ctgagattgcctactttaatttg
pBSΔX-E3F14.5	14.5S121Aas	antisense	taaagtagggaatctcagtggg

b) Oligonucleotides used for cloning 10.4K and 14.5K coding sequences into expression vector pSG5 and pMG

name (specifying restriction sites)	orientation	sequence (5'→3')
10.4 <i>Eco</i> RI- <i>Bam</i> HI	sense	cggaattcggatccgccacatgattcctcaggtc
10.4 <i>Bgl</i> II- <i>Xba</i> I disrupting <i>Eco</i> RI site in 10.4	antisense	cgaagatctagattaaagaatcctgagaagatcagc

10.4LLr <i>Bgl</i> I- <i>Xba</i> I disrupting 10.4 <i>Eco</i> RI site	antisense	cgaagatctagattaagaatcctggcagcatcagc
14.5 <i>Eco</i> RI- <i>Clal</i>	sense	cgaattcatcgatgccaccatgaacggagtgtc
14.5r <i>Bgl</i> I- <i>Nhe</i> I	antisense	ccgagatctgctagctcagtcattctccacctgt
10.4-14.5f <i>Eco</i> RI- <i>Bam</i> HI	sense	cgaattcggatcctgagacatgattcctcgagttc

c) Oligonucleotides for synthesis of mTn containing 10.4K and F14.5K mutant alleles

template	primer name	sequence (5'→3')
pBSΔXE3-10.4LL-F14.5 pBSΔXE3-10.4-F14.5Y74	2395	attggacggctctgaaacc
pAd2-BAC/H7	3468 for	ggtattagagatcttattccattcaac
pBSΔXE3/10.4LL-F14.5; pBSΔXE3/10.4-F14.5Y74; pAd2/10.4ko-14.5ko	3468 rev	gttgaatggaataagatctctaatacc
pAd2-BAC/H7	Ad2/E3-rev	aacatgaggaattgacatcc
pAd2/F14.5; pAd2/10.4ko-14.5ko	2631for	ttcattgactgggtttgtg
pAd2-BAC/H7	2913for	ccatcatctctgtcatgg
pAd2/F14.5	2913rev	ccatgacagatgatgg

d) Oligonucleotides for synthesis of mTn fragments for exon cloning

template	primer name	sequence (5'→3')
pGPS1.1	H5 10.4L	aaa cca tgt tct ctt ctt tta cag tat gat taa atg aga ctg tgg gcg gac aaa ata gtt gg
pGPS1.1	H3 10.4R	cgc aaa aaa tca gca aaa caa aaa tga cac tcc gtt tca ttg tgg gcg gac aat aaa gtc tta aac tga a
pGPS1.1	H3 10.4R Ad4	cta gca ata gta gaa gca tga gaa gta gca aag ccc gca ttg tgg gcg gac aat aaa gtc tta aac tga a
pGPS1.1	H5 14.5L	cag aga cag gac tat agc tga tct tct cag aat tct tta atg tgg gcg gac aaa ata gtt gg
pGPS1.1	H3 14.5R	ttc ggt gtt aat tcc atc caa ttc tag atc tag aga ttc atg tgg gcg gac aat aaa gtc tta aac tga a

Primers named H5 and H3 were used for PCR amplification of mTn containing DNA fragments with homology to the 5' flanking region of the site of mTn insertion (H5) in the upstream primer or homology to the 3' flanking region of the site of mTn insertion (H3) in the downstream primer. Sequences complementary to mTn ends are highlighted in boldface. Oligonucleotides longer than 50 nucleotides were HPLC-purified.

e) Oligonucleotides for amplification of Ad4 10.4K and Ad4 14.5K coding sequences

template	primer name	sequence (5'→3')
pA4E3	Ad4 10.4 NS	gtg tgc tct tca [gac] atg att cct aga cag ttc tt
pA4E3	Ad4 10.4 CS	gtg tgc tct tca [cat] gct tat cag atg agc ct
pA4E3	Ad4 10.4 CS TTATG	gtg tgc tct tca [cat] aat cag atg agc ctg agc agc t
pA4E3	Ad4 14.5 NS	gtg tgc tct tca [taa] gca tgc ggg ctt tgc ta
pA4E3	Ad4 14.5 NS TAAGC	gtg tgc tct tca [taa] taa gca tgc ggg ctt tg
pA4E3	Ad4 14.5 CS	gtg tgc tct tca [tca] gtc atc tcc acc ggt ta

The *Sap*I recognition site is highlighted in boldface. Sequences of trinucleotide single-stranded 5' overhangs resulting from *Sap*I cleavage are written in brackets.

f) Oligonucleotides for sequencing or PCR test

primer name	sequence (5'→3')
2395	attggacggctctgaaacc
3468rev	gttgaatggaataagatctctaatacc
pSG5rev	gacgtaagatcaacaccaacagg

t7	gtaatacgactcactcactatagggc
2913for	ccatcatctctgtcatgg
2913rev	ccatgacagagatgatgg
14.5sigfor	ggagtgtcattttgtttgtctg
14.5sigrev	cagcaaaacaaaaatgacactcc
FLAGrev	tttatcatcatcgctcttatagtc
pTnL	gaatatggctcataacaccc
pTnR	ctctcatcaaccgtggctcc
2631for	ttcattgactgggtttgtg
4913rev (Ad414.5 sequence)	gattcccatgataattatcc
3877rev (Ad414.5 sequence)	cgctgttcggtgtaattcc
4635for (Ad4 10.4 sequence)	ctgggtctttgtgcatcg

Molecular weight markers

DNA 1kb ladder	Molecular Weight Marker (0.07-12.2 kbp) Roche Diagnostics, Mannheim, Germany
Protein marker Dalton VII-L (14-70 kD)	Sigma, Munich, Germany
[¹⁴ C] methylated protein marker CFA645 (5,740-30 kD)	Amersham-Pharmacia, Freiburg, Germany

Kits

BigDye RR Terminator Amplitaq FS Kit	Perkin Elmer, Applied Biosystems Division, Foster City, USA
BCA Protein Assay	Pierce, Rockford, USA
ECL western blotting detection system	Amersham-Pharmacia, Freiburg, Germany
GPS1.1	Genome Priming system, New England Biolabs, Frankfurt, Germany
Nucleobond Kit (PC100, PC500)	Macherey-Nagel, Düren, Germany
Pharmacia GFX Micro Plasmid Kit	Amersham-Pharmacia, Freiburg, Germany
QIAex II Agarose Gel Extraction Kit	Qiagen, Hilden, Germany
QIAquick PCR Purification Kit	Qiagen, Hilden, Germany

Antibodies

a) Primary antibodies

anti-Ad2 E3/10.4K	Bur3 (Elsing and Burgert, 1998), polyclonal rabbit antiserum raised against peptide CYRDRTIADLLRIL comprising the C-terminal 13 amino acids of E3/10.4K with a cysteine added to the N-terminus to allow Cys-mediated coupling to ovalbumin. Unpurified serum obtained after the 6 th boost was used in IP/WB.
anti-Ad2 E3/10.4K	cytoplasmic tail (C-tail), R59 (this study), polyclonal rabbit antiserum generated upon immunization with peptide FIDWVCVRIAYLRHHPQYRDRTIADLLRIL. Unpurified R59 was used in IP/WB after the 8th boost.
anti-Ad2 E3/10.4LLAA	R71 (this study), polyclonal rabbit serum was obtained by immunization of a Newzealand White rabbit with peptide CYRDRTIADAARIL coupled to keyhole limpet hemocyanin (KLH). R71 was used in IP/WB after the 6th boost.
anti-Ad2 E3/14.5K	Bur4 (Elsing and Burgert, 1998), polyclonal rabbit antiserum raised against peptide CEISYFNLTGGDD consisting of the C-terminal 12

	amino acids of E3/14.5K with an additional cysteine added to the N-terminus for directed coupling to ovalbumin. Unpurified serum obtained after the 4th boost was used in IP/WB. Purified rabbit anti-14.5 serum (designated R α 14.5, a kind gift from H.-G. Burgert), was prepared from Bur4 serum by protA affinity chromatography and employed for immunofluorescence or FACS analysis.
anti-Ad2 E3/19K	C-tail (Sester and Burgert, 1994), polyclonal rabbit antiserum raised against KLH-coupled synthetic peptide CKYKSRRSFIDEKKMP, used unpurified after the third boost (serum 83904).
anti-Ad2 E3/19K	mouse mAb Tw1.3, (Cox et al., 1991)
anti-Ad4 E3/19K	rabbit serum 163 (a kind gift from H.-G. Burgert) used unpurified after the 3rd boost.
anti- β 1 \rightarrow 4-Galactosyltransferase	mouse mAb, GTL2, (Kawano et al., 1994)
anti-Calnexin	mAb AF-8, a kind gift from H.-G. Burgert
anti-EGFR	mAb 528, ATCC HB-8509.
anti-GM130	mouse mAb, clone 35, Transduction Laboratories, Lexington, USA.
anti-Lamp-2	mouse mAb 2D5, (Diettrich et al., 1996)
anti-lysobisphosphatidic acid	mouse mAb 6C4 (Kobayashi et al., 1998)
anti-TGN46	sheep polyclonal antiserum, kindly provided by S. Ponnambalam, University of Dundee, Scotland.
anti-EEA1	mouse mAb, clone 14, Transduction Laboratories, Lexington, USA
anti-HLA-A, -B, and -C	mouse mAb, W6/32, ATCC HB95
anti-FLAG octapeptide	mouse mAb, M1, Sigma, Munich, Germany
anti-Fas	mouse mAb B-G27, Chemicon, Hofheim, Germany; mouse mAb B-D29 Chemicon, Hofheim, Germany; mouse mAb DX3, Dianova, Hamburg, Germany; mouse mAb ANC95.1/5E2, Ancell, Bayport USA.
anti-Fas	Rabbit serum anti-Fas was a kind gift of H. Engelmann, University of Munich.
anti-TRAIL-R1, R2	mAbs clone 1H5 (anti-DR4), clone 3F11 (anti-DR5) or polyclonal rabbit antisera recognizing the extracellular domain of DR4 or DR5, respectively, were a kind gift from H.-G. Burgert.

b) Secondary antibodies

Fluorescein-isothiocyanate (FITC)- conjugated:

Goat anti-Mouse IgG (Cat.No. F20-12)	Sigma, Munich, Germany
Goat anti-Rabbit IgG (Cat.No. F05-11)	Sigma, Munich, Germany
Goat anti-Rabbit IgG (Cat.No. 111-095-144)	Dianova, Hamburg, Germany
Donkey anti-Rabbit IgG (Cat.No. 711-095-152)	Dianova, Hamburg, Germany

Rhodamine-, Cy3 or Texas-Red-conjugated:

Goat anti-Mouse IgG (Cat.No. 115-165-068)	Dianova, Hamburg, Germany
Goat anti-Rabbit IgG (Cat.No. 111-295-045)	Dianova, Hamburg, Germany
Donkey anti-Sheep IgG (Cat.No. 713-295-147)	Dianova, Hamburg, Germany
Donkey anti-Mouse IgG (Cat.No. 715-295-151)	Dianova, Hamburg, Germany

Peroxidase-conjugated:

Goat anti-Rabbit IgG (Cat.No. 111-035-144)	Dianova, Hamburg, Germany
--	---------------------------

Enzymes

Expand High Fidelity PCR System Polymerase	Roche Diagnostics, Mannheim, Germany
T4 DNA Ligase	New England Biolabs, Frankfurt, Germany

Phosphatase, alkaline, shrimp (SAP)	Roche Diagnostics, Mannheim, Germany
Restriction Endonucleases	New England Biolabs, Frankfurt, Germany
	For specific enzymes see chapter 2.2. Methods.
Transposase ABC*	New England Biolabs, Frankfurt, Germany
AmpliTaq DNA Polymerase	Roche Diagnostics, Mannheim, Germany

2.2 Methods

2.2.1 Bacterial cultures

Propagation and cryoconservation of bacteria

E. coli strains were grown in LB medium or on LB agar plates with addition of antibiotics for the appropriate selection of plasmid containing bacteria. Incubation was performed at 37°C and liquid cultures were grown with constant shaking at 180 rpm, with the exception of *E. coli* strains containing low copy plasmids pST76A or pST76Tet with a temperature-sensitive origin of replication which were kept at 30°C. For cryoconservation 1,5ml of a bacterial culture in the exponential growth phase obtained after inoculation from single colonies were mixed with 300 µl of glycerol, frozen in liquid nitrogen and stored at -80°C.

LB medium (1 l, pH 7, sterile):

10 g Bacto tryptone
5 g Bacto yeast extract
5 g NaCl
4ml 1M NaOH

LB agar:

LB medium with 1,5 % agar

Selection medium:

LB medium containing either 100 µg/ml ampicillin in general, but 50 µg/ml ampicillin for selection of pBADαβγ or pUCRP12
25 µg/ml chloramphenicol 20 µg/ml kanamycin or two types of antibiotics in combination. Bacteria containing pMG-derived constructs were selected with 50 µg/ml hygromycin B.

Transformation of chemically competent DH5α: Heat-shock method

100 µl of chemically competent DH5α were added to 20 µl of the ligation reaction, mixed and incubated for 30 min. on ice. After the heat-shock for 2 min at 42°C, the mix was briefly put back on ice. 900 µl of prewarmed LB medium were added and bacteria were grown for 1 h at 37°C with constant shaking at 1200 rpm in table top heating block. Then 100 µl were taken and plated on LB agar plates with antibiotic(s). The residual bacteria were pelleted (4000 g, 2 min), resuspended in 100 µl LB and plated the same way. The plates were incubated o/n at 37°C.

Preparation of electrocompetent DH10B strains

a) DH10B and arabinose-induced DH10B strains containing pAd2-BACmid and/or pBADαβγ.

A single bacterial clone of DH10B containing pBADαβγ and pAd2-BACmid (encoding the Ad2 wt genomic sequence, Ad2/10.4-14.5ko or Ad2/(Ad414.5)#7-1) was grown o/n in 5 ml LB

containing 50 µg/ml Ap, 25 µg/ml Cm in a 37°C incubator with shaking at 180 rpm. 2 ml of the o/n culture were used to inoculate 200 ml LB medium (with 50 µg/ml Ap, 25 µg/ml Cm) and grown at 37°C. At OD₆₀₀ of 0.15-0.18 cells 2 ml of a freshly prepared sterile-filtered arabinose solution (10 % w/v) were added for induction of the BAD promoter on pBADαβγ (final conc 0.1 % w/v arabinose) and cells were grown for another 30 min at 37°C. DH10B cells were grown in LB to an OD₆₀₀ of 0.25-0.3 without the addition of antibiotics and without arabinose induction. For preparation of electrocompetent cells all materials and solutions used in the following steps were precooled to below 0°C. The bacterial culture was put on ice for 15 min and then centrifuged for 10 min. at 7000 rpm in Sorvall SLA500 rotor (precooled to -4°C). The supernatant was discarded and the bacterial cells were carefully resuspended on ice in 200 ml 10 % glycerol followed by centrifugation for 10 min. at 7000 rpm in Sorvall SLA500 rotor (precooled to -4 °C). Resuspension in 10 % glycerol and centrifugation were repeated another two times. Finally, the pellet was dried by inverting the tube and taking up residual liquid with a tissue without touching the pellet. Cells were resuspended in a final volume of 900 µl 10 % glycerol and 65 µl aliquots were frozen on dry-ice in pre-cooled 1.5 ml eppendorf tubes and transferred to -80°C for storage.

b) DH10B expressing I-Sce-I for counterselection of mTn containing BACs

A single clone of DH10B transformed with pUCRP12 DNA was grown o/n in 5 ml LB medium containing 50 µg/ml Ap at 37°C with constant shaking at 180 rpm, and 2 ml of the o/n culture were used to inoculate 200 ml of LB (50 µg/ml Ap). The bacterial culture was grown until OD₆₀₀ reached 0.2-0.35 and subsequently transferred on ice. In the following the protocol for preparation of electrocompetent DH10B was followed as described in a).

Transformation of electrocompetent DH10B strains

a) Electroporation of plasmid DNA

About 100 ng of plasmid DNA or 3 µl of a ligation reaction were added to 25 µl of ice-cold electrocompetent DH10B cells, mixed and transferred to a pre-chilled electroporation cuvette (gap 0.2 cm) followed by an electric pulse at 2.5 kV, 200 Ω, 25 µF in BioRad Gene Pulser. Immediately afterwards cells were resuspended in 980 µl LB and incubated for 1 hour at 37°C with constant shaking (heating block, 1200rpm). 1/10 of the cells was plated on a LB agar plate containing the appropriate antibiotic.

b) Cotransformation of target BAC and pBADαβγ into electrocompetent DH10B

65 µl of electrocompetent DH10B were added to 10 ng of target BAC (pAd2-BACmid encoding the Ad2 wt genomic sequence, Ad2/10.4-14.5ko or Ad2/(Ad414.5)#7-1) and 10 ng of pBADαβγ and transferred into a 0.2 cm prechilled cuvette for electroporation at 2.5 kV, 200 Ω, 25

μF in BioRad Gene Pulser. Immediately afterwards 950 μl of LB medium were added for an 1h incubation step at 37°C with constant shaking at 1200 rpm. 100 μl of this culture were plated on an agar plate containing 25 $\mu\text{g}/\text{ml}$ chloramphenicol and 50 $\mu\text{g}/\text{ml}$ ampicillin and incubated o/n at 37°C. A single colony was picked for preparation of electrocompetent cells.

c) ET recombination

65 μl of electrocompetent DH10B containing the target pAd2-BAC and pBAD $\alpha\beta\gamma$ were thawed on ice and added to 2-5 μl of a prepared DNA recombination fragment (100-400 ng). The suspension was immediately transferred to prechilled 0.2 cm electroporation cuvettes and electroporated at 2.5 kV, 200 Ω , and 25 μF in BioRad Gene Pulser. The transformed cells were taken up in 1 ml LB and incubated for 90 min. at 37°C with constant shaking at 1200 rpm. To reduce the volume the cells were pelleted for 1 min. at 6000 rpm in a microcentrifuge and the pellet resuspended in 200 μl LB. The entire suspension was subdivided into two parts (1/5 and the rest) and plated on two agar plates containing 25 $\mu\text{g}/\text{ml}$ Cm and 20 $\mu\text{g}/\text{ml}$ Km, followed by incubation for 16 to 20 hours at 37°C. 10-30 clones were picked and transferred onto a Cm/Km masterplate and analysed by PCR and RFLP. For each type of mTn-containing BAC vector the purified BAC DNA of 3 independent clones was retransformed into DH10B and 3 clones from each retransformation were picked and analyzed by restriction cut of a small scale BAC DNA preparation to obtain a BAC DNA preparation that was free of pBAD $\alpha\beta\gamma$ contaminating DNA.

d) Electroporation of BAC vector DNA

For retransformation of BAC vector DNA 1 μl of a BAC DNA mini-preparation was mixed with 25 μl of electrocompetent DH10B for electroporation as described in a).

2.2.2 DNA techniques

Purification of plasmid DNA from bacteria by alkaline lysis

In small scale plasmid DNA was purified with the Pharmacia GFX Micro Plasmid Kit (3 ml o/n culture) according to the manufacturer's instructions and eluted with 100 μl TE. For minipreparation of BAC-DNA bacteria of 10 ml o/n cultures were pelleted by centrifugation for 10 min at 3500 rpm in Centrifuge Varifuge 3.0R. The pellet was resuspended in 300 μl buffer S1 (50 mM Tris/HCl, 10 mM EDTA, 100 $\mu\text{g}/\text{ml}$ RNase A, pH 8,0) and mixed carefully with 300 μl buffer S2 (200 mM NaOH, 1 % SDS). For separation from cellular DNA and cell debris buffer S3 (2,8 M KAc pH 5.1) was added and the suspension was mixed gently by inverting the tube until a homogenous suspension was formed, followed by centrifugation for 12 min. at 13000 rpm. The supernatant was transferred to a new 2 ml eppendorf cup, and mixed with 900 μl of

phenol/chloroform by constant shaking for 15-30 min. (1200 rpm) followed by phase separation during centrifugation for 5 min. at 13000 rpm. 800 μ l of the DNA containing upper phase was transferred to a fresh tube and precipitated by addition of 560 μ l 2-propanol and centrifugation at 15°C for 10 min. at 14000 rpm. The pellet was washed once with 560 μ l 70% ethanol, dried for 10 min. at RT and dissolved in 65 μ l H₂O.

For large-scale purification plasmid DNA was purified from 200 ml (or 300 ml) o/n cultures using Nucleobond Kit protocol with an AX500 cartridge and resuspended in 300 μ l (or 500 μ l) 10 mM Tris pH 8.5. BAC DNA was isolated from 200ml (midi AX100 cartridge) or 500ml (maxi AX500 cartridge) o/n cultures according to the Nucleobond Kit BAC purification procedure and the precipitated DNA resuspended in 120 to 150 μ l of water.

Determination of DNA concentration

The concentration and purity of the purified DNA was determined by measuring the UV absorbance at 260 and 280 nm. The DNA concentration was calculated with the OD₂₆₀ (OD₂₆₀ = 50 μ g/ml dsDNA or 33 μ g/ml ssDNA). The purity was estimated with the OD₂₆₀/OD₂₈₀ ratio, with a ratio of 1.8 indicating a low degree of protein contamination.

Restriction endonuclease digestion

Restriction endonuclease reactions were performed according to the supplier's recommendations. For restriction cut analysis generally 1 μ g of DNA was digested for 2 h at 37°C with 1-3 U enzyme in a total reaction volume of 20 μ l. For analytical digestion of 1 μ g of BAC DNA or 26 μ l of a BAC miniprep 10 U enzyme were used in 30 μ l of the appropriate buffer. Efficacy of the cleavage reaction was analyzed by agarose gel electrophoresis. For separation of cleaved pAd2-BAC DNA the entire reaction mix was loaded onto a 0.8 % agarose gel (6.5 x 9.5 cm) for horizontal gel electrophoresis at 80 V for 2 h.

Generation of alanine replacement mutants on Ad2/E3 region encoding plasmids

Amino acid replacement mutations were introduced into plasmids pBS Δ X-E3 or pBS Δ X-E3/F14.5 using the PCR-mediated oligonucleotide-directed mutagenesis of Higuchi et al. (Higuchi et al., 1988). Mutagenesis was carried out in a two step PCR reaction with two flanking primers 10.4s (2395) and 14.7as (3468 rev) located 5' and 3' of the site to be mutagenized and two mutant oligonucleotides overlapping this site (see chapter 2.1, Oligonucleotides.). In the first step, two separate PCRs were set up with the respective flanking and mutant oligonucleotides in sense and antisense orientations. The gel purified amplification products of both reactions were combined in

a second PCR using the flanking primers to yield a cDNA spanning the region between the flanking primers 10.4s 2395 and 14.7as 3468.

The DNA fragments obtained in the second PCR step were isolated from the reaction mix using QIAquick PCR purification kit and the DNA obtained in a 100 µl PCR was eluted with 30 µl of 10 mM Tris pH 8.5.

- a) The PCR mixture contained:
10 µl 10x PCR Puffer (100 mM Tris-HCl pH 8.3, 500 mM KCl, 15 mM MgSO₄)
4 µl 5 mM dNTPs (200 µM each)
4 µl 10 µM sense primer (400 nM)
4 µl 10 µM antisense primer (400 nM)
1 µl AmpliTaq (5U) Perkin Elmer
+ 0.1 µg template plasmid DNA in the first PCR step
or 0.1 µg each of gel purified first round PCR products in the second PCR step
+ H₂O ad 100 µl.
- b) PCR cycles: {94°C, 5 min.}, {94°C, 30 sec.; 50° C, 30 sec.; 72°C 30 sec.}₂₅, {72°C, 7 min.}

The cloning vector pBSΔX-E3/F14.5 (4 µg) was digested with restriction endonucleases *Xho*I, *Hpa*I (NEB, Frankfurt, Germany) in 40 µl of 1x NEB4 buffer with BSA for 2h at 37°C followed by gel purification. The purified PCR product (2 µg) was also cleaved by *Xho*I, *Hpa*I and the 773 bp fragment was ligated with (*Xho*I, *Hpa*I)-cut and gel-purified pBSΔX-E3 vectors, giving rise to pBSΔX-E3 or pBSΔX-E3/F14.5 mutant plasmids encoding the desired Ala replacement mutation.

Cloning of 10.4K and 14.5K sequences into vector pSG5 or pMG

For expression of 10.4K and 14.5K from the heterologous SV40 promoter/enhancer the vector pSG5 was used. PCR fragments containing the Ad2 coding sequence of wt 10.4K, 14.5K were cloned into the *Eco*RI and *Bgl*II sites and the wt 10.4-14.5 bicistronic sequence was inserted into *Bam*HI and *Bgl*II sites. PCR fragments were generated by a single round of PCR using pBSΔX-E3/F14.5 as a template, and making use of the primers listed in table below. For optimizing expression from the SV40-driven pSG5 cassette the sequence 5' of the ATG was modified to conform to the Kozak consensus for eucaryotic translation in single expression vectors (Kozak, 1987). 10.4K or F14.5K coding sequences were inserted into the pMG bicistronic vector into MCSI *Bam*HI, *Xba*I sites (10.4) or MCSII *Cl*aI, *Nhe*I sites (14.5), respectively. For generation of pSG5-vectors encoding mutant 10.4LL, F14.5Y122 or 10.4LL-F14.5 and 10.4-F14.5Y122 the inserts were amplified by PCR from the corresponding mutant pBSΔX-E3/F14.5 template. The PCR mixture and conditions were as described above for the generation of alanine replacement mutants on Ad2/E3 region encoding plasmids. The amplified fragments obtained in a 100 µl PCR reaction were concentrated using QIAquick PCR purification kit and elution with 30 µl 10 mM Tris pH 8.5. The entire sample was double-digested in the appropriate 1x buffer

(total volume of 40 μ l) with a combination of two restriction enzymes (listed in table below, 10U each) for 2 h at 37 °C followed by gel purification and ligation.

construct	PCR primer for insert amplification	Enzyme
pSG5-10.4 clone #2	10.4 <i>Eco</i> RI- <i>Bam</i> HI, 10.4r <i>Bgl</i> II- <i>Xba</i> I	<i>Eco</i> RI, <i>Bgl</i> II
pSG5-10.4LL clone # 4	10.4 <i>Eco</i> RI- <i>Bam</i> HI, 10.4LLr <i>Bgl</i> II- <i>Xba</i> I	<i>Eco</i> RI, <i>Bgl</i> II
pSG5-F14.5 clone #2	14.5 <i>Eco</i> RI- <i>Cl</i> aI, 14.5r <i>Bgl</i> II- <i>Nhe</i> I	<i>Eco</i> RI, <i>Bgl</i> II
pSG5-F14.5Y122 clone #1	14.5 <i>Eco</i> RI- <i>Cl</i> aI, 14.5r <i>Bgl</i> II- <i>Nhe</i> I	<i>Eco</i> RI, <i>Bgl</i> II
pMG-10.4	10.4 <i>Eco</i> RI- <i>Bam</i> HI, 10.4r <i>Bgl</i> II- <i>Xba</i> I	<i>Bam</i> HI, <i>Xba</i> I
pMG-10.4 + F14.5	14.5 <i>Eco</i> RI- <i>Cl</i> aI, 14.5r <i>Bgl</i> II- <i>Nhe</i> I	<i>Cl</i> aI, <i>Nhe</i> I
pSG5/10.4-F14.5 clone # 8	10.4-14.5f <i>Eco</i> RI- <i>Bam</i> HI, 14.5r <i>Bgl</i> II- <i>Nhe</i> I	<i>Bam</i> HI, <i>Bgl</i> II
pSG5/10.4LL-F14.5 clone #5	10.4-14.5f <i>Eco</i> RI- <i>Bam</i> HI, 14.5r <i>Bgl</i> II- <i>Nhe</i> I	<i>Bam</i> HI, <i>Bgl</i> II
pSG5/10.4-F14.5Y122 clone #6	10.4-14.5f <i>Eco</i> RI- <i>Bam</i> HI, 14.5r <i>Bgl</i> II- <i>Nhe</i> I	<i>Bam</i> HI, <i>Bgl</i> II

2 μ g of cloning vector DNA were cleaved with the corresponding enzymes (10U) each in 20 μ l of the appropriate buffer (enzymes and restriction endonuclease buffers were from NEB, Frankfurt, Germany) and cleavage efficiency controlled by separation on 1 % agarose gel. The linearized vector DNA was purified using QIAquick PCR purification kit and elution with 30 μ l 10 mM Tris pH 8,5. About 100ng of vector were used for ligation (see below). For insertion of 10.4LL-F14.5 and 10.4-F14.5Y122 the pSG5 vector was cleaved with *Bam*HI only.

All pSG5 constructs were verified by dye terminator cycle sequencing. pMG constructs were analyzed by restriction cut for the presence of the insert, but so far have not been sequenced.

5'-Dephosphorylation reaction

Insertion of the 10.4-14.5K wt encoding DNA fragment with *Bam*HI, *Bgl*II cohesive ends required 5'-dephosphorylation reaction of the target vector DNA pSG5, which had been double-digested with *Bam*HI and *Bgl*II. 5' dephosphorylation of plasmid vector DNA after restriction endonuclease cleavage was performed with the shrimp alkaline phosphatase (SAP). 2 U SAP were added to about 2 μ g restriction enzyme digested plasmid DNA. After 1 hour incubation at 37°C the phosphatase was inactivated by heating to 65°C for 15 min. and the DNA was isolated using QIAquick PCR purification Kit and elution with 30 μ l 10 mM Tris pH 8.5. For generation of pSG5/10.4LL-F14.5 and pSG5/10.4-F14.5Y122 the pSG5 vector was cleaved by *Bam*HI only before SAP treatment.

Gel purification of DNA

DNA fragments were separated by agarose gel electrophoresis, stained with ethidium bromide and detected with UV light (366 nm). The gel slice containing the DNA fragments was cut out and the DNA was isolated using the QIAex II Agarose Gel Extraction Kit according to the manufacturer's instructions. Alternatively, DNA fragments from PCR reactions were purified

using the QIAquick PCR Purification Kit according to the manufacturer's protocol. In general, the DNA obtained in one 100 μ l PCR reaction or extraction of a 300 mg of gel slice was dissolved in 20 μ l of 10 mM Tris pH 8.5.

Phenol/chloroform extraction and ethanol precipitation of DNA

Proteins were removed from DNA preparations by extracting first with 1x volume phenol/chloroform and then with 1x volume of chloroform. After shaking at 1300 rpm for 10 min at 4°C the solution was centrifuged at 14000 rpm (microcentrifuge) for 5 min and the DNA containing upper phase was recovered. Then 0.1x volume 3 M sodium acetate pH 5.2 and 3x volume 100% EtOH (ice-cold) were added, and the mix was incubated at -20°C for 1-12 h. The precipitated DNA was spun down at 14000 rpm for 30 min. (4°C). Then the pellet was washed once with 70% EtOH (cold), and after centrifugation (14000 rpm, 15 min, 4°C) the liquid was removed, the pellet air-dried at RT and resuspended in 22 μ l of H₂O or 10 mM Tris pH 8.0.

Ligation

In a total volume of 20 μ l 1x T4 DNA ligase buffer (NEB, Frankfurt, Germany) 100-200 ng of vector and the insert at a molar ratio of insert/vector of about 3:1 were reacted with 1 U T4 DNA ligase (NEB, Frankfurt, Germany). After incubation o/n at 16 °C the ligase was inactivated by heating 10 min. at 65 °C.

Agarose gel electrophoresis

Analysis of DNA fragments and plasmids was performed by agarose gel electrophoresis in 1x TAE. In general, agarose gels had a content of 0.8 - 1.4 % agarose. The agarose was solubilized in 1x TAE by heating in a microwave oven. Ethidium bromide was added to a final concentration of 0.1 μ g/ml shortly before pouring the gel. Samples were mixed with 1/5 volume loading buffer. Gels (6.5 x 9.5 cm) were run horizontally at 80-120 V. DNA was detected with UV light, λ =254 nm or on preparative gels at λ =366 nm to cut out specific fragments.

Loading buffer (6x in water): 0.25 % bromophenol blue
0.25 % xylene cyanol FF
15 % Ficoll (type 400)

20x TAE: 800 mM Tris
400 mM NaAc
40 mM EDTA
adjusted to pH 7.8 with acetic acid

Ethidium bromide (stock): 10 mg/ml

DNA sequencing

a) PCR

DNA sequencing was performed using the BigDye RR Terminator Amplitaq FS Kit. The reaction mixture contained 8 μ l Premix, as a template 900 ng of plasmid DNA or 100 ng of a PCR fragment per 1kb length of amplification product and 10 pmol primer in 20 μ l final volume. The following PCR was performed: {96°C, 10 sec.; 50°C, 5 sec.; 60°C, 4 min.}₂₅. The PCR product was precipitated by adding 30 μ l H₂O, 5 μ l 3 M sodium acetate pH 5.2 and 135 μ l ethanol (RT) and subsequent centrifugation for 15 min. at 14000 rpm (microcentrifuge). The pellet was washed with 250 μ l 70% EtOH (RT) and centrifuged for 10 min. at 14000 rpm. The EtOH was removed and the pellet air-dried. The DNA was resuspended in 10 μ l loading buffer (1 volume of (50 mg/ml Blue Dextran/25mM EDTA pH 8.0)-solution mixed with 4 volumes of formamide). For DNA sequencing of pAd2-BACs 100-200 ng of a PCR product amplified with primers 2395 and 3468rev served as a template in the sequencing PCR. The PCR product was purified with QIAquick PCR purification kit and elution with 30 μ l autoclaved ddH₂O.

Preparation of the template for a pAd2-BAC sequencing PCR:

a) PCR conditions: {94°C, 5 min.}, {94°C 30 sec ; 55°C 30 sec ; 72°C 30 sec}₃₀, {72°C, 7 min.}

b) PCR reaction mix:

5 μ l 10x PCR Puffer (100 mM Tris-HCl pH 8.3, 500 mM KCl, 15 mM MgSO₄)
 2 μ l 5 mM dNTPs (200 μ M each)
 2 μ l 10 μ M sense primer (400 nM)
 2 μ l 10 μ M antisense primer (400 nM)
 1 μ l AmpliTaq (5U) Perkin Elmer
 + 10 ng of pAd2-BAC to be sequenced
 + H₂O ad 50 μ l.

b) Polyacrylamide sequencing gel

A 5% polyacrylamide gel (8 M urea, 200 x 560 x 0.3 mm) solution was prepared:

5% gel: 30 g urea, 10 ml 30% acrylamide/bisacrylamide (29:1), 6 ml 10x TBE buffer, 22 ml H₂O

10x TBE buffer (1l): 108 g Tris base, 55 g Boric acid, 7.4 g EDTA

The gel solution was incubated at 37°C until the urea was dissolved. Then the solution was passed through a 0.2 μ m filter and degassed for 10 min. 20 μ l TEMED and 350 μ l 10% APS solution were added and the gel was poured and polymerized horizontally for 4 h. The precipitated DNA from the sequencing PCR reaction resuspended in 10 μ l loading buffer was heated for 10 min at 95°C. Then the samples were put on ice for 5 min. After 1 min centrifugation at 14000 rpm (microcentrifuge) 4 μ l of the solution was loaded on the gel. The gel run was performed with 1x TBE buffer at 37 Watt for 18 h (pre-run 30 min). Sequencing data were analyzed using the ABI PRISM software.

2.2.3 Generation of recombinant Ads

Cloning of mutant pAd-BACs: pAd2/10.4LL-F14.5, pAd2/10.4-F14.5Y74, pAd2/10.4ko-F14.5 and pAd2/14.5ko

a) Generation of linear minitransposon (mTn) containing recombination fragment

In a two step PCR reaction a mutant allele containing the mTn sequence was amplified for ET recombination with the target BAC-mid. For generation of the 10.4LL and 14.5Y74 mutant sequences a pBS Δ X-E3/F14.5-derived vector containing the desired mutation served as a template for PCR amplification using oligonucleotides 2395 as sense and 3468rev as antisense primer (compare Fig 24). A partially overlapping DNA fragment encompassing the mTn sequence was amplified by PCR on template pAd2-BAC/H7 with 3468for sense and Ad2/E3rev antisense primers. The two PCR products were assembled in a second round of PCR yielding a fulllength mutant allele spanning the region between flanking primers 2395 and Ad2/E3rev.

As the 10.4ko mutation was not yet existing on pBS Δ X-E3/F14.5 a FLAG-14.5K encoding cDNA was amplified on pAd2/F14.5 BAC with oligonucleotides 2631for as sense and 2931rev as antisense primer, which was combined with the mTn encoding PCR product, that was obtained by PCR with primers 2931for and Ad2/E3rev on pAd2-BAC/H7 (see also Fig. 26). The assembled full-length mutant allele was combined by ET recombination with pAd2/10.4ko-14.5ko BAC, generating pAd2/10.4ko-F14.5. The pAd2-14.5ko BAC was obtained by ET recombination of a full-length mutant allele with wt pAd2-BAC. Primers 2631for (sense) and 3468 rev (antisense) were used to generate a cDNA fragment encompassing the 14.5ko mutation by PCR on template pAd2/10.4ko-14.5ko. PCR product one was assembled with the mTn containing PCR fragment generated with primers 3468for (sense) and Ad2/E3-rev (antisense) on template pAd2-BAC/H7, yielding a full-length mutant allele.

The PCR reaction mix of the first round of PCR was purified using QIAquick PCR purification kit according to the manufacturer's protocol and the DNA eluted with 30 μ l 10 mM Tris pH 8.5. The assembled PCR product of the second round of PCR was gel purified from a 1% agarose gel using QIAex gel extraction kit and the elution buffer was prewarmed to 50°C to assure high yield of the ~3kb fragments.

a) The PCR mixture contained:

10 μ l 10x PCR Puffer (100 mM Tris-HCl pH 8.3, 500 mM KCl, 15 mM MgSO₄)

4 μ l 5 mM dNTPs (200 μ M each final conc)

4 μ l 10 μ M sense primer (400 nM)

4 μ l 10 μ M antisense primer (400 nM)

1 μ l High Fidelity Taq Pol (3.5U/ μ l) (Roche Diagnostics Mannheim)

+ 0.1 μ g template plasmid DNA in the first PCR step

or 0.1 μ g each of gel purified first round PCR products in the second PCR step

+ H₂O ad 100 μ l.

b) PCR cycle parameters: {94°C, 5 min.}, {94°C,30 sec.; 55°C, 30 sec.;72°C, 90 sec.}₂₅, {72°C, 7 min.}

b) ET recombination of 10.4LL, 14.5Y74, 10.4ko, 14.5ko encoding mutant alleles

For ET recombination 120 ng of the linear recombination fragment were mixed with 65 µl of electrocompetent DH10B containing the target BAC vector and pBADαβγ (chapter 2.2). Resulting Cm/Km resistant clones were analyzed by PCR on a boiling prep (see below) for the presence of the mTn sequence in the intergenic space between the 14.7 CDS and fiber region (as in the pAd2-H7 wt clone). A combination of primers 3468for and pTnR was used and the resulting PCR product had a size of 423 bp (67 nt of the Ad2 genomic sequence and 366 nt of the tn sequence). As a positive control the same primers were used for PCR on template pAd2-BAC/H7, whereas PCR on pAd2-BAC yields no amplification product.

Mutant pAd2/10.4ko-F14.5 clones were analyzed for gain of the FLAG-sequence using primers 2395 and FLAGrev for PCR, yielding a 412 bp PCR product which was not cleaved by *XhoI* due to the mutation in 10.4CDS. Similarly, in these clones the PCR product obtained with primers 2395 and 2913rev could not be cleaved by *PacI* proving that the ATG sequence of 14.5K is intact. BAC DNA that was free of pBADαβγ contamination was used for sequencing of mTn containing 10.4LL, 14.574, 10.4*, 14.5* mutant BAC clones to assure that the full-length mutant allele had been inserted by ET recombination.

Generation of recombinant Ad2/Ad4 chimeric viruses: Gene replacement of Ad2 10.4K and/or 14.5K coding sequences with homologous Ad4 sequences in pAd2-BAC

a) Generation of ET recombination fragments containing the mTn sequence

For gene replacement mTn containing fragments were generated with 42 bp homology arms to the sequence flanking the site within target DNA in which the linear fragment should be inserted by ET recombination. Thus, for synthesis of the mTn containing recombination fragment upstream and downstream oligonucleotide PCR primers were designed to possess the homology arms to the target DNA and priming regions with homology to the mTn. The sequences of the priming regions (3' ends of the oligonucleotides) were defined as 5'-tgt ggg cgg aca aaa tag ttg g-3' in the upstream primer and 5'-tgt ggg cgg aca ata aag tct taa act ga-3' in the downstream primer (Ruszics et al., manuscript in preparation). As the PCR cycle parameters are mainly determined by the priming sequences and the length of the PCR product defined priming sequences allowed to fix parameters for PCR amplification of mTn containing DNA which are generally applicable without further optimization (Ruszics et al., manuscript in preparation). The following mTn containing fragments were synthesized by PCR on template pGPS1.1:

a) The PCR reaction was set up as follows:

1.5 µl upstream primer (conc 20 µM)
 1.5 µl downstream primer (conc 20 µM)
 1 µl GPS 1.1 DNA (8 ng)
 2 µl 10 mM dNTPs
 10 µl 10x PCR buffer
 0.8 µl High Fidelity Taq Polymerase (2.5U)
 +H₂O ad 100 µl

b) PCR cycle parameters: {94°C, 4 min.}, {94°C, 30 sec.; 60°C, 30 sec.; 72°C, 90 sec.}₃₀, {72°C, 7 min.}
 The PCR product was purified using QIAquick PCR purification kit and elution with 50 µl 10 mM Tris pH8.5.

CDS to be replaced by ET recombination with mTn	Upstream primer	Downstream primer	mTn containing construct
10.4 CDS within pAd2-BAC	H5 10.4L	H3 10.4R	pAd2/(10.4Tn)#1B
14.5 CDS within pAd2-BAC	H5 14.5L	H3 14.5R	pAd2/(14.5Tn)#1A
10.4-14.5 CDS within pAd2-BAC	H5 10.4L	H3 14.5R	pAd2/(10.4-14.5)Tn#2A
10.4 CDS within pAd2/10.4-Ad414.5#7-1	H510.4L	H3 10.4R Ad4	pAd2/(10.4Tn)(Ad4-14.5)#2

b) Generation of mTn containing pAd2-BAC intermediates for exposon cloning

3 µl (~300ng) of mTn containing recombination fragment DNA were added to 65 µl of electrocompetent DH10B containing pAd2-BAC and pBADαβγ for ET recombination. To get rid of pBADαβγ contamination BAC DNA was retransformed into DH10B and analyzed by restriction endonuclease cleavage. Cm/Km resistant bacterial clones were analyzed by PCR with a boiling prep (see below) for transposon insertion in place of the 10.4 CDS or the 10.4-14.5 CDS using primers 2395 and pTnL (420 bp PCR product, 54 bp of Ad2 sequence and 366 bp of the mTn), and those with the mTn replacing the 14.5 CDS with primers 2631for and pTnL (459 bp PCR product, 93 bp of Ad2 sequence and 366 bp of mTn). Similarly, at the 3' end of the mTn replacing the 14.5 CDS a PCR product of 910 bp (366 bp of mTn and 544 bp of Ad2 sequence) could be amplified using a combination of primers pTnR and Ad2/E3-rev.

c) Generation of Ad4-CDS-containing inserts

Oligonucleotides for amplification of Ad4 inserts were designed to contain a *SapI* recognition site and a priming region with homology to the Ad4 insert. If necessary, an intervening sequence could be included between *SapI* recognition site

construct	Upstream and downstream primer for insert amplification	Target BAC in Tn excision reaction mix
pAd2/(Ad4-10.4)TAAGC14.5 clone #12-1	Ad4 10.4 NS Ad4 10.4 CS	pAd2/(10.4Tn)#1B
pAd2/10.4TAAGC(Ad4-14.5) clone #3-8	Ad4 14.5 NS TAAGC Ad4 14.5 CS	pAd2/(14.5Tn)#1A
pAd2/10.4GC(Ad4-14.5) clone #7-1	Ad4 14.5 NS Ad4 14.5 CS	pAd2/(14.5Tn)#1A
pAd2/(Ad4-10.4)TAAGC(Ad4-14.5) clone #7-4	Ad4 10.4 NS Ad4 14.5 CS	pAd2/(10.4-14.5)Tn#2A
pAd2/(Ad4-10.4)TT(Ad4-14.5) clone #16-1	Ad4 10.4 NS Ad4 10.4 CS TTATG	pAd2/(10.4Tn)-(Ad4-14.5)#2

and the Ad4-specific sequence to introduce a modification of the target site sequence flanking the Ad4 CDS insert. The PCR sample was purified using QIAquick PCR purification kit and elution with 33 μ l 10 mM Tris pH8.5. 2 μ g of the PCR product were digested with 4U *SapI* (NEB, Frankfurt, Germany) in 20 μ l of 1x NEB4 for exactly 6 hours at 37°C, and the enzyme heat-inactivated for 20 min at 65°C. 2 μ l of the *SapI* digest (200ng of insert) were added to the heat-inactivated transposon excision reaction for ligation (see below).

a) The PCR reaction was set up as follows:

- 4 μ l upstream primer (conc 10 μ M)
- 4 μ l downstream primer (conc 10 μ M)
- 1 μ l pA4E3 DNA (100 ng)
- 2 μ l 10 mM dNTPs
- 10 μ l 10x PCR buffer
- 1 μ l High Fidelity Taq Polymerase (2.5U)
- +H₂O ad 100 μ l

b) PCR cycle parameters: {94°C, 5 min.}, {94°C, 30 sec.; 55°C, 30 sec.; 72°C, 2 min.}₃₀, {72°C, 7 min.}

Quick PCR test with a DNA boiling prep

To quickly analyze the DNA content of bacterial colonies single bacterial clones were streaked into an eppendorf tube with a screw lid. Alternatively, several colonies were picked and transferred to the same tube for analysis of a group of clones in one PCR. The bacterial cells were resuspended in 30 μ l (several clones in 70 μ l) of autoclaved ddH₂O. The tubes were tightly closed and immersed in boiling water for 10 min and then put on ice to release the DNA from the cells. The boiling prep was centrifuged and 3 μ l were used to set up a 25 μ l PCR reaction.

a) The PCR mixture contained:

- 2.5 μ l 10x PCR Puffer (100 mM Tris-HCl pH 8.3, 500 mM KCl, 15 mM MgSO₄)
- 1 μ l 5 mM dNTPs (200 μ M each final conc)
- 1 μ l 10 μ M primer 1 (400 nM final conc.)
- 1 μ l 10 μ M primer 2 (400 nM final conc.)
- 0.5 μ l AmpliTaq (5U/ μ l) (Perkin Elmer)
- + 3 μ l of boiling prep
- + H₂O ad 25 μ l.

b) PCR cycles: {95°C, 5 min.}, {95°C, 30 sec.; 55°C, 30 sec.; 72°C, 2 min}₃₅, {72°C, 7 min.}

The entire PCR sample was separated by gel electrophoresis for 30 min at 120 V on a 1.4% agarose gel.

mTn excision *in vitro*

By TnsABC* treatment the Tn7-derived sequence was excised from pAd2-BAC DNA containing the mTn and transferred to a an acceptor suicide plasmid.

The Tn excision reaction mix contained (molar ratio donor:target DNA of 1:4):

- 1-5 μ l of pAd2-BAC as Tn donor (150 ng)
- 1-5 μ l of pST76TET or pST76A (90 ng) as Tn acceptor (high purity!)
- 2 μ l 10x GPS buffer
- autoclaved ddH₂O ad 18 μ l

+ 1 μ l of TnsABC* (NEB, Frankfurt Germany)

After pipetting up and down the mix was incubated at 37 °C for 10 min to allow reaction complex assembly. Then, 1 μ l of 0.3 M sterile MgCl₂ solution was added and quickly mixed by pipetting up and down to start the transposon excision reaction, which was carried out by incubation at 37°C for 1h. To liberate the transposase from the DNA the reaction mix was heated for 15 min to 75 °C and then put on ice. Evaporated liquid was collected at the bottom of the tube by a short centrifuge spin.

For ligation the sample was mixed with 1 μ l T4 DNA ligase (NEB) and if desired a *SapI* cleaved insert (up to 200 ng) was added (see also generation of Ad4 CDS containing inserts) followed by incubation o/n at 16 °C.

After heat-inactivation of the ligase for 15 min at 65 °C, 40 μ l of water were added and the DNA purified by phenol-chloroform extraction and ethanol precipitation. The DNA was dissolved in 10 μ l of autoclaved ddH₂O. 2 μ l of the DNA preparation were mixed with 65 μ l of electrocompetent DH10B expressing I-*Sae* I meganuclease. Following electroporation at 2.5 kV, 200 Ω and 25 μ F cells were resuspended in 1ml LB medium and incubated with constant shaking at 37°C for 1 hour. 1/5 and 4/5 of the bacteria were spread onto two agar plates containing 25 μ g Cm and incubated o/n at 37 °C. 30 single clones were picked and transferred onto Cm and Cm/Km containing LB agar plates and grown o/n at 37 °C to identify clones which lost the Km^r. To get rid of pUCRP12 DNA the BAC DNA was retransformed into DH10B, single clones were picked and transferred onto Cm and Cm/Ap plates to assure that the pUCRP12 DNA was lost. Purified BAC vector DNA was analyzed by PCR and subsequent restriction endonuclease cleavage, and sequencing.

Sequence analysis of newly generated pAd2-BAC-derived vectors after mTn excision

Correct transposon removal introduced a new *NheI* in the Ad2 sequence of pAd2-mutants carrying the 10.4LL, 10.4ko, 14.5ko or F14.5Y74 mutations. By PCR with 1 μ l of a miniprep of pAd2-BAC DNA with primers 2913for and Ad2/E3-rev (50 μ l PCR reaction, conditions as for PCR test with a boiling prep) a ~760 bp DNA fragment was amplified. Half of the PCR product was cut by *NheI* (NEB, Frankfurt, Germany) in 20 μ l NEB2 buffer with BSA for 1 hour at 37 °C and the other half was incubated in parallel without addition of enzyme. Cleavage was analyzed on 1.4% agarose gel to identify clones from which the transposon had been removed and with correct religation of the BAC vector. Purified BAC-DNA preparations were analyzed by restriction endonuclease cleavage (*EcoRV* or *XhoI*) to exclude any unwanted rearrangements and sequencing. Clones obtained by exposon cloning were tested by PCR on a boiling prep for removal of the

mTn and insertion of Ad4 sequence fragments. PCR with primers 2395 and 3468rev would yield a fragment of >1.7kb, whereas insertion of the 10.4-14.5 encoding Ad2 sequence led to generation of a ~1.1 kb fragment. The presence of Ad4 specific sequences was further tested by analytical restriction of a PCR product, obtained with the following PCR:

5 μ l 10x PCR Puffer (100 mM Tris-HCl pH 8.3, 500 mM KCl, 15 mM MgSO₄)
2 μ l 5 mM dNTPs (200 μ M each final conc)
2 μ l 10 μ M primer 1 (400 nM final conc.)
2 μ l 10 μ M primer 2 (400 nM final conc.)
0.5 μ l AmpliTaq (5U/ μ l) (Perkin Elmer)
+ 100ng of purified BAC-DNA
+ H₂O ad 50 μ l.

PCR cycle parameters: {94°C, 5 min.}, {94°C, 30 sec.; 55°C, 30 sec; 72°C, 2 min.}₃₅, {72°C, 7 min.}

10 μ l of the PCR sample were digested with 10 U *Xcm*I or *A*vriI in 40 μ l reaction buffer NEB2 for 2h at 37 °C and 10 μ l of the PCR sample were treated in parallel without the addition of enzyme. The entire reaction was separated by gel electrophoresis on 1.4% agarose gel, 30 min at 120 V. The 1.1kb full-length fragment was cut once by *Xcm*I if the Ad4 10.4CDS was present, and *A*vriI cleaved once within the Ad4 14.5 coding sequence.

2.2.4 Cell culture

Cultivation and cryoconservation

A549, 293 and SeBu cells were maintained in Dulbecco's modified Eagle's medium (DMEM) supplemented with 100 U/ml penicillin, 0.1 mg/ml streptomycin and 10% fetal calf serum at 37°C and 5% CO₂. For propagation of SV80Fas cells and stable E3 transfectants of 293 cells the medium additionally contained 200 μ g/ml G418. Stable A549 transfectants were grown in medium containing 800 μ g/ml G418.

For cryoconservation cells were detached with trypsin and centrifuged at 300 g for 5 min. at 4°C. Then the cells were resuspended in 1 ml 25% FCS/10% DMSO/65% DMEM (4°C) with a final concentration of 0.5-1x10⁷ cells/ml. Cryovials containing aliquots of at least 0.6 ml of the cell suspension were slowly cooled down to -80°C in a tightly closed styropor box. 48 hours later the vials were transferred into liquid nitrogen for long-term storage. Frozen aliquots were quickly thawed at 37°C in a waterbath, one volume DMEM was added and the suspension was carefully pipetted onto a 4 ml FCS cushion. After centrifugation at 300 g for 5 min. the supernatant was removed, cells were resuspended in complete medium without G418 selection and transferred to cell culture dishes. After 24 hours the medium was changed to G418-containing media, if G418 selection was required.

Calciumphosphate transfection

For transient transfection cells were grown on 6 cm Ø dishes to 60-70% confluency. 4 h prior to the transfection the medium was changed to fresh DMEM/10% FCS. If the Bonifacino method (Marks et al., 1996) was employed, cells were seeded on the day of transfection and the transfection mix was added 4 to 6 hours later. For preparation of the transfection mix 250 µl of 2x HBS pH 7.05 were added to a 1.5 ml reaction tube. In another tube 6 µg DNA were combined with H₂O to a total volume of 225 µl. 24.8 µl 2.5 M CaCl₂ solution were added dropwise to the DNA solution while vortexing at low speed (300 rpm), and subsequently mixed by vortexing at 800 rpm. Then, the DNA/CaCl₂ solution was added dropwise to the tube with the 2x HBS constantly vortexed at 300 rpm. Finally, the complete transfection mix was vortexed for 15 sec. at 800 rpm and then incubated for 15-20 min at RT to allow formation of the calcium-DNA precipitate. Subsequently, the suspension was added dropwise to the cultured cells. The next day the medium was changed and protein expression was assessed by immunofluorescence at 40-48h post transfection.

2x HBS pH 7.05: 50 mM HEPES (2-[4-(2-Hydroxyethyl)-1-piperazinyl]-ethane sulfonic acid),
1.5 mM Na₂HPO₄ x 2 H₂O, 280 mM NaCl, 12 mM glucose

Generation of stable 293 E3 transfectants

For generation of stable E3 transfectants 40 µg of pBSΔX-E3/F14.5-derived mutant DNA was linearized by restriction digest with 2U enzyme/µg DNA *ScaI* in a total volume of 200 µl 1x *ScaI* buffer (NEB, Frankfurt, Germany). 15 µg of pSV2-neo^r was cut with *PvuI* (2U enzyme/µg DNA, NEB) in 100 µl 1x NEB3 buffer in the presence of BSA. After 3.5 hours incubation at 37°C the DNA was purified by phenol/chloroform extraction and concentrated by EtOH precipitation. The inner surface of the tube was rinsed with 70% EtOH to assure sterility and the DNA dried in the laminar flow hood for 5-10 min. The pBSΔX-E3/F14.5-derived mutant DNA was resuspended in 22 µl sterile H₂O and pSV2-neo^r in 10 µl. 293 cells were grown to confluency in two T75 flasks. Cell monolayers in each flask were washed once with 8 ml of PBS, trypsinized for 3-5 min with 2 ml Trypsin/EDTA and resuspended in 10 ml DMEM containing 10% FCS. Following centrifugation for 7 min. at 300g the two cell pellets were carefully resuspended in 2ml DMEM without FCS and collected in one tube in a total volume of 10 ml DMEM without FCS. An aliquot was taken to determine the cell number (total number of cells ~3x10⁷). After a second centrifugation step the cells were taken up in DMEM at a cell density of 10⁷ cells/ml. 0.8 ml of this cell suspension was mixed with 20 µg of linearized pBSΔX-E3/F14.5-derived mutant DNA and 2 µg of linearized pSV2-neo^r and incubated for 10 min. at RT. Then, the suspension was transferred

into a 0.4 cm gap electroporation cuvette and electroporated at 0.32kV, 960 μ F on BioRad Gene Pulser. Immediately after the pulse the entire sample was mixed with 1.2ml DMEM/10%FCS and incubated for 10 min at RT. The cells were spread onto two 10 cm \emptyset dishes with 1 ml of the cell suspension each. In parallel, the same number of cells was mock treated by electroporation of an equal volume of sterile water instead of the DNA and a 1 ml and a 0.5 ml aliquot of the suspension were plated. 2 days post transfection each dish was split 1:4 onto four 10 cm \emptyset dishes taking care to spread out single cells and the medium was supplemented with 400 μ g/ml G418 to select transfected clones. Every 3 days the medium was replaced. Six days post transfection no cells of the mock transfection had survived. After 10-14 days clones were trypsinized using cloning cylinders and transferred to 3 cm \emptyset dishes. Usually, 10-20 single clones were obtained per 10 cm \emptyset dish and for each type of transfected DNA 40-50 clones were picked. The clonal lines were kept in DMEM/10%FCS with 200 μ g/ml G418.

Generation of stable transfectants of A549 expressing 10.4K and/or 14.5K

60 μ g of vector pSG5/10.4 and pSG5/F14.5 were cleaved by *Aat*I (2U/ μ g DNA, NEB, Frankfurt, Germany) in 200 μ l NEB4 buffer. 15 μ g of pSV2-neo^r was cut with *Pvu*I (see above). After 3 hours incubation at 37°C, phenol/chloroform extraction and EtOH precipitation the linearized pSG5 vector was resuspended in 25 μ l sterile H₂O and pSV2-neo^r in 10 μ l. Three middle flasks of A549 cells were grown to confluency. The cells of each flask were washed with 8 ml warm PBS, detached with 2 ml Trypsin/EDTA for 5 min. at RT and taken up in 10 ml DMEM/10%FCS. After centrifugation the cells were carefully resuspended and collected in one tube in a total volume of 10 ml. An aliquot was taken for counting the cells (total number of cells $\sim 4 \times 10^7$). After centrifugation the cells were resuspended in DMEM without FCS at a density of 1×10^7 cells/ml. To generate transfectants stably expressing the E3/10.4K and/or 14.5K protein 0.8 ml of the A549 cell suspension were mixed with 12 μ g pSG5-10.4K, 12 μ g pSG5-14.5K and 2 μ g pSV2-neo^r, the latter conferring G418 resistance. As a negative control, an equal number of A549 was mixed with 20 μ g of EtOH-precipitated pBluescript DNA. After incubation for 10 min. at RT the cells were electroporated at 0.27 kV, 960 μ F in BioRad Gene Pulser in a 0.4 cm electroporation cuvette. Immediately after the pulse 1.7 ml of DMEM/10%FCS were added and the cells incubated for at least 10 min at RT before plating onto two 10 cm \emptyset dishes. After two days cells were split 1:5 and the DMEM/10%FCS medium was supplemented with 1.3 mg/ml G418. 6 days post-transfection the medium was replaced with DMEM/10%FCS containing 1 mg/ml G418 and changed every 3 days. After 16 days 5-10 clones were picked from each dish. Clonal lines were

maintained in DMEM/10%FCS containing 1 mg/ml G418 and screened by FACS analysis for intracellular content of 10.4K and/or 14.5K.

Adenovirus infection

Cells were grown to 80-90% confluency in 6 cm (10 cm) Ø dishes and washed once with DMEM without FCS. In general, 10-100 plaque forming units (pfu) were applied per cell in 1 ml (3ml) DMEM without FCS. Dishes were incubated for 90 min. at 37°C, 5% CO₂ and shaken every 10-15 min. Then, the virus-containing medium was removed, and DMEM/2.5 % FCS was added. This time point was defined as the start of infection. Virus containing solutions were inactivated by disposing them in solutions with >1% SDS.

Generation of infectious adenovirus particles from recombinant Ad2 genomic DNA

Adenovirus DNA contained within the pAd2-BAC vector was liberated from the BAC backbone by digestion of 10 µg of BAC DNA with 25 U of *Sna*B1 (5' TAC[▼]GTA 3' blunt end) in a total volume of 120 µl for exactly 3 hours at 37°C. *Sna*B1-digest released linear Ad2 double-stranded genomic DNA with intact ITRs and cleaved the vector backbone into two fragments of 2 and 4 kb. The linearized DNA was concentrated by EtOH precipitation and resuspended in 22 µl sterile H₂O. For transfection 2-5 µg of *Sna*B1-cut DNA were supplemented with EtOH-precipitated pBluescript DNA to give a total of 6 µg and were transfected according to the CaPO₄-transfection protocol into 293 cells. Mock-treated cells were transfected in parallel with 6 µg of pBluescript DNA. 293 cells are ideal hosts for adenovirus replication as they stably express Ad E1A products. It was found to be advantageous to use less rapidly dividing 293 cells (low passage number), because growing cell number should not outcompete the accumulation of viral particles.

293 cells were seeded in 6 cm Ø dishes the day before transfection and reached ~40 % confluency at the time of transfection. The next day transfected cells were split 1:2 and distributed onto two 10 cm Ø dishes. 3 days later dishes were 30% confluent and on day 6-7 small plaques appeared. If necessary, 3 ml of fresh medium were added. 10 days post transfection cpe was extensive and the virus was harvested. Cells and supernatant were centrifuged for 7 min. at 300g. The cell pellet was taken up in 0.5 ml DMEM and saved as a virus prestock at -80°C. The supernatant could be used directly to infect two T75-flasks of A549 cells. 2 days later about 90 % cpe was reached and virus could be harvested. The cell pellet was taken up in 2 ml DMEM without FCS and the virus was released by 3 cycles of freeze and thaw followed by centrifugation to precipitate cell debris. Thereby, 2 ml of a virus stock could be obtained, which generally had a titer of ~3x10¹⁰ pfu on A549. Aliquots of 0.1 or 0.5 ml were stored at -80°C.

Preparation of adenovirus stocks

To prepare high-titer Ad2 virus stocks A549 cells were grown in eight T175-flasks to 90% confluency. The cells were washed once with 10 ml DMEM without FCS. Then 8 ml DMEM without FCS containing 5×10^8 PFUs virus were added and incubated for 1.5 h at 37°C and 5% CO₂ with shaking every 10 min. Subsequently, 32 ml DMEM/2.5% FCS were added and cells were incubated until the cytopathic effect (cpe) reached 100%, which generally took 3 days. Infected cells were detached by shaking the flasks. The cell suspensions were centrifuged for 7 min. at 300 g and 4°C. The cell pellets were resuspended in a total volume of 14 ml sterile 30 mM Tris/HCl pH 8.0. Virus stocks of mutant Ads were prepared at a smaller scale by infection of three T175-flasks and the cell pellets were resuspended in 7 ml sterile 30 mM Tris/HCl pH 8.0. Viruses were released by 3-4 freeze/thaw cycles: Cells were frozen on dry-ice and quickly thawed at 37°C in a water bath. Finally, cell debris was removed by centrifugation (10 min., 3500 rpm, Heraeus Varifuge 3.0R) and the supernatant was split into aliquots of 0.5-1 ml and stored at -80°C.

Plaque assay

Adenovirus stocks were quantified by plaque assays (Mittereder et al., 1996). Virus stocks were diluted $1:10^{10}$, 10^9 , 10^8 , 10^7 in DMEM without FCS. A549 cells were grown to 95% confluency in 6 cm Ø dishes and washed once with DMEM without FCS. Then 1 ml DMEM containing different virus dilutions was added and incubated 1.5 h at 37°C, 5% CO₂ with shaking every 15 min. 2% sterile low melting point agarose (SeaPlaque, in H₂O) was solubilized in the microwave and a sufficient volume was equilibrated to 37°C together with 2x DMEM/6% FCS. At the end of the adsorption time medium was removed from the dishes. 2% low melting point agarose was mixed 1:1 with 2x DMEM/6%FCS and 5 ml per dish was used to overlay the cells. The dishes were left 10 min at RT (lids not tightly closed) until the agarose hardened and then transferred to the incubator (37°C, 5% CO₂). Every 4-5 day the 3 ml DMEM/1% agarose was added onto the overlay to provide sufficient nutritional components. At day 7 p.i. plaques appeared and were counted every day. The final PFU was determined when the plaque count was constant for 2-3 days. To facilitate detection of plaques neutral-red was added to the medium in the last round of overlay.

Preparation of 2x DMEM/6% FCS (250 ml): 6.7 g 2x DMEM powder (Gibco), 1.7 g NaHCO₃ were dissolved in 200 ml ddH₂O, the pH was adjusted to 6.8-7.0 with 1N HCl and ddH₂O added to a final volume of 232 ml. After passing the solution through a sterile filter unit 15 ml FCS (6% final conc), 2.5 ml P/S and 500 µl Fungizone were added.

Immunofluorescence

Subconfluent layers of A549, SV80Fas or SeBu cells were grown on sterile glass coverslips. Cells were rinsed with PBS and fixed with 3% (w/v) paraformaldehyde in PBS for 20 min. After

quenching aldehyde groups with 50 mM NH₄Cl and 20 mM glycine in PBS for 10 min, cells were permeabilized with 0.2% saponin in PBS with 5% FCS to block non-specific binding for 10 min. The cells were incubated with the primary antibody diluted in 0.2% saponin/5% FCS in PBS for 1h, washed four times with 1 ml 0.2% saponin in PBS and incubated with the secondary antibody (fluorescein- or rhodamine-conjugated goat or donkey anti-mouse, anti-rabbit or anti-sheep IgG, respectively, dilution 1:100) for 1 h. After four washing steps with 1 ml 0.2% saponin in PBS, the coverslips were mounted on glass slides with Histogel. The mounted cells were analyzed with a laser scanning confocal microscope.

Antibody	dilution
mouse mAb anti-Calnexin (AF8)	1:100
mouse mAb anti-EEA1	1:100
mouse mAb anti-Fas-Mix	B-G27, B-D27, DX3 each 1:40, ANC95.1/5E2 1:400
mouse mAb anti-FLAG octapeptide (M1)	1:1000 used in the presence of 1 mM CaCl ₂
mouse mAb anti-Galactosyltransferase (GTL-2)	1:200
mouse mAb anti-GM130	1:100
mouse mAb anti-Lamp-2 (2D5, supernatant)	1:10
mouse mAb anti-LBPA (6C4)	1:100
mouse mAb Tw1.3	undiluted hybridoma supernatant with 0.2% saponin
rabbit polyclonal serum anti-10.4K (Bur3)	1:100
rabbit polyclonal serum anti-10.4LLAA (R71)	1:100
rabbit polyclonal serum anti-Fas	1:100
R α 14.5K (prot A purified Bur4)	1:100
sheep anti-TGN46	1:100

Flow cytometry analysis

For flow cytometry analysis cells (293 or A549) in a 6 cm Ø dish were washed once with 5 ml PBS and detached with 0.5 ml warm Trypsin/EDTA for exactly 5 min. Then, the cells were resuspended in 5 ml DMEM containing 10% FCS and centrifuged (300 g, 5 min). Cell pellets were resuspended in ice-cold FACS (fluorescence activated cell sorter) buffer. The following steps were carried out on ice. 30 µl containing 0.5*10⁶ (A549) or 0.5-1*10⁶ (293) cells were added into a well of a 96-well plate prefilled with 70 µl ice-cold FACS buffer containing the first antibody (ca. 1 µg purified antibody or undiluted hybridoma supernatant). In the negative control cells were added to FACS buffer without antibody. After incubation for 45 min at 4°C, the antibody solution was diluted by addition of 70 µl of FACS buffer and cells were centrifuged for 3 min (300g, 4°C). The supernatant was flicked out of the 96 well plate and the cells were resuspended by vortexing the 96-well plate at 1300-1400 rpm. This cycle of washing and centrifugation was repeated 3 times with 190 µl FACS buffer and subsequently 50 µl of secondary antibody solution (G α M or G α R IgG from Sigma, dil. 1:50) was added to the cells. The 96-well plate was gently vortexed to resuspend the cells in the Ab solution. Subsequently, it was incubated for 40 min at 4°C in the dark. The

antibody binding step was stopped by addition of 130 μ l of FACS buffer to each well and centrifugation. After three washing/centrifugation steps with 190 μ l FACS buffer the cells were resuspended in 100 μ l FACS buffer and transferred to plastic tubes with 400 μ l FACS buffer and 5000 cells were analyzed in a FACSCalibur flow cytometer. From the mean value of fluorescence background staining obtained with secondary Ab alone was deducted. If the MVF was measured using polyclonal antibodies (rabbit sera) in the primary Ab incubation step, the background fluorescence was determined on a separate sample incubated in parallel with the corresponding preserum (dil. 1:100). For determination of intracellular FLAG-14.5K content with mAb M1 background control was carried out by incubating cells IgG2b isotype control Ab MA215. Whereas hybridoma supernatant of mAb Tw1.3 was used for determination of intracellular E3/19K content in 293 E3-transfectants, this primary antibody gave a high background on infected A549 cells, and supernatant 3A9 was used instead.

FACS buffer: 3% (v/v) FCS, 0.02% (w/v) NaN_3 in PBS

For intracellular staining FACS buffer with 0.1% (w/v) saponin was used.

Antibody	dilution
3A9 anti-Ad2 E3/19K	Hybridoma supernatant undil.
528 anti-EGFR	Hybridoma supernatant undil.
B-G27 anti-Fas	1:10
M1 anti-FLAG	1.1 μ g/sample with or without addition of 0.1% saponin
mAb DR4 1H5	0,9 μ g/sample
mAb DR5 3F11	0,8 μ g/sample
Polyclonal Ab R α DR4	1:100
Polyclonal Ab R α DR5	1:100
Polyclonal Ab R59 anti-10.4K	1:100 in FACS buffer with saponin
Tw1.3 anti-Ad2 E3/19K	Hybridoma supernatant, used with 0.1% saponin and the additon of 0.7 μ g/sample purified Tw1.3
Tw1.3 anti-Ad2 E3/19K purified	3.6 μ g/sample dil. in FACS buffer with saponin
W6/32 anti-HLA-A,-B,-C	1:40 (3 μ g/sample)

2.2.5 Protein techniques

Metabolic labeling and immunoprecipitation

Cells were grown on 6 cm \varnothing culture dishes to 80-90% confluency. After washing once with 3 ml RPMI without methionine and cysteine, cells were incubated with 2 ml RPMI without methionine and cysteine for 1h to deplete the intracellular levels of methionine and cysteine. Then cells were metabolically labeled (293 E3 transfectants: 200 μ Ci of each [35 S]-methionine and [35 S]-cysteine in 1 ml RPMI) for 1 hour. The cells were washed once with cold DMEM, once with cold PBS and then lysed with 1 ml IP-lysis buffer containing freshly added protease inhibitors at 4°C for 15 min. The supernatant was transferred to 1.5 ml tubes. After 15 min centrifugation at 14000

rpm (4°C, cooled microcentrifuge) supernatants were transferred to new 1.5 ml tubes. To monitor the incorporation of radioactive label 5 µl lysate were added to 1 ml scintillation cocktail and the amount of radioactivity was measured with a β-counter. All further incubations were performed at 4°C. Preequilibrated protein A-Sepharose (see below) was washed 3x with buffer B and a 50% slurry was prepared. 50 µl of the 50% slurry was added to each sample, followed by incubation for 50 min. rotating in a head-over-tail shaker. The protein A-Sepharose beads were spun down for 30 s at 14000 rpm (microcentrifuge). The clear lysate was added to 7 µl monoclonal TW1.3 (5-10 µg) in a fresh 1.5 ml tube and incubated for 45 min rotating head-over-tail. 50 µl of a 50% protein A-Sepharose slurry was added followed by another incubation for 45 min rotating in an overhead mixer. The protein A-Sepharose beads were centrifuged for 30 s at 14000 rpm (microcentrifuge). The pellet was washed 3x with 1 ml buffer B, 2x with 1 ml buffer C and 1x with 1 ml 10 mM Tris pH 8.0. Finally, the pellet was centrifuged for 2 min. at 14000 rpm (microcentrifuge). The supernatant was completely removed and the samples were resuspended in complete SDS sample buffer for SDS-PAGE on a 11.5-13.5% gradient Maxigel. For testing different boosters of rabbit serum R59 and R71 for specific antibody development infected A549 cells (12 h p.i., 10 pfu/cell) were labeled with 100 µCi each [³⁵S]-methionine and [³⁵S]-cysteine and the serum and corresponding pre-serum were used for IP in a 1:200 dilution. Immunoprecipitates were separated on a 15% maxigel.

Promix™: 70% L-[³⁵S]-methionine, 30% [³⁵S]-cysteine, 14.3 mCi/ml, specific activity >1000 Ci/mmol

IP-lysis buffer: 1% Triton X-100 or digitonin

140 mM NaCl

5 mM MgCl₂

20 mM Tris pH 7.6

8 µg/ml PMSF (stock 20 mg/ml in isopropanol)

10 µg/ml trypsin inhibitor (stock 10 mg/ml)

0.5 µg/ml leupeptin (stock 2 mg/ml)

Buffer B: 0.2% Triton X-100 or digitonin

150 mM NaCl pH 8.0

2 mM EDTA pH 8.0

10 mM Tris pH 7.6

Buffer C:

0.2% Triton X-100 or digitonin

500 mM NaCl

2 mM EDTA pH 8.0

10 mM Tris pH 7.6

Preequilibration of protein A-sepharose:

1.5 g protein A-sepharose CL-4B were washed with 20 ml 100 mM Tris pH 8.0 for 30 min. on a rolling shaker at 4°C followed by centrifugation at 2200 rpm in a Varifuge 3.0R centrifuge. Subsequently, washing was repeated 2x with 20 ml 50 mM Tris pH 8.0 for 5 min. and once with 20 ml 10 mM Tris pH 8.0. Finally, the protein A-Sepharose was resuspended in 10 mM Tris pH 8.0 to obtain a 50% slurry.

SDS PAGE**a) Maxigel**

Gel electrophoresis was performed using a 15% gel or a (11.5 % to 13.5 %) gradient gel (200 x 300 x 1 mm) (Laemmli, 1970). For pouring gradient separation gels the two solutions were mixed in a gradient former. During polymerization the gel was overlaid with isopropanol. The stacking gel solution was poured on top of the separation gel and a comb (20 wells, 0.8 cm wide) was inserted. The gel electrophoresis apparatus was assembled. IP samples in 25 μ l complete sample buffer were heated for 5 min. to 95°C. After cooling to RT 5 μ l 0.5 M iodacetamide was added and samples were incubated for 15 min at RT. Then the samples were centrifuged for 2 min. at 14000 rpm (microcentrifuge) and loaded on the gel. 10 μ l of ¹⁴C-methylated proteins were used as molecular weight marker (5,740-30 kD). Separation was performed at 18-25 mA constant current for 12-18 h. Then the gel was fixed in fixing solution for 45 min, transferred to Whatman paper, covered with plastic foil and dried for 2 h at 80°C under vacuum in a gel dryer. Dried gels were exposed to BioMaxMR films at -80° C or phosphorimager screens at RT. Radioactive bands were quantified using a Storm 860 Molecular Imager. films were developed using an automatic film developing machine.

Separation gel:	11.5%	13.5%	15%
Acrylamide/Bisacrylamide (29:1)	15.3 ml	18 ml	40 ml
2 M Tris pH 8.8	8.4 ml	8.4 ml	16.8 ml
20 % SDS	0.2 ml	0.2 ml	0.4 ml
H ₂ O	16.1 ml	3.3 ml	22.6 ml
60% sucrose	-	10 ml	-
10 % APS	120 μ l	120 μ l	120 μ l
TEMED	20 μ l	20 μ l	40 μ l
Stacking gel:	5%		
Acrylamide/Bisacrylamide (29:1) 5 ml			
0.5 M Tris pH 6.8	4 ml		
20 % SDS	0.15 ml		
H ₂ O	14 ml		
60% sucrose	7 ml		
10 % APS	150 μ l		
TEMED	15 μ l		
Sample buffer pH 8.8 (stock):	10 ml 2 M Tris pH8.8 (200 mM final conc.) 57.14 ml 60% sucrose (1M final conc.) 1 ml 500 mM EDTA (5mM final conc.) 0.01 g bromophenolblue (0.01% final conc.) H ₂ O ad 100 ml		
Sample buffer (complete):	1 ml sample buffer pH 8.8, 100 μ l 0.5 M DTT , 200 μ l 20% SDS		
Fixing solution (1 l):	8% acetic acid, 46% methanol		
Electrophoresis buffer (5 x):	30 g/l Tris, 144 g/l glycine, 0.5% SDS (added just before use)		

b) Minigel

Gel electrophoresis with minigels was performed using the Protean II system (Bio-Rad) with 15% gels (80 x 50 x 1 mm). IP samples were mixed with 25 µl sample buffer and further processed as described for maxigels. As molecular weight marker 10 µl of Protein marker Dalton VII-L (14-70 kD, 3.5mg of lyophilized mix dissolved in 1.5ml complete sample buffer) were loaded.

Separation gel:	15%	Stacking gel:	5%
Acrylamide/ Bisacrylamide (29:1)	5 ml	Acrylamide/ Bisacrylamide (29:1)	1.7 ml
2 M Tris pH 8.8	2.1 ml	0.5 M Tris pH 6.8	1.4 ml
H ₂ O	2.8 ml	H ₂ O	6.8 ml
20 % SDS	50 µl	20 % SDS	50 µl
10 % APS	40 µl	10 % APS	50 µl
TEMED	5 µl	TEMED	10 µl

Electrophoresis buffer (10 x): 30.28 g/l Tris, 144 g/l glycine, 1% SDS (added directly before use)

Immunoprecipitation and Western blotting**a) Preparation of cell lysate**

Cells were grown to nearly 100% confluency in 6 cm Ø (10 cm Ø) culture dishes, washed with ice-cold PBS and lysed with 1ml (3ml) IP-lysis buffer containing freshly added protease inhibitors at 4°C for 15 min. The supernatant was transferred to 1.5 ml tubes. After 15 min centrifugation at 14000 rpm (4°C, cooled microcentrifuge) the supernatants were transferred to new 1.5 ml tubes or samples with volumes of more than 1 ml were pooled in a 15ml Falcon tube. At this point aliquots were taken for determination of the total protein content using BCA protein assay kit. 1 ml aliquots of equal protein content were prepared from all samples and used for immunoprecipitation or if not used immediately, stored at -80°C.

b) Immunoprecipitation

In modification of the immunoprecipitation protocol for radioactively labeled lysates 5 µl preserum (rabbit polyclonal Ab) were added to a 1 ml aliquot of the lysate, mixed by vortexing and incubated on ice for 20 min. Preequilibrated protein A-Sepharose was washed 3x with buffer B and a 50% slurry was prepared. 50 µl of the 50% slurry was added to each sample, followed by incubation for 50 min rotating in a head-over-tail shaker. The protein A-Sepharose beads were centrifuged for 30 s at 14000 rpm (microcentrifuge). Then 980 µl of lysate was transferred to a new 1.5 ml tube and incubated on ice with 5 µl of specific serum (rabbit) for 20 min.. 50 µl of a 50% protein A-Sepharose slurry was added followed by another incubation for 45 min rotating in an overhead mixer. The protein A-Sepharose beads were centrifuged for 1 min at 14000 rpm (microcentrifuge). The pellet containing the immunocomplexes was washed 3x with 1 ml buffer B, 2x with 1 ml buffer C and 1x with 1 ml 10 mM Tris pH 8. Finally, the pellet was centrifuged for 2

min at 14000 rpm (microcentrifuge). The liquid was completely removed and the pellets were resuspended in 25 μ l SDS sample buffer and analyzed by SDS-PAGE on a 15 % minigel.

c) Protein blotting and detection

Proteins were blotted onto nitrocellulose membranes using the Trans-Blot SD Semidry Transfer Cell (Bio-Rad). A sheet of nitrocellulose membrane and eight pieces of Whatman filter paper of the same size as the gel were soaked with transfer buffer. A stack of four sheets of filter paper, the nitrocellulose membrane, the gel and another four sheets filter paper was assembled avoiding inclusion of air-bubbles and with the nitrocellulose facing the anode. Blotting was performed at 0.8 mA/cm² for 80 min. Protein bands were visualized after 2 min incubation of the membrane in Ponceau staining solution, to cut out lanes for separate antibody incubations. Ponceau staining solution was removed by washing the membrane with PBS. Unspecific binding sites were blocked by incubation o/n at 4°C in PBS/0.05% Tween 20, 5% skim milk powder, 0.02% NaN₃. Then, incubation with the primary antibody (rabbit sera, dil. 1:200) was performed at RT for 1 hour in 2-4 ml PBS/0.05% Tween 20 in a rotating Falcon tube. After five washing steps for 15 min. in 200 ml PBS/0.05% Tween 20 the membrane was placed for 1 hour in 25 ml PBS/0.05% Tween 20 containing the secondary antibody Peroxidase-conjugated goat anti-Rabbit IgG (1:10000 – 1:20000) with constant shaking at 40 rpm. Subsequently, the membrane was washed 5x 10 min and 1x 30 min in 200 ml PBS/0.05% Tween 20. Then the blotted proteins were detected using the ECL Western blotting detection system (Amersham-Pharmacia) according to the manufacturer's instructions. The membrane was exposed to BIOMAX-MR autoradiography films for different time periods.

Transfer buffer (1l): 5.8 g Tris base, 2.9 g Glycine, 0.37 g SDS, 200 ml Methanol, H₂O ad 1l

Ponceau solution (100 ml): 0.5 g Ponceau S, 1 ml Glacial acetic acid, 98.5 ml H₂O

d) Coomassie blue staining

For Coomassie blue staining of proteins, SDS-PAGE gels were incubated in Coomassie blue staining solution (0.25% Coomassie brilliant blue R-250, 45% methanol, 10% acetic acid) for 12 h and destained with 30% methanol/10% acetic acid by changing the destaining solution until the desired protein staining was visible.

Surface plasmon resonance

In order test the *in vitro* binding of the clathrin adaptor complexes AP-1 and AP-2 an interaction analysis was performed by Stefan Höning, University of Göttingen, Göttingen, Germany. Wt and mutant 10.4 and 14.5 cytoplasmic tail peptides were coupled to a CM5 sensor chip. Interaction was analyzed using a BIAcore 2000 (BIAcore AB). Purified AP-1 and AP-2 were used at 100 nM in buffer A (20 mM HEPES pH 7.0, 150 mM NaCl, 10 mM KCl, 2 mM MgCl₂,

0.2 mM dithiothreitol) and injected at a flow rate of 20 $\mu\text{l}/\text{min}$. Association (2 min) was followed by dissociation (2 min) during which buffer A was perfused. The equilibrium constant (K_D) was determined as described (Honing et al., 1997).

Production of rabbit polyclonal antibodies

For generation of antiserum R59 one Newzealand White rabbit was immunized with approximately 1 mg of 10.4 cytoplasmic tail peptide in 500 μl PBS mixed with 500 μl complete Freund's adjuvant by subcutaneous injection. For generation of R71 another rabbit was immunized with a mixture of KLH-coupled mutant peptide and free peptide (total 725 μg of peptide) emulsified with complete Freund's adjuvant. In 4 week intervals the rabbits were immunized with the same dose of immunogen mixed with incomplete Freund's adjuvant. 20-25 ml blood were taken (i.v.) on day 10 after each boost. All immunization steps and bleedings were performed by Christian Kuenzel, Max-von-Pettenkofer Institut, Munich, Germany. Serum was recovered by incubation at RT for several hours, 30 min. incubation at 37°C and o/n at 4°C followed by centrifugation of the blood sample for 15 min at 3000 rpm (Heraeus Varifuge 3.0R). A serum aliquot of 0.5 ml was kept at 4°C (0.02 % sodium azide), the rest was stored at -80°C. Specific antibody development was tested in immunoprecipitation/metabolic labeling experiments on infected A549 cells. The rabbit was sacrificed when the specific activity of the antibodies remained constant.

Results

3. Relevance of strictly conserved amino acids for Ad2 10.4-14.5K function

3.1 Identification of strictly conserved amino acids within 10.4K and 14.5K

The adenovirus E3/10.4K and E3/14.5K proteins are encoded by a clustered sequence block which is found in all subgroups of human adenoviruses. Interestingly, these sequences exhibit a high degree of variability. It is thus conceivable, that amino acids conserved among 10.4-14.5K proteins from different subgenera might be required for 10.4-14.5-induced down-regulation of plasma membrane receptors. Recently, the sequences of the 10.4K and 14.5K genes of subgenus D (Burgert and Blusch, 2000) and subgenus E Ads (Burgert et al., 2002) were determined allowing a complete comparison of 10.4K and 14.5K proteins from Ads of all subgroups. (Fig. 8A and 8B). Except for the subgenus F homologs Ad40 and Ad41 (90 residues), 10.4K sequences share a length of 91 amino acids, but only 15 amino acids are strictly conserved. The majority of strictly conserved residues is distributed over the C-terminal cytoplasmic tail sequence, which is rather short (~30 amino acids). Remarkably, a highly polar cysteine-serine pair is conserved in the central part of the predicted transmembrane domain. In the extracellular domain the cysteine residue that forms the disulfide bond between 10.4K species is strictly conserved (Fig. 8A).

By contrast to the constant length of 10.4K, the length of the mature 14.5K protein varies from 91 to 127 amino acids (Fig. 8B). Furthermore, the sequence homology between 14.5K proteins of different subgenera is significantly lower (average ~30%) than that of its interaction partner 10.4K (40 to 52%). In the mature 14.5K protein, only 9 amino acids are strictly conserved. Three of them are adjacent to each other forming a SYF triplet positioned 10 amino acids upstream from the C-terminus.

Another remarkable feature of the 14.5K cytoplasmic tail sequence is the high content of proline residues (especially in subgenus D proteins), one proline being strictly conserved. Proline-rich sequences containing a PXXP consensus might act as protein interaction modules for SH3 domain-containing proteins (Mayer, 2001), which might also be true for the 14.5K proline-rich region (Burgert and Blusch, 2000). Some of the conserved amino acids within 10.4K and 14.5K may be part of putative tyrosine-based or dileucine-type transport motifs, consensus sequences previously shown to mediate transport into endosomes/lysosomes (Bonifacino and Traub, 2003; Kirchhausen, 1999): In 14.5K, two YXX Φ motifs, designated Y⁷⁴XX Φ and Y¹²²XX Φ according to the position of the Y in the Ad2 14.5K sequence, are strictly conserved (Fig. 8B). The Y¹²²XX Φ motif is commonly found in position -9 from the C-terminus, whereas Y⁷⁴XX Φ may be located

◀ Fig.8 Identification of strictly conserved amino acids within 10.4K and 14.5K proteins from Ads of all human adenovirus subgenera

Amino acid sequence comparison of E3/10.4K (A) and E3/14.5K (B) proteins. Multiple alignment was carried out with DNAMAN software using the optimal alignment instruction. For each subgroup representative members were chosen (listed on the left of the sequence comparison). The 14.5K sequence alignment was further refined manually in accordance with a more extensive sequence comparison (see (Burgert et al., 2002)). The predicted signal sequences and transmembrane domains are underlined. Amino acids present with >50% homology between the given examples are shaded, a dash marks the lack of the corresponding amino acid. Stars (*) denote amino acids identical in all serotypes sequenced to date (Burgert et al., 2002). YXXΦ and LL consensus motifs are indicated on top of the sequence comparison. Genbank accession numbers and references for E3 sequences are as follows: Ad2 (Herisse et al., 1980; Herisse and Galibert, 1981), Ad5 M73260, Ad3 (Signas et al., 1986), Ad35 (Basler et al., 1996), Ad4 AF361223 (Burgert et al., 2002), Ad15, Ad19a (Burgert and Blusch, 2000), Ad12 (Sprengel et al., 1994) and Ad40 (Davison et al., 1993). ‡ D not strictly conserved, as e.g. N instead of D in Ad8 of subgenus D. For details refer to text.

close to or within the lipid bilayer (Fig. 8B and Fig. 5). A third YXXΦ sequence element with Y at position 76, overlapping the Y⁷⁴XXΦ element, is present only in 14.5K proteins of subgenus C Ads. These tyrosine-based consensus motifs appear to be in close proximity to the putative interface with the transmembrane domain (Burgert and Blusch, 2000). Two putative dileucine motifs reminiscent of transport motifs can be recognized in the cytoplasmic tail of 10.4K (Fig. 8A). One LL motif is conserved at position -4/-5 (in Ad12 at -5/-6) from the C-terminus (L⁸⁷L⁸⁸ in the Ad2 sequence) with the first Leu being replaced by Ile in subgenus D proteins. The last two amino acids, either IL in subgenus C or LI in subgenera B, D and E may also constitute transport motifs. Additional YXXΦ motifs can be recognized in the cytosolic portion of 10.4K proteins of subgenus D and F exclusively.

3.2 Functional relevance of strictly conserved amino acids in 14.5K

To investigate whether some of the strictly conserved amino acids within the 14.5K protein sequence are functionally relevant, the corresponding residues in the Ad2 14.5K sequence were replaced by alanine. Mutations were introduced into plasmid pBSΔX-E3/F14.5, containing the entire Ad2 E3 region which was modified to encode a FLAG-tagged version of 14.5K, with an octapeptide-tag fused to the N-terminus of the mature 14.5K. First, it was ensured that FLAG-tagged 14.5 (F14.5) had a functional activity similar to unmodified 14.5. Stable E3/F14.5⁺ 293 transfectants, namely E3/F14.5-19, E3/F14.5-8, and E3/F14.5-16 cells provided by A. Elsing (in Fig. 9 referred to as F-19, F-8, F-16, respectively) were selected that expressed similar levels of intracellular E3/19K and surface HLA molecules as the E3⁺ reference cell line (E3-45) expressing untagged 14.5 (Fig. 9). Comparison of the FACS data for surface expression of Fas and the EGFR demonstrated that receptor down-modulation is as effective in cells expressing FLAG-tagged 14.5K

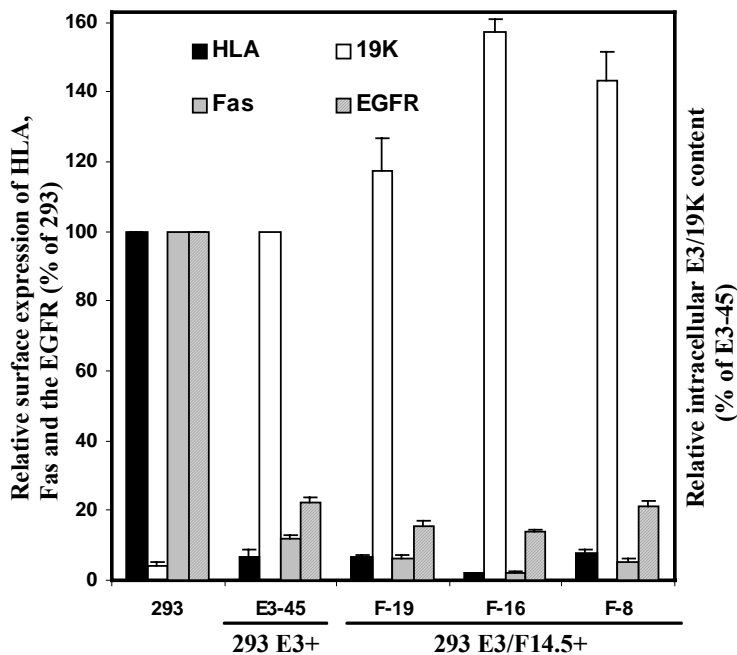


Fig. 9 Down-regulation of Fas and the EGFR in E3+ 293 cells expressing Flag-14.5K

Relative expression of plasma membrane proteins HLA, Fas, EGFR and intracellular content of E3/19K as determined by FACS analysis on 293 cells and 293 E3 transfectants expressing unmodified 14.5K (clone E3-45) or FLAG-tagged 14.5K (clones F-19, F-16, F-8). HLA and E3/19K expression was measured with mAbs W6/32 and Tw1.3, respectively, followed by incubation with FITC-labeled goat anti-mouse IgG (SIGMA, Munich, Germany). Analysis of intracellular E3/19K content was carried out in the presence of 0.1 % saponin. Fas and EGFR were detected by mAbs B-G27 and 528, respectively. After deduction of the background staining obtained with the secondary antibody alone, the mean value of fluorescence (MVF) for each cell clone was related to that of 293 cells, which was set to 100%. The 19K MVFs were related to E3-45 cells, a representative clone of 293 cells expressing wild-type E3 proteins. The bars denote the mean value calculated from three measurements. Error bars depict the standard error of the mean (SEM).

as in cells expressing unmodified 14.5K. The E3/F14.5-19 cell line, hereafter referred to as F-19, was chosen as a positive control for protein expression in E3/F14.5-transfected 293 cells.

Upon transfection of mutant plasmids into 293 cells and selection of stable transfectants with G418, the effect of the mutation was quantitatively assessed by measuring Fas and EGFR cell surface expression using FACS analysis. The 293 system was previously shown to allow efficient expression of E3 proteins, due to the presence of E1A proteins in 293 cells which transactivate the E3 promoter (Burgert and Kvist, 1985; Elsing and Burgert, 1998; Korner et al., 1992; Sester and Burgert, 1994). The system has the additional advantage of easy standardization of E3 protein expression levels (copy number) by monitoring expression of E3/19K, an unrelated E3 protein not affected by the mutations introduced in 10.4K and 14.5K (Elsing and Burgert, 1998). Thus, upon standardizing E3 expression, the effect of each mutation on Fas and EGFR modulation was compared. Transfectant clones were first screened for intracellular E3/19K expression. In general, 5 or 8 independent clones from each transfection with levels comparable to transfectants expressing wild-type E3 proteins and with similar HLA modulation (Burgert and Kvist, 1985;

Elsing and Burgert, 1998) were selected for further analysis. In a series of at least three independent measurements the mean value of fluorescence (MVF) for each clone was determined and related to that of untransfected 293 cells measured in parallel. Thereby, variations introduced by different experimental conditions were compensated. Additionally, receptor surface expression levels on pSV2-neo^r-transfected 293 cells (pneo) were analysed. For each individual clone relative receptor expression levels (% of 293 cells) determined in different experiments were combined to calculate the arithmetic mean. Mean values of 5-8 individual clones were used to determine the overall arithmetic mean value and standard error for each cell line (depicted in Fig. 10). For simplicity mutant cell lines are designated with the single letter code of the amino acid that was replaced by alanine and its position in the Ad2 14.5K protein sequence. Results for the mutant cell lines were compared to those of the reference cell line F-19 expressing wt E3 proteins.

The average level of intracellular E3/19K content was very similar among the selected clones and was comparable to that of F-19 cells set to 100% (Fig. 10A, white bars). Accordingly, cell surface expression of HLA in all these clones was reduced by at least 75% (Fig. 10A, black bars). Having established a comparable E3 protein expression level, the relative efficacy of each 10.4-14.5K mutant to modulate Fas and EGFR was determined by flow cytometric analysis of their cell surface expression (Fig. 10B and 10C). In F-19 cells which expressed wild-type 10.4-14.5K proteins Fas surface expression was reduced to ~10% of the levels expressed on 293 cells. EGFR levels corresponded to ~20% of those on 293 cells.

The down-modulating capacity was largely retained in cells expressing the 14.5Y⁴⁴A mutant, as Fas levels on these cells were drastically reduced and similar to those of F-19. EGFR surface expression was decreased to 35% of the levels on 293 cells, corresponding to at least 80% of the reduction determined for F-19 (Fig. 10B and 10C). Replacing the neighbouring amino acid C43 by alanine more severely affected function. Fas expression corresponded to ~47% of that on the surface of 293 cells. EGFR levels were only slightly decreased, ranging at about 80% as compared to 293 cells. Interestingly, the other conserved cysteine in the luminal domain, C32, showed a remarkably similar phenotype. The C32 cell line had mean values of E3/19K expression and HLA levels comparable with those of the C43 mutant, permitting to compare the results for receptor down-modulation of these two cell lines. Inspection of the mean values for Fas and EGFR levels on these transfectants revealed that on average Fas levels on C³²A transfectants (37,6%) reached only 80% of those on C⁴³A clones. Despite a higher variation in EGFR surface expression among individual C⁴³A clones, the mean value of their EGFR levels (64,4%) appeared to be increased at a similar ratio. Thus, in both mutants the reduction in EGFR levels was less efficient than that of Fas and the C⁴³A substitution had a slightly higher impact on Fas

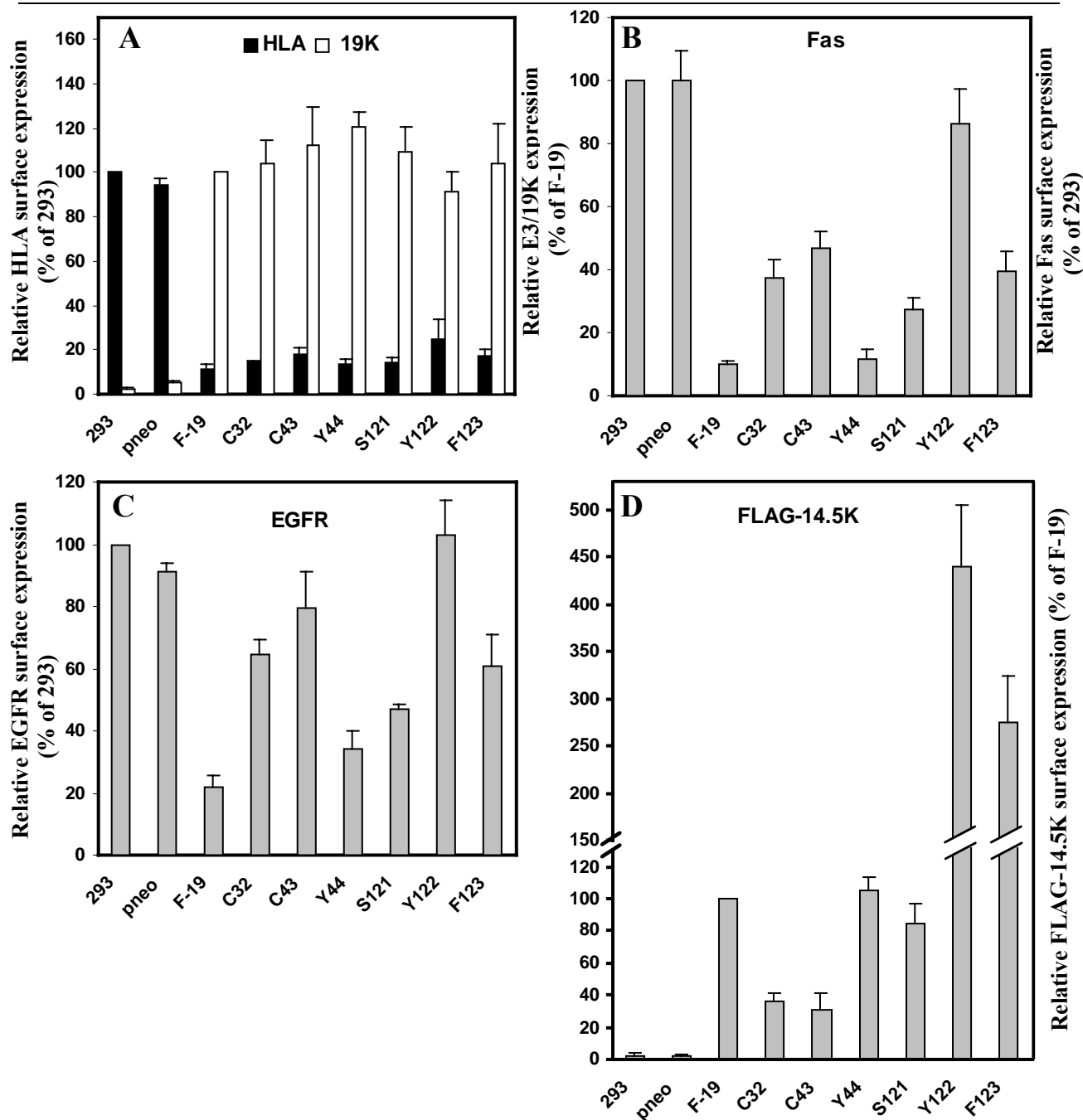


Fig. 10 Cell surface expression and function of wt and mutant FLAG-14.5K

(A) Relative cell surface expression of HLA (black bars) and intracellular E3/19K content (white bars) as determined by FACS analysis on E3/F14.5+ 293 transfectants expressing wt (F-19) or mutant FLAG-14.5K, pSV2-neo^r-transfected (pneo) or untransfected 293 control cells. Mutant E3/F14.5+ cell lines are designated with the substituted amino acid. Antibodies were as described in Fig. 9. After deduction of the background staining obtained with the secondary antibody alone, the mean value of fluorescence (MVF) for each cell clone was related to that of 293 cells (HLA) or F-19 cells (19K), which was set to 100%. Data were compiled from 3 independent experiments using 3 to 8 representative clones from each mutant cell line and the control cells. Error bars represent the SEM. **(B)+(C)** Relative Fas and EGFR surface expression on cell lines analyzed in A. Data were derived as described in (A) except for the EGFR levels on mutant Y122 which were determined in a single experiment with three selected clones. **(D)** Anti-FLAG mAb M1 was employed for monitoring FLAG-14.5K surface exposure, followed by incubation with FITC-labeled goat anti-mouse IgG. After deduction of background staining obtained with secondary antibody alone the MVFs for each cell line were related to that of F-19 cells (set to 100%) determined in the same experiment.

and EGFR down-modulation (Fig. 10B and 10C).

Mutations of strictly conserved amino acids (S121, Y122, F123) within the 14.5K cytoplasmic tail sequence also affected down-modulation of both Fas and the EGFR (Fig. 10B and 10C). As expected from the results obtained with E3/14.5Y¹²²A mutants (see Fig.7, chapter 1.9) the corresponding FLAG-tagged mutant (designated Y122) showed no loss in Fas and EGFR surface expression. In the previous series of experiments with non-FLAG-tagged E3/14.5Y¹²²-transfectants Fas and EGFR expression levels were similar to those seen for 293 E3-transfectants that lack expression of 10.4K and 14.5K (Fig. 7, (10.4-14.5)ko cell line). In good correlation, the FLAG-tagged mutant cell line 14.5Y¹²²A exhibited 85% of the Fas surface expression on 293 cells, which corresponded exactly to the mean value of 293 E3 transfectants expressing non-FLAG-tagged 14.5Y¹²²A (see Fig. 7). EGFR surface expression on Y¹²²A clones was restored to the levels seen on 293 cells, indicating a complete loss of function regarding down-modulation of the EGFR. In conclusion, alanine replacement mutation of Y122 in 14.5K severely suppressed down-regulation of both receptor targets, Fas and the EGFR.

The serine S121, directly preceding Y122, seemed not to be essential for down-modulation to occur. Fas levels were reduced to below 30%, and EGFR levels below 50% of those on 293 cells. Substitution of F123, the C-terminal neighbour of Y122, more severely affected functional activity of 14.5K, with 40% Fas and at least 60% EGFR surface expression as compared to 293 cells. If one compares the reduction of surface expression levels on F-19 cells with that of the mutant cell lines it becomes obvious that all the mutations introduced in 14.5K caused a more pronounced suppression of EGFR modulation than Fas down-regulation (Fig. 9). Similarly, in the wild-type situation the reduction in relative surface expression on 293 E3+ cells was generally less for the EGFR than for Fas (Fig. 9 and Fig. 10).

3.3 Surface expression levels of mutant FLAG-14.5K

The FLAG-tag fused to the N-terminus of the mature 14.5K allowed to quantitatively monitor 14.5K expression on the cell surface by flow cytometry with monoclonal antibody (mAb) M1. 14.5K mutant Y⁴⁴A had been shown to retain most of its functional activity and appeared to have normal surface expression levels (Fig. 10D). By contrast, the functional knock-out Y¹²²A resulted in a 4-5 fold increase of 14.5K surface expression. Thus, functional loss by this single amino acid substitution in 14.5K was accompanied by a profound alteration of intracellular localization of the 14.5K protein. Similarly, the other alanine replacement mutations which had been shown to impair functionality of the 10.4-14.5K complex to some extent were associated with

altered surface expression levels of 14.5K. Mutation of the cysteines in the extracellular domain reduced 14.5K surface expression to 30-40%. The S¹²¹A mutant, which exhibited higher down-modulation capacity also showed higher surface expression of 14.5K reaching 84% of those on F-19 cells. Similar to the phenotype observed for the Y¹²²A mutant, substitution of F123 led to a dramatic increase in 14.5K surface expression levels. About 3 fold higher amounts of 14.5K were detected on the cell surface as compared to F-19. Thus, strictly conserved residues Y122 and F123 contained within the Y¹²²XXΦ consensus caused an increase in 14.5K surface expression, whereas the strictly conserved residue S121 preceding this sequence element seemed not to be essential, as on these cells FLAG-14.5K surface expression reached 80-90% of the levels of wild-type E3/F14-5 transfectants. The integrity of tyrosine Y122 seemed to be most critical as it was associated with an immense increase in FLAG-14.5K surface expression, even higher than that on F¹²³A cells, and it was shown to be of crucial functional importance *in vivo*, inhibiting down-modulation of both Fas and the EGFR.

In addition to tyrosine Y122, a second strictly conserved tyrosine within the 14.5K cytoplasmic tail, Y74, had previously been shown to be functionally relevant, as Fas levels on the mutant E3-transfectants remained at 74% and EGFR levels even higher, corresponding to 90% of the levels on 293 cells (as depicted in Fig. 7). Both tyrosines are part of YXXΦ consensus sequences found in all human adenovirus subgroups. In subgroup C viruses a third YXXΦ motif starting with tyrosine Y76, and partially overlapping the Y⁷⁴XXΦ motif, is present in the 14.5K sequence. The Y⁷⁶A substitution only slightly decreased the efficiency of Fas and EGFR down-regulation, and therefore, Y⁷⁶ does not seem to be critical for 10.4-14.5 function (Fig. 7).

Taken together, the FACS analysis of 293 E3-transfectants revealed that among the strictly conserved amino acids of 14.5K two strictly conserved tyrosines at position Y¹²² and Y⁷⁴ of the Ad2 14.5K sequence are of crucial functional importance *in vivo*. The aim of the following study was to explore the function of these critical tyrosines and their implication in the mechanism of receptor down-regulation. As loss of function mutant Y122A was associated with an alteration of 14.5K surface expression levels, the importance of putative YXXΦ and dileucine type sorting signals for 10.4-14.5K function was analyzed.

3.4 Complex formation of 10.4K with 14.5K mutants

Given that both 10.4K and 14.5K are required for down-regulation of Fas and the EGFR and that they form a complex in infected cells *in vivo* (Elsing and Burgert, 1998; Tollefson et al., 1991), it is conceivable that complex formation is a prerequisite for 10.4-14.5 function. Therefore,

14.5K mutants with a loss of function phenotype were examined for their ability to interact with 10.4K. Alanine replacement mutants of Y⁷⁴ and Y¹²² were analyzed. Additionally, the mutant cell line Y76 was included in the experiment, as Y⁷⁶ is also the first residue of a YXXΦ consensus sequence in Ad2 14.5K.

Complex formation was assayed by immunoprecipitation of 14.5K from detergent lysates and subsequent detection of associated 10.4K by western blotting (see also *Materials and Methods*). Interestingly, immunoprecipitation of 10.4K did not coimmunoprecipitate the 14.5K protein, presumably because the epitope in the 10.4K cytoplasmic tail was masked by 14.5K in the complex (data not shown). This is in accord, with results reported by another group, that a peptide serum directed against the C-terminal 15 amino acids of the Ad2 10.4K protein immunoprecipitated solely 10.4K, whereas immunoprecipitation of Ad5 14.5K with sera directed against amino acids 19-34 or 118-132 efficiently coimmunoprecipitated 10.4K (Tollefson et al., 1991), indicating that the extreme N- and C-termini of 14.5K are accessible in the 10.4-14.5K complex.

One representative clone from each transfection was lysed in Triton X-100 (Trit) or the less stringent detergent Digitonin (Dig) and from all the lysates equal amounts of protein were subjected to immunoprecipitation. In addition to being as effective in down-modulation of Fas and the EGFR on E3-transfectants as the unmodified version, the FLAG-tagged 14.5K wt protein was found to associate with 10.4K (Fig. 11A, lane 2). The immunoblot signal of 10.4K revealed two bands corresponding to the two isoforms of 10.4K. The protein represented by the upper band retains the N-terminal signal sequence for membrane insertion, whereas the cleaved isoform migrated as the lower band (Tollefson et al., 1990b). Similar to the wild-type proteins, both isoforms of 10.4K are visualized in the extracts containing the Y¹²² mutant (Fig. 11A, compare lanes 2 and 5). Thus, the interaction of the 14.5Y¹²²A mutant with 10.4K was not significantly altered. Digitonin lysis allowed to detect higher amounts of 10.4-14.5K complexes than Triton X-100 lysis. Therefore, the non-covalent association of 10.4K with 14.5K was sensitive to different types of detergents and digitonin was better suited for analysis of 10.4-14.5K complex formation. The interaction of the Y⁷⁶A mutant seemed to be reduced as the 10.4 bands could only be detected after lysing the cells in the mild digitonin buffer (Fig. 11A, lane 4). Obviously, this reduced stability of the complex in Triton extracts was not critical for the *in vivo* function (compare Fig. 7). Remarkably, no significant interaction of 10.4K with 14.5 Y⁷⁴A was detected in either detergent. This was not due to an inefficient E3 expression in this particular clone, as E3/19K levels were comparable to wild-type and the other mutant cells (Fig. 11B). To examine whether the altered complex formation is caused by an altered expression of the individual subunits, the total

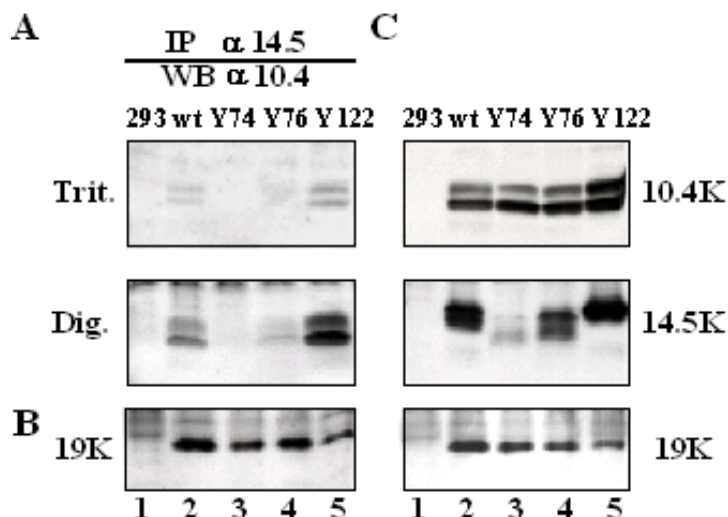


Fig. 11 Association of 10.4K with mutant 14.5K

(A) Representative clones of 293 E3⁺ cell lines, expressing F14.5K wt (F19), 14.5Y74, 14.5Y76 or F14.5Y122 and 293 control cells were lysed in either Triton X-100 (Trit.) or Digitonin (Dig.) buffer and subjected to immunoprecipitation (IP) with polyclonal antiserum Bur4 against 14.5K. Immunocomplexes were separated by SDS-PAGE and analyzed by western blotting (WB) for the presence of 10.4K with serum Bur3. **(B)** Parallel IP/WB analysis of E3/19K expression in digitonin lysates of 293 cells (lane 1) and selected 293 E3⁺ clones studied in A (lanes 2-5) using polyclonal serum R α E3/19K in a second IP step following immunoprecipitation of 14.5K. **(C)** Parallel IP/WB analysis of the total amounts of 10.4K, 14.5K, and E3/19K in Triton X-100 lysates of clonal lines studied in (A, B). 10.4K steady-state levels were determined by immunoprecipitation with polyclonal Ab R59 and western blot detection by Bur3. For detection of 14.5K Bur4 was used in both IP and WB. 19K levels were monitored using R α E3/19K in IP and WB. Differences in the apparent MW between mutants 14.5Y74 (lane 3), 14.5Y76 (lane 4) and wt (lane 2) and 14.5Y122 (lane 5) are due to insertion of the FLAG-tag in the latter two.

amounts of 10.4K and 14.5K were determined by immunoprecipitation/western blotting (Fig. 11C, 10.4K and 14.5K). For the comparative analysis of 10.4K and 14.5K contents the corresponding E3 expression levels in the selected clones were determined by immunoprecipitation/western blot detection of E3/19K (Fig. 11C, 19K), in a second IP step following immunoprecipitation of 14.5K. While the total amount of 10.4K in the 14.5Y⁷⁴A expressing cells was comparable to wild-type, steady-state expression of 14.5Y⁷⁴A was greatly reduced (Fig. 11C, 14.5K). Thus, substitution of Y⁷⁴ selectively reduced the stability of 14.5K, most likely by disrupting its association with 10.4K. The impaired interaction of 14.5Y⁷⁴A with 10.4K might have caused the dramatic loss of functional activity observed in 293 transfectants *in vivo* (Fig. 7). The amount of 10.4K isolated in complex with FLAG-modified 14.5Y¹²²A was markedly increased compared to that associated with wild-type FLAG-14.5 (Fig. 11A). This was accompanied by increased total amounts of immunoprecipitated 10.4 and 14.5Y¹²²A proteins (Fig. 11C, 10.4K and 14.5K), if one takes into account the lower E3/19K expression in these mutant cells (Fig. 11C, 19K, compare lanes 2 and 5). Therefore, the data indicated an increased stability of 10.4K and 14.5K in the Y¹²²A transfectant.

3.5 Functional relevance of dileucine type sequence elements within 10.4K

In a previous FACS analysis of 293 E3-transfectants it had been shown, that substitution of the dileucine sequence element at position L⁸⁷L⁸⁸ in the 10.4K cytoplasmic tail sequence by alanine inhibited down-modulation of Fas and the EGFR (Fig. 7). In order to characterize this loss of function mutant in greater detail the mutation was introduced into pBSΔX-E3/FLAG-14.5, encoding a FLAG-tagged version of 14.5K. Thereby, it is possible to investigate by FACS analysis whether the mutation in 10.4 had any influence on 14.5K surface expression. Furthermore, it remained to be analyzed whether substitution of a single leucine accounted for the knock-out phenotype or whether the integrity of the dileucine pair was required for efficient receptor down-regulation. Therefore, additional mutants were created with single leucine residues L⁸⁷ (mutant cell line L1), L⁸⁸ (mutant cell line L2) replaced by alanine. To examine all potential cytosolic dileucine motifs within 10.4K, the last two residues at the 10.4K C-terminus, representing an IL element in the Ad2 10.4K sequence (10.4I⁹⁰L⁹¹), were mutated to alanine as well. Upon transfection of mutant plasmids into 293 cells and selection of stable transfectants in G418, functional activity of 10.4-14.5K was assessed by FACS analysis. Transfectants were selected for similar E3/19K expression levels and HLA down-modulation. In a series of three independent experiments a representative clone of the 10.4L⁸⁷L⁸⁸ mutant cell line (hereafter referred to as LL-11) was compared with three clones from each of the 293 transfectant cell lines 10.4L⁸⁷A (L1) and 10.4L⁸⁸A (L2). In addition, the results determined in another series of three experiments with 3 representative clones of the 10.4I⁹⁰L⁹¹ mutant cell line (IL) are included in Fig. 12. The mean value of fluorescence (MVF) for each clone was determined and related to that of untransfected 293 cells or 293 cells expressing wild-type E3 proteins. Whereas cell surface expression of HLA was efficiently reduced (Fig. 11A, black bars) in all transfectants, intracellular 19K levels (Fig. 11A, white bars) in the selected L1, L2 clones reached only 64% of those in F-19. Nonetheless, metabolic labeling and immunoprecipitation of E3/19K confirmed that individual clones synthesized E3/19K at a rate similar to LL-11 and E3-45, but less than F-19 cells (Fig. 13). However, the analysis of single clones can yield only an estimate of a mutation's effects on receptor down-regulation, because variations in receptor expression among individual clones cannot be excluded. Therefore the analysis was based on a spectrum of three clones, and with respect to lowered E3 gene expression in these clones, the results give a rough approximation of the phenotype.

In F-19 cells which expressed wild-type 10.4K and F14.5K proteins Fas surface expression was reduced to below ~10% of the levels expressed on 293 cells. EGFR levels corresponded to ~20% of those on 293 cells (Fig. 12B and 12C). Upon mutation of the last two amino acids (I⁹⁰L⁹¹)

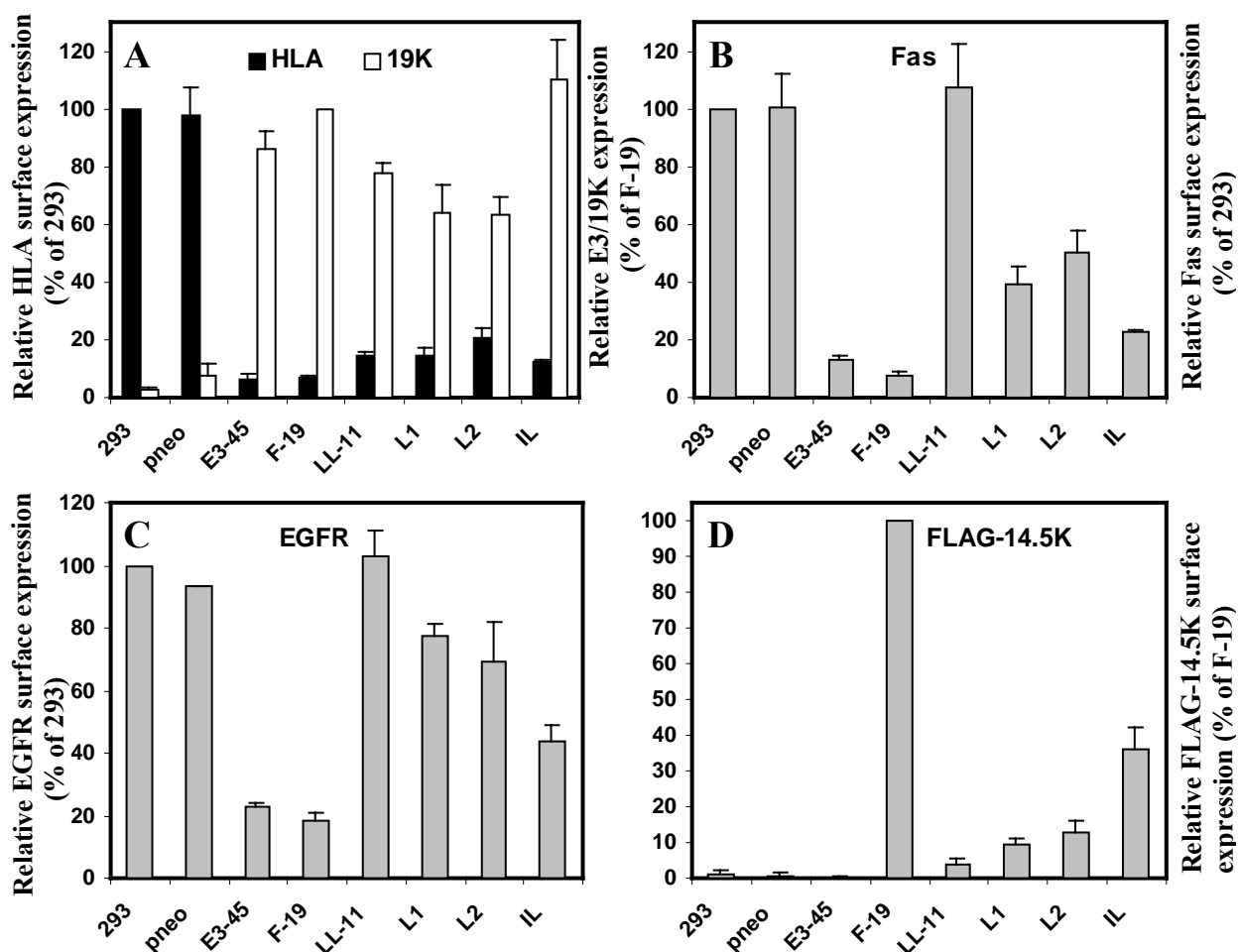


Fig. 12 Functional relevance of dileucine type sequence elements within 10.4K

(A) Relative cell surface expression of HLA (black bars) and intracellular E3/19K content (white bars) as determined by FACS analysis on E3/F14.5+ 293 transfectants expressing wt (E3-45, F-19) or mutant 10.4K, pSV^{neo}+-transfected (pneo) and untransfected 293 control cells. Mutant E3/F14.5+ cell lines are designated LL for both 10.4L⁸⁷ and 10.4L⁸⁸ replaced by alanine, whereas L1 indicates substitution of L⁸⁷ and L2 of L⁸⁸, respectively. Bars denote the relative percentage of expression compared to that seen on 293 cells (HLA) or F-19 (E3/19K). The mean value of fluorescence (MVF) of reference cell lines was set to 100%. Antibodies were as described in the legend to Fig. 2. Data were compiled from 3 independent experiments using cell clone LL-11 and 3 representative clones of L1 and L2. In another series of three experiments three representative clones expressing the 10.4IL mutant were compared to F-19 and control cells. Error bars represent the standard error (SEM). **(B)+(C)** Relative Fas and EGFR surface expression on the same 293 E3/F14.5+ transfectants analyzed in A. Data were derived as described in (A). **(D)** FLAG-14.5K surface expression of the same clones analyzed in A, B and C by the method described in Fig. 10D.

of Ad2 10.4, the capacity of 10.4-14.5K to down-modulate Fas and EGFR was largely retained, exhibiting Fas levels corresponding to 30% and EGFR levels of 40% of those on 293 cells. This revealed that the IL sequence element was not essential for 10.4-14.5K function. On 293 cells transfected with the dileucine pair mutant (LL-11) Fas and EGFR levels were restored, indicating that at least one of the two leucine residues was required for 10.4-14.5K function. Single alanine replacement mutations of either the first or second leucine resulted in significant reduction of Fas expression levels, whereas EGFR expression remained at 70-80% of that on 293 cells. Thus,

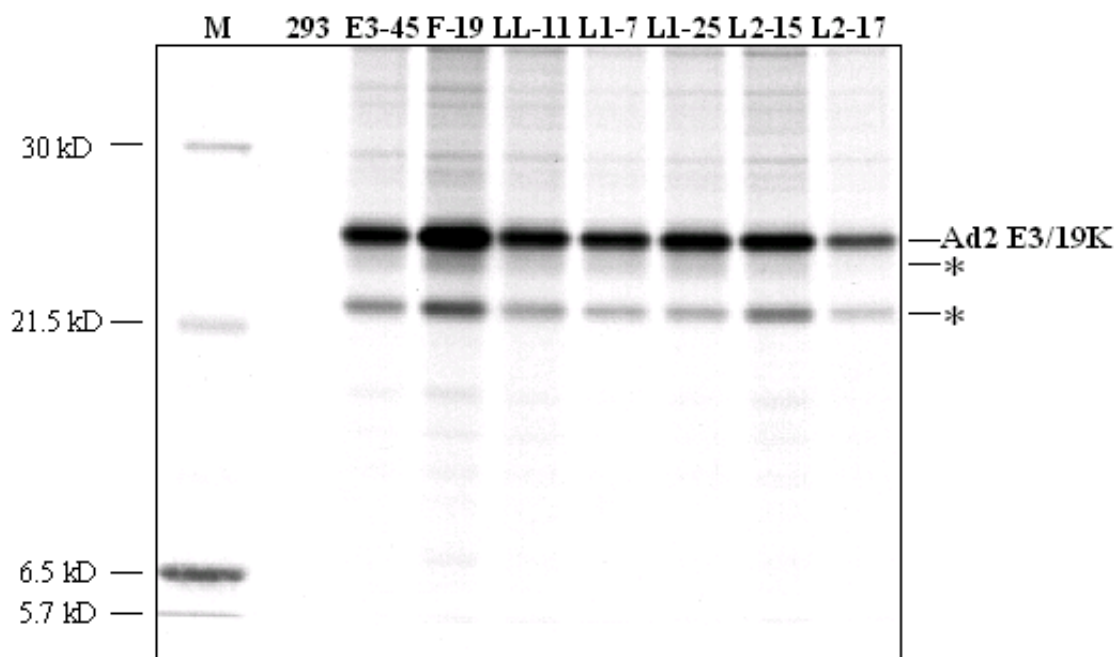


Fig. 13 E3/19K synthesis in 293 E3+ clones expressing 10.4K dileucine pair mutants

Autoradiogram of a 11.5-13.5% acrylamide gel filmed 14 hours. 293 E3+ transfectants were labeled for 1h with 200 μ Ci of each [35 S] methionine and [35 S] cysteine per ml and lysed in Triton-X 100 lysis buffer for immunoprecipitation of Ad2 E3/19K. Immunoprecipitates were separated by SDS-PAGE. TW1.3 mAb precipitated a major protein as well as two less abundant products marked with asterisks. Cell clones are designated LL for both L⁸⁷ and L⁸⁸ replaced by alanine, whereas L1 indicates substitution of L⁸⁷ and L2 of L⁸⁸, respectively. Clone numbers are added to the name. M = molecular weight marker containing 14 C methylated proteins (5.7-30kD). Quantitative phosphorimager (Storm 860 Molecular Imager, Molecular Dynamics, Sunnyvale, USA) analysis of band intensities confirmed that selected clones were similar in E3/19K synthesis to E3-45 cells, except for L2-17 which was not included in the FACS analysis, because of too little E3 gene expression.

mutation of single leucines differentially affected Fas and EGFR down-regulation, exhibiting only a small reduction of EGFR levels. As the second leucine residue (L⁸⁸) within the dileucine sequence is strictly conserved among 10.4K proteins of Ads of different subgroups (Fig. 8), this residue might be expected to be critical. However, disruption of either one of the two leucines led to a rather similar phenotype. Thus, both leucines contribute to the 10.4-14.5K function and it appeared that a pair of leucine residues was important. The results suggest that efficient modulation of cell surface receptors *in vivo* requires the integrity of both leucines or a dileucine-type sequence element. In good agreement with this hypothesis, a dileucine type sequence element is commonly found in 10.4K proteins of all subgenera, represented by an IL pair in 10.4K proteins of subgroup D Ads.

3.6 Influence of mutations in 10.4K on FLAG-14.5K surface expression

The FLAG-tag allowed to quantitatively monitor 14.5K expression on the cell surface by FACS analysis on 293 E3/F14.5-transfectants expressing mutant 10.4K. Flow cytometry with

monoclonal antibody M1 revealed that cells expressing the 10.4IL mutant exhibited a significant reduction of 14.5K cell surface expression as compared with the MVF of FLAG-tagged 14.5K on F-19 cells set to 100% (Fig. 12D). As this altered expression was associated with only a marginal effect on Fas and EGFR modulation, the observed steady-state surface expression level of about 40% is obviously sufficient for functional activity (Fig. 12B, 12C).

Remarkably, Flag-14.5K cell surface exposure was dramatically reduced in cells expressing 10.4K proteins with a disrupted dileucine motif. As the specific signal obtained by FACS analysis of 14.5K surface expression on 293 E3/F14.5+ transfectants consisted of only 10 fluorescent units the corresponding signal for the dileucine pair mutant was only slightly above unspecific background signals. Relative to the steady-state surface expression levels of F-19 cells less than 5% were detected in the dileucine pair mutant. Replacement mutations of single leucine residues also significantly lowered surface expression to below 10% of wild-type. This major decrease in surface expression might be a consequence of either enhanced degradation of 14.5K in the early secretory pathway, a reduced efficiency of cell surface transport, or a reduction in its residence time at the cell surface, due to enhanced degradation upon internalization. Why would a mutation in 10.4K have such a drastic effect on the 14.5K protein? A possible reason might be a loss of interaction with the mutant 10.4K protein, as complex formation of 10.4-14.5K is a prerequisite for efficient transport to the cell surface (Stewart et al., 1995). Loss of complex formation can be due to disruption of the interaction interface by the mutation, or enhanced degradation of 10.4K. To investigate the latter question, complex formation of mutant 10.4K with 14.5K was analyzed.

3.7 Complex formation of mutant 10.4K with 14.5K

By immunoprecipitation and western blotting the role of putative dileucine transport motifs in 10.4K for interaction with 14.5K and protein stability was examined. As the 10.4 antiserum Bur3 proved to be ineffective for detection of the mutant 10.4 proteins (data not shown), new antisera R59 and R71 were generated, directed to the entire 10.4 cytoplasmic tail and the mutated 10.4 LLAA peptide, respectively (see *Materials and Methods*).

The interaction of mutant 10.4K with wild-type FLAG-14.5K was assayed in Digitonin lysates allowing coprecipitation of 10.4K with 14.5K (Fig. 14A) and the total amounts of immunoprecipitated 10.4K, 14.5K and 19K (Triton X-100) were analyzed in parallel (Fig. 14B). Lysates were adjusted to equal contents of total protein and E3/19K expression of the different clonal lines was analyzed by immunoprecipitation/western blot detection of E3/19K in a second IP following immunoprecipitation of 14.5K. Alanine replacement of the C-terminal two amino

acids (IL) of 10.4K had no obvious influence on its interaction with 14.5K (Fig. 14A, compare lanes 3 and 7), nor did it reduce the overall stability of the individual subunits (Fig. 14B). This is reflected by a nearly unaltered functional activity of 10.4-14.5K in the E3 transfectants expressing mutant 10.4I⁹⁰L⁹¹ (see Fig. 12B,C). By contrast, no interaction could be detected for the 10.4L⁸⁷L⁸⁸ mutant (Fig. 14A, lane 5), although the serum readily recognized the mutant protein (Fig. 14B, 10.4K, lane 5). Whereas levels of 19K were similar in all transfectants, the level of 14.5K was strongly reduced in the 10.4L⁸⁷L⁸⁸ mutant cell line (Fig. 14B, 14.5K, lane 5). Furthermore, these cells exhibited a comparably low signal of 10.4K detected by the dileucine pair mutant specific serum R71 (Fig. 14B, 10.4K, lane 5). The diminished 14.5K content may indicate a reduced stability of 14.5 (and possibly also of 10.4LL), which is obviously a direct consequence of the L⁸⁷L⁸⁸ mutation in 10.4K. These mutually dependent steady-state levels suggest that 10.4K forms complexes with 14.5K and that both proteins have a common fate. Therefore, one attractive hypothesis was that the dileucine motif in 10.4 may prevent transport of the complex into a degradative compartment. In support of this hypothesis, steady-state levels of 10.4 and 14.5 in 10.4LL transfectants could be reconstituted to nearly wt levels by treatment of the cells with Bafilomycin A₁ (Baf), an inhibitor of the vesicular ATPase which impairs endosomal/lysosomal acidification (van Weert et al., 1995) and protein degradation by lysosomes (Fig. 14B, 10.4K, 14.5K, compare lanes 5 and 6 with 3 and 4). Baf-treatment increased the levels of the 10.4LL mutant and 14.5 by at least 10-fold, an effect repeatedly observed in multiple independent experiments. Interestingly, a 2 to 5-fold increase in signal intensity was observed for the wt proteins (Fig. 14B, compare lanes 3 and 4), indicative of lysosomal protein degradation. This protective effect of Baf seemed to be specific, since steady-state levels of the ER-located E3/19K protein were not significantly altered by this treatment (Fig. 14B, 19K). Thus, Baf affected primarily trafficking and degradation at the post-ER level.

The data strongly suggested that a significant proportion of wild-type 10.4K and 14.5K was degraded in a Baf-sensitive compartment, and mutation of the dileucine pair in 10.4 markedly promoted this degradation. Bafilomycin treatment also increased the amount of 10.4K isolated in complex with 14.5K (Fig. 14A, compare lanes 3 and 4). Remarkably, in the mutant LL-11 cells (Fig. 14A, compare lanes 5 and 6) treated with Baf the 10.4LL mutant protein could be coprecipitated with 14.5K, clearly demonstrating that the mutant protein was still capable of interacting with 14.5K. Thus, in the mutant cell line the complex can be formed, degradation of both subunits is increased and steady-state expression levels are lowered.

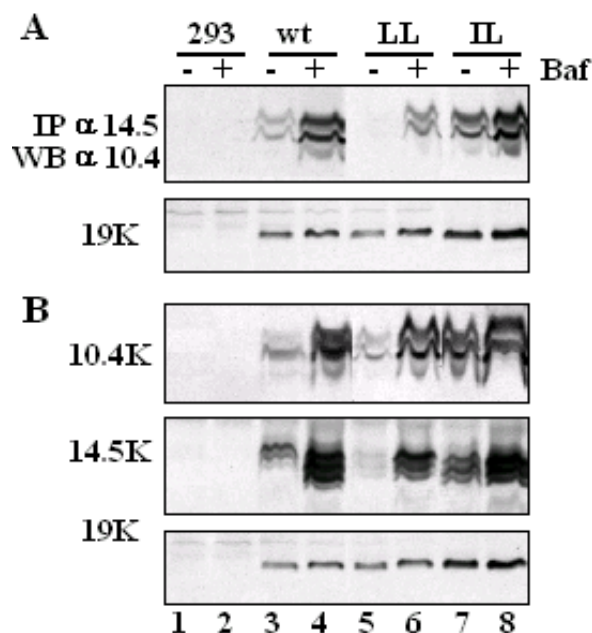


Fig. 14 Mutation of the conserved 10.4K dileucine motif results in reduced 10.4K and 14.5K steady-state levels that can be rescued by Bafilomycin treatment

(A) Association of mutant 10.4K with wt FLAG-14.5K with (+) or without (-) Bafilomycin A₁ (Baf) treatment (cells in culture were incubated with 100 nM Baf for 11h prior to lysis).

Representative clones derived from transfection of 293 cells with the indicated pBSΔX-E3/F14.5 constructs were lysed in Digitonin buffer and subjected to immunoprecipitation (IP) with polyclonal antiserum Bur4 against 14.5K. Immunocomplexes were separated by SDS-PAGE and analyzed by western blotting (WB) for the presence of wt 10.4K with serum Bur3 (lanes 1-4), for 10.4LL with specific serum R71 (lanes 5,6) and R59 was used to detect 10.4IL (lanes 7,8). In a second IP step from the same lysates E3/19K was detected using RαE3/19K in IP and WB. **(B)** Parallel IP/WB analysis of the total amounts of 10.4K, 14.5K, and E3/19K in Triton X-100 lysates of clonal lines studied in (A). 10.4K steady-state levels were determined by immunoprecipitation with polyclonal Ab R59 and western blot detection by Bur3 (lanes 1-4), or IP/WB using R71 (lanes 5,6), or R59 (lanes 7,8). 14.5K and 19K levels were analysed by IP/WB with Bur4 and RαE3/19K, respectively.

3.8 The cellular adaptor proteins AP-1 and AP-2 bind to 10.4K and 14.5K cytoplasmic tail peptides in a motif-dependent fashion

The observation that mutants 14.5Y¹²² and 10.4L⁸⁷L⁸⁸ were functionally defective without destroying complex formation, but were associated with a drastically altered cell surface exposure of 14.5K, suggested that Y122 and the dileucine pair may be part of transport signals that are critical for intracellular trafficking of the two viral proteins. To test this hypothesis, it was investigated whether the cytoplasmic tails of 10.4K and 14.5K were able to bind to the prominent cellular adaptor proteins AP-1 and AP-2 *in vitro*. AP-1 and AP-2 have been shown to recognize both dileucine- and YXXΦ-type motifs in the cytoplasmic tails of cargo proteins and are involved in clathrin-mediated transport (Heilker et al., 1999; Kirchhausen, 1999). To this end surface plasmon resonance spectroscopy (SPR) with purified AP-1 and AP-2 adaptor proteins and

immobilized 10.4K and 14.5K cytoplasmic tail peptides encompassing the putative transport motifs in native or mutated form was carried out (Table 3, the N-terminal cysteine was added to the peptides as these were also used for immunization which required coupling to KLH). The results demonstrated a significant affinity of both AP-1 and AP-2 for wild-type cytoplasmic tail peptides of 10.4 and 14.5 with equilibrium dissociation constants (K_D) below 600nM (Table 3, 10.4 and 14.5, respectively). Binding required the integrity of the putative transport motifs, as disruption of the dileucine pair in 10.4 (10.4L⁸⁷L⁸⁸) or mutation of Y122 to alanine in 14.5 (14.5Y¹²²) dramatically reduced binding. Mutation of the dileucine motif reduced the affinity to AP-1 and AP-2 by 154-fold and 300-fold, respectively. Similarly, the substitution of Y122 by alanine reduced the affinity of AP-1 and AP-2 to the tail peptide of 14.5 by a factor of 108 and 167, respectively. Interestingly, both the 10.4K and 14.5K peptides exhibited a higher affinity towards AP-2 than AP-1.

In summary, the cytoplasmic tail peptides of 10.4 and 14.5 bind to the adaptor proteins AP-1 and AP-2 *in vitro*, and this binding is dependent on the integrity of both types of motifs. Thus, these *in vitro* data provided further evidence for a role of these motifs in intracellular transport.

Table 3 Binding of adaptor proteins AP-1 and AP-2 to cytoplasmic tail peptides of 10.4 and 14.5 as determined by Surface Plasmon Resonance spectroscopy (data provided by Stefan Höning, University of Göttingen)

Peptide		AP-1		AP-2	
	peptide sequence	K_D	affinity reduction	K_D	affinity reduction
10.4	CYRDDRTIADLLRIL	0,52 ^{a)}		0,4	
10.4 L ⁸⁷ L ⁸⁸	CYRDDRTIADAARIL	80,0	154x ^{b)}	120,0	300x
14.5	CEISYFNLTGGDD	0,48		0,3	
14.5 Y ¹²²	CEISAFNLTGGDD	52,0	108x	50,0	167x

^{a)} K_D equilibrium dissociation constants in μ M

^{b)}fold reduction

4 Importance of the 10.4K dileucine and 14.5K Y¹²²XXΦ motifs for intracellular trafficking of 10.4-14.5K

4.1. Establishment of an efficient heterologous expression system for 10.4-14.5K suitable for analysis of intracellular localization by immunofluorescence

It remained to be tested whether the observed loss of binding of the mutated proteins to the adaptor proteins *in vitro* was reflected by an altered trafficking of 10.4K and 14.5K mutant proteins *in vivo*. To analyze the intracellular distribution of the viral proteins in greater detail, 10.4 and 14.5 had to be expressed in cells more suitable for immunofluorescence than 293 cells. Therefore, plasmid pBSΔX-E3/FLAG-14.5 was transiently transfected into SV80Fas cells, a human fibroblast cell line expressing SV40 T antigen and Fas. At 40h post transfection the intracellular localization of E3 proteins was analyzed. Upon CaPO₄-mediated transfection of SV80Fas cells only 25% of the cells stained positive for E3/19K in the endoplasmic reticulum. Moreover, 14.5K could only be detected in one third of these E3 positive cells (Fig. 15). This is consistent with the generally lower abundance of the 10.4-14.5K encoding mRNA species of subgroup C Ads as compared with those encoding E3/19K (Wold et al., 1995). 14.5K localized to a perinuclear compartment, which was stained specifically by rabbit serum anti-14.5K (Rα14.5) and monoclonal anti-FLAG antibody M1 (data not shown). But, the number of positive cells as well as the staining intensity was insufficient for a detailed analysis of the intracellular distribution of 10.4-14.5K proteins by immunofluorescence.

Therefore, an efficient 10.4-14.5 expression system independent of AdE1A products, which upregulate E3 expression in 293 cells had to be established. To this end, Ad2 10.4K and FLAG-14.5K encoding ORFs were cloned separately into pSG5 expression vectors to drive 10.4K and 14.5K synthesis by the SV40 promoter/enhancer (Fig. 16). A potentially important feature of this vector is the intron II of the rabbit β-globin gene for splicing of the expressed transcript. Inclusion of the intron might help to enhance expression by increasing mRNA half-life and improving the efficiency of RNA processing and transport to the cytoplasm (Kim et al., 2002). As both proteins are known to function as a complex it was also aimed at expressing both proteins from a single vector. The entire Ad2 10.4-14.5K encoding sequence was cloned into the pSG5 vector, and in parallel individual ORFs were introduced into the multigenic expression vector pMG (Fig. 16). This vector provides two different multiple cloning sites, each with a strong promoter for eucaryotic expression, a viral and a housekeeping promoter, thus limiting transcription interference. The 10.4K open reading frame was inserted into the first MCS under the control of the immediate-early HCMV enhancer promoter (HCMV-IA prom) and located downstream of

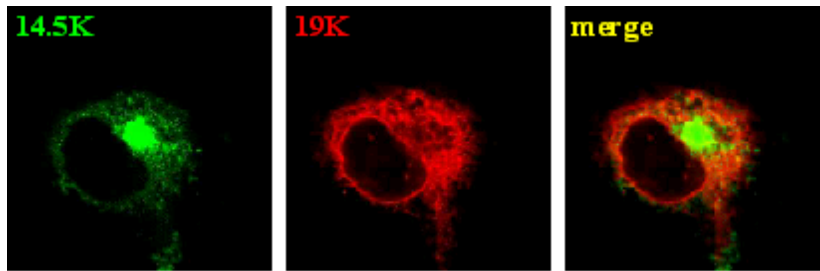


Fig. 15 Costaining of Ad2 14.5K and E3/19K in SV80Fas cells transiently transfected with plasmid pBSΔX-E3/FLAG-14.5

SV80Fas cells were transiently transfected with plasmid pBSΔX-E3/FLAG-14.5 (calciumphosphate method) for immunofluorescence analysis at 40 hours post-transfection. 14.5K was detected with polyclonal serum Rα14.5 and 19K was stained using mAb Tw1.3 as described in *Materials and Methods*.

intron A. The 14.5K ORF was cloned into the second MCS with expression driven by the Elongation factor 1 alpha (hEF1) promoter in combination with the Human T-Cell leukemia virus (HTLV) 1 Long terminal Repeat for stabilization of the mRNA followed by an intron sequence (intron 117). The introns preceding the inserted ORFs are spliced out in mammalian cells. Insert amplification primers for the cloning of individual ORFs were designed to yield a modified sequence 5' of the ATG that conforms to the Kozak consensus of translation initiation (Kozak, 1987), for optimized heterologous expression. Expression of the proteins was analyzed upon transient transfection of SV80Fas or A549 cells with vector DNA followed by immunofluorescence detection at 40 hours post-transfection. For improved transfection efficiency cells were seeded on the day of transfection and the DNA/CaPO₄ mix was added to the cells 4-6

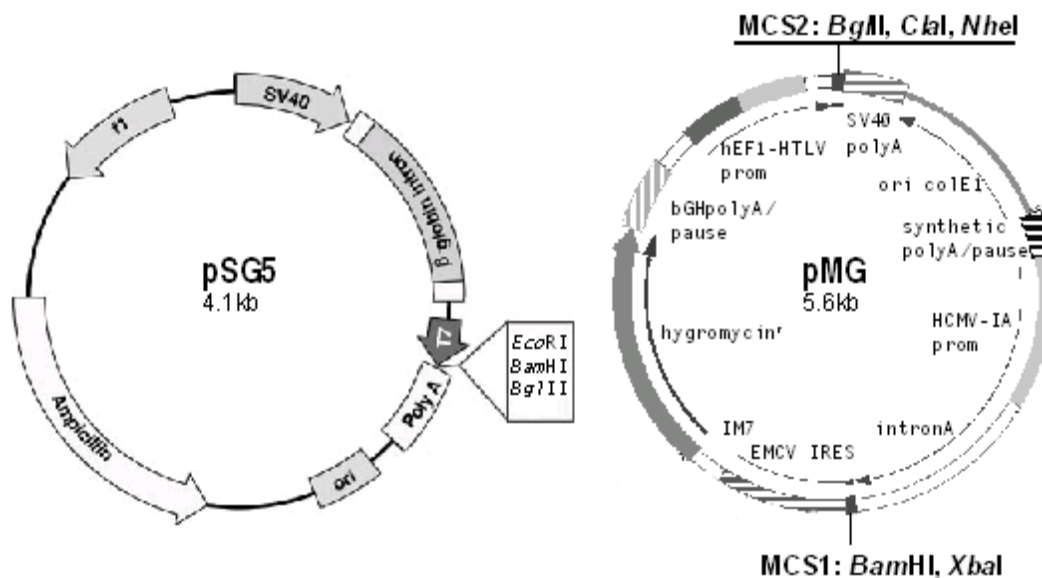


Fig. 16 Circular map of pSG5 (Stratagene, Amsterdam, The Netherlands) and pMG (InvivoGen, San Diego, USA) used for construction of 10.4K and 14.5K expression vectors

Coding sequences of 10.4K, 14.5K or both were inserted into the MCS of pSG5, as described in *Materials and Methods*. Additionally, the 10.4 ORF was cloned into the *BamHI*, *XbaI* sites of pMG and the FLAG-14.5K CDS into the *ClaI*, *NheI* sites of construct pMG10.4. For a description of vector features see text.

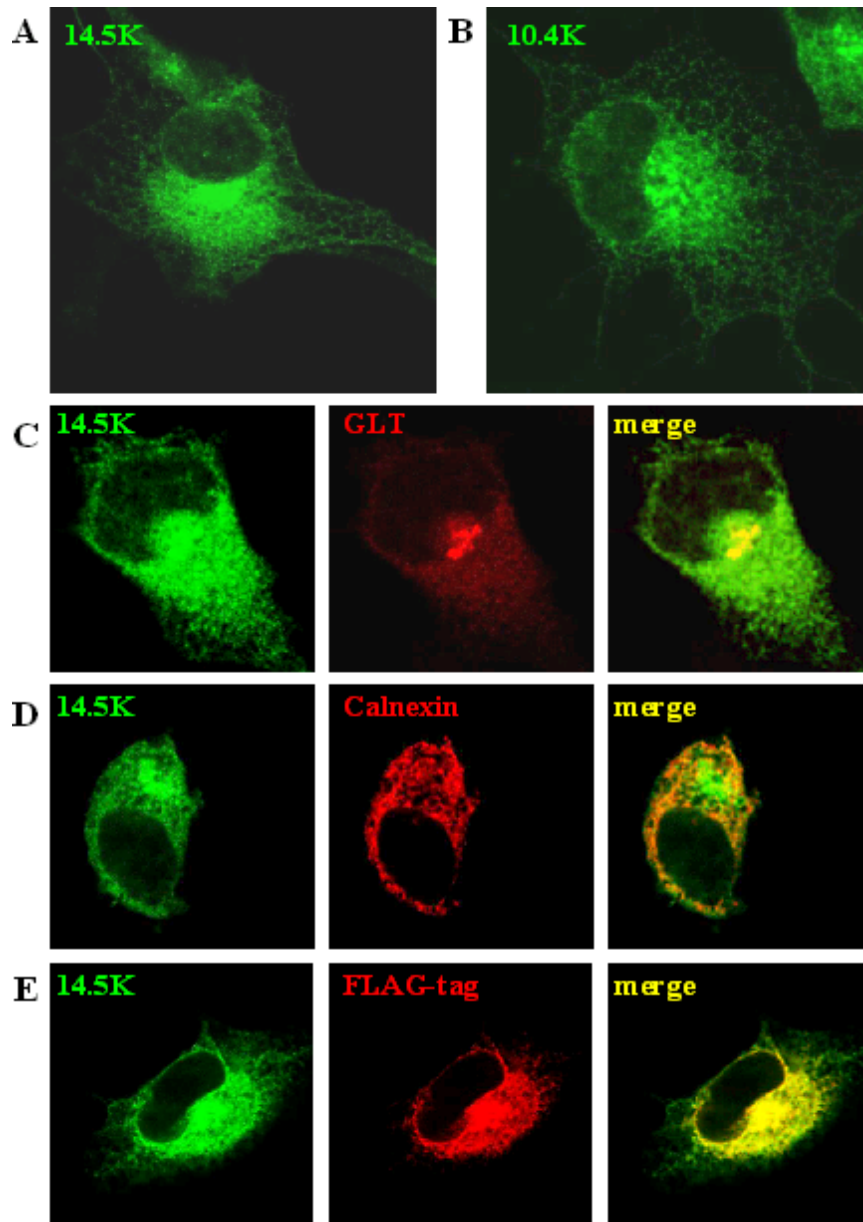


Fig. 17 Intracellular localization of 10.4K in SV80Fas cells and FLAG-14.5K in SV80Fas or A549 cells following transient transfection of single expression vectors

SV80Fas cells were transfected with pSG5/F14.5K (A, C, D) or pSG5/10.4K (B) and processed for confocal laser microscopy at 40 h post transfection using polyclonal Ab Bur3 or R α 14.5 to detect 10.4 and 14.5K, respectively (green). Localization of 14.5K was compared with the Golgi marker galactosyltransferase, GLT (red, mAb GTL-2) (C), and ER-resident protein Calnexin (red, mAb AF-8) (D). (E) In A549 cells transfected with pSG5/F14.5K a similar distribution of FLAG-14.5K was detected using R α 14.5 or mAb M1 anti-FLAG (40 h post transfection).

hours after plating, at which time the cells had adhered to the plastic dishes but not yet extended (Marks et al., 1996).

Despite the presence of strong promoters transfection of the bicistronic vector pMG yielded only a low percentage of positive SV80Fas cells. 10.4K was barely detectable whereas about 20% of the cells showed a specific staining for FLAG-14.5K in a perinuclear compartment (data not shown). Even a smaller number of positive cells were observed upon transfection of the pMG

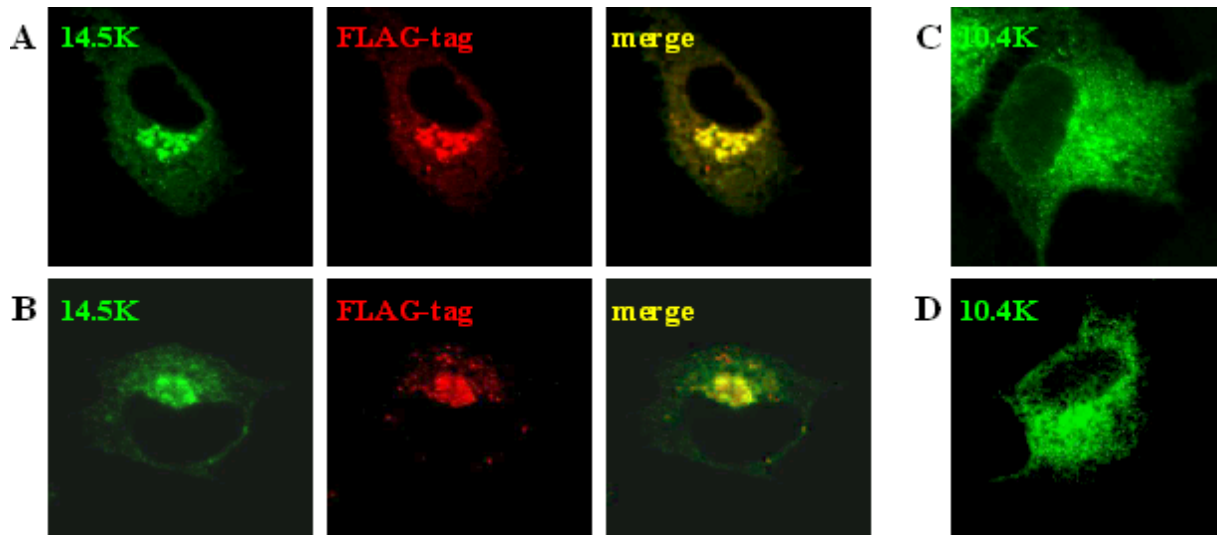


Fig.18 Intracellular localization of 10.4K and F14.5K expressed in A549 (A, C) or SV80Fas (B,D) cells, upon transfection of pSG5/10.4-F14.5

At 40 hours post-transfection with pSG5/10.4-F14.5 vector DNA cells were processed for immunofluorescence analysis. Transfected A549 cells (**A**) or SV80Fas cells (**B**) were costained for 14.5K with R α 14.5K (green) and mAb M1 against FLAG (red). For detection of 10.4K a single stain with Bur3 was performed on transfected A549 (**C**) or SV80Fas cells (**D**).

vector into A549 cells (~10%). By contrast, a satisfactory expression level suitable for immunofluorescence analysis of intracellular protein localization could be achieved upon transfection of pSG5 vectors. Up to 60% of the cells exhibited a strong staining for 10.4K and 14.5K in SV80Fas cells transfected with pSG5/10.4K or pSG5/F14.5K (Fig. 17A, 17B). A similar pattern was observed for 14.5K expression in A549 cells. 14.5K specific rabbit serum and monoclonal antibody M1 directed against the FLAG-tag revealed an identical staining pattern (Fig. 17E). The 14.5K positive perinuclear structure corresponded to the Golgi/trans-Golgi network as it costained with galactosyltransferase (Fig. 17C, red) and human TGN46 (data not shown), which are cellular marker proteins for this compartment. Furthermore, 14.5K colocalized with Calnexin in the endoplasmic reticulum (Fig. 17D). In cells transfected with pSG5/10.4K 10.4K could be specifically stained using polyclonal rabbit serum Bur3 (Fig. 17B), or antiserum R59 directed against the entire cytoplasmic tail of 10.4K (data not shown). In pSG5/10.4K positive SV80Fas cells 10.4K localized to the ER and Golgi/TGN.

In cells transfected with the pSG5/10.4-F14.5 vector 14.5K was detected in a perinuclear compartment identified to correspond to the Golgi/TGN, which also stained positive for 10.4K. Additionally, 14.5K localized to a few dot-like structures surrounding the perinuclear compartment (Fig. 18A, 18B, 14.5K). 10.4K (Fig. 18C, 18D, 10.4K) localized to the endoplasmic reticulum and the Golgi/TGN, as observed in cells transfected with pSG5/10.4K (Fig. 17B). Interestingly, 14.5K specific staining of the endoplasmic reticulum was significantly reduced as

compared to cells transfected with pSG5/F14.5K (compare Fig.17A, 17E and Fig. 18A, 18B, 14.5K). Thus, coexpression of 10.4K in the transfected cells caused a shift in 14.5K steady-state localization, as evidenced by a reduced ER staining. This correlates with biochemical evidence presented for the Ad5 14.5K protein. Ad5 14.5K can form a complex with Ad2 10.4K and it has been reported that the efficiency and site of cleavage of the Ad5 14.5K signal sequence depends on the presence of 10.4K (Krajcsi et al., 1992b). Moreover, the extent of glycosylation and phosphorylation of Ad5 14.5K depends on expression of 10.4K (Krajcsi et al., 1992c; Krajcsi and Wold, 1992). Therefore, the 10.4K-induced loss of 14.5K ER staining might be the consequence of association of 10.4K with 14.5K and efficient signal sequence cleavage in the 14.5K protein, which is then no longer retained in the ER.

In SV80Fas cells the number of cells bearing 14.5K at the cell surface was higher than in A549 cells, whereas in about 5% of the transfected A549 cells 14.5K was also detected in the ER. The increase in 14.5K signal intensity at the cell surface of SV80Fas cells suggested enhanced expression of 10.4-14.5K in these cells. Given that transfection efficiency was very similar in both cell types increased expression in SV80Fas cells might be due to SV40 T antigen-mediated amplification.

In sum, upon transient transfection of pSG5 expression constructs into SV80Fas cells a high number of cells could be efficiently transfected yielding expression levels that were suitable for immunofluorescence analysis of 10.4K and 14.5K intracellular localization. Therefore, for most studies the pSG5 expression constructs were introduced into SV80Fas cells.

4.2. Functional activity of 10.4 and 14.5K proteins encoded by single expression vectors

Apart from Fas, A549 cells express also other target molecules of E3/10.4-14.5K, like EGFR, TRAIL-R1 (DR4) and TRAIL-R2 (DR5). To analyse whether heterologous expression of 10.4K and/or 14.5K was sufficient to down-modulate these latter targets pSG5/10.4K and pSG5/F14.5K vectors were cotransfected together with the pSV2-neo^r plasmid into A549 cells (see also *Materials and Methods*) to generate stable transfectants expressing either 10.4K, 14.5K or both proteins. Receptor surface expression levels were determined by FACS analysis. FACS analysis also allowed to qualitatively determine the intracellular content of 10.4K and/or 14.5K using polyclonal immune sera R59 directed against 10.4K and monoclonal Ab M1 against FLAG-14.5K. Clones could be grouped according to their expression profile being positive for 10.4K, 14.5K or both. Expression levels of 10.4K and 14.5K in the preselected clones were subsequently analysed quantitatively by immunoprecipitation and western blot. 10.4K was immunoprecipitated from

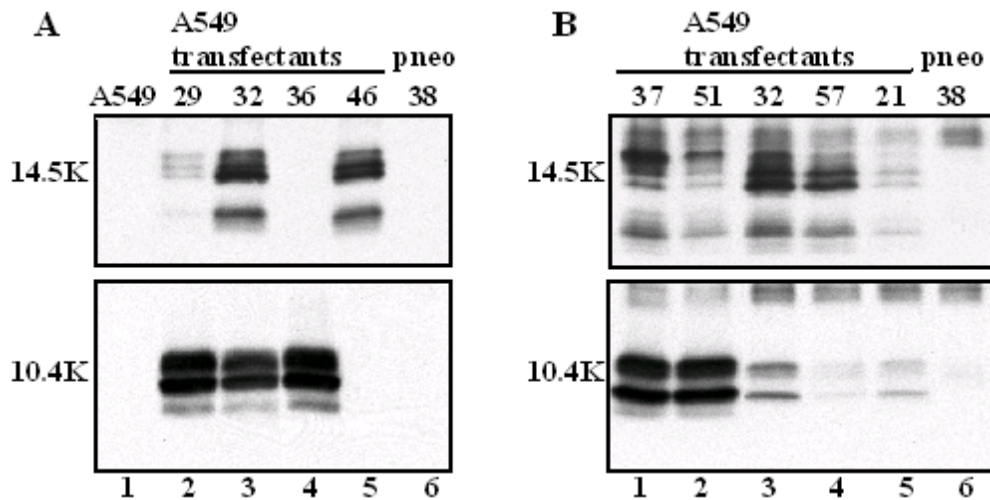


Fig. 19 Expression levels of 10.4K and FLAG-14.5K in selected A549 transfectants

Parallel immunoprecipitation and western blot analysis of F14.5K and 10.4K in Triton X-100 lysates of stable A549 transfectants expressing 10.4K (panel A, lane 4, clone number 36), 14.5K (panel A lane 5, clone number 46) or both (clones number 21, 29, 32, 37, 51, 57). Lysates were adjusted to equal protein content (BCA protein assay) prior to immunoprecipitation of 14.5K with polyclonal serum Bur4 and 10.4K with R59. Immunoprecipitates were separated on a 15% mini-gel by SDS-PAGE and analyzed by western blotting with Bur4 and Bur3 for the presence of 14.5K and 10.4K, respectively. The fastest migrating band on the 14.5K immunoblot likely represents 14.5K degradation products. As negative control lysates of A549 or pSV2-neo^r transfected cells (pneo, clone number 38) were analyzed.

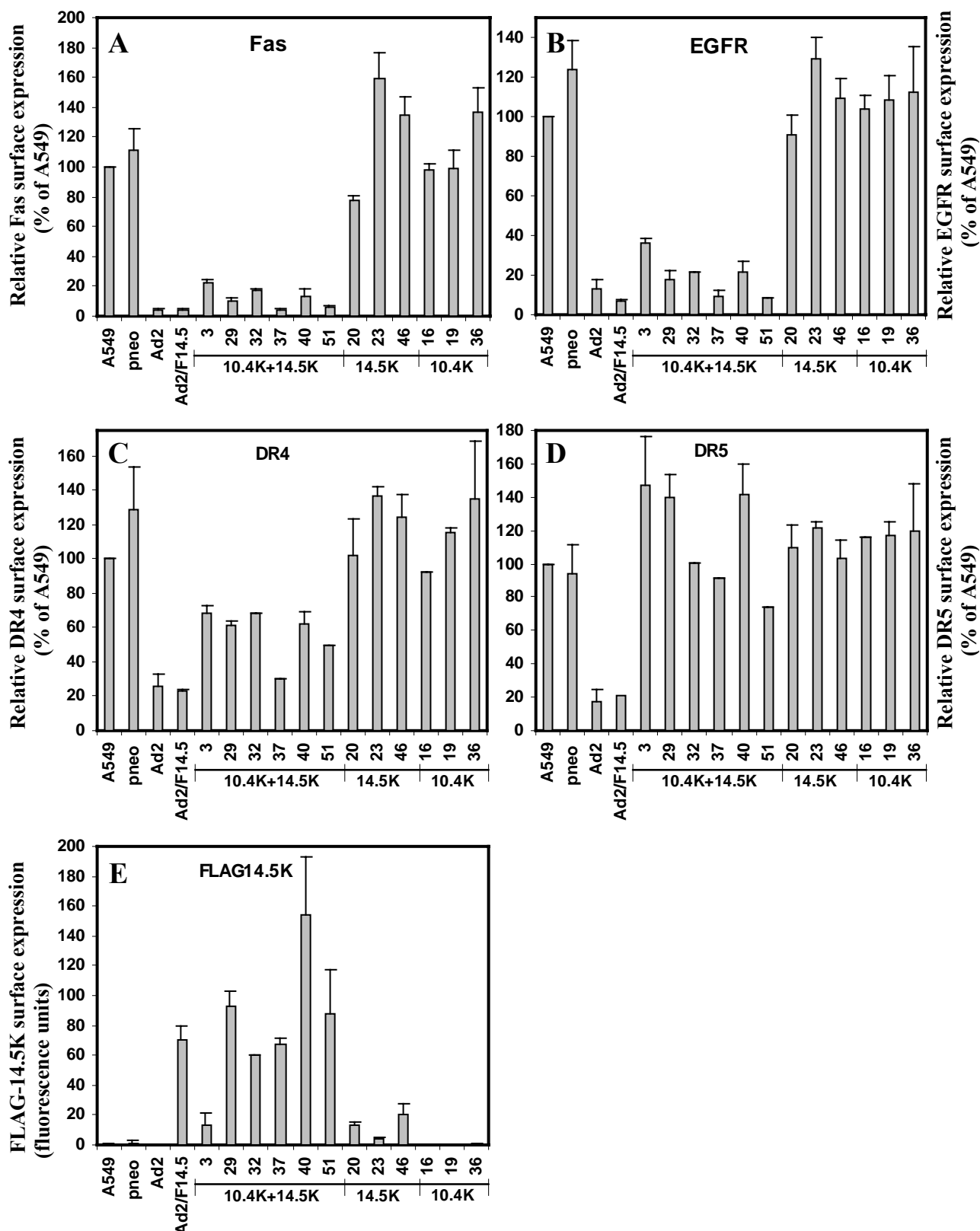
Triton X-100 lysates with polyclonal immune serum R59 and western blot detection with Bur3.14.5K content was determined by immunoprecipitation and western blot with Bur4. Thereby, single positive clones could be identified which expressed solely 10.4K (Fig. 19A lane 4, clone number 36) or 14.5K (Fig. 19A lane 5, clone number 46). In selected clones expressing 10.4K together with 14.5K different ratios of 10.4K and 14.5K proteins were observed. Moreover, the pattern of the immunoblot signal for 14.5K differed among the clones and the intensity of the uppermost 14.5K band seemed to correlate with the amount of 10.4K expressed in these clones (Fig. 19B). As cleavage of the 14.5K signal sequence has been shown to depend on the presence of 10.4K (Krajcsi et al., 1992c) the association of 14.5K with 10.4K in the ER might be a prerequisite for efficient processing and cell surface transport of 14.5K. Along this line, the observed differences in the abundance of different processed forms of 14.5K suggest that the top band corresponds to the fully processed form of 14.5K that is transported to the cell surface in the presence of 10.4K. In good correlation, for mutant 14.5K Y¹²²A which had been shown to accumulate at the cell surface of 293 transfectants, the banding pattern of the 14.5K signal was shifted towards bands of high MW (compare Fig. 11C, 14.5K, lane 5). Thus, one would expect to see an increase in F14.5K cell surface exposure in the presence of 10.4K as compared to clones expressing 14.5K alone. Therefore, Flag-14.5K surface expression was determined by FACS analysis

on selected A549 transfectants (see below). For FACS analysis of receptor surface expression levels, at least three independent clones expressing 10.4K, 14.5K or both were chosen (Fig. 20). On stable A549 transfectants coexpressing 10.4K and 14.5K Fas and EGFR levels were efficiently down-modulated. On average Fas surface expression was decreased to 10% of the levels on A549 cells, and EGFR to 15%. For some of these clones receptor levels were similar to those on virus-infected A549 cells determined in parallel (Fig. 20A, 20B, clones number 37 and 51). By contrast, receptor surface expression levels remained unchanged in cell clones which expressed either 10.4K or 14.5K alone. Thus, heterologous expression of both 10.4K and 14.5K is necessary and sufficient to achieve down-regulation of Fas and the EGFR..

TRAIL-R1 (DR4) expression levels on A549 cells infected with Ad2 were reduced to 25%. Among the stable transfectants the clone with the highest expression of both 10.4 and 14.5K (clone number 37) exhibited down-regulation to a similar degree. On average DR4 surface expression on selected 10.4-14.5K expressing clones was decreased by 50% as compared to A549 cells. By contrast, combined expression of 10.4 and 14.5K was not sufficient to achieve down-modulation of TRAIL-R2 (DR5), whereas in virus-infected cells levels were reduced to below 20%. Thus, apart from 10.4K and 14.5K another viral function or protein was required to bring about down-regulation of DR5. It had been shown by Benedict et al. that in addition to 10.4 and 14.5K a third adenovirus E3 protein, E3/6.7K, was required for DR5 down-regulation. Moreover, the authors demonstrated that E3/6.7K can physically interact with the 10.4-14.5K complex in living cells (Benedict et al., 2001).

Fig. 20 FACS analysis of Fas, EGFR, DR4, DR5 and F14.5K surface expression on A549 transfectants expressing 10.4K, 14.5K or both viral proteins

Relative expression of plasma membrane proteins Fas **(A)**, EGFR **(B)**, DR4 **(C)**, DR5 **(D)** as determined by FACS analysis on stable transfectants of A549 cells, which had received pSG5/10.4 (clones number 16, 19, 36), pSG5/F14.5 (clones 20, 23,46) or both plasmids (3, 29, 32, 37, 40, 51) together with the pSV2-neo^r plasmid. Clone number 38 (pneo) had incorporated only the pSV2-neo^r plasmid. As positive measure for a reduction in cell surface receptor levels, A549 cells infected with Ad2 or Ad2/F14.5 viruses (18-22 h p.i.) were processed in parallel. Infection efficiency was monitored by determination of the percentage of E3/19K positive cells (purified mAb Tw1.3 was used) and reached about 100%. Fas (mAbs B-G27) and EGFR (mAb 528) surface expression levels were determined as described in *Materials and Methods*. After deduction of the background staining obtained with the secondary antibody alone, the mean value of fluorescence (MVF) for each cell clone was related to that of A549 cells, which was set to 100%. DR4 and DR5 levels were determined with rabbit polyclonal Ab, followed by incubation with FITC-labeled secondary Ab GαR IgG (SIGMA, Munich, Germany) and background staining with the corresponding pre-sera and secondary Ab was deducted. The bars denote the mean value calculated from one to three experimental values. Error bars depict the SEM. **(E)** Anti-FLAG mAb M1 was employed prior to incubation with FITC-labeled goat anti-mouse IgG for monitoring FLAG-14.5K surface exposure. After deduction of background staining obtained with secondary antibody alone the mean value calculated from MVFs of three measurements was plotted in the bar diagram. Error bars depict the SEM. ►



Flag-14.5K surface exposure was low in clones lacking expression of 10.4K reaching at most 30% of the 14.5K surface expression on infected cells. Upon coexpression of 10.4K, many clones exhibited FLAG-14.5K surface expression levels comparable or even higher than those on infected

cells. Thus, the steady-state level of F14.5K surface expression was not only a function of the amount of 14.5K synthesized, but varied depending on the presence of the 10.4K protein, with high amounts of 10.4K increasing 14.5K surface expression. Clearly, coexpression of 10.4K with 14.5K was required to achieve efficient down-modulation of plasma membrane receptors, but no direct correlation was found between down-regulation capacity and FLAG-14.5K surface expression levels. Interestingly, down-regulation efficiency was increased with increasing levels of 10.4K (compare the results of the FACS analysis for 10.4-14.5+ clones in Fig. 20 with the intensity of the bands in the IP/WB experiment Fig. 19).

4.3. Analysis of intracellular trafficking of 10.4K and FLAG-14.5K coexpressed upon transfection of separate expression vectors

SV80Fas cells received equimolar amounts of both types of expression vectors pSG5/10.4 and pSG5/F14.5K (3 μ g of DNA each) and were processed for immunofluorescence at 40 h post transfection. Localization of 10.4K and 14.5K was analyzed by costaining of both proteins to identify cells that expressed both 10.4K and 14.5K. As expected from the results obtained with construct pSG5/10.4-F14.5K, coexpression of 10.4K resulted in localization of 14.5K to the perinuclear compartment of the cells, ER staining being greatly reduced (Fig. 21A). Remarkably, the number of cells exhibiting 14.5K at the cell surface was increased as compared to cells transfected with pSG5/10.4-F14.5K (compare Fig. 18). Some cells exhibited a clear surface staining for 14.5K, lining the border of the cells (Fig. 21B). In at least 50% of 14.5K positive cells surface staining was composed of distinct patches or stippled staining which appeared at the inner rim of the plasma membrane and surrounding the perinuclear compartment. Surprisingly, in the majority of these 10.4-14.5K positive cells 10.4K was also no longer found in the ER, but localized exclusively to the perinuclear compartment (Fig. 21A, 21B). In cells exhibiting the most intensive staining, 10.4K colocalized with 14.5K at the cell surface (Fig. 21C). This phenotype had not been observed upon coexpression of 10.4K and 14.5K from a single vector (pSG5/10.4-F14.5), with both translation initiation codons residing in their natural context. In the expression vectors pSG5/10.4 and pSG5/F14.5K the 6 bases preceding the start codon had been optimized to fit the Kozak consensus for eucaryotic translation initiation and therefore increased synthesis of 10.4K and 14.5K was expected. Moreover, expression of 14.5K from a separate vector independent of the 10.4K encoding upstream sequence might also have contributed to higher expression. A comparably high expression of 14.5K might have facilitated its detection at the cell surface, which is in agreement with the increase in number of cells exhibiting 14.5K surface staining.

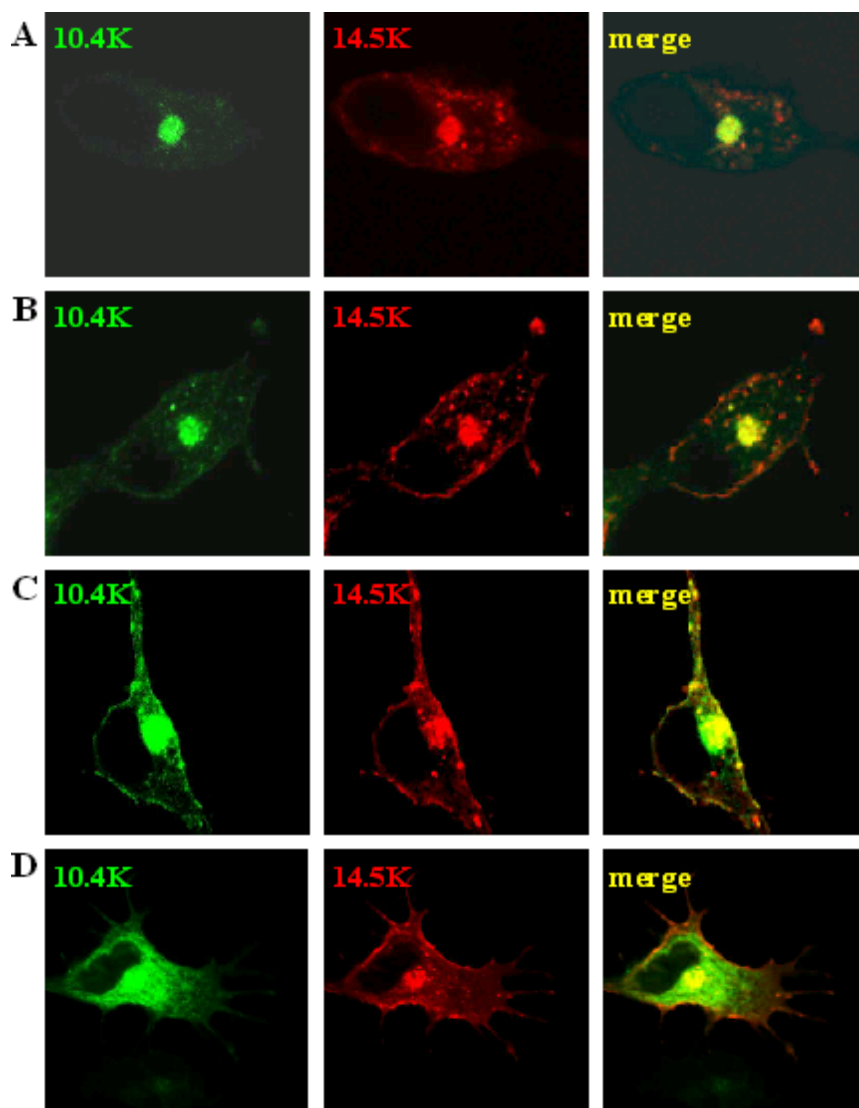


Fig. 21 Intracellular localization of 10.4K and FLAG-14.5K in SV80Fas cells transiently transfected with a combination of pSG5/10.4 and pSG5/F14.5

At 42 hours post-transfection cells were processed for confocal laser scanning microscopy. Costaining with Bur3 against 10.4K and mAb M1 against FLAG-14.5K identified cells that expressed both 10.4K and 14.5K.

Therefore, the difference in 10.4K intracellular distribution might be interpreted as a consequence of a different ratio of 10.4K and 14.5K levels in these cells. Increased synthesis of both 10.4K and 14.5K might have elevated 10.4K surface expression to levels that allowed immunofluorescence detection of 10.4K at the cell surface. Taken together, the data suggest that cell surface transport of 10.4K requires coexpression of 14.5K, as 10.4K is found in the ER/Golgi, when expressed alone, whereas 10.4K localization is shifted to Golgi and post-Golgi compartments with increasing amounts of 14.5K.

The observation that in some cells 10.4K colocalized with 14.5K at the plasma membrane suggested that the two proteins exist as a complex at the cell surface. But as the rabbit serum directed against the 10.4K cytoplasmic tail had been shown to be unable to coprecipitate 14.5K

from detergent extracts it remained unknown whether it would allow immunofluorescence detection of 10.4K complexed to 14.5K. Thus, the 10.4K positive structures may well correspond to free 10.4K. In general, the intensity of surface staining detected with monoclonal Ab M1 against FLAG-14.5K was higher and a greater number of surface staining bearing cells was counted than for the cells stained with rabbit serum against 10.4K. This does not necessarily reflect differences in the level of surface expression, provided that antibody was used in excess, but could be due to differences in the affinities of the antibodies or the different epitopes involved. 10.4K epitopes may be inaccessible due to its association with 14.5K.

In the population of 10.4K expressing cells which were obtained by transfection of equimolar amounts of pSG510.4 and pSG5/F14.5K, less than one third exhibited ER and Golgi-like perinuclear staining. These cells were mostly negative for 14.5K, thus had been transfected only with the pSG5/10.4 construct. But in some of these cells strong surface staining for 14.5K was observed (Fig. 21D). This phenotype resembled the one that was observed with the pSG5/10.4-F14.5K vector except for a higher intensity of FLAG-14.5K surface staining.

In conclusion, upon introduction of separate expression plasmids different populations of transfected cells were obtained: Cells expressing only one of the two proteins in significant amounts were characterized by ER/Golgi localization of the corresponding protein. Upon coexpression of both proteins the cells exhibited less ER staining and the two proteins colocalized in the perinuclear Golgi-like structure. As compared to transfection of pSG5/10.4-F14.5K vector an increased number of cells exhibiting 14.5K surface staining and increased signal intensity was noted. Cell surface expression of 14.5K and/or 10.4K could only be detected in cells expressing both proteins. The observation that different ratios of 10.4K and 14.5K can cause a redistribution of both proteins from the ER to the perinuclear compartment and the cell surface suggested that a complex of 10.4-14.5K assembles prior to exit from the Golgi to allow efficient transport to the cell surface.

4.4. Mutations of 10.4LL and 14.5Y122 induce missorting of 10.4-14.5K

In order to study the intracellular distribution of mutant proteins 10.4LL/AA (abbreviated as 10.4LL) and FLAG-14.5Y¹²²A, the corresponding nucleotide sequences were inserted separately into the MCS of the pSG5 vector. As with the pSG5/10.4K and pSG5/F14.5 vectors the sequence directly preceding the start codon was modified to conform to the Kozak consensus of translation. SV80Fas cells were cotransfected with different combinations of 10.4K and 14.5K wt and mutant plasmids and localization of 10.4K and 14.5K was analyzed by immunofluorescence.

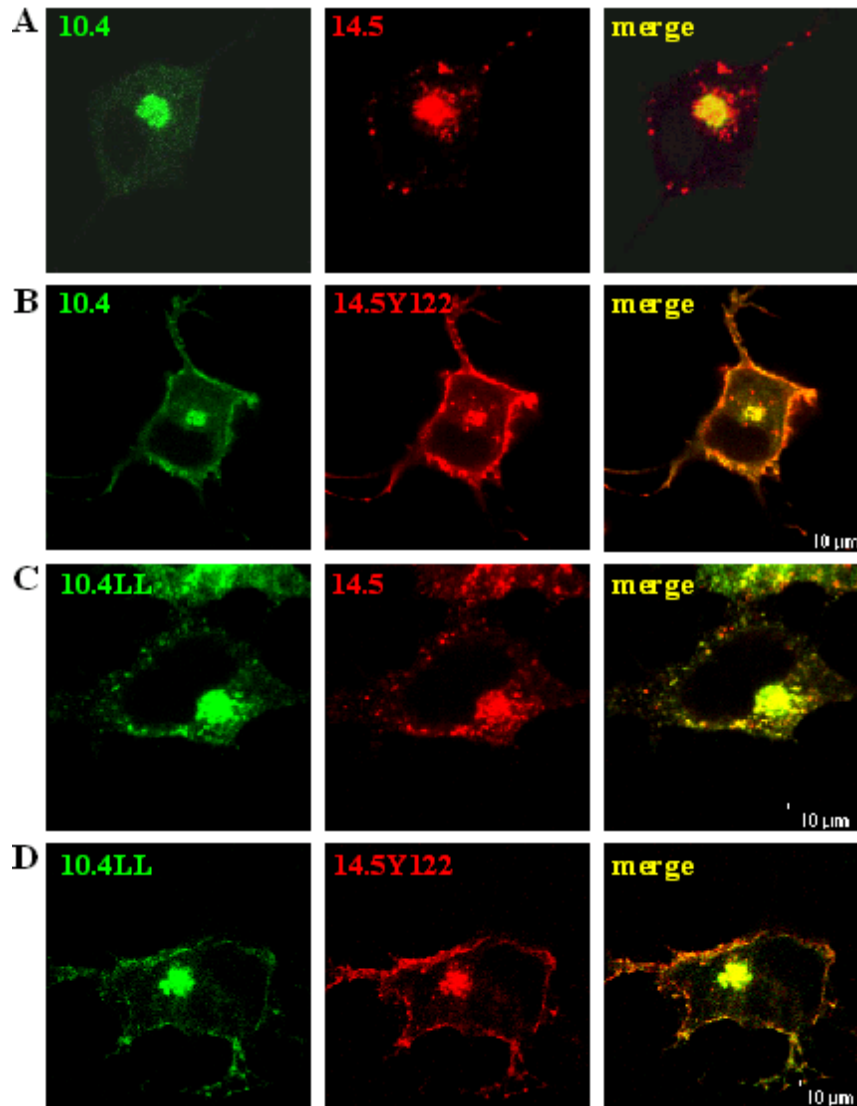


Fig.22 Missorting of 14.5Y122 mutant to the cell surface and 10.4LL to intracellular vesicles

Steady-state localization of 10.4K and 14.5K was analyzed by immunofluorescence in transiently transfected SV80Fas cells at 42 h post-transfection. Different combinations of 10.4 and 14.5 wt and mutant expression plasmids were transfected: pSG5/10.4 + pSG5/F14.5 (**A**), pSG5/10.4 + pSG5/F14.5Y122 (**B**), pSG5/10.4LL + pSG5/F14.5 (**C**), pSG5/10.4LL + pSG5/F14.5Y122 (**D**). Cells were costained for 14.5K with mAb M1 against FLAG (red) and for 10.4 or 10.4LL with polyclonal antiserum Bur3 and R71, respectively (green). The right column shows the overlay of the red and green channel. Bars = 10 μ m.

The effect of the Y122 mutation in 14.5K was analyzed by combining wt 10.4K with the 14.5Y¹²²A mutant. This resulted in a marked increase of cells exhibiting 14.5K plasma membrane staining, confirming the FACS data obtained for stable 293 transfectants. Whereas transfection of the pSG5/10.4 together with pSG5/F14.5 revealed surface exposure of 14.5K in about 50% of 14.5K positive cells, introduction of the 14.5K Y¹²²A mutant resulted in 14.5K surface staining on the entire population of (10.4+F14.5Y¹²²A) positive cells (Fig. 22B). In addition, the surface staining appeared more intense than that of wt 14.5K and lined the rim of the cells, whereas in the wt situation stained patches on the plasma membrane were the most common phenotype (Fig.

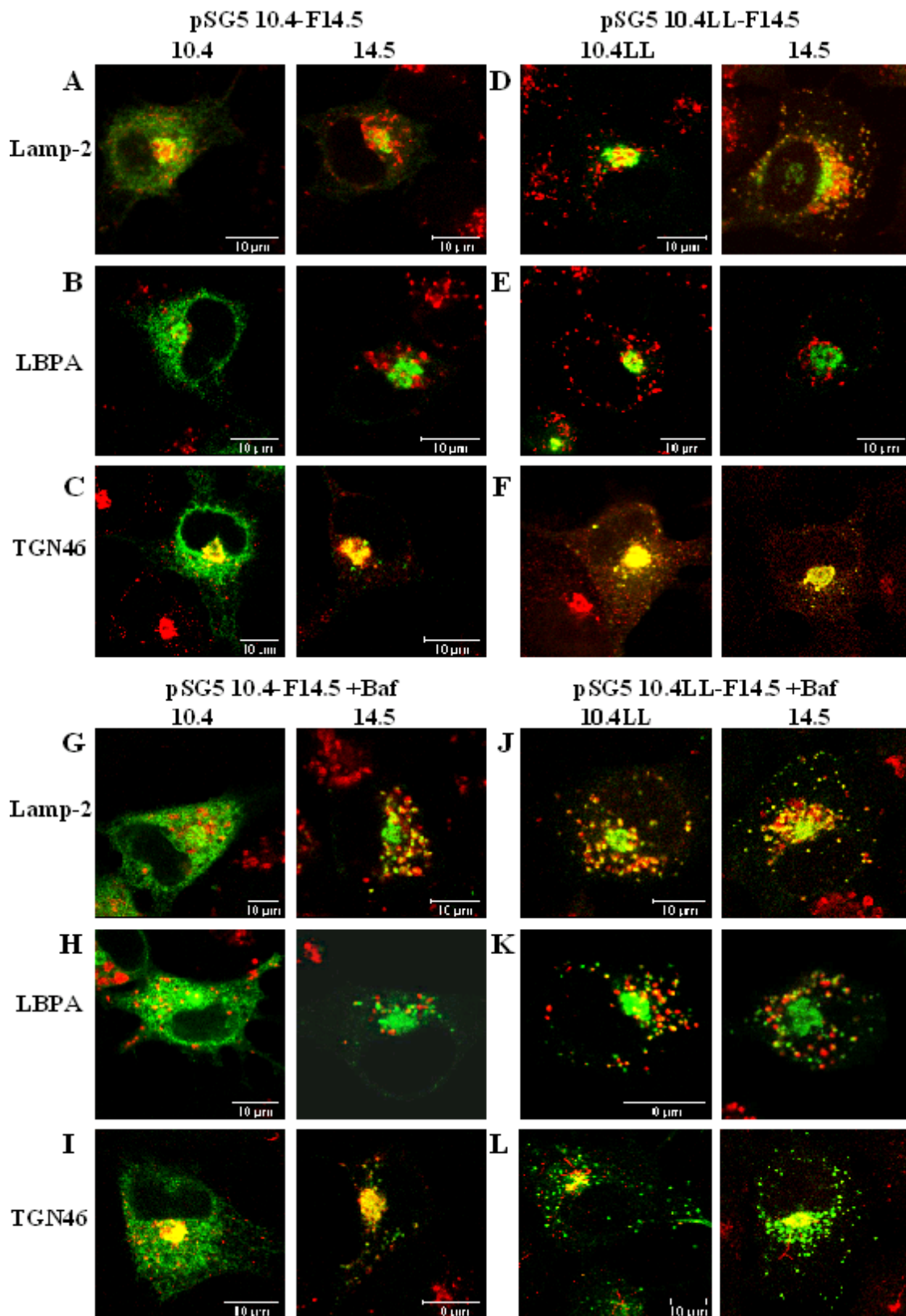
22A). Remarkably, in combination with 14.5K mutant Y¹²²A, the 10.4K protein could also be detected at the plasma membrane and colocalized with 14.5K (Fig. 22B). Thus, both 10.4K and 14.5K were expressed at the plasma membrane, where they presumably exist as a complex. The increased cell surface staining induced by the 14.5Y¹²²A mutant might be explained by a prolonged residence time on the surface, caused by inhibition of endocytosis, due to the lack of a functional Y¹²²XXΦ motif. If so, the dileucine pair present in 10.4 was obviously unable to mediate efficient endocytosis in the absence of the Y¹²²FNL motif.

When the 10.4LL mutant was coexpressed with wt F14.5, an increased staining of intracellular vesicles, but no surface staining of 10.4 or 14.5 was observed (Fig. 22C). Interestingly, 14.5K also localized to 10.4LL⁺ vesicles, indicating that the dileucine mutation in 10.4 influenced trafficking of 14.5. This mutual dependence of 10.4 and 14.5 trafficking on the integrity of the studied motifs confirmed the idea that i) the proteins act as a complex and ii) that trafficking of the complex depends on two signals present in the two subunits. The prominent vesicular staining together with the loss of cell surface expression caused by mutating the dileucine motif could be explained by missorting of the 10.4-14.5 proteins either at the TGN or following endocytosis. To distinguish between these two possibilities, the two mutant proteins, 10.4LL and 14.5Y¹²² were coexpressed (Fig 22D). If sorting by the LL motif occurred prior to the proposed activity of the Y¹²²XXΦ motif in endocytosis, the double-mutant was expected to be localized in intracellular vesicles and not at the cell surface. If it acted subsequently to endocytosis, a similar phenotype to that of the Y¹²² mutant could be expected. Fig. 22D shows that the latter was indeed the case. The majority of the cells exhibited a strong cell surface staining of both proteins. This indicated that i) the two mutant proteins are capable of interacting with each other and are transported together to the cell surface, and ii) the dileucine motif does not seem to act as sorting motif at the TGN. As no prominent vesicular staining was detected in this combination, it was concluded that an intact Y¹²²XXΦ motif in 14.5 is required for generation of the vesicular phenotype by the 10.4 dileucine mutant. Therefore, the Y¹²²XXΦ motif seemed to act upstream of the LL motif, which appeared to have a sorting function subsequent to endocytosis. In agreement with the FACS data the 14.5Y¹²²A mutant caused missorting of the 10.4-14.5K complex to the cell surface, whereas mutant 10.4LL caused localization of both 10.4K and 14.5K to intracellular vesicles. Thus, the presence of the dileucine motif prevents transport of 10.4-14.5 into intracellular vesicles and thereby may contribute to its efficient cell surface expression.

4.5. Enhanced transport of 10.4-14.5 to late endosomes/lysosomes in the absence of the 10.4K dileucine motif

To identify the cellular compartments in which wt 10.4-14.5K are localized and to which these molecules are diverted to upon disruption of the dileucine pair in 10.4K the two proteins were coexpressed from a single vector by transfection of pSG5/10.4-F14.5 (Fig. 23A-C, 23G-I) or pSG5/10.4LL-F14.5 (Fig. 23D-F, 23J-L). This system was used to assure that both viral proteins are coexpressed in the same cell. Subsequently, their distribution was determined by costaining with cellular markers. In this expression system the majority of the cells exhibited a prominent ER staining of 10.4 in addition to the perinuclear staining seen before (Fig. 23A). This is presumably due to lower amounts of 14.5 synthesized, as evidenced by the reduced 14.5 cell surface expression seen compared to cotransfection of single expression vectors (see above). The perinuclear compartment was identified as the Golgi/TGN, because it stained with mAbs against galactosyltransferase (data not shown) and TGN46 (Fig. 23C). Only a small number of cells exhibited 14.5 positive vesicles close to the perinuclear compartment, but these did not colocalize with TGN46+ vesicles (Fig. 23C).

The dileucine mutant of 10.4 was no longer found in the ER, but predominantly in the Golgi/TGN where it colocalized with 14.5K (Fig. 23D-F). This phenotype suggested an enhanced export of the dileucine mutant from the ER or a reduced steady-state expression level of the protein, possibly due to increased degradation. The latter suggestion is supported by the restoration of 10.4K dileucine mutant levels to wild-type levels by treatment with Bafilomycin A₁ (Fig. 14B). Therefore, it was tested whether this drug influenced the steady-state localization of wt 10.4-14.5K. Baf treatment of cells transfected with wt 10.4-14.5K induced the appearance of a small but significant number of 14.5 positive vesicles, indicating that wt 14.5K enters Baf-sensitive endosomal/lysosomal compartments. No changes in ER/Golgi localization of 10.4K (Fig. 23G-I) were observed. In cells expressing the 10.4 dileucine mutant Baf triggered the appearance of a high number of 10.4-14.5+ vesicles, which were identified as late endosomal/lysosomal compartments, as they co-stained with Lamp-2 and partially also with lysobisphosphatidic acid (LBPA, Fig. 23J, K), but not with TGN46 (Fig. 23L). These findings corroborated the previous suggestion that mutation of the dileucine motif of 10.4K causes enhanced degradation of 10.4 and 14.5 in late endosomes/lysosomes. Therefore, the two leucines in the cytoplasmic tail of 10.4 may act as a sorting signal to prevent internalized 10.4-14.5 from being transported into a degradative vesicular compartment, and thereby protect 10.4-14.5K from degradation. Taking into account the drastically low 10.4-14.5K levels at the cell surface of the 293 10.4LL mutant the LL motif may be required to direct the viral proteins into a recycling compartment.

**Fig. 23**

Disruption of the dileucine motif in 10.4K influences the steady-state localization of 10.4K and 14.5K
 SV80Fas cells transfected with pSG5/10.4-F14.5 (A-C and G-I), or pSG5/10.4LL-F14.5 (D-F, J-L), respectively, were processed for immunofluorescence analysis. At 40h post transfection without (A-F) or with (G-L) treatment with Bafilomycin A₁ (11h, 100 nM) localization of 10.4 or 14.5 (green) was compared to that of marker proteins for different cellular compartments (red): Lamp-2 (late endosomes/lysosomes), LBPA late endosomes, TGN46 (TGN). Bars = 10 μm. The antibodies are given in *Materials and Methods*.

5. Characterization of 10.4-14.5K loss of function mutants in infected cells

To examine the phenotype of mutant 10.4-14.5 proteins in the viral context and to extend the analysis to primary cells, the mutations that caused a loss of 10.4-14.5 function in stable transfectants were incorporated into the Ad genome. To achieve this, a novel method for manipulation of complete viral genomes was employed, that is independent of any restriction enzyme sites (Ruszics et al., manuscript in preparation).

5.1. BAC technology for manipulation of Ad2 genomic DNA

The entire genome of adenovirus type 2 had been inserted by homologous recombination directed by the left and right ITRs into plasmid pKBS2 yielding BACmid pAd2-BAC (Ruszics et al., manuscript in preparation). pKBS2 and its derivative BAC constructs are based on the well-studied *Escherichia coli* F factor. Replication of the F factor in *E. coli* is strictly controlled, maintaining a low copy number (1 or 2 copies per cell), and thus reducing the potential for recombination between DNA fragments carried by the plasmid. pKBS2 incorporates regulatory genes of F factor replication including parA, parB, parC, which serve to maintain a low copy number, as well as the repE gene and oriS that mediate the unidirectional replication. In addition, pKBS2 encodes a chloramphenicol resistance marker for selective amplification of the vector. Incorporation of large inserts, such as adenoviral genomic DNA, into pKBS2 generates a BAC vector that permits easy isolation and manipulation of the large viral DNA in solution with minimal breaking. BAC vectors based on F factor replication exist as supercoiled circular plasmids in *E. coli*, and therefore can be stably maintained and grown up in bacteria (Shizuya et al., 1992). Moreover, they can be transformed into *E. coli* by electroporation. Compared with the chemical transformation procedure electroporation usually yields a higher number of transformants and does not bias against large molecules (>20kb). For the BAC vector pAd2-BAC with an overall size of 42 kb electroporation proved very useful and a sufficient number of transformants was readily obtained.

5.2. Generation of recombinant Ad mutants by ET cloning:

5.2.1. Generation of 10.4LL-F14.5 and F14.5Y74A mutant alleles by PCR

The BAC vector pAd2-BAC had been employed to generate recombinant Ad2 expressing a FLAG-tagged version of wt 14.5K, and FLAG-14.5Y¹²²A instead of wt 14.5K (Ruszics, unpublished). In this study a similar approach was used to create virus mutants Ad2/10.4LL-F14.5 and Ad2/FLAG-14.5Y⁷⁴A. The procedure was based on a gene replacement strategy, replacing the wt by

the mutant allele. Advantage was taken of the fact that mutations for the generation of 14.5Y^{74A} and 10.4LL/AA were preexisting on plasmid pBSΔX-E3/FLAG-14.5 expressing FLAG-tagged versions of 14.5K, and therefore this plasmid was used as a template to amplify a linear fragment of DNA encompassing the mutant sequence by PCR (Fig. 24, primers 1 and 2).

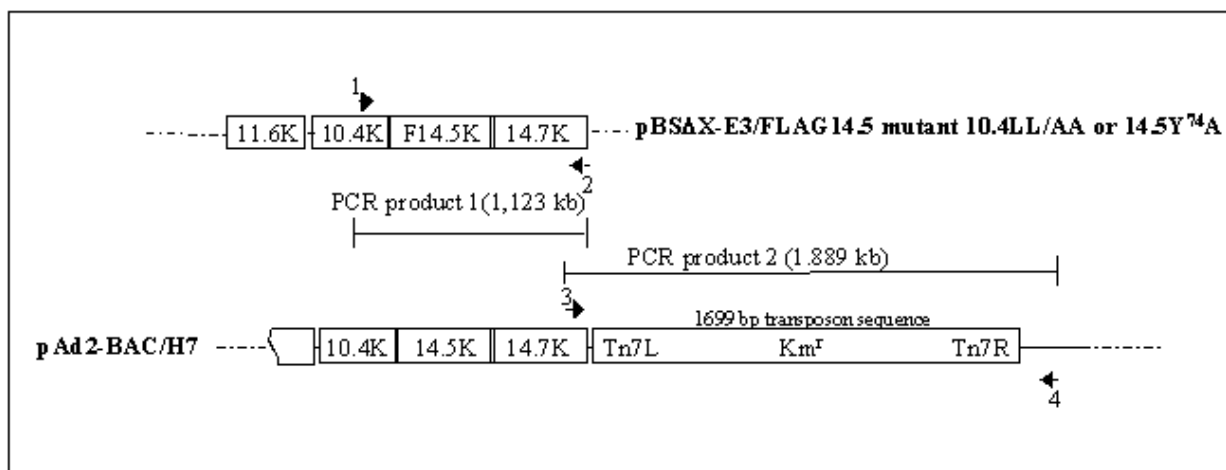


Fig.24 Generation of linear recombination fragment for ET recombination

Mutant alleles were combined with the mTn sequence in a two-step PCR, making use of the following primers: 1, 2395; 2, 3468rev; 3, 3468for; 4, Ad2/E3-rev.

In order to be able to control the replacement process and to select for clones carrying the mutant allele, a selection marker was fused to the mutant allele. In a second PCR reaction using a forward primer (primer 3) that overlaps with primer 2 a fragment of the Ad2 genome sequence was amplified which possessed a transposon (mTn) harboring a Km resistance gene cassette (Fig. 24, primers 3 and 4). BACmid pAd2-H7, which corresponds to the pAd2-BAC with a Tn7 kanamycin resistance gene (Km^r) inserted into the intergenic region between E3B polyadenylation site and the E3 fiber protein served as a template. By assembly PCR using primers 1 and 4 and the two primary PCR products a full-length mutant allele containing the transposon encoded kanamycin resistance gene as a marker was obtained. The assembled PCR product was purified by gel extraction to exclude any contamination with other types of DNA, e.g. the vector template.

5.2.2. ET recombination strategy

For gene replacement to occur the assembled PCR product had to be introduced into an appropriate bacterial strain that would allow homologous recombination of the mutant allele with the target BAC. This was achieved by electroporation into DH10B cells containing pAd2-BAC and pBAD $\alpha\beta\gamma$. High-copy plasmid pBAD $\alpha\beta\gamma$ (Zhang et al., 1998b) encodes gene products of the λ

phage red operon, which is similar to the RecET recombination system, to promote efficient homologous recombination. In a method referred to as ET cloning *recE* and *recT* recombinases, encoded by part of the RAC prophage integrated in *E. coli* K12, have been transferred to a mobile unit, plasmid pBADE γ and exploited to force homologous recombination of linear DNA

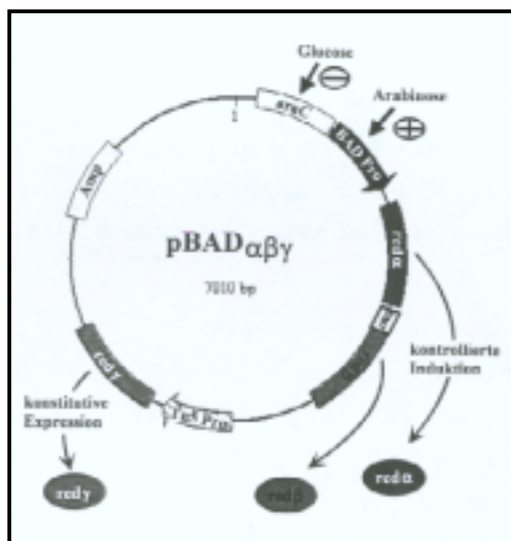


Fig.25 Circular Map of plasmid pBAD $\alpha\beta\gamma$ encoding genes of the phage λ red operon.

Red α expression is controlled by the pBAD promoter, which is repressed by the regulatory protein *araC*. Addition of arabinose (0,1% w/v in the culture medium) frees the promoter from the bound regulatory protein, leading to promoter activation. In the presence of glucose dissociation of the *araC* protein is blocked and promoter activity is inhibited. Red β expression is driven by the EM7 promoter and red γ by the Tn5 promoter. pBAD $\alpha\beta\gamma$ has a size of 7010 bp and encodes an ampicillin (Amp) resistance gene.

fragments with circular DNA in various *E. coli* hosts. (Zhang et al., 1998b). For the same purpose plasmid pBAD $\alpha\beta\gamma$ had been developed (Zhang et al., 1998b). In pBAD $\alpha\beta\gamma$ (Fig. 25) expression of Red α (*exo*), a 5'→3' exonuclease, is regulated by an arabinose-inducible pBAD promoter (Invitrogen). It progressively degrades the 5'-ended strand of double-stranded DNA, generating 3' overhangs (Poteete, 2001). Red β (*bet*), binds to single-stranded DNA, promotes renaturation of complementary strands and is capable of mediating strand annealing and exchange reactions *in vitro* (Li et al., 1998b). The strong, constitutive EM7 promoter permits a high level of red β expression in order to promote efficient recombination. Red γ (*gam*) is required to suppress cellular *recBCD*-mediated degradation of the introduced linear double-stranded DNA (Murphy, 1991). Therefore, it is constitutively expressed upon Tn5 promoter transcription.

For the red recombination system 25 to 60 bp homology ends suffice to direct efficient recombination (Muyrers et al., 1999). The amplification primers 1 and 4 had been chosen in a way that the full-length mutant allele carrying the transposon insertion had sufficient flanking homology regions to the wild-type sequence to be replaced. Red α , Red β mediated a double crossing-over between the homologous ends of the linear PCR fragment and the wt pAd2-BAC generating a mutant pAd2-BAC containing the transposon sequence (mTn), which could be selectively amplified in Cm/Km containing media.

5.2.3. ET cloning strategy for the generation of 10.4K and 14.5K single knock-out viruses

Instead of deleting the 10.4K or 14.5K open reading frames, which might have caused alteration of gene expression in the complex E3 transcription unit (Brady and Wold, 1988; Wold et al., 1995) 10.4K and 14.5K coding sequences were modified by introducing a frameshift in 10.4K or mutating the start codon of 14.5K to create single knock-outs. The mutations were identical to those on plasmids pBSΔX-E3-10.4*, pBSΔX-E3-14.5* (Elsing and Burgert, 1998), and had been introduced into the BAC vector yielding pAd2/(10.4-14.5)ko (Obermaier, unpublished). For generating pAd2-BAC vectors with the desired mutation the above described ET recombination strategy was applied with the following modifications. To generate PCR product 1 encompassing the 14.5ko mutation, BAC vector pAd2/10.4ko-14.5ko was used as a template (Fig. 26A, primers 1 and 2). PCR product 1 was assembled with the minitransposon- containing DNA fragment of the second PCR reaction (Fig. 26A, primers 3 and 4). The assembled PCR product

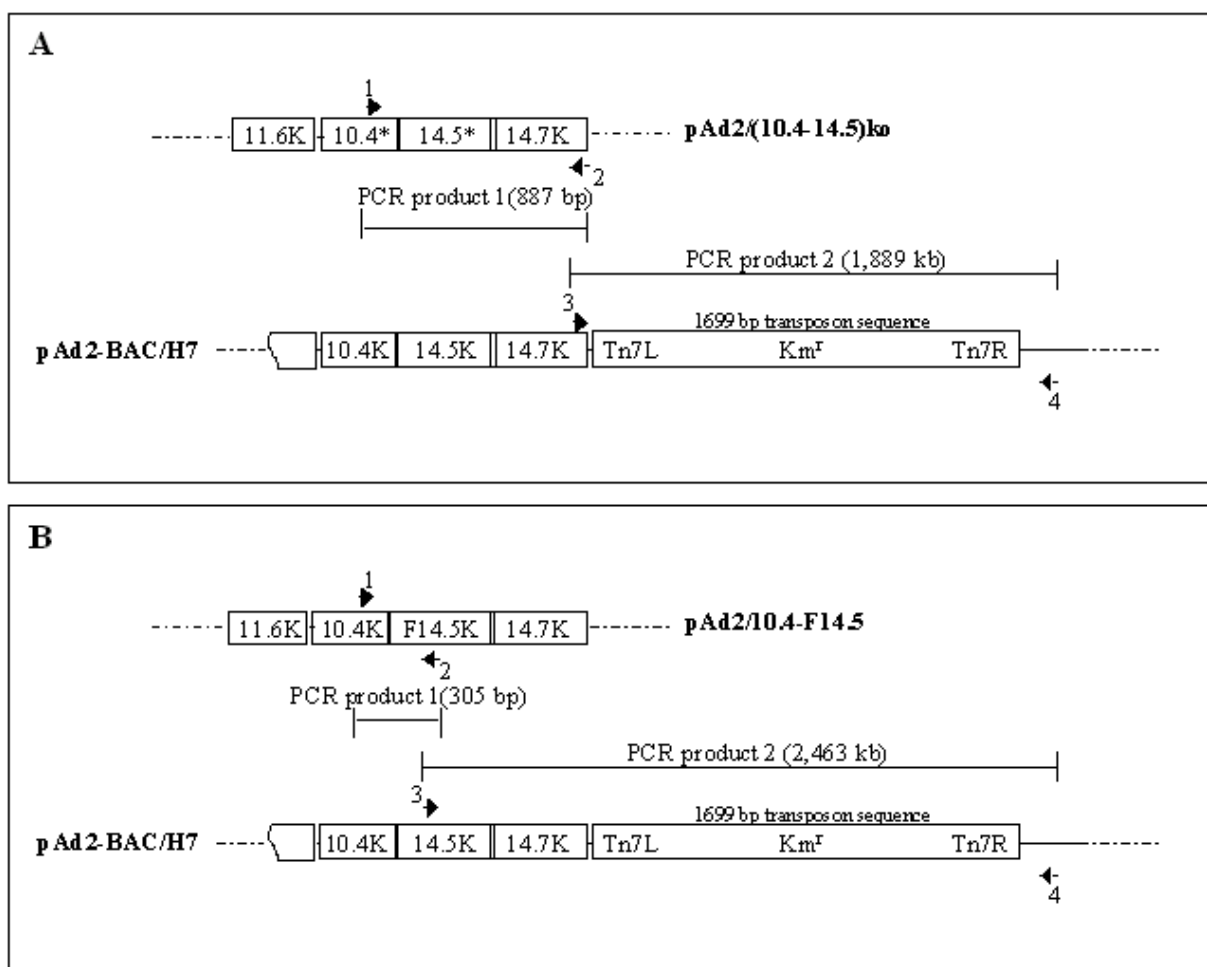


Fig.26 (A) primer 1, 2631for; primer2, 3468rev; primer 3, 3468for; primer 4, Ad2/E3-rev. **(B)** primer 1 2631for; primer 2, 2913rev; primer 3, 2913for; primer 4, Ad2/E3-rev.

was gel-purified and transformed into DH10B cells containing pAd2-BAC and pBAD $\alpha\beta\gamma$ for ET recombination. To create pAd2/10.4ko-F14.5 a FLAG-14.5K encoding fragment was used to replace the mutant 14.5K sequence in pAd2/10.4ko-14.5ko. Thus, as a first PCR product a short fragment overlapping the 10.4K 3' end and the first 210 nt of the FLAG-14.5K sequence was synthesized and assembled with PCR product 2 (Fig. 26B). The assembled PCR product was gel-purified and transformed into DH10B containing pAd2/10.4*-14.5* and pBAD $\alpha\beta\gamma$ for ET recombination.

5.2.4 Analysis of minitransposon-containing mutant pAd2-BACs

Even though pBAD $\alpha\beta\gamma$ lacks Cm/Km resistance genes it usually was found to copurify with a first round of small scale preparation of pAd-BAC mutant DNA. As a high copy plasmid it could hardly be diluted out in subsequent rounds of bacterial growth in ampicillin-free liquid cultures. Retransformation of the BAC-DNA into DH10B allowed to generate clones which were Cm/Km-resistant, but could not grow on ampicillin-containing media. Only bacterial clones that were rid of this contaminant were used for large scale purification of Cm/Km-resistant pAd2-BAC mutant DNA.

Correct insertion of the mutant allele was analyzed by restriction cut of BAC DNA. The mutation in the 14.5ko Ad2 genome could be identified by gel electrophoresis of mutant BAC DNA cleaved by *Pad*. The mutation introduced to eliminate the 14.5K start codon had caused a 1 bp frameshift and a new *Pad* site, which resulted in generation of an additional 1.5 kb band that could be visualized on the gel (Fig. 27A, *Pad*). A complete list of *Pad* restriction sites of wt and mutant BAC DNA and resulting restriction fragment size is given in annexe. Similarly, mutation of 14.5K Y74 introduced a new *Pvu* site and therefore an additional DNA fragment of 1.5kb appeared on the gel (Fig. 27A, *Pvu*, refer to annexe for a list of *Pvu* sites). To exclude any unwanted rearrangements of the BAC sequence mutant clones were cut by *EcoRV*, which yielded the correct banding pattern expected for mTn-containing clones (Fig. 27A, *EcoRV*, constructs 1-4, and *EcoRV*-list in annexe). The mTn sequence contains two *EcoRV* sites. Therefore, the *EcoRV* cleavage of mTn containing BAC constructs generated three characteristic fragments that were not obtained upon cleavage of the pAd2-BAC without the transposon (Fig. 16A, *EcoRV*, compare constructs 1-4 with construct 5).

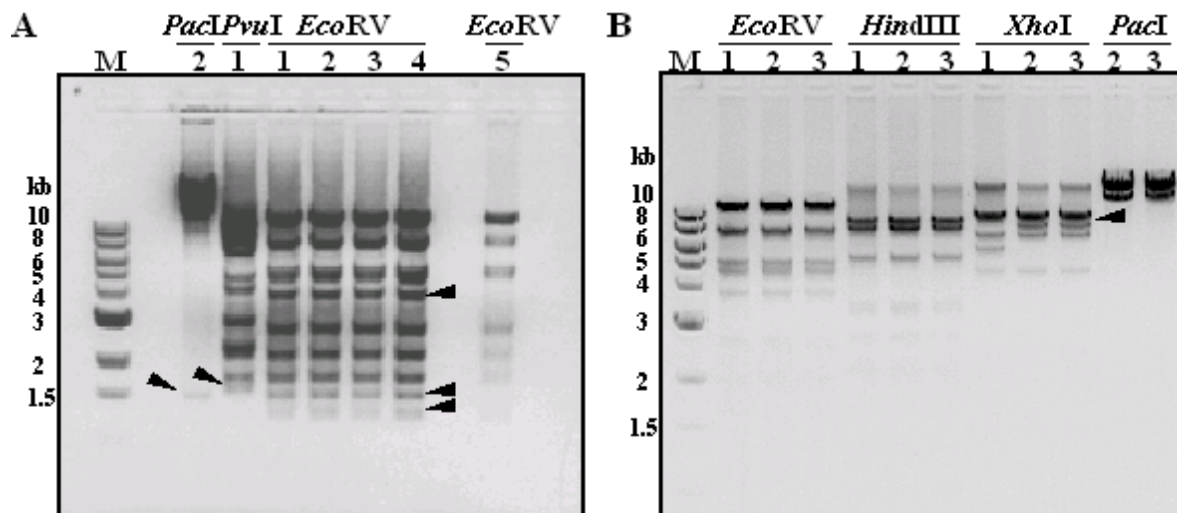


Fig. 27 Analytical restriction cut of mTn-containing mutant pAd2-BACs

Analytical restriction digests of mutant pAd2-BAC DNA were separated on a 0.8% agarose gel. Restriction enzymes used are listed above the lanes. Numbers on top of the lanes denote the type of BAC DNA analyzed. M, 1kb DNA ladder. Arrowheads highlight the appearance of additional fragments, that were not obtained with wt pAd2-BAC.

(A) construct number 1, pAd2-H7/F14.5Y74; 2, pAd2-H7/14.5ko; 3, pAd2-H7/10.4ko-F14.5; 4, pAd2-H7/10.4LL-F14.5; 5, pAd2-BAC.

(B) construct number 1, pAd2-H7; 2, pAd2-H7/10.4ko-F14.5 #37; 3, pAd2-H7/10.4ko-F14.5 #41.

Disruption of the 10.4K open reading frame was achieved by deletion of a *XhoI* site within the 10.4K coding sequence which introduced a 4bp frameshift 13 bp downstream of the 10.4K start codon. Therefore, the banding pattern of a *XhoI* restriction cut was different from the one obtained with the wt sequence (clone pAd2-H7) with a 8.3kb band instead of two smaller fragments (Fig. 27B, *XhoI*), but the *EcoRV* and *HindIII* restriction pattern was identical to that of unmodified pAd2-H7. A complete list of *XhoI*, *EcoRV* and *HindIII* restriction sites and resulting fragment sizes in the mTn-containing BAC vectors is given in annexe). The mutagenized part of the E3 region was sequenced to assure the correctness of 10.4K or 14.5K mutant gene sequences.

5.2.5. Transposon removal

As the Km^r gene was part of a bacterial Tn7-derived transposon sequence, it could be excised from pAd2-BAC mutant DNA *in vitro* by use of a Tn7 transposition system, TnsABC*, and subsequent religation of the gap (Ruzsics et al in preparation).

TnsABC* (New England Biolabs, Frankfurt, Germany) consists of wt bacterial proteins TnsA, TnsB, which act interdependently to execute the catalytic steps of the transposition reaction (Biery et al., 2000a), and a mutant variant of TnsC. Wt TnsC is an ATP-dependent DNA-binding protein (Gamas and Craig, 1992). TnsC binds DNA without any obvious sequence specificity, but

it depends on Tn7-encoded TnsD or TnsE target selection proteins to enable transposition. Gain of function mutant TnsC* (TnsC^{A225V}) can activate TnsA+B in the absence of TnsD or TnsE to give very robust levels of recombination with low target site selectivity (Biery et al., 2000b; Stellwagen and Craig, 2001). The TnsABC*-mediated transposon excision reaction is initiated following specific recognition of the inverted repeats at the Tn7 transposon ends by TnsB. TnsC* binds to target DNA and interacts with TnsB. TnsA associates with TnsB:DNA. Thus, a three protein, two DNA complex is assembled and allows TnsA and TnsB to carry out the strand transfer reaction in the presence of cofactors ATP and Mg²⁺. The donor DNA is cleaved three bases 5' to the transposon in one strand and precisely at the transposon 3' end in the other strand. This occurs on both sides of the transposon, creating three base single-stranded 5' overhangs in the donor DNA. In the target DNA a five-base staggered cut is made. Transposon insertion results in a five-base duplication of target sequences (Craig, 1996).

For transposon excision from Km-resistant mutant pAd2-BAC DNA to occur, TnsABC* was applied to an *in vitro* reaction mix containing both pAd2-BAC donor DNA and plasmid pST76Tet as transposon acceptor (as described in *Materials and Methods*). Plasmid pST76Tet carries a temperature-sensitive mutation in the pSC101 replicon and cannot replicate at 37-42°C (Posfai et al., 1997; Posfai et al., 1999). Thus, the transposon will be received by a suicide plasmid and during bacterial growth cells are easily cured of that plasmid.

TnsABC*-mediated transposon excision from pAd2-H7-derived mutant BAC vectors created 3'-overhangs which could anneal as they contained complementary bases (Ruszics et al, manuscript in preparation). These cohesive ends were religated by addition of T4 DNA ligase. Correct transposon removal from pAd2-H7-derived mutant BAC vectors and religation of the gap was characterized by creation of a new *NheI* restriction site (Ruszics et al., manuscript in preparation, and data not shown).

To efficiently eliminate Km-resistant BAC vectors that persist due to incomplete transposition a strong counterselection tool was applied. The reaction mix was electroporated into *E. coli* strain RP-12, which constitutively expressed a meganuclease I-*Sce* I from high copy plasmid pUC19RP12 (Posfai et al., 1999). Meganuclease I-*Sce* I (Intron encoded meganuclease from *Saccharomyces cerevisiae*) recognizes a specific sequence of 18 nucleotides in the transposon sequence. Because of the length of the recognition sequence such a meganuclease target site is extremely rare and thus not present in the BAC vector backbone, in the *E. coli* genome, nor in the Ad2 genomic sequence (Posfai et al., 1999), Ruszics et al, manuscript in preparation). Meganuclease cleavage induces a double-stranded break in the mTn containing DNA, generating free DNA ends that trigger degradation of these DNA species.

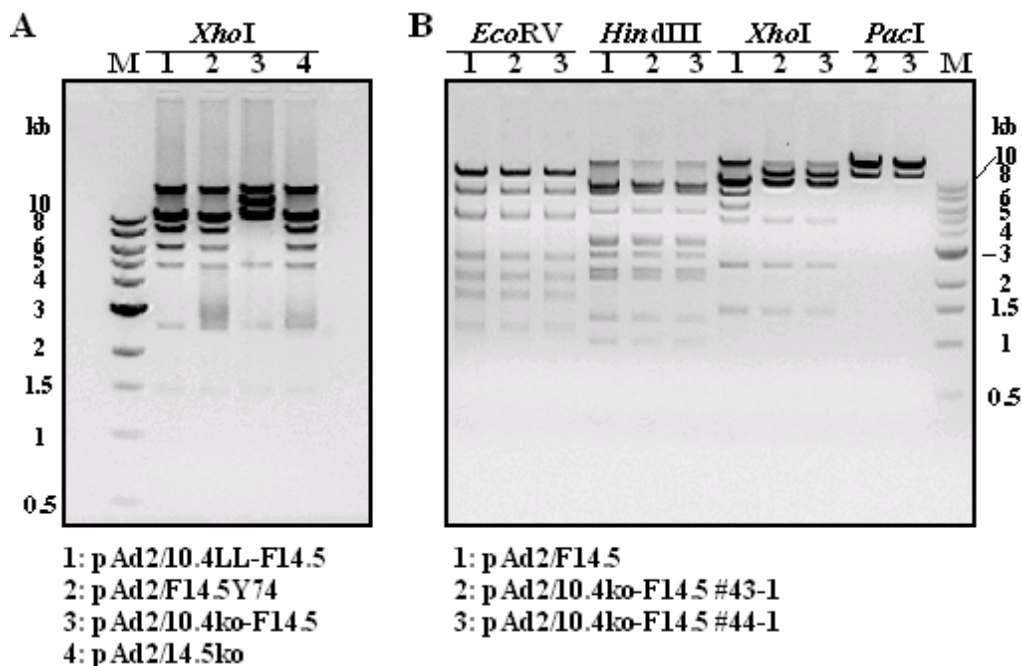


Fig. 28 Analysis of mutant pAd2-BACs by restriction cut

Analytical restriction digests of mutant pAd2-BAC DNA were separated on a 0.8% agarose gel.

Enzymes used for the restriction cut are listed above the lanes. Numbers on top of the lanes denote the type of BAC DNA analysed, as listed below the gel pictures. M, 1kb DNA ladder.

To eliminate contamination by high copy plasmid pUC19RP12, the BAC-DNA was isolated from RP-12 cells, retransformed into DH10B and Cm^r/Ap^s clones were selected. The integrity of the newly generated mutant pAd2-BAC vectors was analyzed by restriction cuts (Fig. 28). For a detailed overview of restriction fragments, see annexe.

XhoI cleavage of the mutant BACs pAd2/14.5ko (no FLAG-sequence), pAd2/10.4LL-F14.5, pAd2/F14.5Y74 (Fig. 28A) yielded the expected band pattern which was similar to that of pAd2/F14.5 (shown in Fig. 28B, *XhoI* cut of construct 1, and annexe). The top band that was present in all *XhoI* restriction cuts seemed to result from incomplete digestion. The 10.4ko mutation abolished one *XhoI* site, thus the 5864 bp and 7918 bp fragments were not generated, but migrated as one band of 13778 bp in size (Fig. 28A, *XhoI*, and annexe). The mutant BAC clone pAd2/10.4ko-F14.5 was additionally cut by *PacI* to confirm that the 14.5* ORF in the acceptor BAC DNA had been replaced by the FLAG-14.5K sequence. The mutated 14.5K start codon had been successfully replaced, as no 1.5kb fragment was obtained (Fig. 28B, *PacI*, annexe). *EcoRV* and *HindIII* digestion of pAd2/10.4ko-F14.5 yielded the correct pattern, identical to the wt situation (Fig. 28B, annexe).

SnaB1 digestion liberated the viral DNA framed by intact flanking ITRs from the BAC vector backbone and a purified preparation of 2-6 µg of linear Ad2 mutant genomes was

transfected into 293 cells ($\sim 2 \times 10^6$ cells) for reconstitution of viral particles (described in *Materials and Methods*).

5.3. Recombinant Ads expressing 10.4-14.5 mutants are defective in receptor down-modulation

With the gene replacement strategy for manipulation of entire Ad genomes described above the desired mutations could be introduced into the viral genes in their native location, allowing to study mutant proteins in the context of Ad infection and under natural conditions of viral protein expression. Moreover, virus mutants would allow to extend the analysis to primary cells. Therefore, the mutations that caused a loss of 10.4-14.5 function in stable transfectants were incorporated into the Ad genome. Recombinant adenoviruses expressing wt 10.4K and FLAG-14.5K (Ad2/F14.5) and mutant viruses encoding FLAG-tagged versions of 14.5 were created. The mutant viruses expressed 10.4LL, 14.5Y⁷⁴A or 14.5Y¹²²A mutant proteins.

For functional characterization of the mutant proteins A549 cells were infected with recombinant Ads at MOI 100 pfu/cell and receptor levels were measured by FACS analysis at 21-24 hours p.i. On A549 cells the entire series of surface receptors identified as targets of 10.4-14.5K induced down-regulation, namely Fas, EGFR and both TRAIL receptors DR4 and DR5 are sufficiently expressed to allow FACS analysis of their surface expression levels. As a marker of infection efficiency the cell population was analyzed for intracellular E3/19K levels. Cells infected with mutant viruses expressed at least as much E3/19K as those infected with wt and in all cases infection efficiency was close to 100% (data not shown). Thereby, it was ascertained that receptor surface expression levels were determined on a similar population of cells infected with wild-type or mutant Ads. Similar to wt Ad2 (Elsing and Burgert, 1998), Ad2/F14.5 infection of A549 cells diminished cell surface expression of Fas and EGFR by more than 95%, as measured by FACS analysis (Fig. 29A, B). By contrast, recombinant viruses lacking expression of either 10.4K, 14.5K or both were incapable of down-modulating Fas, but rather induced its cell surface expression. This may be due to Ad-induced NF- κ B activation which in turn stimulates the Fas promoter (Gil et al., 1999; Kuhnel et al., 2000) or by Ad-induced activation of p53 resulting in a transient upregulation of Fas on the cell surface (Bennett et al., 1998). Independent of which 10.4-14.5 knock-out Ad was utilized for infection, EGFR levels consistently declined to about 80% of that in uninfected cells, indicating an additional, 10.4-14.5K-independent modulation, presumably caused by E1A-induced transcriptional repression (Prudenziati et al., 2000). Of note, the Ad2/14.5ko virus caused an even stronger reduction in EGFR surface expression levels.

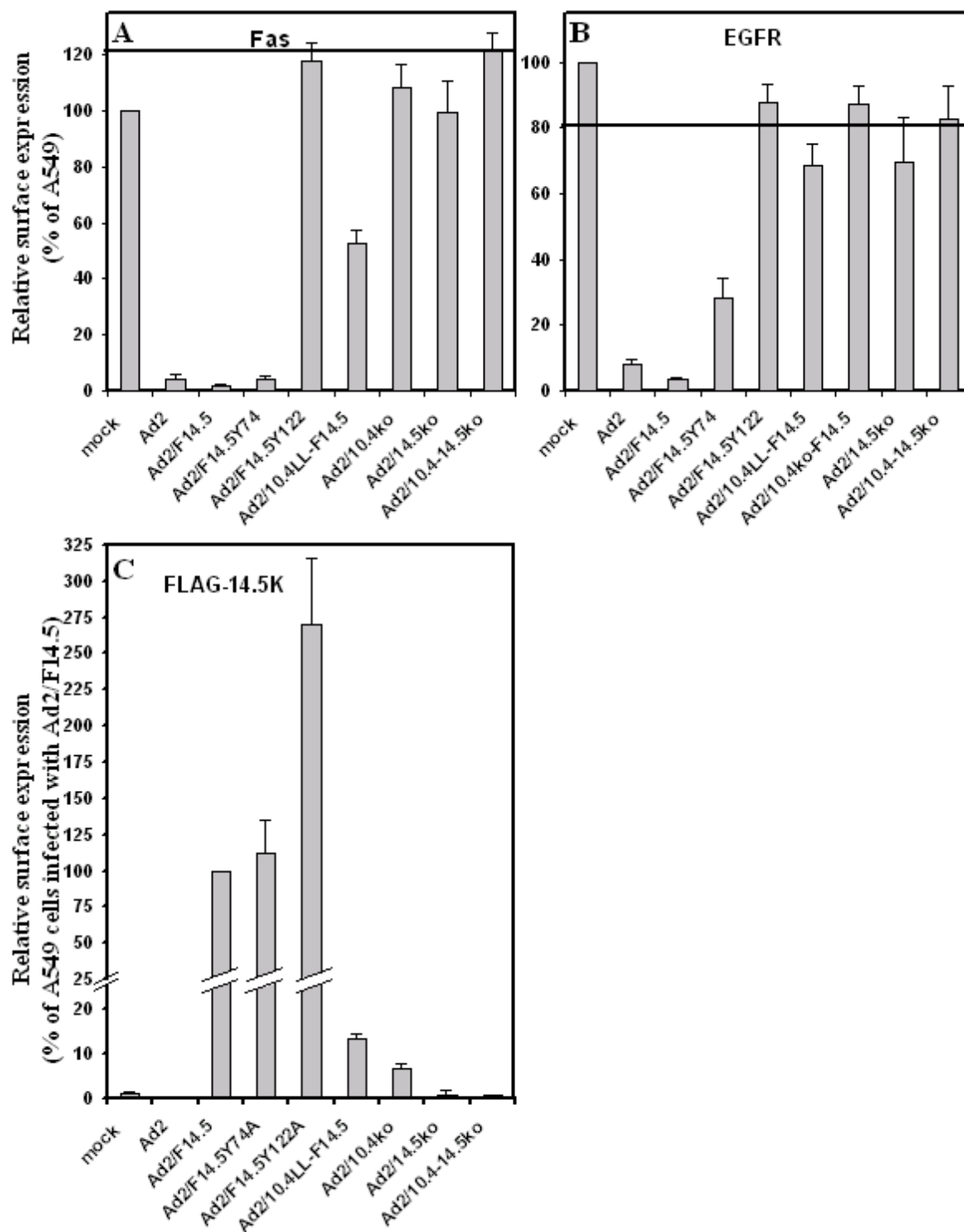
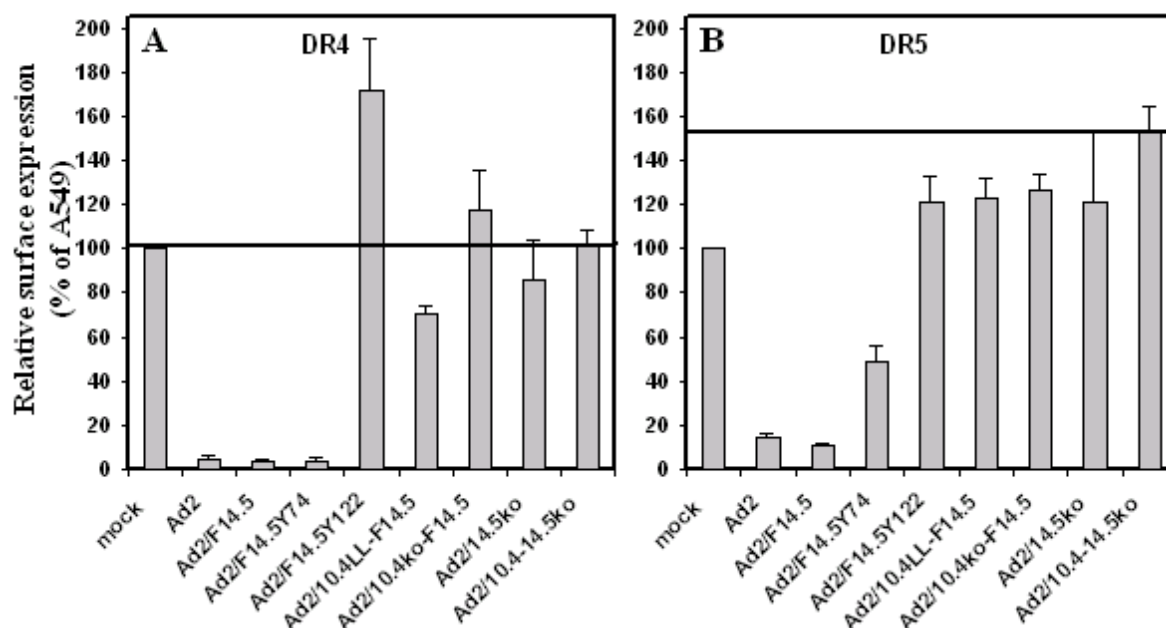


Fig. 29 Functional activity of mutant 10.4-FLAG-14.5K in infected cells

A549 cells were infected at equal MOI (100 pfu/cell) with wt Ad2 or recombinant Ads expressing 10.4-F14.5 wt and mutant proteins or lacked expression of 10.4K, 14.5K or both, as indicated below the figure. At 21 – 24 hours p.i. cell surface expression of Fas (**A**, mAb B-G27), EGFR (**B**, mAb 528) and FLAG-14.5K (**C**, mAb M1) were determined by FACS analysis, as described in *Materials and Methods*, and related to those on mock-infected A549 cells (**A**, **B**) or Ad2/F14.5-infected cells (**C**), determined in parallel and set to 100%. Infection efficiency was nearly 100%, as judged by parallel FACS analysis of intracellular E3/19K levels (mAb 3A9). Data were compiled from at least 5 independent experiments. Error bars represent the SEM.

**Fig. 30****Relative cell surface expression of DR4, DR5 on A549 cells infected with 10.4-14.5K mutant viruses**

A549 cells were infected with wt Ad2 or recombinant Ads (MOI 100 pfu/cell) that expressed 10.4-F14.5K wt and mutant proteins or lacked expression of 10.4K, 14.5K or both (as indicated below the figure). Relative DR4 (**A**) and DR5 (**B**) surface expression levels were determined by FACS analysis at 24 hours p.i. MAb 1H5 and 3F11 were used to detect DR4 and DR5, respectively, and G α M FITC (SIGMA, Munich, Germany) was used as secondary Ab. Experimental values minus unspecific background were related to those on mock-infected A549 cells determined in parallel and set to 100%. Results from 3 independent experiments were compiled to calculate the arithmetic mean (bars) and SEM (error bars). For clarity a horizontal line is drawn to illustrate the levels on cells infected with Ad2/(10.4-14.5)ko.

Confirming the data obtained in transfectants, the Y¹²²A mutation completely abolished the function of the 10.4-14.5K complex, in that both Fas and EGFR expression on the cell surface remained unaffected upon infection with Ad2/F14.5Y122. Fas and EGFR levels were comparable to those on Ad2/10.4-14.5ko-infected cells. Furthermore, in line with the accumulation seen in the 293 transfectants, the Y¹²²A substituted FLAG-14.5K protein accumulated to roughly 2.7 fold higher levels at the plasma membrane compared to wild-type FLAG-14.5 (Fig. 29C). Remarkably, in cells infected with Ad2/10.4ko-F14.5, lacking coexpression of 10.4K, F14.5K surface expression reached only 6.5% of wt levels. This underscores the results of the immunofluorescence analysis which suggested that efficient cell surface transport of 14.5K depends on 10.4K. As illustrated in Fig. 17 and Fig. 18 steady-state localization of 14.5K changed upon coexpression of 10.4K, 14.5K was relocated from the ER into post-Golgi compartments.

Interestingly, inactivation of 10.4-14.5K was incomplete in the Ad2/10.4LL-F14.5 virus lacking the di-leucine pair of 10.4K. While down-regulation of the EGFR was similarly compromised as upon infection with the 14.5ko virus, Fas levels were reduced to 53 % of the levels on mock-infected cells. Related to levels on cells infected with the double knock-out virus

the mutant 10.4LL-14.5 retained 56 % of the activity of wt 10.4-14.5 towards Fas. Strikingly, in Ad2/10.4LL-F14.5-infected cells F14.5 surface expression levels reached only 13 % of the wild type (Fig. 29C), a level only slightly above that seen upon infection with the Ad2/10.4ko-F14.5 virus (6.5% of wt). Thus, also in the virus context disruption of the 10.4K di-leucine pair caused a strong reduction of F14.5 surface expression levels. The Y⁷⁴A mutant exhibited normal F14.5 surface expression and retained the capacity to efficiently down-regulate Fas (98 % of the reduction on Ad2/F14.5 as related to levels on Ad2/10.4-14.5ko-infected cells), but induced only a partial (69% of the reduction on Ad2/F14.5 compared with Ad2/10.4-14.5ko-infected cells) down-modulation of the EGFR (Fig. 29A, B). This differs from the phenotype seen in stable transfectants, in which EGFR levels were similar to those of (10.4-14.5)ko transfectants and Fas levels indicated a residual activity of only 20% (Fig. 7). The differential effect of the 10.4LL and 14.5K Y74 mutation on Fas and the EGFR down-modulation might argue for a different mechanism of receptor down-modulation. Presumably, the increased de novo synthesis in the infected versus transfected cells could partially compensate the defects of the 14.5Y74 and 10.4 di-leucine mutants.

Concerning down-modulation of DR4 and DR5, respectively, a similar picture was obtained (Fig. 30). Recombinant Ads lacking expression of either 10.4K, 14.5K or both were incapable of down-modulating these receptors. DR4 levels remained equivalent to those on mock-treated A549 cells, and similar to the situation with the EGFR the Ad2/14.5ko virus caused a slight reduction (see discussion). DR5 levels on A549 cells were generally increased upon infection with 10.4ko, 14.5ko and 10.4-14.5ko viruses, to at least 120% of those on mock-infected cells. Wt Ad2 and Ad2/F14.5K efficiently reduced receptor levels of DR4 and DR5 to below 5% and 10-15%, respectively, of those seen in A549 cells. Virus mutant Ad2/F14.5Y¹²² was incapable of reducing receptor levels. Instead, DR4 levels appeared to be significantly increased by at least 50% on cells infected with this mutant. As lack of either 10.4K, 14.5K or both did not induce an increase in surface expression, this effect seems to be a specific consequence of the mutation in 14.5K. Given that substitution of Y¹²² resulted in a 2.7fold increase in F14.5K levels at the plasma membrane the observed increase of DR4 receptor levels might be caused by interference of 10.4-F14.5Y¹²²A complexes with internalization of the receptor. This scenario is consistent with 10.4-14.5K interacting with DR4 at the plasma membrane, the interaction being either direct or indirect. Surface expression levels of the other 10.4-14.5K receptor targets, Fas, EGFR and DR5, were not specifically increased on cells infected with Ad2/F14.5Y¹²². This suggests that 10.4-14.5K act on these receptor targets subsequent to internalization, perhaps in an endosomal compartment.

Down-modulation of the TRAIL-R2 depends on a third E3 protein, E3/6.7K, which has been reported to exist in complex with 10.4-14.5K at the plasma membrane (Benedict et al., 2001). It is not known whether the mutation in 14.5K might disrupt the functional interaction with E3/6.7K, but coexpression of E3/6.7K can obviously not rescue the functional defect of the 10.4-14.5Y¹²²A complex, nor compensate the trafficking defect of the 14.5Y¹²²A mutant.

Thus, in the virus context, substitution of Y122 by alanine was detrimental to down-regulation of 10.4-14.5K receptor targets Fas, EGFR, DR4 and DR5 and caused a dramatic increase in F14.5K surface expression.

Ad2/F14.5Y4 mutant viruses efficiently down-regulated DR4, preserving nearly the activity of the wt proteins, whereas DR5 levels remained at about 50% of the levels on A549 cells. This accounted for about 70% of the reduction observed in Ad2/F14.5 infected cells as related to levels on Ad2/10.4-14.5ko virus-infected cells. Thus, 14.5K Y⁷⁴ is not essential for receptor down-modulation in virus-infected cells. FLAG-14.5K surface expression levels on cells infected with the Y74A mutant were as high as those on Ad2/F14.5-infected cells, a phenotype that affords an interaction of mutant 14.5Y⁷⁴ with 10.4K (see below).

The dileucine mutant of 10.4K appeared to differentially affect down-modulation of different receptor targets: Whereas DR5 levels were comparable to those seen on cells infected with the Ad2/10.4ko virus and only a low reduction in EGFR levels could be observed, DR4 levels were decreased to 70% and Fas levels to 53%. Related to the levels on A549 cells infected with Ad2/10.4-14.5ko this reduction accounted for 32 % of DR4-specific activity and 57 % of Fas-specific activity of wt 10.4-14.5K. The increased efficiency of receptor down-regulation in the infected cells as compared to the stable E3 10.4LL mutant transfectant might be explained by increased 10.4-14.5K expression in infected cells and likely a higher gene copy number. In good correlation, F14.5K levels at the cell surface of the Ad2/10.4LL-F14.5-infected cells reached 13% of Ad2/F14.5 infected cells, whereas in the stable transfectant LL-11 F14.5K surface expression was below 5% of that on F-19 cells. Nonetheless, the drastically decreased F14.5K steady-state surface expression levels indicated that the 10.4LL mutation significantly affected transport of 10.4-14.5K in infected cells (see immunofluorescence analysis below).

Thus, it can be concluded that the Y¹²²XXΦ motif is essential for down-regulation of all known receptor targets of 10.4-14.5, whereas the dileucine motif was primarily critical for down-modulation of DR5 and the EGFR and less important for modulation of DR4 and Fas. This differential effect may indicate mechanistic differences in the targeting of these receptors.

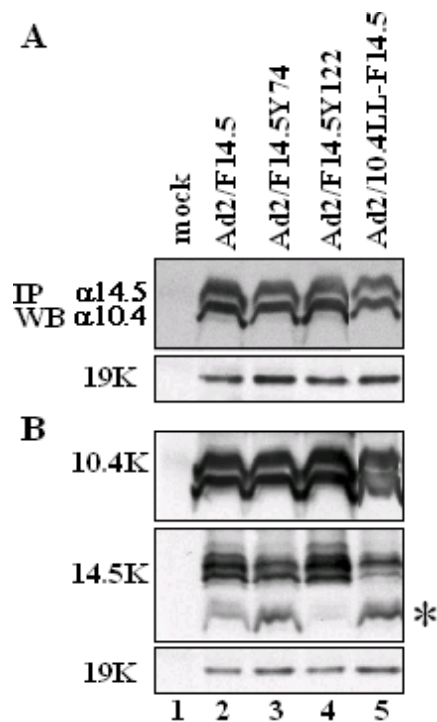


Fig. 31 10.4-14.5K complex formation upon infection of A549 cells with recombinant Ads

(A) Digitonin extracts of infected or mock-infected A549 cells (21 h p.i.) were subjected to IP with polyclonal serum Bur4 directed to 14.5. After separation of immunoprecipitated material by SDS-PAGE the presence of 10.4 was visualized by western blotting, using antiserum Bur3 (α 10.4) in lanes 1-4 (lane 1, mock-infected A549 cells; and infected cells in lane 2, Ad2/F14.5; lane 3, Ad2/F14.5Y74; lane 4, Ad2/F14.5Y122) and R71 specific for 10.4LL in lane 5 (Ad2/10.4LL-F14.5). The same lysates were subsequently reacted with Ranti-E3/19K and blotted material was detected with the same antibody. **(B)** Total amounts of 10.4K, 14.5K and 19K as determined by immunoprecipitation from Triton X-100 lysates and western blotting using the corresponding antisera, as described in Fig. 14.

5.4. Complex formation of mutant 10.4-14.5K in infected cells

For analysis of complex formation A549 cells were infected at a MOI 40 pfu/cell, and at 17 hours p.i. complex formation was analyzed in digitonin extracts of infected and mock-infected cells (Fig. 31A). Prior to immunoprecipitation cell lysates were adjusted to equal protein content. As a control E3/19K was isolated from the same lysates in a second IP step (Fig. 31A). Total amounts of 10.4K, 14.5K and 19K proteins were analyzed in parallel by immunoprecipitation and western blotting in Triton X-100 cell lysates (Fig. 31B). In infected cells, 10.4-14.5 interaction was detectable for all three virus mutants (Fig. 31A), although, in line with the results obtained with E3-transfectants complex formation seemed to be reduced for the 14.5Y74 and the 10.4LL mutants. For the latter, this was accompanied by somewhat lower amounts of 10.4 and 14.5 and markedly increased amounts of low molecular weight products, that presumably represented 14.5K degradation products (Fig. 31B, marked with a *). Remarkably, these lower molecular weight 14.5

products were not visualized in cells infected with mutant Ad2/F14.5Y122, indicating that their generation depends on the presence of tyrosine 122.

5.5. Immunofluorescence of infected primary cells

The recombinant adenovirus mutants allowed to express and localize the mutant 10.4-14.5 proteins in primary fibroblasts, such as SeBu cells (Fig. 32A-D). In SeBu cells infected with wt Ad2/F14.5 the ER and Golgi stained positively for 10.4K and 14.5K, and 14.5K was additionally detected at the plasma membrane. While upon infection with mutant Ad2/F14.5Y74 14.5 surface staining was similar to infection with wt Ad2 (Fig. 32B), ER/Golgi staining appeared less pronounced. Upon infection with the Ad2/F14.5Y122 mutant, cellular extrusions were prominently stained, indicating a markedly increased surface staining of 10.4-14.5K (Fig. 32C), compatible with the proposed role of the Y¹²²XXΦ motif in directing internalization of the 10.4-14.5K complex. By contrast primary fibroblasts infected with Ad2/10.4LL-F14.5 showed no surface staining. Even without Bafilomycin treatment a significant proportion of the cells exhibited a highly vesicular staining for both 10.4 and 14.5 (Fig. 32D), instead of the ER/Golgi staining seen for wt proteins (Fig. 32A). To characterize the nature of the vesicles SeBu cells were infected with Ad2/F14.5 or Ad2/10.4LL-F14.5 and processed for dual label immunofluorescence analysis to compare steady-state localization of 14.5K with cellular marker proteins. In the mutant (Fig. 33A) and the wt (Fig. 33B) situation the perinuclear compartment was costained with GM130, a cis-Golgi marker protein. Upon Bafilomycin treatment, the number of cells bearing 14.5+ vesicles was further increased in cells infected with mutant Ad2/10.4LL-F14.5, but not in cells infected with wt Ad2, in which ER/Golgi staining for 14.5K (Fig. 33D, F, H) remained unaltered. In Ad2/10.4LL-F14.5- infected primary fibroblasts the distribution of 14.5+ vesicles was distinct from the localization of EEA1, a marker for early endosomes (Fig. 33C). Similarly, vesicles did only partially overlap with LBPA which represents late endosomes (Fig. 33E). But both 14.5K (Fig. 33G) and 10.4LL (Fig. 34E) extensively colocalized with Lamp-2+ vesicles.

Remarkably, the reduction of ER staining and redistribution of 10.4K to Lamp-2+ vesicles occurred selectively in cells expressing the 10.4 dileucine mutant (Fig. 34A). In cells infected with Ad2/F14.5 (Fig. 34B) or virus mutants Ad2/10.4-F14.5Y74 (Fig. 34C), Ad2/10.4-F14.5Y122A (Fig. 34D) 10.4K was found in the ER and the Golgi, and did not colocalize with Lamp-2+ vesicles following Bafilomycin treatment (Fig. 34 F-H). Thus, disruption of the 10.4K dileucine motif leads to a profound redistribution of 10.4-14.5K into Lamp-2+ vesicles,

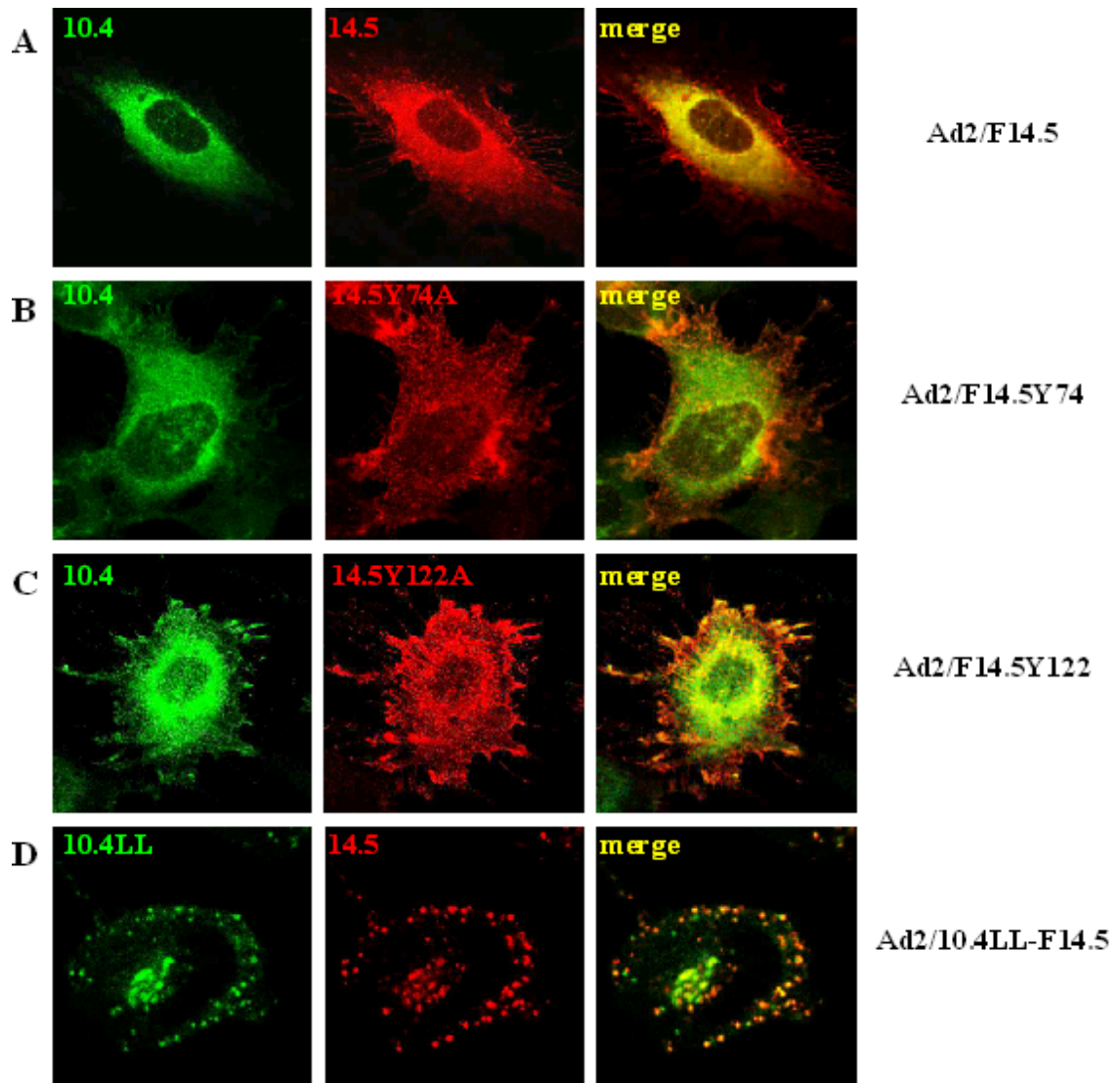


Fig. 32 Localization of 10.4-14.5 complexes in primary fibroblasts infected with Ad2 mutants

Primary fibroblasts (SeBu cells) were infected with 200 PFU/cell of wt **(A)** or mutant Ad2/F14.5 viruses **(B-D)** as indicated on the right. Cells were processed for immunofluorescence analysis at 21h p.i. and stained for wt 10.4 or 10.4LL with polyclonal serum Bur3 or R71, respectively (green), and mAb M1 directed to FLAG-14.5 (red). Upon infection with Ad2/F14.5 **(A)** or Ad2/F14.5Y74 **(B)** 10.4 and 14.5 colocalize extensively in the ER/Golgi and 14.5K can be detected at the cell surface. **(C)** Increased cell surface staining of both 10.4K and 14.5K upon infection with mutant Ad2/F14.5Y122. **(D)** Infection with Ad2/10.4LL-F14.5: 10.4LL and 14.5K colocalize in a perinuclear compartment and vesicular structures.

accompanied by a reduction of ER staining, which indicated an increased ER export rate and a faster delivery of the complex into lysosomes. In the absence of the dileucine motif 10.4-14.5 is deviated from its normal trafficking route and is primarily transported to lysosomes for degradation. Together with the drastically lowered steady-state surface expression levels of Flag-14.5K, the data suggest that LL may contribute to recycling to the plasma membrane.

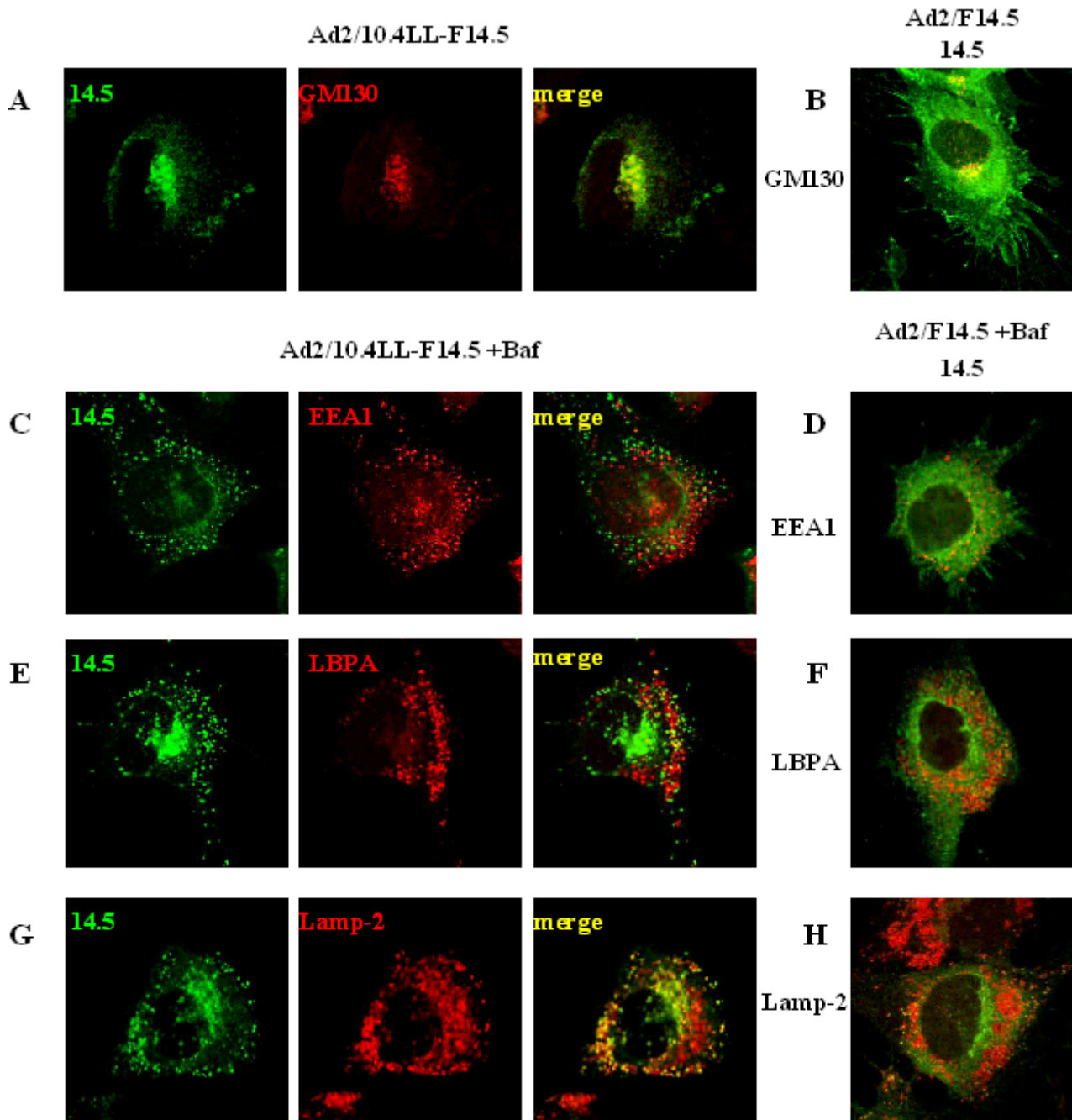


Fig. 33 Disruption of the dileucine motif in 10.4K redistributes the steady-state localization of 14.5K in infected primary fibroblasts (SeBu cells)

SeBu cells were infected with 200 PFU/cell of Ad2/10.4LL-F14.5 (A, C, E, G) or wt Ad2/F14.5 (B, D, F, H) viruses. Infected cells remained untreated (A, B) or were treated for 11 hours with 100nM Bafilomycin A₁ (C-H) before processing for immunofluorescence at 21 h p.i. Intracellular localization of 14.5K (Bur4, green) was compared to that of marker proteins (red) for the cis-Golgi (A, B: GM130) and different endosomal compartments: EEA1 (early endosomes in C,D), lysobisphosphatidic acid (LBPA, late endosomes in E, F), Lamp-2 (late endosomes and lysosomes in G, H). The mAbs used are listed in *Materials and Methods*.

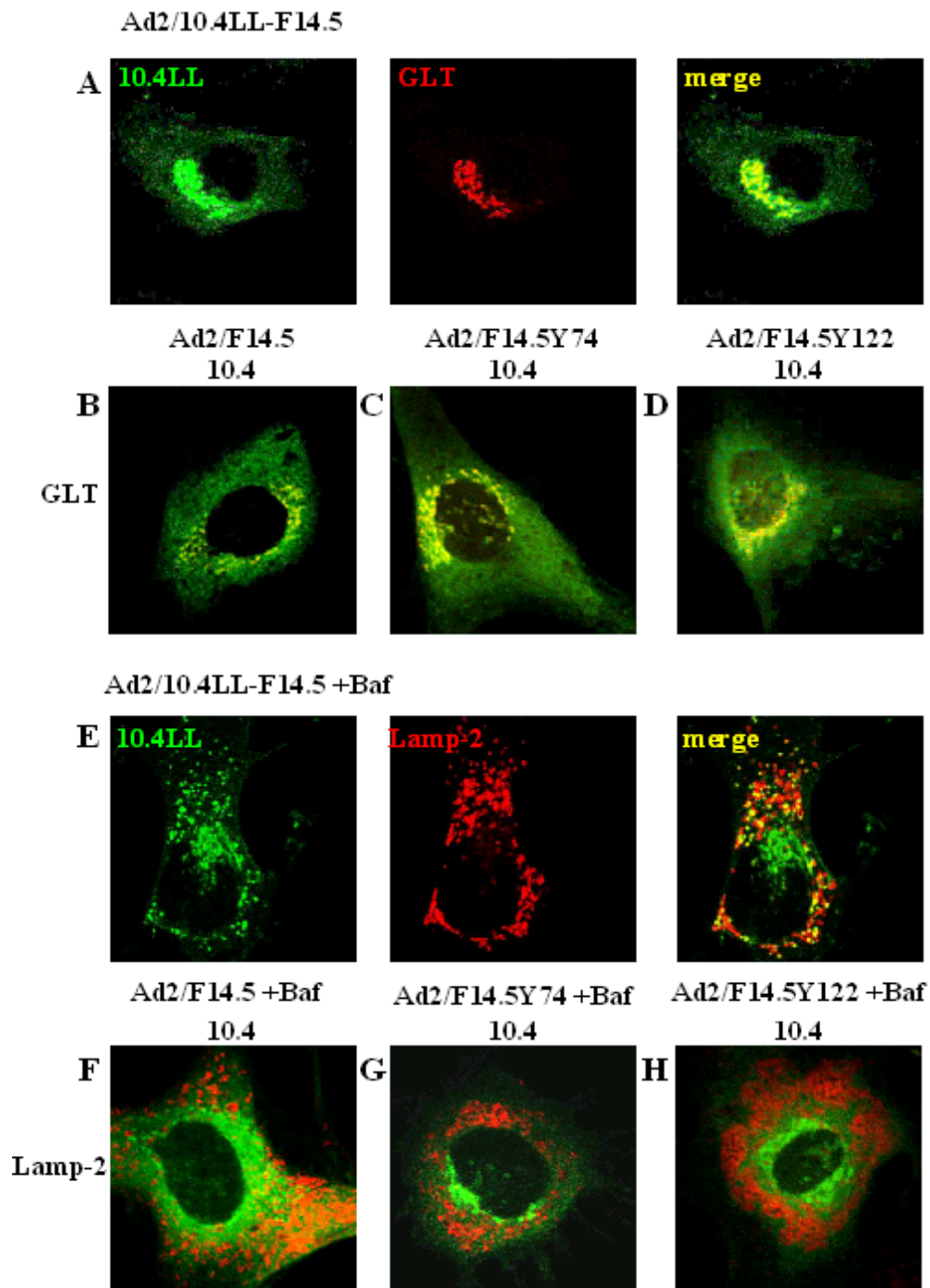


Fig. 34 In infected primary fibroblasts disruption of the 10.4K dileucine motif diverts the mutant protein to lysosomes resulting in increased degradation

Primary fibroblasts (SeBu cells) were infected with 200 PFU/cell of Ad2/10.4LL-F14.5 (A,E) Ad2/F14.5 (B, F), Ad2/F14.5Y74 (C, G), Ad2/F14.5Y122 (D, H) viruses and processed for immunofluorescence at 21 h p.i. Wt 10.4K was detected with polyclonal Ab Bur3 and the 10.4K dileucine mutant with R71 (D, H). Intracellular localization of 10.4K (green) was compared to localization of galactosyltransferase (GLT, red, mAb GTL2), a cellular Golgi-resident protein (A-D). Subsequent to treatment for 11 hours with 100nM Bafilomycin A₁ (E-H) cells were costained for 10.4K (green) and Lamp-2 (red, mAb 2D5, late endosomes/lysosomes).

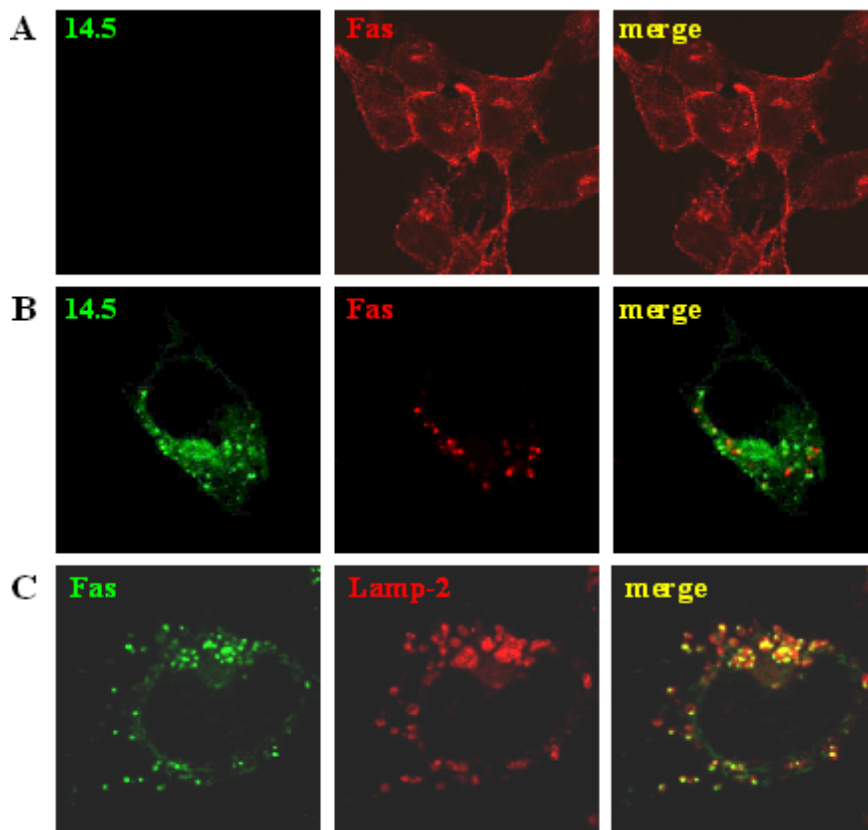


Fig. 35 10.4-14.5K-induced internalization and degradation of Fas in late endosomes/lysosomes SV80Fas cells overexpressing Fas were mock-infected (**A**) or infected with Ad2 (**B-C**) and processed for confocal laser scanning microscopy at 16 h p. i., subsequent to treatment with 100 nM Baf for 11h. (**A, B**) Intracellular localization of 14.5K (green, Ra14.5) was compared to Fas (red), which was detected using a combination of different mAb against Fas (anti-Fas-Mix). (**C**) Costaining of Fas (green, polyclonal rabbit serum anti-Fas) and Lamp-2 (red, mAb 2D5). Magnification was 100x instead of 63x as in A, B.

5.6. 10.4-14.5K and Fas do not profoundly colocalize in Ad2-infected cells

In Ad2-infected cells 10.4-14.5K induce internalization of Fas and its degradation in late endosomes/lysosomes (Elsing and Burgert, 1998; Tollefson et al., 1998). But it remained unknown, whether or not 10.4-14.5K localizes to the same endosomal/lysosomal vesicles. Therefore, the intracellular distribution of 10.4-14.5K and Fas was analyzed in infected SV80Fas cells which had been treated with Bafilomycin to inhibit Fas degradation. Bafilomycin treatment did not affect distribution of Fas in mock-infected cells and Fas was detected at the cell surface (Fig. 35A). By contrast, in the infected cells Fas was no longer found at the plasma membrane, but exclusively in vesicles (Fig. 35B). Fas⁺ vesicles costained with Lamp-2 (Fig. 35C). As Bafilomycin treatment inhibits the acidification of late endocytic compartments Lamp-2⁺ late endosomes/lysosomes (van Weert et al., 1995; Yoshimori et al., 1991) were increased in size and anti-Lamp-2 antibody stained outer membranes which appeared as red circles (Fig. 35C). Fas was found in dense, dot-like

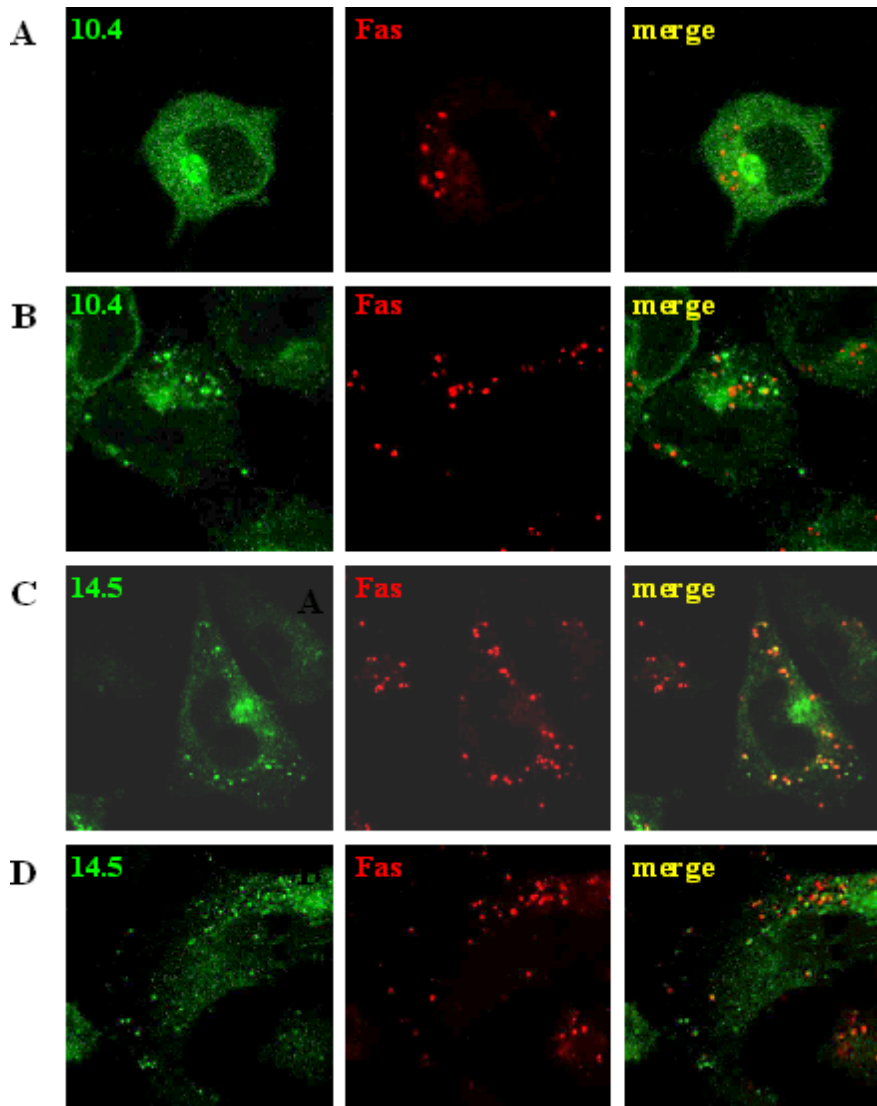


Fig. 36 In Ad2-infected SV80Fas cells 10.4-14.5K do not profoundly colocalize with Fas

SV80Fas cells overexpressing Fas were infected with Ad2, treated with 100 nM Baf for 11h and processed for confocal laser scanning microscopy at 16 h p. i. Intracellular localization of 10.4K (A, B) or 14.5K (C, D) was compared to Fas localization. 10.4K and 14.5K (green) were detected using polyclonal Ab Bur3 and Ra14.5), respectively, and Fas (red) was costained using a combination of different mAb (anti-Fas-Mix).

structures that localized at the outer rim, but also in the inner core of lamp-2+ vesicles (Fig. 35C).

Thus, following 10.4-14.5K-induced down-regulation Fas becomes incorporated into the inner core of lysosomes. Despite Bafilomycin treatment the majority of 10.4K positive cells retained the ER/Golgi staining pattern (Fig. 36A). Fas could be detected in vesicles which did not colocalize with the 10.4K positive structures, even if 10.4K was detected in swollen vesicles (Fig. 36B). Like for Fas, Bafilomycin-treatment also increased the number of 14.5K vesicles, but strikingly these 14.5 vesicles only partially overlapped with Fas+ late endosomes/lysosomes (Fig. 36C, D). Thus, at steady state no extensive colocalization of 10.4-14.5 with Fas was observed, suggesting that the association of Fas with the viral proteins might be rather short-lived.

6. Analysis of homologous E3/10.4-14.5K proteins of adenovirus 4 (subgenus E)

6.1. Down-regulation of cell surface receptors following infection with Ad4

Adenovirus 4 (Ad4), the only member of human subgroup E adenoviruses encodes two E3/ORFs homologous to the adenovirus 2 E3/10.4-14.5K proteins (see Fig. 4). However, Ad4 infection of A549 cells does not cause down-modulation of Fas (Fig. 37, Burgert, unpublished). FACS analysis of Ad4-infected A549 cells revealed that Fas, EGFR and TRAIL-R2 remained almost unchanged during infection with Ad4, but TRAIL-R1 levels were efficiently reduced to about 10% of the levels on uninfected A549 cells (Obermaier, unpublished). To investigate the molecular basis of these functional differences and to characterize a potentially different receptor target specificity of the Ad4 E3/10.4-14.5K proteins, Ad2/Ad4 chimeric viruses were generated with Ad4 homologous ORFs replacing the Ad2 10.4 and/or 14.5K ORFs. Coexpression of subgenus E protein homologues should reveal whether a functional 10.4-14.5K complex can be established, and whether one of the subunits can confer target specificity to the complex.

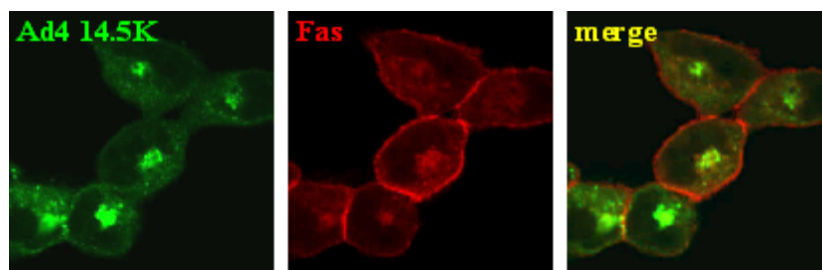


Fig. 37 Fas is expressed at the cell surface of SV80Fas cells infected by adenovirus 4 (subgroup E)
SV80Fas cells infected with Ad4 were processed for dual label CLSM at 22 h p.i., and subsequently to 11 h treatment with 100nM Bafilomycin A₁. Costaining for Ad4 14.5K (R α 14.5) and Fas (mAb anti-Fas-Mix) revealed Fas surface staining in cells expressing Ad4 14.5K.

6.2. Generation of recombinant Ad2 viruses encoding Ad4 homologues of 10.4K and 14.5K

To analyze whether the different effects of Ad4 versus Ad2 on target receptor modulation is an intrinsic property of the corresponding subunits of the 10.4-14.5K complex the homologous Ad4 CDS were introduced into the adenovirus 2 genome. This approach may offer several advantages: (i) Both 10.4K and 14.5K are expressed from a single vector backbone, allowing to maintain a constant ratio of 10.4K and 14.5K expression. (ii) The splicing of the Ad2 E3 region is well-characterized (Imperiale et al., 1995). (iii) E3 gene expression could be standardized by monitoring expression of the Ad2 E3/19K protein. iv) In infected cells a high number of Ad

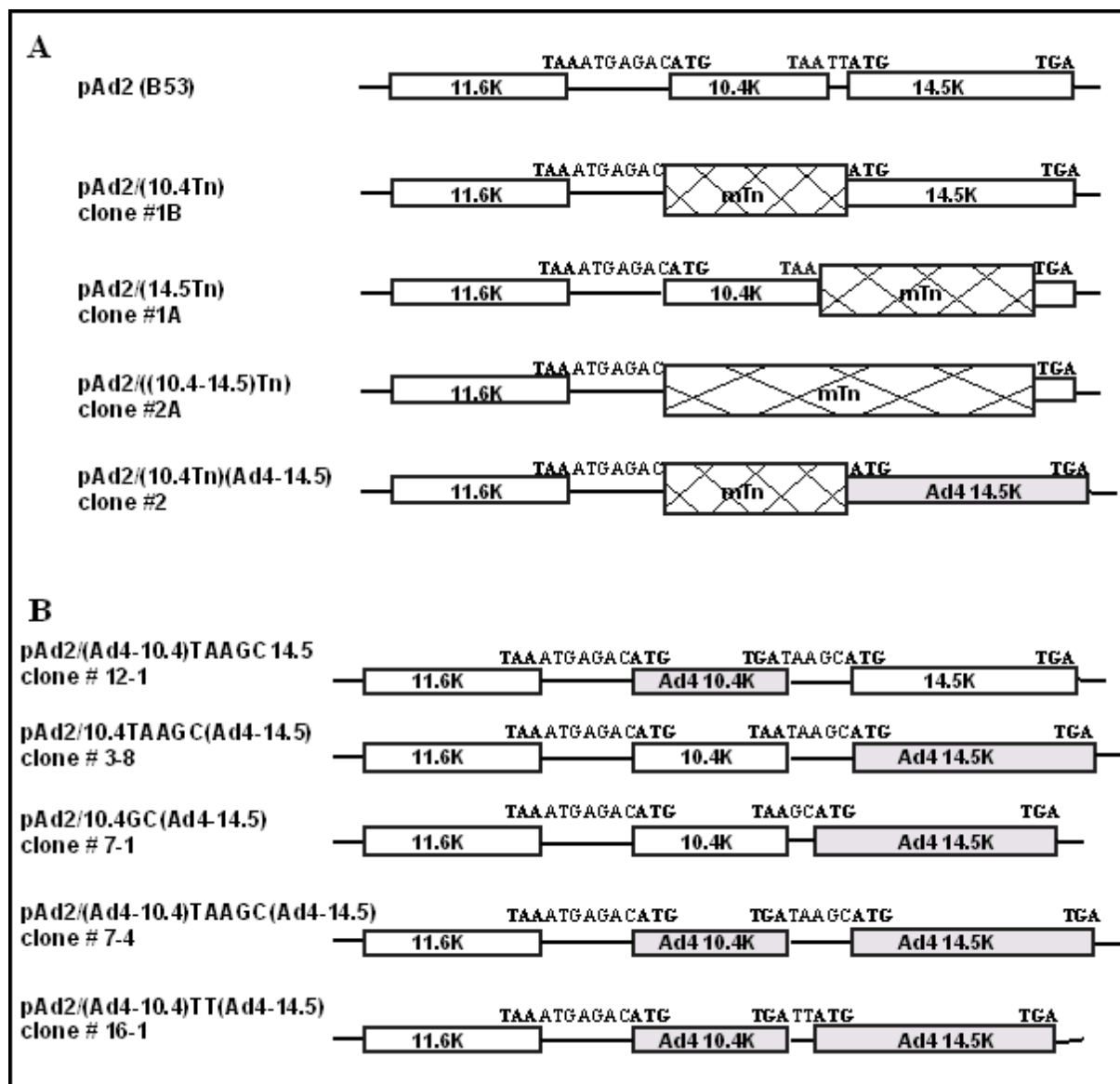


Fig. 38 Sequence composition of the mTn-containing pAd2 intermediates (A) and pAd2/Ad4 chimeric constructs (B).

Nucleotide sequences are given for the coding strand (5' to 3'), start and stop codons of the ORFs are highlighted in boldface. **(A)** mTn encoding sequences are indicated by checked boxes and adjacent nucleotide sequences are given to specify their position. **(B)** 11.6K, 10.4K and 14.5K represent Ad2 ORFs, whereas Ad4 CDS are designated Ad410.4K and Ad414.5K (shaded boxes). Refer to text for details.

genome copies is present, thus a high E3 protein expression level can be attained. Infection can be carried out at equal infection efficiency (equal MOI). (v) Since the target specificity of Ad2 is well-known, the effect of the gene replacement on down-regulation of plasma membrane receptors can be analysed. The adenovirus 2 genome had been cloned into a BAC vector facilitating manipulation of the viral genomic DNA (Ruzsics et al., in preparation). In order to exchange the coding regions, the Ad2 10.4 and 14.5 ORFs were removed from the pAd2-BAC vector in a first step by ET recombination with a kanamycin cassette encoding a mini-transposon sequence (mTn), generating mTn-containing intermediate BAC vectors (Fig. 38A).

The mTn-containing replacement sequences were amplified by PCR using pGPS1.1 as a template. The linear recombination fragments had 40-43 base pair homology arms to the sequence flanking the target site within the pAd2-BAC, which served to direct ET recombination (described in *Materials and Methods*). For ET recombination the mTn containing PCR products were transformed into DH10B containing pBAD $\alpha\beta\gamma$ and the target BAC pAd2. mTn-containing intermediate pAd2BAC vectors could be selected by growth of the bacteria in Cm/Km-containing media. The transposon sequence was excised from the pAd2-BAC vector in an *in vitro* reaction using TnsABC* (see chapter 5.2.5 Tn removal) and the gap in the pAd2 vector was ligated with an insert encoding the Ad4 replacement sequence. Transposase excises the transposon with trinucleotide 5' overhangs on both sides of the transposon. Thereby, distinct trinucleotide single stranded overhangs are generated in the open vector, which preclude recircularization of the pAd2-BAC vector and allow directed insertion of the Ad4 sequence with its correct 5'→3' orientation. Ad4 inserts were amplified by PCR on plasmid pA4E3, containing part of the Ad4 E3 region (Genbank AF361223). Primers for synthesis of Ad4-CDS inserts (see also *Materials and Methods*) encompassed a priming region with 20 bp homology to the Ad4 sequence and *SapI* recognition sites at the 5' ends. A trinucleotide sequence complementary to the corresponding 3 nt overhang in the pAd2-BAC vector was incorporated in the primer 3' to the *SapI* recognition site. By this approach, referred to as exposon cloning (Ruszics et al., manuscript in preparation), different pAd2/Ad4 chimeric constructs were generated with 10.4, 14.5 or both CDS replaced by the corresponding Ad4 sequences. Interestingly, the Ad4-14.5K coding sequence was found to be 48 nucleotides longer than the Ad2-14.5K ORF and in addition the spacing of the Ad4-10.4 and Ad4-14.5 ORFs is different from the one in Ad2. In Ad4 the intercistronic sequence is 5 nt (nucleotide sequence TAAGC) in length instead of 2 nt (TT) in Ad2. In order to be able to generate Ad2/Ad4 constructs with different intercistronic sequences, the position of the mTn sequence was defined in a way (Fig. 38A) that allowed to modify the 10.4-14.5K intercistronic sequence by incorporating sequence changes in the corresponding Ad4 insert. The desired sequence was included in the inserted fragment between the *SapI* cleavage site and the Ad4-specific sequence by modification of insert amplification primers (see also *Materials and Methods*). The pAd2/(10.4Tn) construct was used for generation of pAd2/(Ad4-10.4) by Tns excision and ligation with an Ad4-10.4 encoding insert (Fig. 38B, see *Materials and Methods*). pAd2/(Ad4-14.5) constructs #3-8 and #7-1, were obtained by Tn removal from pAd2/(14.5Tn) and ligation of the open vector with two different types of Ad4-14.5 inserts. These were designed to yield pAd2/(Ad4-14.5) constructs #3-8 and #7-1, with 10.4-14.5K intercistronic sequences of 5 or 2 nucleotides in length, respectively (refer to Fig. 38B and

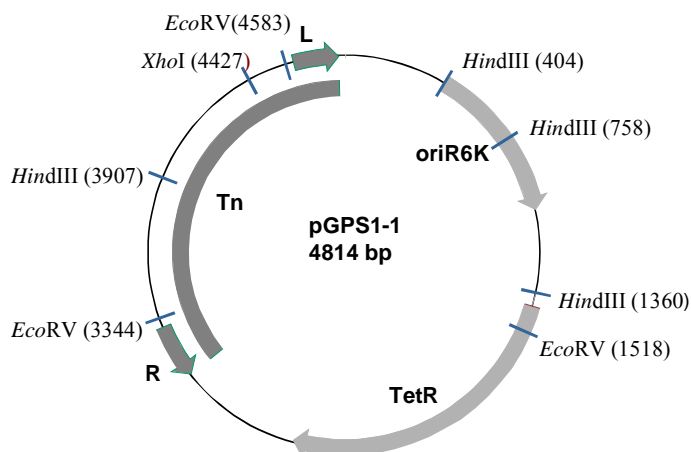


Fig. 40 Circular Map of pGPS1.1, illustrating the position of *EcoRV*, *HindIII* and *XhoI* sites which also cleave within the transposon (Tn) sequence.

The Tn sequence is contained in pGPS1.1 between map position 3068-4767. L and R denote the left and right transposon ends, respectively.

In order to generate pAd2/(Ad4-10.4)TT(Ad4-14.5) #16-1 with a modified intercistronic sequence between the Ad4 ORFs, an additional mTn-containing intermediate, pAd2/(10.4Tn)Ad414.5, was created (Fig. 38A). pAd2/(10.4Tn)(Ad4-14.5) was obtained from pAd2/10.4GC(Ad4-14.5)#7-1 by ET recombination. The mTn-containing linear recombination fragment consisted of a 40 bp homology region to the Ad2 sequence preceding the 10.4 ORF upstream of the mTn sequence and at the 3' mTn end a homology to the first 40 nucleotides of the Ad4-14.5 CDS. Following transposon removal from pAd2/(10.4Tn)(Ad4-14.5) the ends of the BAC vector were ligated with a (Ad4-10.4)-containing insert, which had a dinucleotide (TT) insertion preceding the 3' *SapI* site (Fig. 38B, pAd2/(Ad4-10.4)TT(Ad4-14.5) #16-1).

The Tn-containing pAd2-BAC vectors were analysed by restriction cut with *EcoRV*, *HindIII* and *XhoI* to prove that they contained the full-length genome with the desired transposon insertions (Fig. 39). The inserted mTn sequence contains two *EcoRV*, one *HindIII* and one *XhoI* site (Fig. 40). *EcoRV* and *HindIII* do not cut within the Ad2-(10.4-14.5), whereas one *XhoI* site is present in the Ad2 10.4K sequence. For a list of the expected fragment sizes refer to annex.

Accurate incorporation of the Ad4 inserts was ascertained by sequencing of the corresponding region in the chimeric pAd2-BAC vectors containing Ad4 coding sequences. In addition the BAC vectors were cleaved by *EcoRV* and *XhoI* yielding the correct restriction pattern (Fig. 41). Neither Ad2 nor Ad4 10.4-14.5K coding sequences contain *EcoRV* sites. Therefore the *EcoRV* restriction pattern was similar among all constructs (Fig. 41A), and comparable to the that of the wt pAd2-BAC, although depending on the type of Ad4 insert, the fragment which

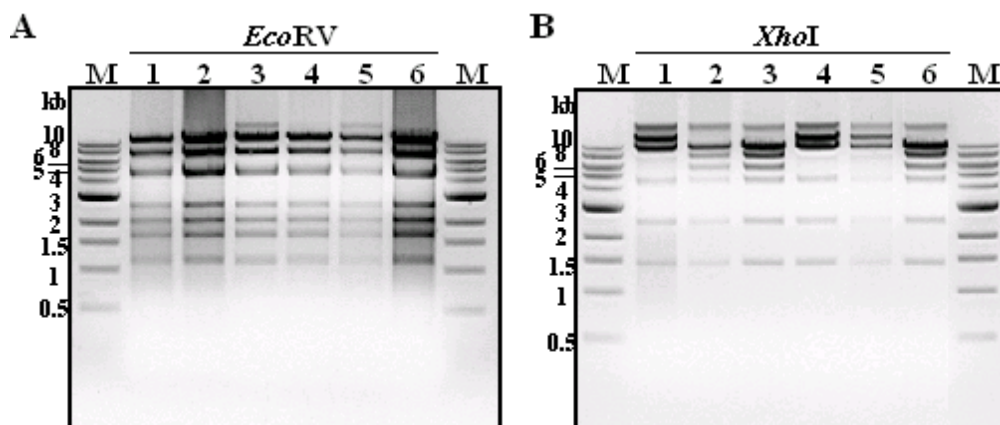


Fig. 41 Analytical restriction cut of pAd2/Ad4 BAC DNA

BAC DNA was digested with *EcoRV* (A) or *XhoI* (B) and separated on a 0.8% agarose gel. Numbers on top of the lanes indicate the type of construct analyzed. 1, pAd2/(Ad410.4) #12-1; 2, pAd2/(Ad414.5) #3-8; 3, pAd2/(Ad414.5) #7-1; 4, pAd2/(Ad410.4-14.5) #7-4; 5, pAd2/(Ad410.4-14.5) #16-1; 6, pAd2-BAC. M = 1kb DNA ladder.

encompasses the 10.4-14.5K CDS slightly varied in length (4755-4803 bp). All the constructs containing the Ad4-10.4K sequence lack one *XhoI* site, which is present in Ad2-10.4K. Therefore, upon *XhoI* cleavage of these constructs one ~13.8 kb band was obtained instead of two smaller fragments (Fig. 41B). For a list of the exact fragment sizes refer to annexe.

For reconstitution of infectious viral particles the modified Ad2 genomes were released from the BAC vector by *SnaB1* digest and the linear double-stranded genome was transfected into 293 cells.

6.3. Expression of Ad4 10.4K and Ad4 14.5K proteins in cells infected with Ad2/Ad4 chimeric viruses

To evaluate the amounts of 10.4K and 14.5K in cells infected with the Ad2 recombinant viruses encoding Ad4 10.4K and/or 14.5K proteins A549 cells were either infected at a MOI of 25 pfu/cell with Ad2, Ad4, and Ad2-recombinants or were mock-infected. Cells were lysed in Triton X-100 buffer at 17 hours post infection. Cell lysates were subjected to immunoprecipitation and western blot detection of E3/19K, 10.4K and 14.5K. Indicative of equal infection efficiency and E3 gene expression, all five Ad2/Ad4 chimeric viruses exhibited a similar level of E3/19K expression as wt Ad2 (Fig. 42A, 19K). Detection of the Ad4 E3/19K homologue required the use of Ad4 E3/19K specific serum and thus the intensity of the band could not be directly compared to the Ad2 E3/19K signals.

Ad4 14.5K was detected with polyclonal serum Bur4 directed against the cytoplasmic tail peptide (CEISYFNLTGGDD) of Ad2 14.5K (Fig. 42A, 14.5K), which is nearly identical to the

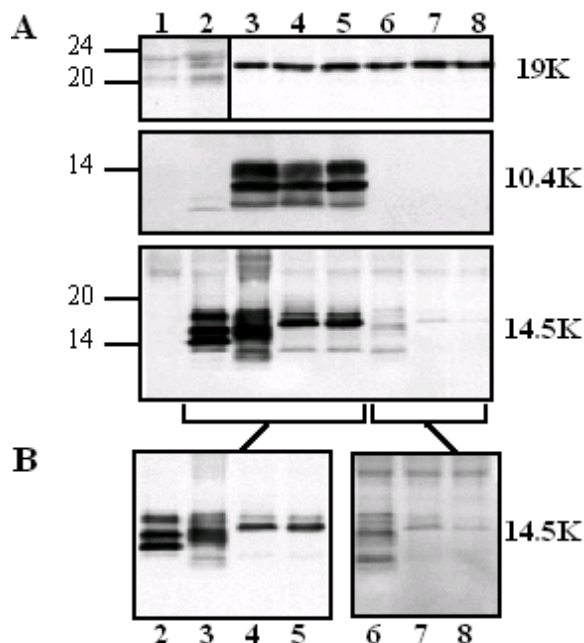


Fig. 42 10.4 and 14.5K levels in A549 cells infected with Ad2 recombinant viruses

Parallel immunoprecipitation and western blot analysis of E3/19K, 10.4K and 14.5K in Triton X-100 lysates of mock-infected A549 cells (lane 1), or A549 cells infected (MOI 25 pfu/cell) with Ad4 (lane 2), Ad2 (lane 3), Ad2/(Ad4-14.5) #7-1 (lane 4), Ad2/(Ad4-14.5) #3-8 (lane 5), Ad2/(Ad4-10.4) #12-1 (lane 6), Ad2/(Ad4-10.4-14.5) #7-4 (lane 7), Ad2/(Ad4-10.4-14.5) #16-1 (lane 8). Immunoprecipitates were separated on a 15% minigel by SDS-PAGE, prior to transfer to a nitrocellulose membrane for western blot detection.

(A) Immunoprecipitation and western blot detection of E3/19K employing rabbit serum against Ad4 19K (lanes 1,2) or Ad2 19K (lanes 3-8). Rabbit serum Bur4 was used in IP/WB of E3/14.5K and E3/10.4K was analyzed using rabbit serum R59 in IP and Bur3 for western blot detection.

(B) Different exposures of the left and right portion of the western blot anti-14.5K depicted in **(A)** to visualize bands of different intensities.

corresponding Ad4 sequence (see Fig. 8). In the immunoblot three major protein species were obtained from lysates of Ad4-infected cells, which migrated with the expected MW of about 14 to 18 kD. The Ad4 14.5K bands differed from those of the Ad2 14.5K protein (Fig. 42 B, left panel). Instead of one more intense faster migrating species and two of higher MW, as seen for Ad2 14.5K, the Ad4 14.5K protein was represented by three bands of equal intensity. Thus, in addition to the expected variation in size, Ad4 14.5K being 16 amino acids longer than the Ad2 homologue, the processing of Ad4 14.5K might differ from that of Ad2 14.5K. In any case, the Ad4 14.5K protein is in fact synthesized in Ad4-infected cells, and lack of 14.5K expression is not the reason for the impaired down-regulation of Fas, EGFR and DR5 by this virus.

10.4-like protein species were also detected in Ad4-infected cells, using the Ad2 10.4K specific reagents R59 and Bur3. The two protein species (faint bands) migrated somewhat faster than their Ad2 counterparts (compare lanes 2 and 3). As the Ad2 10.4K homologue, the Ad4 10.4K protein is predicted to consist of 91 amino acids. The cytoplasmic tail sequence of the Ad4 10.4K protein differs in 9 residues from the Ad2 peptide sequence, which was used to generate

polyclonal serum R59. Bur3 serum recognizes a stretch of 13 amino acids at the C-terminus of 10.4K, but the corresponding Ad4 sequence differs in 6 positions. Therefore, the Ad2-specific sera are likely to bind the Ad4 10.4K protein with lower affinity, which is consistent with the faint appearance. However, the apparent MW of the detected bands is lower than expected, although the Ad5 version of the 10.4K protein, which also consists of 91 amino acids, has been reported to migrate with apparent MW of 7kD (a doublet) and 15kD (Tollefson et al., 1990b). Thus, by analogy and as the doublet bands were not present in lysates of uninfected A549 cells, they may correspond to the Ad4 10.4K protein.

A549 cells infected with Ad2 recombinants Ad2/(Ad4-14.5) #3-8 and #7-1 encoding the Ad4 14.5K protein, produced qualitatively and quantitatively the same 10.4 species as seen in Ad2 (Fig. 42A, 10.4K, compare lane 3 with lanes 4, 5). However, the corresponding Ad4 14.5K signal was different from that obtained by infection with wt Ad4 (Fig. 42, 14.5K, lane 4,5). Instead of 3 bands of equal intensity two major species were detected, which migrated at an apparent MW different from any of the bands observed in Ad4-infected cells. Moreover, the amounts of Ad4 14.5K isolated from lysates of cells infected with Ad2/Ad4 recombinants were lower than those obtained with Ad4-infected cells. Similar amounts of 14.5K were detected for both chimeric constructs, which differed in the spacing of 10.4-14.5K ORFs, but contained the natural context of translation initiation of Ad4 14.5K (TAAGC).

Thus, the Ad4 14.5K protein encoded within the Ad2/E3 region is expressed in infected cells, but is less abundant and might be differently processed compared to that produced during Ad4 infection. None of the Ad2 recombinants in which the Ad2 10.4K sequence was replaced by that of Ad4 10.4K did reveal the doublet band observed after IP/WB of lysates from Ad4-infected cells (Fig. 42A, 10.4K, compare lane 2 with lanes 6-8). Moreover, signal intensities for both Ad2 and Ad4 14.5K proteins were very faint (Fig. 42A, 14.5K, lanes 6-8). Qualitatively, the 14.5K pattern seemed to resemble that observed after infection with wt Ad2 (compare Fig. 42B lanes 3 and 6) or with chimeric constructs Ad2/(Ad414.5) #7-1, Ad2/(Ad414.5) #3-8 (compare Fig. 42B, lanes 7, 8 to 4, 5), respectively. The drastic reduction in signal intensity cannot be explained by reduced protein stability due to the absence of the Ad2 10.4K protein, as in 293 (E3-10.4*)-transfectants, lacking Ad2 10.4K 14.5K was stable and synthesized at a similar rate as in wt E3 transfectants (Elsing and Burgert, 1998). Thus, replacing the Ad2 10.4K ORF and intercistronic sequence upstream of Ad2 14.5K with the corresponding Ad4 sequence seemed to interfere with Ad2 E3/14.5K expression.

Independent of whether the intervening sequence was derived from Ad2 or Ad4, insertion of the Ad4(10.4-14.5) encoding sequence as a whole into the E3 region of Ad2 (Fig. 42, lane 7, 8)

did not allow expression of the Ad4 proteins in a manner similar to that found in Ad4-infected cells. Ad4 14.5K levels were drastically reduced and migrated as differently processed forms.

In conclusion, the Ad4 10.4-14.5K proteins were not sufficiently expressed when placed within the Ad2/E3 region. For all chimeric virus constructs, the Ad2/E3 19K protein was constantly expressed, suggesting that the splicing of the E3 19K encoding mRNA is normal. Normal 10.4K expression was detected as long as the Ad2-10.4 sequence remains intact (Fig. 42, compare lane 3 with lanes 4,5), and was not significantly altered by insertion of Ad4 sequences downstream of the 10.4K ORF. By contrast, replacement of the Ad2 10.4K coding sequence and intercistronic sequence by the corresponding Ad4 nucleotide sequence strongly reduced the amounts of the Ad2 14.5K protein isolated from infected cells. Similarly, Ad4 14.5K levels were also drastically reduced when the Ad4 10.4K CDS was preceding the 14.5K ORF. This reduction of 14.5K levels was not influenced by the type of intercistronic sequences (Ad2- or Ad4-like), or spacing of 10.4-14.5K coding sequences. The coordinated lack of Ad4 10.4 and Ad4 14.5 expression suggested, that the mRNA(s) for Ad4 10.4-14.5K is not synthesized and inappropriate expression of the Ad4 10.4K protein may contribute to differential processing of Ad4 14.5K encoded by Ad2. In subgroup C viruses Ad2 10.4-14.5K have been reported to be translated from the same bicistronic mRNA, but so far it is unknown, how initiation of translation at the downstream 14.5K ORF occurs. The Ad2/Ad4 chimeric viruses reveal that expression of 14.5K in the Ad2 E3 region is influenced by sequences preceding the 14.5K ORF. Taken together, the data suggest, that expression of Ad4 10.4-14.5K is differently regulated in the Ad4 E3 region, which differs in size and composition from E3 region of subgenus C viruses (Fig. 4).

Discussion

7.1. Importance of strictly conserved amino acids for the function of Ad2 10.4-14.5K

E3/10.4-14.5K proteins are transmembrane proteins encoded by all subgroups of human adenoviruses, but only a small number of amino acids are strictly conserved (Fig. 8). To determine the role of these strictly conserved residues for 10.4-14.5K-mediated down-regulation of Fas and the EGFR, stable 293 E3-transfectants expressing mutant forms of 10.4-14.5K were generated and screened by FACS analysis for expression and down-regulation of target proteins. Analysis was carried out for the Ad2 FLAG-14.5K mutant proteins in which the strictly conserved residues C32, C43, Y44 in the extracellular domain and S121, Y122, F123 within the cytoplasmic tail were replaced alanine (Fig. 10).

Besides mutant Y122 for which the results will be discussed below, the mutation of C32, C43, F123 and S121 significantly impaired the functional activity of 10.4-14.5K. Y44 was not essential for 10.4-14.5K function as this mutant cell line exhibited a reduction in Fas and EGFR surface expression comparable to E3-transfectants expressing wt 10.4K and F14.5K. No alteration of F14.5K surface expression levels was observed for the F14.5Y⁴⁴A mutant. Mutant C43 had a clearly reduced efficiency in down-regulation of both Fas and the EGFR, which was accompanied by drastically decreased F14.5 surface levels. Interestingly, a similar phenotype was observed upon mutation of the other strictly conserved cysteine residue C32 in the extracellular domain. One possible explanation for this similar phenotype might be that both are linked by a disulfide bond. A coordinated change of phenotype of cysteine mutants was previously observed for E3/19K. In that case, the existence of intramolecular disulfide bonds was confirmed biochemically (Sester and Burgert, 1994). So far, the 14.5K protein has not been examined for the presence of intramolecular disulfide bonds. This will be difficult to perform, as the loop created by the putative disulfide bond will be very small and migration differences are expected to be extremely difficult to detect. The elimination of cysteines will further complicate an analysis by metabolic labeling. How the Cys mutations affect surface expression and receptor target down-modulation remains unclear. The efficiency of 14.5K association with 10.4K, which is known to influence cell surface transport, should be investigated by IP/WB. Immunofluorescence analysis in suitable cells, should give sufficient information as to whether mutants are retained in the ER/Golgi or delivered to endosomes/lysosomes.

Substitution of single residues within the strictly conserved triplet S¹²¹Y¹²²F¹²³ in the 14.5K cytoplasmic tail also impaired down-regulation of both Fas and the EGFR. Whereas S121 and F123 mutants retained functional activity (80% and 67% of wt activity, respectively, towards Fas

and 68% and 50% towards the EGFR) a complete loss of function was observed for mutant Y122. FLAG-14.5Y¹²²A was shown to accumulate at the cell surface, exhibiting about 4 to 5 times higher steady-state expression levels than wt (F-19). 14.5F¹²³A also showed a strong increase of surface expression, which reached ~60 % of surface levels of FLAG-14.5Y122, whereas the preceding serine residue exhibited slightly reduced 14.5K surface levels. All our experimental evidence suggests that the increased surface expression levels reflect a prolonged residence time of mutant 14.5 at the cell surface, indicative of a defect in internalisation (see below). Y122 represents the first and most essential residue of a strictly conserved YXXΦ transport motif. F123 being part of this motif may also have a profound influence on recognition of this motif by AP complexes to direct internalization of 14.5K. Consistent with the data shown here for S121 of Ad2 14.5K, the corresponding serine residue in the Ad5 protein was not phosphorylated and alanine replacement did not abolish functional activity of the Ad5 10.4-14.5K complex (Lichtenstein et al., 2002).

Surprisingly, we did not observe any significant effect upon replacement of Y44 by alanine although the nature of the introduced amino acid is considerably different from tyrosine. Perhaps, there are other constraints to keep this mutant protein functional.

So far, no direct interaction of 14.5K with receptor targets has been detected, and it is possible that 10.4-14.5 mediate down-regulation of targets via interaction with other cellular proteins (Fig. 43, factor x). Thus, it remains unknown whether strictly conserved amino acids of 14.5K are determinants of its affinity towards the target molecules or some unknown intermediate interaction partner. Interestingly, in both the wt and the mutant 293 E3+ cells the reduction in relative surface expression was less for the EGFR than for Fas. This difference was also noted with fixed cells (Elsing and Burgert, 1998). This might reflect a difference in the mechanism of 10.4-14.5K-mediated down-regulation of these receptors or a different affinity of 10.4-14.5 towards these receptors or towards different types of cellular factors that may be involved. Since equivalent amounts of Fas and EGFR were detected at the surface of 293 cells by flow cytometry, a dosage effect can be excluded.

7.2. Functional relevance of putative transport motifs within 10.4-14.5K for receptor down-modulation

Based on the previous observation that the 10.4-14.5 target proteins, the EGFR and Fas, are rerouted to a late endocytic/lysosomal compartment (Elsing and Burgert, 1998; Tollefson et al., 1998), it was investigated whether putative transport signals in 10.4-14.5K are functionally important. Of the three YXXΦ motifs present in 14.5, those at position 74 and 76 may be located

adjacent to or even within the lipid bilayer (Fig. 8). Previous studies showed that YXX Φ sequences have to retain a minimal distance of 5-7 amino acids to the lipid bilayer in order to be recognized as transport motifs (Collawn et al., 1990; Rohrer et al., 1996). This argues against a role of these motifs in trafficking. Indeed, mutation of Y76, which is found only in subgenus C Ads, had no profound effect on the capacity of 10.4-14.5K to down-regulate Fas and the EGFR (Fig. 10). Interestingly, in this mutant a reduced stability of 10.4-14.5K complexes in Triton extracts was observed, indicative of a decreased affinity of the 14.5 Y76 mutant towards 10.4K (Fig. 11).

In contrast, mutation of the strictly conserved tyrosine Y74 within a potential YXX Φ motif either containing leucine (YXXL) in subgenera C, A and F or F (YXXF) in subgenera B, E and D, nearly abrogated the functional activity in transfected 293 cells (Fig. 7). The functional deficiency correlated with a markedly reduced 10.4-14.5Y⁷⁴A complex formation, presumably caused by enhanced degradation of 14.5Y74 (Fig. 11). Levels of 10.4K were not affected (Fig. 11C). Taken together, Y74 rather than being part of a transport motif appears to be required for efficient complex formation between the viral proteins. In infected cells, a differential effect of the Y⁷⁴A mutation on target modulation was noted. While the 10.4-14.5K-mediated EGFR modulation was impaired, Fas removal from the cell surface occurred with similar efficiency as in Ad2-infected cells (Fig. 29). This suggests that increased expression of 14.5Y⁷⁴ (and 10.4) during infection can partially or completely overcome the decreased 10.4-14.5 association. Consistent with this idea 10.4-14.5Y⁷⁴A complexes could be isolated from digitonin extracts of infected cells (Fig. 31A, lane 3), but not from transfected cells. The reduced ER and Golgi staining (Fig. 32B) suggests that the resident time of the viral proteins in these compartments may be shorter, in line with the suggested higher degradation rate. The latter is also indicated by an increased amount of 14.5 degradation product (Fig. 31B, lane 3*). At present, it is unclear whether the decreased complex formation is a direct consequence of the lower affinity of the 14.5Y⁷⁴A mutant to 10.4 or is rather due to the decreased steady-state levels of mutant 14.5, presumably caused by an increased degradation rate. Possible alterations in the metabolic half-life of 14.5K caused by the Y⁷⁴A mutation remain to be analysed quantitatively by metabolic labeling.

The third YXX Φ motif (Y¹²²XX Φ motif of Ad2 14.5K) is strictly conserved and consists of the sequence YXXL in subgenera B, C, E, and F, YXXI in subgenus D and YXXF in Ad12 (Fig. 8). The tyrosine residue is commonly found in position -9 from the C-terminus and remarkably, amino acids flanking the tyrosine are strictly conserved: A serine residue in position -1 and phenylalanine in +1. In a comparison of the sequence context of 48 functional YXX Φ motifs no preference for phenylalanine has been noted, but serine in position -1 is somewhat preferred

(Windheim et al., 2003, *in press*). Prominent examples are endocytosis signals in furin and the transferrin receptor, which have been shown to bind AP-2 *in vitro* (Ohno et al., 1995; Teuchert et al., 1999). Regarding the sequence context and position in the 14.5K cytoplasmic tail, the Y¹²²FNL motif does not exhibit the characteristics of known GYXXΦ lysosomal targeting signals, found in Lamp-1, Lamp-2 or CD63 which share a remarkably small distance (6-9 residues) to the transmembrane domain (Bonifacino and Traub, 2003). The short spacing of the Lamp-1 signal to the transmembrane domain has been shown to be critical for the lysosomal targeting step, whereas endocytosis of mutant Lamp-1 could still occur (Rohrer et al., 1996). The position of the YXXΦ motif at the end of the cytoplasmic tail should make it easily accessible for recognition by adaptor protein complexes and suggests that it might constitute a functional transport motif. Indeed, surface plasmon resonance spectroscopy confirmed that adaptor protein complexes AP-1 and AP-2 bound to the 14.5K tail peptide *in vitro*. *In vivo*, this Y¹²²XXΦ motif, seems to be crucial both for function and transport. In 293 E3 transfectants expressing the 14.5 Y122 mutant as well as in cells infected with mutant Ad2/F14.5Y122, down-regulation of Fas and the EGFR is abolished, like in cells lacking expression of either 10.4 or 14.5 or both (Fig. 7 and 29). In these cells, steady-state levels of both 10.4 and 14.5 are significantly increased as are the amounts of detectable complexes (Fig. 11 and 31). The apparently increased stability correlated with only small amounts of 14.5K degradation products in extracts from Ad2/F14.5Y122-infected cells (Fig. 31B, lane 4*). Several lines of evidence suggest that Y122 is part of a transport motif: First of all, SPR studies *in vitro* showed that Y¹²² is essential for efficient binding to the 14.5-tail of the adaptor protein complexes AP-2 and AP-1, which are known to mediate endocytosis and transport between intracellular compartments, respectively. Secondly, mutation of Y¹²² alters the subcellular distribution of the 10.4-14.5 complex *in vivo*. FACS analysis demonstrated a dramatic increase in 14.5Y¹²² cell surface expression, to 400-500% of the F14.5 levels on wt 293 E3-transfectants (Fig. 10). Similarly, in infected cells F14.5Y122 surface expression level was increased to 280% of that of the wt F14.5 (Fig. 29C). A corresponding increase in cell surface expression is also observed for the 10.4 subunit in these cells by immunofluorescence (Fig. 32C). Together with the higher affinity of the 14.5 tail to AP-2, this suggested that the Y¹²²XXΦ motif serves as a recognition signal for AP-2 binding which might trigger rapid endocytosis of the complex.

This is in agreement with data obtained upon expression of Ad5 10.4-14.5K proteins in transiently transfected COS cells: Alanine replacement of the corresponding tyrosine Y124 in Ad5 14.5K caused a loss of function, whereas substitution by phenylalanine did not abolish function, indicating that phosphorylation of 14.5K Y124 was not required for internalisation and

degradation of Fas and the EGFR (Lichtenstein et al., 2002). Thus, phosphotyrosine, a characteristic of an SH2-ligand motif doesn't seem to play a role in 10.4-14.5K function. These authors also concluded that the tyrosine in 14.5K might rather be part of a tyrosine-based transport signal (Lichtenstein et al., 2002).

Interestingly, also the 10.4 tail seems to contain sequence elements important for transport and function. The C-terminal residues of 10.4K represent an IL pair in subgenus C viruses and LI in subgroups B, E, and D, but this potential dileucine motif is not present in 10.4K proteins from subgroup A or F. Mutation of the Ad2 10.4K IL pair did not alter the ability to form complexes with 14.5 in Triton X-100 (data not shown) or Digitonin extracts (Fig. 14A), and had only a minor effect on the down-regulation capacity of 10.4-14.5 (Fig. 12, Fas and EGFR cell surface levels were about 10-15% higher as compared to cells expressing wild-type proteins). But cell surface display of 14.5 in 10.4IL mutant cell lines reached only 30-40% of wild-type (Fig. 12D). Obviously, this reduced level is still sufficient to bring about most of the 10.4-14.5K activity. As the functionality of 10.4-14.5K was only slightly affected by the mutation, the molecular basis for the decreased surface expression was not further investigated. In contrast to this very slight effect, mutation of the LL motif in position -4/-5 from the C-terminus of 10.4 abolished the function of the 10.4-14.5 complex in 293 transfectants (Fig. 7). Notably, complete loss of 10.4-14.5K function was observed upon substitution of the dileucine pair, whereas single replacement mutants retained a significant part of functional activity (Fig. 12B, C). Consistent with the profound effect, the dileucine-type consensus sequence is strictly conserved among 10.4K proteins from different subgroups, and represented by two leucines in all subgenera except for subgenus D viruses which encodes an IL pair instead. If isoleucine is part of functional di-leucine motifs in mammalian proteins, it is more frequently found in position L2 than L1. Nonetheless, functionality of an IL internalisation signal has recently been reported for the type II TGF- β receptor (Ehrlich et al., 2001). Comparing the sequence composition flanking the LL element of 10.4K with the amino acid environment of functional LL motifs (35 LL motifs in 31 proteins) it was noted that a number of overrepresented amino acids are commonly found in 10.4K proteins of subgenera C, B, D and E (Windheim et al., 2003, *in press*): these are R in (+1), A in (-2), R in (-7) and Y in (-8). Ad12 (subgenus A) lacks two of these favorable residues, but is also able of reducing Fas and EGFR expression (Burgert, unpublished). But, the 10.4K dileucine pair lacks acidic residues in positions -3 to -5 from the first leucine, which are frequently found in functional dileucine motifs (Bonifacino and Traub, 2003). Sometimes these are implicated in a specific sorting step, e.g. in LimpII glutamic acid at position -4 is required for sorting to late endosomes/lysosomes, but not for internalization

(Sandoval et al., 2000). A subgroup of dileucine-type signals, the acidic cluster dileucine signals, are characterized by a DXXLL consensus which is strictly required for GGA-mediated cargo selection at the TGN (Bonifacino and Traub, 2003). According to this definition the 10.4LL motif does not conform to the consensus of an acidic cluster dileucine motif and is therefore unlikely to be recognized by GGAs. However, the position of the dileucine pair close to the C-terminus may facilitate recognition by adaptor protein complexes and supports the idea that this motif might be functional. Consistent with this hypothesis, adaptor protein complexes AP-1 and AP-2 bound to a 10.4K cytoplasmic tail peptide *in vitro* (Table 3).

In 10.4LL stable transfectants Fas and EGFR cell surface expression was similar to untransfected cells (Fig. 12 B, C). Lack of modulation correlated with a dramatically decreased stability of both 10.4LL and 14.5 (Fig. 14B, lane 5), which hindered the detection of 10.4LL-14.5 complexes in these cells (Fig. 14A, lane 5). Baf-treatment restored steady-state levels of both 10.4LL and 14.5, indicating that a Baf-sensitive compartment (e.g. lysosomes) is responsible for their accelerated degradation. Moreover, Baf-treatment revealed that the 10.4LL mutant has the ability to form complexes with 14.5K (Fig. 14A, lane 6). Interestingly, Baf also strongly increased the stability of wild-type 10.4-14.5K proteins, suggesting that normally a profound proportion of the viral complex is transported to and degraded in late endosomes or lysosomes. It was concluded that the LL/AA substitution drastically enhances degradation of the 10.4-14.5 complex and this may be the prime reason for the dramatic reduction (95%) of 14.5 cell surface expression (Fig. 12D). Immunofluorescence studies showed a decreased ER staining for 10.4LL and a greatly increased labeling of 10.4-14.5+ intracellular vesicles after Baf-treatment which colocalized mostly with late endosomal and lysosomal markers (Fig. 23). Taken together, it appears that LL prevents extensive degradation of the 10.4-14.5 complex in late endosomes/lysosomes.

Incorporation of the 10.4LL/AA mutation into the virus background confirmed the important role of the motif for both trafficking and target protein modulation, although some of the defects caused by the mutation were ameliorated, presumably due to the increased expression of viral proteins. However, some viral-induced regulatory phenomena, such as possible p53- or NF- κ B-mediated increase in Fas expression (Bennett et al., 1998; Gil et al., 1999; Kuhnel et al., 2000; Wallach et al., 1999), or the transcriptional repression of the EGFR promoter by E1A (Prudenziati et al., 2000) complicate the interpretation. Relative to levels on Ad2/(10.4-14.5)ko-infected cells, 10.4LL-14.5 proteins exhibited 57% and 17% of the activity of wt 10.4-14.5K towards Fas and the EGFR, respectively (Fig. 29 A, B). Strikingly, the amount of F14.5 on the cell surface was reduced to ~13% of that seen upon infection with wild-type virus (Fig. 29C). Thus, the residence time on

the cell surface appeared to be dramatically reduced. Reduced 14.5K surface expression, together with the increased amounts of 14.5K degradation products (Fig. 31, lane 5*) and the vesicular localization (Fig. 32D) suggested that in the absence of the LL motif 10.4 and possibly 14.5 are preferentially degraded. Similarly to the transient transfection experiments (Fig. 23), Bafilomycin treatment of SeBu cells infected with Ad2/10.4LL-F14.5, revealed an increased number of 10.4-14.5+ intracellular vesicles which colocalized with Lamp-2 (Fig. 33G, 34E). The infection experiments confirmed that the LL mutation has no detrimental effect on 10.4-14.5 association (Fig. 31A, lane 5). Thus, also in the infected cells, substitution of the 10.4K dileucine motif caused increased degradation of both 10.4LL and 14.5K in late endosomes/lysosomes. Increased degradation of 10.4LL and 14.5K was associated with concomitant reduction of 14.5K steady-state cell surface expression, suggesting that the di-leucine motif acts as a transport motif that profoundly influences intracellular transport of 10.4-14.5K complexes. This hypothesis is underscored by the fact that the di-leucine pair is an essential determinant for the affinity of 10.4K cytoplasmic tail peptides towards AP-1 and AP-2 adaptor molecules (Table 3).

In conclusion, the data suggest that full activity of 10.4-14.5K requires the combined action of two sorting motifs, one (LL) in 10.4 and another one ($Y^{122}XX\Phi$) in 14.5. Disruption of the 14.5 $Y^{122}FNL$ or the 10.4 dileucine motif causes missorting of the two viral proteins, illustrated by markedly different surface expression levels, but does not destroy the 10.4-14.5K complex. The findings obtained upon coexpression of both mutants suggest that the two sorting motifs are not functionally redundant, as the dileucine pair cannot substitute for the $Y^{122}XX\Phi$ motif in directing rapid internalization of 10.4-14.5K. Moreover, the $Y^{122}XX\Phi$ motif functions upstream of the LL motif (Fig. 22), which appears to have a sorting function subsequent to endocytosis. Thus, two distinct transport motifs encoded by two physical entities appear to act in concert in order to bring about efficient down-modulation of Fas and the EGFR.

7.3. Importance of putative transport motifs for down-regulation of TRAIL-receptors DR4 and DR5

Whereas down-regulation of Fas and EGFR by 10.4-14.5K occurs independently of other viral proteins, E3/6.7K has been reported to be required for down-modulation of DR5, and to augment 10.4-14.5K-induced down-regulation of DR4 in some cell lines (Benedict et al., 2001). E3/6.7K has been proposed to be an ER transmembrane protein (Wilson-Rawls and Wold, 1993). A tagged version of 6.7K has been shown to interact with 10.4-14.5K and to be expressed at the plasma membrane, suggesting that the natural 6.7K might also be expressed at the cell surface

(Benedict et al., 2001). In its short cytoplasmic tail 6.7K contains a YXXL sequence element, which conforms to the consensus of YXX Φ -type transport motifs (Windheim et al., 2003, *in press*). Therefore, it was of particular interest to investigate, whether similar to the situation with Fas and the EGFR, infection with the virus mutants would reveal a defect in TRAIL-R down-regulation.

Wt Ad2 and Ad2/F14.5 reduced receptor levels of DR4 to below 5% and of DR5 to below 10-15% on infected A549 cells. A549 cells infected with virus mutants that lack expression of either 10.4K or 14.5K showed an upregulation of DR5 levels to at least 120% of the levels on A549 cells, whereas DR4 remained unchanged. This might be due to transcriptional upregulation of DR5 expression by NF- κ B activation following infection, since a similar observation has recently been described for epithelial cells, in that TRAIL-mediated NF- κ B activation led to a specific increase of DR5 expression, without upregulation of DR4 (Shetty et al., 2002). Potential NF- κ B and p53 binding sites have been mapped to the first intronic region of the DR5 gene and the p53 DNA binding site is involved in increased DR5 expression in lung carcinoma cell lines (Wu et al., 1999; Yoshida et al., 2001). It is unknown, whether AdE1A functions, which sensitize infected cells to TRAIL-induced apoptosis in the absence of AdE1B-19K and E3 proteins (Routes et al., 2000), also upregulate cell surface expression of the TRAIL-receptors. In cells infected with the Ad2/14.5k.o. DR4 surface expression levels were decreased by 16% as compared to levels on Ad2/(10.4-14.5)ko-infected cells. A similar reduction was observed for the EGFR (13%), whereas Fas and DR5 levels remained unchanged. This effect on the DR4 and the EGFR seems to be related to the retained expression of 10.4K in this mutant. For the EGFR a direct interaction with 10.4K has been reported (Crooks et al., 2000), suggesting that isolated expression of 10.4K might cause retention of the EGFR in intracellular stores. This may also be the case for DR4.

Studying down-regulation of DR4 and DR5 on A549 cells infected with mutant viruses Ad2/F14.5Y74, Ad2/F14.5Y122 or Ad2/10.4LL-F14.5, it initially appeared that DR4 down-regulation was similarly affected as Fas-modulation and that for the DR5 a similar picture as for the EGFR was obtained.

Mutant Y74, which exhibited normal F14.5 surface expression levels, differentially affected down-regulation of the two TRAIL receptors. In Ad2/F14.5Y74-infected cells DR4 levels were reduced as efficiently as in cells infected with wt, but DR5 surface expression remained at 49% of the levels on A549 cells. Relative to the levels on cells infected with the Ad2/(10.4-14.5)ko virus the Ad2/F14.5Y74-induced decrease in DR5 levels accounted for 66 % of that observed with Ad2/F14.5 (Fig. 30B). These data are very similar to the results described above for Ad2/F14.5Y74-

induced down-regulation of Fas and the EGFR corresponding to 100% and 69% of the activity of wt 10.4-14.5K, respectively.

Strikingly, substitution of Y122 was detrimental to the down-regulation of all target molecules. However the relative expression level of the individual receptor targets differed: EGFR levels were at 80% (relative to the levels on A549 cells) like in cells infected with Ad2/(10.4-14.5)ko (Fig. 29B) and Fas and DR5 were expressed at 120% as observed after infection with virus mutants lacking expression of 10.4K and/or 14.5K (Fig. 29A, Fig. 30B). But DR4 surface expression levels were dramatically increased (170%, Fig. 30A), similar to F14.5Y¹²²A itself. The increased expression of 10.4-14.5Y¹²²A complexes and DR4 at the cell surface suggested, that 10.4-14.5K may physically interact with DR4 at the plasma membrane and mutation of Y122 would prevent internalization of the DR4/10.4-14.5 complex. Thus, with the exception of DR4 which is upregulated concomitantly to mutated F14.5 cell surface expression of Fas, EGFR and DR5 is regulated independently of 14.5. Consequently, it is likely that receptor/10.4-14.5K complexes do not exist at the cell surface, but may be formed subsequent to endocytosis. This is consistent with data published by Crooks et al., who coimmunoprecipitated 10.4K and EGFR in an early endosome cell fraction (Crooks et al., 2000). Localization of the EGFR to specialized plasma membrane sections, known as caveolae (Mineo et al., 1999), might prevent its association with 10.4-14.5K at the cell surface. The deficiency of 14.5Y122 to be internalized did not allow to test experimentally whether Y122 plays a role subsequent to endocytosis. Obviously, neither in the E3 transfectants nor in the virus-infected cells coexpression of 6.7K can compensate the internalization defect of 10.4-14.5Y¹²²A (Fig. 10D, 29C) and down-regulation of DR5 by 10.4-14.5K and 6.7K seems to require an intact 14.5K Y¹²²XXΦ motif.

The dileucine pair in 10.4K is essential for down-regulation of DR5 by 10.4-14.5 and 6.7K, since DR5 levels remained nearly unchanged with levels higher than those on mock-infected cells. The presence of E3/6.7K cannot prevent enhanced degradation of 10.4LL and 14.5K in the virus-infected cells (Fig. 33G, 34E). 6.7K has been reported to interact with 14.5K, forming a heterotrimeric complex (Benedict et al., 2001). It remains to be tested experimentally whether the 10.4K dileucine mutant also induces degradation of 6.7K in late endosomes/lysosomes. As 10.4-14.5K appears to interact with DR4 at the plasma membrane the reduced expression of 10.4LL-14.5K at the plasma membrane might be associated with a coordinate reduction in the efficiency down-modulation of DR4. Indeed, in cells infected with this mutant the decrease of DR4 levels corresponded only to 30% of that observed upon infection with wt.

Taken together, mutation of the 10.4K dileucine pair and 14.5K Y122 also impaired down-regulation of TRAIL-R1 and TRAIL-R2, implying a general role of these two sequence elements in

the process of 10.4-14.5K-induced receptor modulation. Furthermore, the results demonstrate that down-regulation of TRAIL-R2, which requires additionally E3/6.7K, also depends on the integrity of these motifs. These data allow to propose a transport mechanism underlying 10.4-14.5K-mediated down-modulation of apoptosis receptors and the EGFR, which will be outlined in the following chapter.

7.4. Transport processes underlying the mechanism of down-modulation of plasma membrane receptors by 10.4-14.5K

10.4 and 14.5K are known to associate non-covalently with each other (Tollefson et al., 1991) and are both required to induce down-regulation of Fas, the EGFR and DR4, DR5 (Elsing and Burgert, 1998; Shisler et al., 1997; Tollefson et al., 1991; Tollefson et al., 1998; Tollefson et al., 2001). Thus, 10.4-14.5K complex formation appears to be a prerequisite for down-modulation of plasma membrane receptors and consistent with previous reports we found that individual subunits were incapable of reducing receptor expression levels in stable transfectants of A549 cells (Fig. 20) or upon infection with Ad2/10.4ko-F14.5 and Ad2/14.5ko viruses (Fig. 29, 30). 10.4-14.5 complexes seem to assemble at the level of the ER (Fig. 43), as illustrated by the influence of 10.4K on signal sequence cleavage site selection in 14.5K (Krajcsi et al., 1992c). It is well-documented that trafficking of individual subunits to the cell surface depends on concomitant expression of the other protein (Stewart et al., 1995). If expressed without the interaction partner individual proteins localize to the ER and Golgi compartment (Fig. 17A, 17B), whereas upon coexpression both proteins can be detected at the cell surface (Fig. 21), where they presumably exist as a complex (Stewart et al., 1995). The E3/6.7K cannot replace the 10.4K protein in assisting transport of 14.5K protein to the cell surface (Benedict et al., 2001) and the trafficking pathway of 6.7K within post-ER compartments remains elusive.

Based on the observation that the rapid loss of Fas/EGFR surface expression upon infection with Ad2 is opposed to the slow decrease observed upon transport inhibition of newly synthesized molecules by Brefeldin A (Elsing and Burgert, 1998), we suggested that the 10.4-14.5K complex is likely to bind to the receptor target at the cell surface or shortly after internalization in early endosomes (Fig. 43). This would predict that 10.4-14.5K does not interact with the receptor in the ER or Golgi to deregulate biosynthetic cell surface transport, but may rather interfere with receptor trafficking at a later stage, possibly regulated through interaction with other cellular factors. So far, no direct interaction of 10.4-14.5K with Fas or DR4, DR5 could be observed, but when overexpressed, 10.4K could be isolated in complex with the EGFR in a cell fraction enriched for early endosomes (Crooks et al., 2000). Thus, the interaction of 10.4-14.5K with receptor targets

appears to be rather short-lived or possibly mediated by other cellular proteins (Fig. 43, cellular factor x). At present it is not known whether viral protein-receptor complexes are existing at the cell surface or formed subsequent to internalisation of the receptor in early endosomes. Cross-linking experiments aimed at isolating viral protein-receptor complexes at the cell surface might allow to distinguish between these possibilities. Data obtained with stable transfectants of A549 cells coexpressing 10.4-14.5K revealed no direct correlation between the level of FLAG-14.5K cell surface expression and the efficiency of receptor down-regulation. First of all, clones with Flag-14.5K surface levels higher than those observed in infected cells did not exhibit a higher efficiency of receptor down-regulation (Fig. 20). Secondly, 10.4-14.5K-induced down-regulation appeared to tolerate tremendous variations in surface expression levels since significant down-regulation could still occur in a 10.4-14.5K+ clone exhibiting only 20% of F14.5K levels of the infected cells (Fig. 20). However, as both 10.4K and 14.5K can be detected at the cell surface in transfected (Fig. 21) and infected cells (Fig. 32) the normal trafficking route of 10.4-14.5K complexes likely involves the cell surface. Further experimental evidence for this idea was obtained studying mutant 14.5Y¹²²A. 14.5Y¹²²A accumulates together with 10.4K at the cell surface (Fig. 22B, 32C), 10.4-14.5K steady-state levels are increased and in Ad2/F14.5Y122-infected cells the appearance of 14.5K degradation products is greatly diminished (Fig. 31, lane 4), suggesting that biosynthetic transport of 10.4-14.5K involves an obligatory cell surface intermediate. However, in both stable transfectants and infected cells expressing the 14.5Y122 mutant receptor levels were not reduced indicating that plasma membrane localization of 10.4-14.5 is not sufficient for receptor down-regulation.

At the cell surface the 10.4-14.5K complex, possibly in association with the receptor target, may be recognized via its tyrosine-based sorting signal by the AP-2 adaptor. Thereby, the complex is recruited into coated pits and rapidly internalized into endosomes (Fig. 43). Several lines of experimental evidence support this hypothesis: (i) The 14.5K cytoplasmic tail bound AP-1 and AP-2 heterotetrameric adaptor protein complexes in a Y122-dependent manner, exhibiting higher affinity towards AP-2 (Table 3). (ii) As observed by immunofluorescence the single amino acid substitution of tyrosine 122 in 14.5 caused accumulation of both 10.4K and 14.5K at the plasma membrane. (iii) In both transfectants and infected cells 10.4-14.5Y¹²²A complexes can be isolated, demonstrating that replacement of Y122 causes missorting of 10.4-14.5K without disrupting complex formation. Taken together, this experimental evidence suggests that 10.4 and 14.5 are internalized as a complex, and its endocytosis critically depends on the Y¹²²FNL motif in 14.5. If 10.4-14.5K interacted with the receptors at the plasma membrane one would expect that missorting of 10.4-14.5Y122 to the cell surface affects surface expression of the target receptors. But, whereas

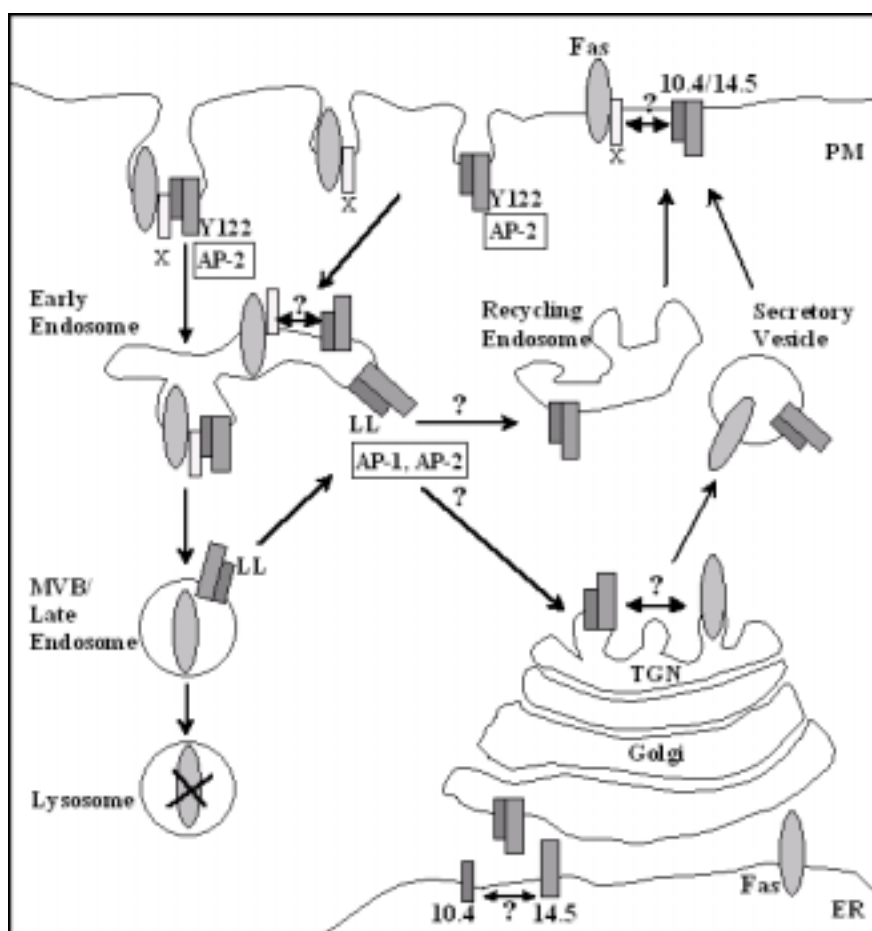


Fig. 43 Model for 10.4-14.5K-mediated down-regulation of plasma membrane receptors, e.g. Fas/CD95

The 10.4-14.5K heteromeric complex reroutes Fas from the cell surface to late endosomes/lysosomes for degradation, but the viral proteins escape from degradation in lysosomes. Sorting signals within the cytoplasmic tails of both 10.4K and 14.5K are required for efficient down-regulation of plasma membrane receptors. 14.5K Y122 appears to be part of a YXX Φ transport motif that can be recognized by AP-2 to direct endocytosis of 10.4-14.5K complexes at the plasma membrane. The 10.4K dileucine motif plays a role subsequent to endocytosis. Disruption of the 10.4K dileucine motif diverts 10.4-14.5K from a recycling pathway to late endosomes/lysosomes for degradation. ER, endoplasmic reticulum; PM, plasma membrane; AP, adaptor protein complex. See text for details.

DR4 was upregulated in cells infected with Ad2/F14.5Y122, the increase in F14.5Y¹²²A at the cell surface was not paralleled by a similar increase in Fas, EGFR or DR5 levels. Together with the critical role of Y122 in the process of receptor down-regulation these data suggest the 14.5Y¹²²FNL motif is most likely required for transport of 10.4-14.5K complexes into endosomes to promote degradation of the receptors within the endocytic route (Fig. 43), rather than for internalisation of viral protein-receptor complexes. However, according to the FACS data a significant fraction of DR4 is likely to be internalised in complex with 14.5K.

In the absence of Y122 the dileucine motif in 10.4 is insufficient to promote endocytosis (Fig. 22B and 32C). In the literature, dileucine motifs have been described acting as internalisation signals, as e.g. in the TGF- β receptor, CD4 and HIV-1 nef (Ehrlich et al., 2001; Greenberg et al., 1998; Shin et al., 1991), but the experimental data clearly indicate that the dileucine motif in 10.4 is not responsible for internalization of 10.4-14.5K.

However, the dileucine pair is likely to function as a transport signal: (i) AP-1 and AP-2 adaptor molecules (Table 3) bind to 10.4K cytoplasmic tail peptides *in vitro*, exhibiting the expected requirement for the critical dileucine pair. (ii) In both transfected and infected cells alanine substitution of the dileucine pair stimulates enhanced degradation of mutant 10.4K and its interaction partner without disrupting complex formation (Fig. 14). (iii) Immunofluorescence studies revealed that disruption of the dileucine motif in 10.4K causes 10.4-14.5K to accumulate in late endosomes/lysosomes, with a concomitant reduction of 10.4K ER staining (Fig. 23). (iv) enhanced degradation of 10.4LL and 14.5K is not due to a defect in the interaction, as the combined expression of 10.4LL/AA and 14.5Y¹²²A exhibits a high surface expression. As the vesicular phenotype of 10.4LL/AA requires an intact Y¹²²XX Φ motif in 14.5K (Fig. 22D), LL seems to be required subsequent to internalization for sorting within an endosomal compartment. Remarkably, the massive degradation of 10.4LL-14.5K in late endosomes/lysosomes is associated with a drastic decrease in 14.5K surface expression. IP/WB of 10.4-14.5K following treatment with or without Bafilomycin revealed that a significant fraction of wt 10.4-14.5K is degraded in a Bafilomycin-sensitive compartment, possibly late endosomes/lysosomes. This degradation is strongly increased upon disruption of the 10.4K dileucine pair, leading to a dramatic reduction of 10.4-14.5K steady-state levels in the mutant transfectant (Fig. 14B). Taken together, these data suggest that the dileucine pair functions within endosomes to direct recycling of 10.4-14.5K complexes to the plasma membrane (Fig. 43). The functional defect observed for the 10.4K dileucine mutant in both stable transfectants and infected cells, emphasizes the important role of the 10.4-14.5K recycling for the mechanism of receptor down-regulation. Consistent with the proposed role of the 10.4K-encoded dileucine motif in recycling of 10.4-14.5K, the efficiency of receptor down-regulation in (10.4-14.5K)+-stable transfectants was enhanced with increasing amounts of 10.4K (Fig. 19 and Fig. 20). Furthermore, enhanced degradation of 10.4LL-14.5K in late endosomes/lysosomes was not associated with an increased reduction of DR4 surface levels, although DR4 appears to physically interact with 10.4-14.5K at the plasma membrane. This suggests that the process of 10.4-14.5K-induced receptor down-regulation likely involves a more complex regulation, which is not determined solely at the level of internalisation of viral protein-

receptor complexes from the plasma membrane but requires reutilization of 10.4-14.5K to establish efficient down-regulation of target receptors. Remarkably, the 10.4K dileucine pair was most critical for down-regulation of DR5, the EGFR and DR4 whereas Fas levels could be significantly reduced (Fig. 29, Fig. 30). Receptors such as the unoccupied EGFR, which have the intrinsic capacity to rapidly recycle from endosomes to the plasma membrane (Herbst et al., 1994), might be able to escape 10.4-14.5K-induced degradation, and recycling 10.4-14.5K molecules would be required to establish efficient reduction of receptor surface expression levels. However, except for the EGFR little is known about intracellular trafficking of the other 10.4-14.5K target receptors. On the other hand, 10.4-14.5K are expressed at relatively low abundance during natural infection, as compared to other E3 proteins (Tollefson et al., 1990b; Tollefson et al., 1990a), thus reutilization of 10.4-14.5K might be required to maintain a sustained depletion of cell surface receptor pools.

In sum, our experimental data support the view that 10.4-14.5K might function within early endosomes to reroute internalised receptors to late endosomes/lysosomes for degradation, whereas a major fraction of 10.4-14.5K proteins is rescued from degradation into a recycling pathway (Fig. 43). Thereby, 10.4-14.5K might be able to target receptor molecules at the plasma membrane and early endosomes, but also within recycling compartments.

Endosomal localization of wt 10.4-14.5 is consistent with results published by Crooks et al., showing that upon infection with a virus mutant overexpressing 10.4K, 10.4K transiently colocalizes with the EGFR in early endosomes (Crooks et al., 2000). Interestingly, the LLRIL sequence found in 10.4K proteins of subgenus C is also present in the EGFR adjacent to the TMD and has been described as being necessary for efficient sorting of ligand-receptor complexes in early endosomes en route to lysosomes (Kil et al., 1999; Kil and Carlin, 2000). It was proposed that interaction of 10.4K with EGFR might lead to oligomerization of dileucine-type signals (Crooks et al., 2000), which might be important for regulating the sorting activity of these signals in different compartments (Arneson and Miller, 1995), and that the 10.4K LLRIL sequence may function to enhance recognition of the lysosomal targeting signal of the EGFR. However, despite the sequence similarity with the lysosomal sorting signal of the EGFR our experimental evidence supports the idea that the 10.4K dileucine motif functions independently from the EGFR signal in regulating transport of 10.4-14.5K to avoid extensive degradation in lysosomes. In support of our model 10.4K was not found to be degraded at the same rate as internalized EGFR in virus-infected cells (Crooks et al., 2000). Cell fractionation and immunocytochemistry indicated that the interaction of 10.4K with the EGFR in an early endosomal compartment was only transitory and 10.4K only partially colocalized with the EGFR and subsequent to early endosomes 10.4K and the

EGFR follow divergent pathways. Whereas EGFRs proceed to lysosomes for degradation, 10.4K is retained within endosomes (Crooks et al., 2000). By immunoelectron microscopy of infected cells 10.4K colocalized with endocytosed tracers in early endosomes and on limiting membranes of multivesicular endosomes (Crooks et al., 2000). However, the results of this study have to be interpreted with caution, since a virus-mutant overproducing 10.4K was used, and steady-state distribution of 10.4K differed from that observed after infection with wt Ad2. A549 cells infected with this virus mutant exhibited a highly vesicular staining for 10.4K which colocalized with transferrin receptor and RhoB in infected A549 cells (Crooks et al., 2000), leading the authors to suggest that 10.4K is located primarily to early endosomes and RhoB-positive immature multivesicular endosomes at steady-state. But in infection with wt Ad2, in both A549 cells (data not shown) or primary fibroblasts, 10.4K is detected in the ER and a perinuclear compartment, identified as the Golgi/TGN (compare Fig. 34), hindering the identification of 10.4-14.5K+ vesicular structures. However, in good agreement with the results obtained by Crooks et al. for down-regulation of the EGFR, in SV80Fas cells infected with wt Ad2 10.4-14.5K and Fas exhibit only a limited colocalization in endosomal/lysosomal compartments, even in the presence of Bafilomycin A₁ (Fig. 36). Whereas Fas receptors seem to be delivered into lysosomes where they are degraded, the majority of 10.4 and 14.5 is retained in a prelysosomal compartment (multivesicular endosome or late endosome) or retrieved to early endosomes from which they might recycle to the plasma membrane (Fig. 43). The data presented here provide evidence that the LL motif in 10.4 is crucially involved in this latter sorting step and in rescuing of 10.4-14.5 from degradation. But the precise endosomal compartment at which LL may act remains unclear. One possibility is that LL is required for recruiting and directing 10.4-14.5K from the limiting membrane of late endosomes into a recycling pathway to the plasma membrane either via early/recycling endosomes or the TGN. Alternatively, LL may be important for sorting and recycling of 10.4-14.5 at the early endosome (Fig. 43).

At present the mechanism for transfer from EE to RE is unclear. It may either involve transport vesicles or alternatively tubular RE may derive directly from EE. Despite the wealth of information that has been gained on the other transport steps of the biosynthetic and endocytic pathways no recycling motif has been identified yet, leading to the proposal that recycling from EE to the cell surface occurs by default. This view is difficult to reconcile with the situation in polarized epithelial cells in which transcytosed and recycling receptors transit through a common recycling endosome before being transported to opposite plasma membrane domains (Futter et al., 1998). Remarkably, endosomal tubules have been found to generate clathrin-coated vesicles (Stoorvogel et al., 1996), that in polarized have been proposed to carry transferrin receptor to the

basolateral membrane (Futter et al., 1998). But although γ -adaptin was contained in these clathrin-coated domains, it remains unclear whether transferrin receptors are actively sorted, possibly by AP-1, into these vesicles. Localization of 10.4-14.5K to recycling endosomes is particularly difficult to identify, since in most cell types the recycling compartment is concentrated predominantly in the perinuclear area, and thus by immunofluorescence it can hardly be distinguished from the strong signal of 10.4-14.5K in the Golgi/TGN compartment. To circumvent this problem, one might impose a block on 10.4-14.5K neosynthesis by cycloheximide treatment of the infected cells and follow 10.4-14.5K trafficking in post-Golgi compartments in a pulse-chase analysis.

The dependence of recycling pathways from endosomes to the TGN on the presence of transport motifs has been demonstrated. A tyrosine-based signal in beta2 integrin has been shown to be required for recycling to the plasma membrane (Fabbri et al., 1999), since disruption of the motif diverts internalized integrins from a recycling compartment into a degradative pathway. The SXYQRL sequence of TGN38 can confer TGN localization to a plasma membrane protein (Wong and Hong, 1993). Our experimental evidence argues against a dominant role of the 14.5K Y¹²²FNL transport motif in such a recycling step, as this motif cannot prevent enhanced degradation in the absence of the 10.4K dileucine pair. The cellular factor PACS-1 is important for TGN localization of Furin and the cI-MPR by a retrieval mechanism from late endosomes (Wan et al., 1998), and also for the ability of HIV-1 Nef to redistribute MHC-I from the cell surface to the TGN (Piguet et al., 2000). PACS-1 is thought to recognize acidic cluster signals in cytosolic domains of membrane proteins and to function as a connector molecule by linking these proteins to adaptor complexes, such as AP-1 (Crump et al., 2001; Wan et al., 1998). But sorting of 10.4-14.5K is unlikely to involve recognition by PACS-1 as neither 10.4K nor 14.5K contains a stretch of acidic residues in its cytoplasmic tail.

A dileucine pair has been described to be implicated in sorting of MPR46 within endosomes (Tikkanen et al., 2000). MPR46 binds AP-1 and AP-2 and normally cycles between the TGN, endosomes and the plasma membrane (Rohn et al., 2000). The MPR46 LL/AA mutant accumulates in early endosomes and at the plasma membrane and was proposed to exhibit an impaired sorting within endosomes eliminating its return to the TGN (Tikkanen et al., 2000). In good correlation in AP-1 knock-out cells retrograde transport of MPRs from the endosome to the Golgi is inhibited (Meyer et al., 2000). By analogy the 10.4K dileucine pair may also be recognized by AP-1 within endosomes. But, 10.4-14.5K trafficking differs from that of MPR46 in that in the absence of the 10.4K dileucine pair the viral proteins cannot return to the plasma membrane.

At present, the molecular mechanism how segregation of 10.4-14.5K receptor targets into lysosomes is achieved is unknown. The observation that proteins which undergo ligand-induced

down-regulation, such as the EGFR, have the capacity to recycle back to the plasma membrane argues against the simple model that receptor down-regulation is determined solely at the level of internalization from the plasma membrane. It rather appears to require in addition an active sorting determinant for entry into the lysosomal pathway. Sorting between cargo destined for degradation in lysosomes from material supposed to be recycled occurs in a prelysosomal, late endosomal compartment, named multivesicular bodies (MVBs). The signals and the protein machinery involved in this sorting step are being intensively studied [reviewed in (Piper and Luzio, 2001)]. Invagination of vesicles from the limiting membranes to the interior of the MVB, has been proposed to be promoted by segregation of lysobisphosphatidic acid and phosphatidylinositol 3'phosphate. As a consequence, integral membrane proteins with special properties of the transmembrane domain (TMD), e.g. containing polar residues may partition together with these lipids (Reggiori et al., 2000; Zaliauskiene et al., 2000). Interestingly, both the 10.4 and the 14.5 proteins contain an unusually high number (6-10) of polar residues, like serine, threonine, cysteine or tyrosine in their TMD. This feature is conserved in proteins of Ads from all subgenera, with subgenus B 14.5 proteins even containing a centrally located asparagine residue in the TMD (Fig. 8). Therefore, compatible with the proposed role of polar residues in sorting to the luminal membranes, it is an attractive possibility that 10.4-14.5 may reroute their target proteins by providing a polar characteristic to the intrinsically hydrophobic TMDs of Fas (3 pol. aa), the EGFR (none) and the TRAIL-Rs (DR4 none, DR5 2). However, this model is difficult to reconcile with the observation that a significant proportion of 10.4-14.5K is not present in the same vesicles as the target protein.

One sorting tag involved in directing internalized receptors into a pathway that results in lysosomal degradation, has been identified as ubiquitin (Hicke, 2001; Urbanowski and Piper, 2001). The ubiquitin tag can be recognized by members of the class E vacuolar protein-sorting (Vps) proteins, such as tumor susceptibility gene 101 (TSG101)/VPS28 and mammalian cells lacking TSG101 cannot effectively down-regulate the activated EGFR (Babst et al., 2000). Entry of the activated EGFR into the MVB pathway involves EGFR tyrosine kinase activity, sorting signals in the EGFR cytoplasmic tail and the ubiquitin ligase c-Cbl (Felder et al., 1990; Kil et al., 1999; Kil and Carlin, 2000; Kornilova et al., 1996; Levkowitz et al., 1998). The E3 ubiquitin ligase c-Cbl is phosphorylated upon tyrosine kinase activation, associates with the EGFR and mediates receptor ubiquitination (Levkowitz et al., 1998; Levkowitz et al., 1999; Lill et al., 2000). At present it is debated whether the interaction between c-Cbl and EGFR occurs at the plasma membrane and/or at the level of endosomes (de Melker et al., 2001; Levkowitz et al., 1998; Stang et al., 2000), but Cbl-mediated ubiquitination is not required for EGFR endocytosis (Longva et al., 2002).

Overexpression of c-Cbl greatly enhances the level of EGFR ubiquitination and rate of ligand-induced degradation without altering the rate at which it is internalized from the plasma membrane (Levkowitz et al., 1998). It remains to be tested whether in the presence of 10.4-14.5K the EGFR becomes phosphorylated and/or ubiquitinated, but as 10.4-14.5K do not activate the receptor tyrosine kinase ubiquitination may occur by a different mechanism than ubiquitination of ligand-activated EGFRs. Recently, the human herpes virus 8 (HHV8) gene product K3 was shown to usurp the ubiquitin-dependent endosomal sorting machinery of the host cell for down-regulation of MHC class I from the plasma membrane (Lorenzo et al., 2002). K3 possesses E3 ubiquitin ligase activity and promotes ubiquitylation of class I molecules after export from the ER. Ubiquitylation provides the signal for class I internalization at the plasma membrane and late endosomal sorting for degradation by a mechanism involving TSG101 (Hewitt et al., 2002). However, 10.4K and 14.5K cytoplasmic tails do not possess any sequence homology to the ubiquitin ligase plant homeodomain of K3 (HHV8 K3: AAC57091.1).

A mechanism which proposes that 10.4-14.5K functions within endosomes to enhance the efficiency of sequestration of the EGFR within MVBs is in accord with the observation that 10.4-14.5K down-regulation of the EGFR is not accompanied by an increased rate of receptor internalization (Hoffman and Carlin, 1994). 10.4-14.5K might link the receptor to an intrinsic MVE sorting signal located in the viral proteins, but this would predict that 10.4-14.5K are degraded at the same rate as the receptor. Alternatively, the association of 10.4 with the EGFR in early endosomes may induce conformational changes similar to ligand-occupancy of the receptor, and thereby expose cryptic sorting signals in the receptors cytoplasmic tail that enhance trafficking to late endosomes/lysosomes. Such a sorting signal, which is active in C-terminally truncated or ligand-activated EGFRs of the receptor, has been identified surrounding the critical residues L679L680 of the receptor. This region within the receptor's cytoplasmic tail has been reported to be required for 10.4-14.5K-mediated down-regulation of the EGFR, whereas other sorting signals located within sequences downstream of the EGFR kinase domain were dispensable for Ad-induced down-regulation of cytoplasmically truncated receptors (Crooks et al., 2000). However, it has not been tested experimentally whether this region is necessary for the interaction of viral proteins with the receptor or functions as a sorting signal in the process of 10.4-14.5K-induced down-regulation. It appears likely that 10.4-14.5 target constitutively internalized EGFRs to the same endocytic compartment as ligand, but how 10.4-14.5K achieve segregation of the receptor from the recycling pathway into lysosomes independently of the EGFR kinase activity remains unclear.

Whereas the EGFR is known to be constitutively internalized by a default pathway that does not involve signals within the receptors cytoplasmic tail (Herbst et al., 1994), very little is known about trafficking of Fas and other members of the TNF/NGFR superfamily. In some cells (e.g. in untransformed vascular smooth muscle cells), Fas is predominantly intracellular, colocalizing with the Golgi marker galactosyltransferase, and to a lesser degree on the cell surface (Bennett et al., 1998). Likewise the TGN is the principal intracellular location of TNFR1, and sorting signals for localization to the TGN have been identified in the receptors cytoplasmic tail (Storey et al., 2002). But the TGN is not a site of TNFR1 signaling. Therefore, it has been proposed that there may be a regulated recycling pathway between the TGN and cell surface, allowing control of the amount of TNFR1 on the cell surface and other sites of the pathway, thus influencing signaling (Jones et al., 1999; Storey et al., 2002). In support of this model, after TNF-binding and TNFR1 internalization from the cell surface TRADD has been shown to dissociate from the receptor and signaling terminates (Jones et al., 1999). The region within TNFR1 that contains a TGN localization signal is not conserved in the Fas cytoplasmic tail. Nonetheless, regulated trafficking between the Golgi and the cell surface might also be an important determinant of Fas signaling (Augstein et al., 2002; Bennett et al., 1998; Haynes et al., 2002). Stimulation of Fas by agonistic antibodies or Fas ligand results in microaggregation and clustering of the receptor at the plasma membrane which is followed by internalization and transport into transferrin receptor positive endosomes (Algeciras-Schimmich et al., 2002). Thus, Fas can enter the endocytic pathway in the presence of ligand. Internalization of Fas upon stimulation with ligand appears to modulate cell death-signaling (Strasser and O'Connor, 1998), in that rapid internalization may prevent assembly of the death inducing signaling complex at the receptor's cytoplasmic tail. TRAIL-R1 and TRAIL-R2 have also been reported to be internalized into endosomes after ligand binding (Zhang et al., 2000). Thus, all known target molecules of 10.4-14.5 seem to be able to enter the endocytic pathway in the absence of 10.4-14.5. This observation is compatible with the hypothesis that 10.4-14.5 do not induce endocytosis, but rather regulate a subsequent sorting step directing targets into lysosomes. Close inspection of the Fas sequence reveals four potential LL transport motifs and one YXX Φ motif. The YXX Φ motif is located in the death domain and a similar motif is conserved among the death domains of TRAIL-R1, TRAIL-R2 and TNF-R1. At present, it is unclear whether these motifs are involved in trafficking or rather represent ITAMs. Moreover, it remains to be investigated how the 10.4-14.5K YXX Φ and LL motifs would contribute to the lysosomal sorting via endogenous sorting signals in the target receptor. First experiments have been carried out to test which elements in the Fas receptor

contribute to 10.4-14.5-mediated modulation. Interestingly, both the transmembrane part and the cytoplasmic tail of Fas are required for 10.4-14.5 mediated down-regulation (Obermeier et al., unpublished observation). Down-modulation of the TRAIL-R2 by the E3 complex has been reported to depend on the receptor's cytoplasmic tail, but the death domain alone is not sufficient (Benedict et al., 2001). This is in accord with the observation that other death domain-containing receptors such as TNFR1 are not targeted by 10.4-14.5K.

Thus, interestingly, adenovirus seems to have evolved two transmembrane proteins, E3/10.4-14.5K, which exploit the cellular protein sorting machinery to achieve selective down-regulation of different immunologically relevant cell surface receptors, thereby contributing to immune evasion. This strategy appears to be specifically adapted to the target molecules, as it differs from the ER-retention mechanism employed by E3/19K to down-regulate MHC class I molecules. Apparently, E3/10.4-14.5K do not escort the receptor targets into lysosomes, therefore it will be interesting to identify cellular interaction partners of the targeted receptors that might play a role in this process.

7.5. Differential requirements for expression of Ad4 10.4-14.5K proteins

The Ad2 10.4-14.5K proteins are capable of specific down-modulation of receptor targets that are members of two different receptor families and therefore have different sequence requirements. It would be interesting to find out what elements define the specificity of 10.4-14.5K towards different types of receptors. Remarkably, the Ad4 10.4-14.5K proteins appear not to have the same target specificity, since in cells infected with Ad4 solely TRAIL-R1 surface expression levels are efficiently reduced (Burgert, unpublished observation). To test whether indeed the Ad4 10.4-14.5K proteins are sufficient for the Ad4 target specificity the coding sequences of Ad4 10.4 and/or 14.5 proteins were inserted into the Ad2 genome, replacing the Ad2 homologues. Surprisingly, expression of the Ad4 10.4-14.5K proteins encoded by the Ad2 E3 region differed from the pattern observed in Ad4-infected cells. The Ad4 10.4K protein was not detected and very little Ad4 14.5K was expressed independently of whether the Ad2 specific nucleotides or the Ad4 5 nucleotide intercistronic sequence was present (Fig. 41, lane 7,8). For all chimeric virus constructs, the Ad2 E3/19K protein was constantly expressed, suggesting that the splicing of the E3/19K encoding mRNA is normal. Ad2 10.4K expression was not changed by insertion of Ad4 sequences downstream of the 10.4K ORF (Fig. 31, 10.4K, compare lane 3 with lanes 4,5). By contrast, replacement of the Ad2 10.4K coding sequence and intercistronic sequence by the corresponding Ad4 nucleotide sequence strongly reduced the amounts of the Ad2 14.5K protein isolated from

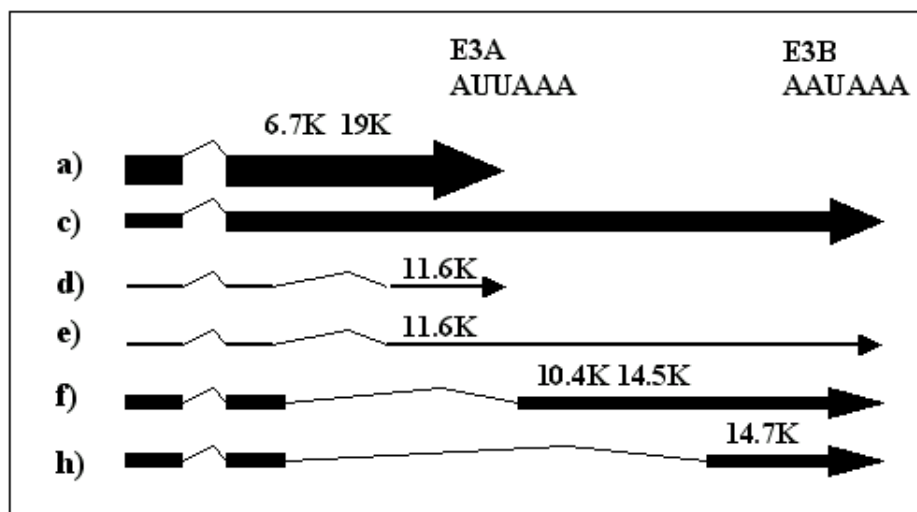


Fig. 44 Physical Map of the E3 transcription unit of subgroup C adenoviruses (adapted from (Brady et al., 1992)). Arrows represent the exons of mRNAs a-h, with the thickness of the arrow indicating the relative abundance of the mRNA. E3 proteins expressed from the different mRNA species are listed on top of the arrows. Thin lines indicate the introns removed during mRNA maturation. E3A and E3B denote two alternative polyadenylation sites used during E3 mRNA formation.

infected cells (Fig. 31, 14.5K, compare lane 3 with lane 6). Similarly, Ad4 14.5K levels were also drastically reduced when the Ad4 10.4K CDS was preceding the 14.5K ORF. This reduction of 14.5K levels was not influenced by the type of intercistronic sequences (Ad2- or Ad4-like), or spacing of 10.4-14.5K coding sequences. Therefore, these Ad2/Ad4 chimeric viruses reveal that expression of 14.5K in the Ad2 E3 region is influenced by sequences preceding the 14.5K ORF.

In cells infected with subgroup C viruses both 10.4 and 14.5K seem to be translated from mRNA f (Fig. 44), as they were coordinately overexpressed or underexpressed *in vivo* by virus mutants that under- or overproduce mRNA f (Tollefson et al., 1990b; Tollefson et al., 1990a). Thus, the 14.5K protein appears to be translated mainly from a bicistronic mRNA, the 14.5K ORF being located two nucleotides downstream of that translated into 10.4K. In this respect the 14.5K ORF differs from the other Ad2 E3 ORFs which are located on separate mRNAs, mRNA d, e for 11.6K, mRNA h for 14.7K and are directly preceded by a 3' splice site (the same is true for 10.4K on mRNA f), which reduces the number of upstream AUGs and putative cistrons (Fig. 44). 14.5K can be translated *in vitro* in a reticulocyte extract from mRNA f purified from virus-infected cells (Tollefson et al., 1990a), but so far it is unknown, how initiation of translation at the downstream 14.5K ORF occurs. Most eucaryotic RNAs are translated by a scanning mechanism that initiates at the mRNA 5' terminal cap and initiates translation at the 5' proximal efficient AUG, the consensus sequence being GCC(A,G)CCA⁺UGG (Kozak, 1987), whereas suboptimal AUG are

bypassed (Kozak, 1999). The start codons of Ad2 10.4 and 14.5 appear to be of similar efficiency, as none of them contains G in +4, but both do contain A in -3. Besides the 10.4K start codon no other AUG matching the consensus of translation initiation have been identified (Tollefson et al., 1990a). The sequence context of the Ad2 10.4 AUG seems to be suboptimal and therefore may allow initiation of translation at the downstream 14.5K AUG. It has been proposed that ribosomes may terminate translation of 10.4K and then reinitiate translation of 14.5K from the same mRNA (Wold et al., 1995). The balance of E3 mRNA production in subgroup C viruses is regulated by two polyadenylation (poly(A)) signals, an atypical AUUAAA E3A signal and a typical AAUAAA termed E3B (Fig. 44). Interestingly, the 3' splice site for mRNA f is only 4 bp upstream of the E3A polyadenylation/cleavage signal. A competition between splicing and polyadenylation factors has been proposed and as a result mRNA a, encoding E3/19K, is three times more abundant than mRNA f (Wold et al., 1995). In addition cis-acting sequences around the E3 poly(A) site have a crucial effect on E3 mRNA processing, e.g. a splice suppressor sequence within the 11.6K ORF favors production of mRNAa and downstream from the actual E3A poly A signal a GU rich sequence forms part of the core poly(A) site (reviewed in (Imperiale et al., 1995).

Introduction of the Ad4 10.4K nucleotide sequence into Ad2 E3 leaves both the polypyrimidine tract and 3' splice site for mRNA f intact, but introduces sequence changes downstream of the E3A poly(A) signal and these might influence the efficiency of 3' end processing. Therefore, it cannot be predicted from the sequence whether mRNA f is being made in the chimeric viruses encoding Ad4 10.4K. Apparently, no increase in E3/19K production is observed in the chimeric viruses (Fig. 41), indicating that the balance of E3 splicing is not shifted towards mRNAa. To clarify this issue mRNA levels need to be analyzed experimentally.

Since Ad2 and Ad4 10.4K CDS are of identical length, and neither the type of intercistronic sequence (Ad2 or Ad4), nor the spacing of 10.4 and 14.5K ORFs appeared to be the prime reason for drastically reduced expression of 14.5K, this defect might be attributed to differences between the 10.4K nucleotide sequences of Ad4 and Ad2. Sequence comparison revealed a remarkably higher content of GC residues in Ad4 10.4K (data not shown). The RNA secondary structure prediction algorithm mfold (Zuker, 1989) suggested that these differences might permit the Ad4 10.4K encoding RNA to fold into a hairpin structure close to the 3' end of the 10.4K ORF. Interestingly, among the 15 predicted secondary structures 14 contained an identical hairpin structure whereas another structure represented an alternative stem loop involving residues further downstream. Thus, an equilibrium of 5' and 3' hairpin structures was predicted which might allow formation of a pseudoknot intermediate (Fig. 45 A).

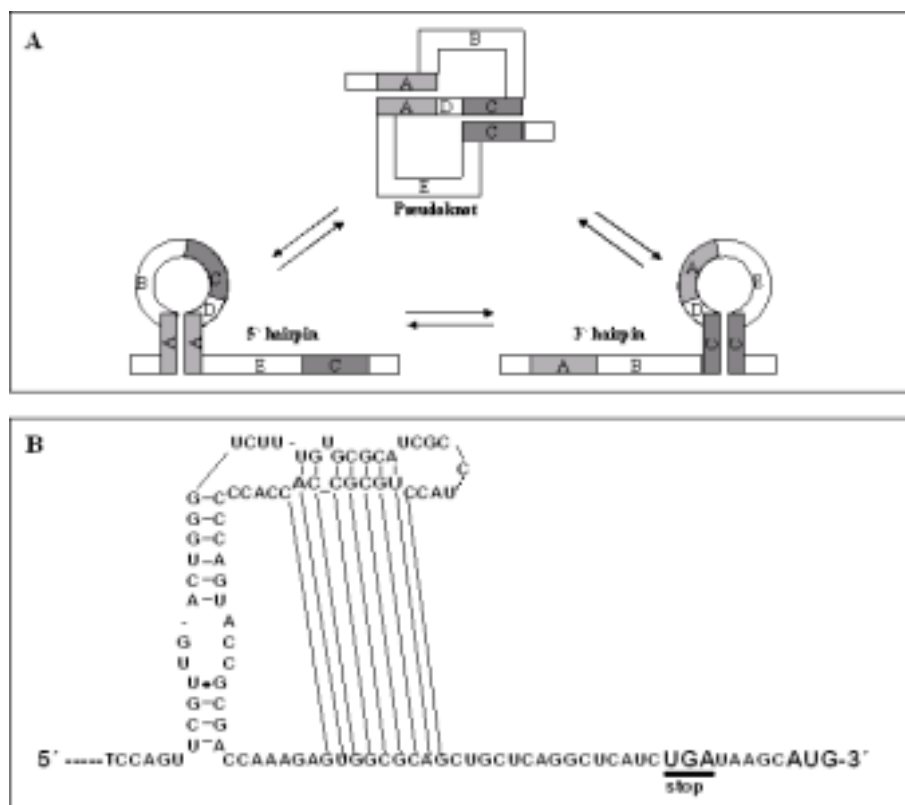


Fig. 45 The nucleotide sequence in the 3' part of an Ad4 10.4K encoding mRNA can adopt a pseudoknot structure

(A) A sequence with the potential to form a pseudoknot can also form two hairpin structures. **(B)** The mfold algorithm (<http://bioinfo.rpi.edu/mfold/rna/form1-2.3.cgi>) developed by M. Zuker was used to predict the secondary structure of an RNA sequence of 290 nt in length encompassing the sequence TGAGAC upstream and TAAGCAUG downstream of the Ad4 10.4K coding sequence. The predicted pseudoknot structure is positioned close to the stop codon of the Ad4 10.4K ORF.

This is an interesting finding, since pseudoknots have been proposed to slow elongating ribosomes and thereby inhibit reinitiation of translation at a downstream ORF (Kozak, 2001). A possible pseudoknot structure formed at the 3' end of the Ad4 10.4K RNA sequence is shown in Fig. 45B. This would suggest that in the organization of the Ad4 genome 14.5K is located on a separate mRNA.

In conclusion, the data suggest that expression of Ad4 10.4-14.5K is differently regulated in the Ad4 E3 region, which differs in size and composition from E3 region of subgroup C viruses (Fig. 4). Ad4 is unusual in that it is the only known serotype of subgroup E, and it has been proposed that Ad4 originated only recently by recombination of genomes resembling contemporary subgroup B and subgroup C viruses (Gruber et al., 1993). Therefore the regulation of the Ad4 E3 region might resemble that of subgroup B viruses. Despite the fact that subgroup B adenovirus type 35 encodes homologous proteins to subgroup C the quantity of individual

mRNAs differs substantially among Ad2 and Ad35 (Basler and Horwitz, 1996). Moreover, in Ad35 10.4K and 14.5K are encoded by two separate mRNAs. Whereas subgroup C Ads devote nearly half of their E3 mRNAs to the production of mRNAs a and c which encode the class I MHC binding protein gp19K and relatively less mRNA to the production of 10.4, 14.5, 14.7K proteins, the Ad35 RNAs encoding 10.4K and 14.5K, respectively, are the most abundant comprising 20% and 48% (Basler and Horwitz, 1996; Wold et al., 1995). Analysis of Ad35 E3 mRNA regulation revealed that there is only one polyadenylation signal (the equivalent of the E3B poly(A)) while two polyadenylation signals are used in the formation of subgroup C mRNAs. In support of the view that E3 splicing in Ad4 might be regulated differently than that of subgroup C viruses, the E3A poly(A) signal of Ad2 is not conserved in Ad4. The 3' splice site preceding the 10.4K CDS is present in Ad4 and it remains to be explored whether the Ad4 14.5K ORF is also preceded directly by a functional 3' splice site, generating a 14.5K mRNA.

We have chosen to use the Ad2 background in this study, since this context allows to monitor down-regulation of all target proteins by infection of A549 cells, which express sufficient amounts of all receptor targets. Moreover, we have reagents to determine expression of other E3 proteins, e.g. E3/19K. But obviously, the viral system is highly regulated, with complex requirements for splicing to occur correctly and disabling successful transfer of Ad4 genes into Ad2. Thus, to reproduce and analyze the Ad4-specific modulation pattern, a non-viral expression system has to be established despite the major disadvantage that no 10.4-14.5K-independent standard for E3 protein expression is available in such a system. In order to be able to quantitatively monitor expression of Ad4 10.4K and 14.5K, Ad4-specific antibodies need to be developed. Functional analysis may be carried out on stable transfectants of A549 cells expressing the Ad4 10.4-14.5K proteins.

References

- Aguilar,R.C., Boehm,M., Gorshkova,I., Crouch,R.J., Tomita,K., Saito,T., Ohno,H., and Bonifacino,J.S. (2001). Signal-binding specificity of the mu4 subunit of the adaptor protein complex AP-4. *J. Biol. Chem.* **276**, 13145-13152.
- Ahn,S., Kim,J., Lucaveche,C.L., Reedy,M.C., Luttrell,L.M., Lefkowitz,R.J., and Daaka,Y. (2002). Src-dependent tyrosine phosphorylation regulates dynamin self-assembly and ligand-induced endocytosis of the epidermal growth factor receptor. *J. Biol. Chem.* **277**, 26642-26651.
- Algeciras-Schimmich,A., Shen,L., Barnhart,B.C., Murmann,A.E., Burkhardt,J.K., and Peter,M.E. (2002). Molecular ordering of the initial signaling events of CD95. *Mol. Cell Biol.* **22**, 207-220.
- Allan,B.B. and Balch,W.E. (1999). Protein sorting by directed maturation of Golgi compartments. *Science* **285**, 63-66.
- Andersson,M., Paabo,S., Nilsson,T., and Peterson,P.A. (1985). Impaired intracellular transport of class I MHC antigens as a possible means for adenoviruses to evade immune surveillance. *Cell* **43**, 215-222.
- Andrade,F., Bull,H.G., Thornberry,N.A., Ketner,G.W., Casciola-Rosen,L.A., and Rosen,A. (2001). Adenovirus L4-100K assembly protein is a granzyme B substrate that potently inhibits granzyme B-mediated cell death. *Immunity* **14**, 751-761.
- Arneson,L.S., Kunz,J., Anderson,R.A., and Traub,L.M. (1999). Coupled inositide phosphorylation and phospholipase D activation initiates clathrin-coat assembly on lysosomes. *J. Biol. Chem.* **274**, 17794-17805.
- Arneson,L.S. and Miller,J. (1995). Efficient endosomal localization of major histocompatibility complex class II-invariant chain complexes requires multimerization of the invariant chain targeting sequence. *J. Cell Biol.* **129**, 1217-1228.
- Ashcroft,M. and Vousden,K.H. (1999). Regulation of p53 stability. *Oncogene* **18**, 7637-7643.
- Ashkenazi,A. and Dixit,V.M. (1998). Death receptors: signaling and modulation. *Science* **281**, 1305-1308.
- Augstein,P., Dunger,A., Salzsieder,C., Heinke,P., Kubernath,R., Bahr,J., Fischer,U., Rettig,R., and Salzsieder,E. (2002). Cell surface trafficking of Fas in NIT-1 cells and dissection of surface and total Fas expression. *Biochem. Biophys. Res. Commun.* **290**, 443-451.
- Babst,M., Odorizzi,G., Estepa,E.J., and Emr,S.D. (2000). Mammalian tumor susceptibility gene 101 (TSG101) and the yeast homologue, Vps23p, both function in late endosomal trafficking. *Traffic* **1**, 248-258.
- Bache,K.G., Raiborg,C., Mehlum,A., and Stenmark,H. (2003). STAM and Hrs are subunits of a multivalent ubiquitin-binding complex on early endosomes. *J. Biol. Chem.* **278**, 12513-12521.
- Balsinde,J., Balboa,M.A., Insel,P.A., and Dennis,E.A. (1999). Regulation and inhibition of phospholipase A2. *Annu. Rev. Pharmacol. Toxicol.* **39**, 175-189.
- Bao,J., Gur,G., and Yarden,Y. (2003). Src promotes destruction of c-Cbl: Implications for oncogenic synergy between Src and growth factor receptors. *Proc. Natl. Acad. Sci. U. S. A* **100**, 2438-2443.
- Barkett,M. and Gilmore,T.D. (1999). Control of apoptosis by Rel/NF-kappaB transcription factors. *Oncogene* **18**, 6910-6924.
- Barlowe,C. (2000). Traffic COPs of the early secretory pathway. *Traffic* **1**, 371-377.
- Barraza,E.M., Ludwig,S.L., Gaydos,J.C., and Brundage,J.F. (1999). Reemergence of adenovirus type 4 acute respiratory disease in military trainees: report of an outbreak during a lapse in vaccination. *J. Infect. Dis.* **179**, 1531-1533.
- Basler,C.F., Droguett,G., and Horwitz,M.S. (1996). Sequence of the immunoregulatory early region 3 and flanking sequences of adenovirus type 35. *Gene* **170**, 249-254.

References

- Basler,C.F. and Horwitz,M.S. (1996). Subgroup B adenovirus type 35 early region 3 mRNAs differ from those of the subgroup C adenoviruses. *Virology* **215**, 165-177.
- Benedict,C.A., Norris,P.S., Prigozy,T.I., Bodmer,J.L., Mahr,J.A., Garnett,C.T., Martinon,F., Tschopp,J., Gooding,L.R., and Ware,C.F. (2001). Three adenovirus E3 proteins cooperate to evade apoptosis by tumor necrosis factor-related apoptosis-inducing ligand receptor-1 and -2. *J. Biol. Chem.* **276**, 3270-3278.
- Benedict,C.A., Norris,P.S., and Ware,C.F. (2002). To kill or be killed: viral evasion of apoptosis. *Nat. Immunol.* **3**, 1013-1018.
- Bennett,E.M., Bennink,J.R., Yewdell,J.W., and Brodsky,F.M. (1999). Cutting edge: adenovirus E19 has two mechanisms for affecting class I MHC expression. *J. Immunol.* **162**, 5049-5052.
- Bennett,M., Macdonald,K., Chan,S.W., Luzio,J.P., Simari,R., and Weissberg,P. (1998). Cell surface trafficking of Fas: a rapid mechanism of p53-mediated apoptosis. *Science* **282**, 290-293.
- Bewley,M.C., Springer,K., Zhang,Y.B., Freimuth,P., and Flanagan,J.M. (1999). Structural analysis of the mechanism of adenovirus binding to its human cellular receptor, CAR. *Science* **286**, 1579-1583.
- Biery,M.C., Lopata,M., and Craig,N.L. (2000a). A minimal system for Tn7 transposition: the transposon-encoded proteins TnsA and TnsB can execute DNA breakage and joining reactions that generate circularized Tn7 species. *J. Mol. Biol.* **297**, 25-37.
- Biery,M.C., Stewart,F.J., Stellwagen,A.E., Raleigh,E.A., and Craig,N.L. (2000b). A simple in vitro Tn7-based transposition system with low target site selectivity for genome and gene analysis. *Nucleic Acids Res.* **28**, 1067-1077.
- Biron,C.A. and Brossay,L. (2001). NK cells and NKT cells in innate defense against viral infections. *Curr. Opin. Immunol.* **13**, 458-464.
- Bishop,N., Horman,A., and Woodman,P. (2002). Mammalian class E vps proteins recognize ubiquitin and act in the removal of endosomal protein-ubiquitin conjugates. *J. Cell Biol.* **157**, 91-101.
- Black,M.W. and Pelham,H.R. (2000). A selective transport route from Golgi to late endosomes that requires the yeast GGA proteins. *J. Cell Biol.* **151**, 587-600.
- Black,M.W. and Pelham,H.R. (2001). Membrane traffic: how do GGAs fit in with the adaptors? *Curr. Biol.* **11**, R460-R462.
- Blagoveshchenskaya,A.D., Thomas,L., Feliciangeli,S.F., Hung,C.H., and Thomas,G. (2002). HIV-1 Nef downregulates MHC-I by a PACS-1- and PI3K-regulated ARF6 endocytic pathway. *Cell* **111**, 853-866.
- Boehm,M., Aguilar,R.C., and Bonifacino,J.S. (2001). Functional and physical interactions of the adaptor protein complex AP-4 with ADP-ribosylation factors (ARFs). *EMBO J.* **20**, 6265-6276.
- Boehm,M. and Bonifacino,J.S. (2001). Adaptins: the final recount. *Mol. Biol. Cell* **12**, 2907-2920.
- Boll,W., Ohno,H., Songyang,Z., Rapoport,I., Cantley,L.C., Bonifacino,J.S., and Kirchhausen,T. (1996). Sequence requirements for the recognition of tyrosine-based endocytic signals by clathrin AP-2 complexes. *EMBO J.* **15**, 5789-5795.
- Boll,W., Rapoport,I., Brunner,C., Modis,Y., Prehn,S., and Kirchhausen,T. (2002). The mu2 subunit of the clathrin adaptor AP-2 binds to FDNPVY and YppO sorting signals at distinct sites. *Traffic.* **3**, 590-600.
- Bonifacino,J.S. and Traub,L.M. (2003). Signals for Sorting of Transmembrane Proteins to Endosomes and Lysosomes. *Annu. Rev. Biochem.*
- Borgland,S.L., Bowen,G.P., Wong,N.C., Libermann,T.A., and Muruve,D.A. (2000). Adenovirus vector-induced expression of the C-X-C chemokine IP-10 is mediated through capsid-dependent activation of NF-kappaB. *J. Virol.* **74**, 3941-3947.
- Brady,H.A., Scaria,A., and Wold,W.S. (1992). Map of cis-acting sequences that determine alternative pre-mRNA processing in the E3 complex transcription unit of adenovirus. *J. Virol.* **66**, 5914-5923.

- Brady,H.A. and Wold,W.S. (1988). Competition between splicing and polyadenylation reactions determines which adenovirus region E3 mRNAs are synthesized. *Mol. Cell Biol.* **8**, 3291-3297.
- Bremnes,T., Lauvrak,V., Lindqvist,B., and Bakke,O. (1998). A region from the medium chain adaptor subunit (mu) recognizes leucine- and tyrosine-based sorting signals. *J. Biol. Chem.* **273**, 8638-8645.
- Bruder,J.T. and Kovesdi,I. (1997). Adenovirus infection stimulates the Raf/MAPK signaling pathway and induces interleukin-8 expression. *J. Virol.* **71**, 398-404.
- Burgert,H.G. (1996). Subversion of the MHC class I antigen-presentation pathway by adenoviruses and herpes simplex viruses. *Trends Microbiol.* **4**, 107-112.
- Burgert,H.G. and Blusch,J.H. (2000). Immunomodulatory functions encoded by the E3 transcription unit of adenoviruses. *Virus Genes* **21**, 13-25.
- Burgert,H.G. and Kvist,S. (1985). An adenovirus type 2 glycoprotein blocks cell surface expression of human histocompatibility class I antigens. *Cell* **41**, 987-997.
- Burgert,H.G., Maryanski,J.L., and Kvist,S. (1987). "E3/19K" protein of adenovirus type 2 inhibits lysis of cytolytic T lymphocytes by blocking cell-surface expression of histocompatibility class I antigens. *Proc. Natl. Acad. Sci. U. S. A* **84**, 1356-1360.
- Burgert,H.G., Ruzsics,Z., Obermeier,S., Hilgendorf,A., Windheim,M., and Elsing,A. (2002). Subversion of host defense mechanisms by adenoviruses. *Curr. Top. Microbiol. Immunol.* **269**, 273-318.
- Carlin,C.R., Tollefson,A.E., Brady,H.A., Hoffman,B.L., and Wold,W.S. (1989). Epidermal growth factor receptor is down-regulated by a 10,400 MW protein encoded by the E3 region of adenovirus. *Cell* **57**, 135-144.
- Chang,C.P., Lazar,C.S., Walsh,B.J., Komuro,M., Collawn,J.F., Kuhn,L.A., Tainer,J.A., Trowbridge,I.S., Farquhar,M.G., Rosenfeld,M.G., and . (1993). Ligand-induced internalization of the epidermal growth factor receptor is mediated by multiple endocytic codes analogous to the tyrosine motif found in constitutively internalized receptors. *J. Biol. Chem.* **268**, 19312-19320.
- Chen,P., Tian,J., Kovesdi,I., and Bruder,J.T. (1998). Interaction of the adenovirus 14.7-kDa protein with FLICE inhibits Fas ligand-induced apoptosis. *J. Biol. Chem.* **273**, 5815-5820.
- Chen,Y.A. and Scheller,R.H. (2001). SNARE-mediated membrane fusion. *Nat. Rev. Mol. Cell Biol.* **2**, 98-106.
- Chepenik,K.P., Diaz,A., and Jimenez,S.A. (1994). Epidermal growth factor coordinately regulates the expression of prostaglandin G/H synthase and cytosolic phospholipase A2 genes in embryonic mouse cells. *J. Biol. Chem.* **269**, 21786-21792.
- Chin,L.S., Raynor,M.C., Wei,X., Chen,H.Q., and Li,L. (2001). Hrs interacts with sorting nexin 1 and regulates degradation of epidermal growth factor receptor. *J. Biol. Chem.* **276**, 7069-7078.
- Chirmule,N., Moscioni,A.D., Qian,Y., Qian,R., Chen,Y., and Wilson,J.M. (1999). Fas-Fas ligand interactions play a major role in effector functions of cytotoxic T lymphocytes after adenovirus vector-mediated gene transfer. *Hum. Gene Ther.* **10**, 259-269.
- Clarke,P., Meintzer,S.M., Gibson,S., Widmann,C., Garrington,T.P., Johnson,G.L., and Tyler,K.L. (2000). Reovirus-induced apoptosis is mediated by TRAIL. *J. Virol.* **74**, 8135-8139.
- Collawn,J.F., Stangel,M., Kuhn,L.A., Esekogwu,V., Jing,S.Q., Trowbridge,I.S., and Tainer,J.A. (1990). Transferrin receptor internalization sequence YXRF implicates a tight turn as the structural recognition motif for endocytosis. *Cell* **63**, 1061-1072.
- Confalonieri,S., Salcini,A.E., Puri,C., Tacchetti,C., and Di Fiore,P.P. (2000). Tyrosine phosphorylation of Eps15 is required for ligand-regulated, but not constitutive, endocytosis. *J. Cell Biol.* **150**, 905-912.
- Cox,J.D., Bennink,JR., and Yewdell,J.W. (1991). Retention of adenovirus E19 glycoprotein in the endoplasmic reticulum is essential to its ability to block antigen presentation. *J. Exp. Med.* **174**, 1629-1637.
- Craig,N.L. (1996). Transposon Tn7. *Curr. Top. Microbiol. Immunol.* **204**, 27-48.

References

- Cress,W.D. and Nevins,J.R. (1996). Use of the E2F transcription factor by DNA tumor virus regulatory proteins. *Curr. Top. Microbiol. Immunol.* **208**, 63-78.
- Crooks,D., Kil,S.J., McCaffery,J.M., and Carlin,C. (2000). E3-13.7 integral membrane proteins encoded by human adenoviruses alter epidermal growth factor receptor trafficking by interacting directly with receptors in early endosomes. *Mol. Biol. Cell* **11**, 3559-3572.
- Crump,C.M., Xiang,Y., Thomas,L., Gu,F., Austin,C., Tooze,S.A., and Thomas,G. (2001). PACS-1 binding to adaptors is required for acidic cluster motif- mediated protein traffic. *EMBO J.* **20**, 2191-2201.
- Cuconati,A., Degenhardt,K., Sundararajan,R., Ansel,A., and White,E. (2002). Bak and Bax function to limit adenovirus replication through apoptosis induction. *J. Virol.* **76**, 4547-4558.
- Dai,Y., Schwarz,E.M., Gu,D., Zhang,W.W., Sarvetnick,N., and Verma,I.M. (1995). Cellular and humoral immune responses to adenoviral vectors containing factor IX gene: tolerization of factor IX and vector antigens allows for long-term expression. *Proc. Natl. Acad. Sci. U. S. A* **92**, 1401-1405.
- Davison,A.J., Telford,E.A., Watson,M.S., McBride,K., and Mautner,V. (1993). The DNA sequence of adenovirus type 40. *J. Mol. Biol.* **234**, 1308-1316.
- de Melker,A.A., van der,H.G., Calafat,J., Jansen,H., and Borst,J. (2001). c-Cbl ubiquitinates the EGF receptor at the plasma membrane and remains receptor associated throughout the endocytic route. *J. Cell Sci.* **114**, 2167-2178.
- Dell'Angelica,E.C. (2001). Clathrin-binding proteins: got a motif? Join the network! *Trends Cell Biol.* **11**, 315-318.
- Dell'Angelica,E.C., Shotelersuk,V., Aguilar,R.C., Gahl,W.A., and Bonifacino,J.S. (1999). Altered trafficking of lysosomal proteins in Hermansky-Pudlak syndrome due to mutations in the beta 3A subunit of the AP-3 adaptor. *Mol. Cell* **3**, 11-21.
- Deryckere,F., Ebenau-Jehle,C., Wold,W.S., and Burgert,H.G. (1995). Tumor necrosis factor alpha increases expression of adenovirus E3 proteins. *Immunobiology* **193**, 186-192.
- Desagher,S. and Martinou,J.C. (2000). Mitochondria as the central control point of apoptosis. *Trends Cell Biol.* **10**, 369-377.
- Diaz,E. and Pfeffer,S.R. (1998). TIP47: a cargo selection device for mannose 6-phosphate receptor trafficking. *Cell* **93**, 433-443.
- Dietrich,J., Hou,X., Wegener,A.M., and Geisler,C. (1994). CD3 gamma contains a phosphoserine-dependent di-leucine motif involved in down-regulation of the T cell receptor. *EMBO J.* **13**, 2156-2166.
- Dietrich,O., Gallert,F., and Hasilik, A. (1996). Purification of lysosomal membrane proteins from human placenta. *Eur. J. Cell Biol.* **69**, 99-106.
- Dimitrov,T., Krajcsi,P., Hermiston,T.W., Tollefson,A.E., Hannink,M., and Wold,W.S. (1997). Adenovirus E3-10.4K/14.5K protein complex inhibits tumor necrosis factor-induced translocation of cytosolic phospholipase A2 to membranes. *J. Virol.* **71**, 2830-2837.
- Doray,B., Ghosh,P., Griffith,J., Geuze,H.J., and Kornfeld,S. (2002). Cooperation of GGAs and AP-1 in packaging MPRs at the trans-Golgi network. *Science* **297**, 1700-1703.
- Duerksen-Hughes,P., Wold,W.S., and Gooding,L.R. (1989). Adenovirus E1A renders infected cells sensitive to cytolysis by tumor necrosis factor. *J. Immunol.* **143**, 4193-4200.
- Ehrlich,M., Shmueli,A., and Henis,Y.I. (2001). A single internalization signal from the di-leucine family is critical for constitutive endocytosis of the type II TGF-beta receptor. *J. Cell Sci.* **114**, 1777-1786.
- Elkon,K.B., Liu,C.C., Gall,J.G., Trevejo,J., Marino,M.W., Abrahamsen,K.A., Song,X., Zhou,J.L., Old,L.J., Crystal,R.G., and Falck-Pedersen,E. (1997). Tumor necrosis factor alpha plays a central role in immune-mediated clearance of adenoviral vectors. *Proc. Natl. Acad. Sci. U. S. A* **94**, 9814-9819.
- Ellgaard,L., Molinari,M., and Helenius,A. (1999). Setting the standards: quality control in the secretory pathway. *Science* **286**, 1882-1888.

- Elsing, A. and Burgert, H.G. (1998). The adenovirus E3/10.4K-14.5K proteins down-modulate the apoptosis receptor Fas/Apo-1 by inducing its internalization. *Proc. Natl. Acad. Sci. U. S. A* **95**, 10072-10077.
- Fabbri, M., Fumagalli, L., Bossi, G., Bianchi, E., Bender, J.R., and Pardi, R. (1999). A tyrosine-based sorting signal in the beta2 integrin cytoplasmic domain mediates its recycling to the plasma membrane and is required for ligand-supported migration. *EMBO J.* **18**, 4915-4925.
- Fanger, N.A., Maliszewski, C.R., Schooley, K., and Griffith, T.S. (1999). Human dendritic cells mediate cellular apoptosis via tumor necrosis factor-related apoptosis-inducing ligand (TRAIL). *J. Exp. Med.* **190**, 1155-1164.
- Felder, S., Miller, K., Moehren, G., Ullrich, A., Schlessinger, J., and Hopkins, C.R. (1990). Kinase activity controls the sorting of the epidermal growth factor receptor within the multivesicular body. *Cell* **61**, 623-634.
- Fessler, S.P. and Young, C.S. (1998). Control of adenovirus early gene expression during the late phase of infection. *J. Virol.* **72**, 4049-4056.
- Folsch, H., Ohno, H., Bonifacino, J.S., and Mellman, I. (1999). A novel clathrin adaptor complex mediates basolateral targeting in polarized epithelial cells. *Cell* **99**, 189-198.
- Futter, C.E., Collinson, L.M., Backer, J.M., and Hopkins, C.R. (2001). Human VPS34 is required for internal vesicle formation within multivesicular endosomes. *J. Cell Biol.* **155**, 1251-1264.
- Futter, C.E., Gibson, A., Allchin, E.H., Maxwell, S., Ruddock, L.J., Odorizzi, G., Domingo, D., Trowbridge, I.S., and Hopkins, C.R. (1998). In polarized MDCK cells basolateral vesicles arise from clathrin-gamma- adaptin-coated domains on endosomal tubules
7. *J. Cell Biol.* **141**, 611-623.
- Gallimore, P.H. and Turnell, A.S. (2001). Adenovirus E1A: remodelling the host cell, a life or death experience. *Oncogene* **20**, 7824-7835.
- Gamas, P. and Craig, N.L. (1992). Purification and characterization of TnsC, a Tn7 transposition protein that binds ATP and DNA. *Nucleic Acids Res.* **20**, 2525-2532.
- Geisler, C., Dietrich, J., Nielsen, B.L., Kastrup, J., Lauritsen, J.P., Odum, N., and Christensen, M.D. (1998). Leucine-based receptor sorting motifs are dependent on the spacing relative to the plasma membrane. *J. Biol. Chem.* **273**, 21316-21323.
- Gil, J., Alcamí, J., and Esteban, M. (1999). Induction of apoptosis by double-stranded-RNA-dependent protein kinase (PKR) involves the alpha subunit of eukaryotic translation initiation factor 2 and NF-kappaB. *Mol. Cell Biol.* **19**, 4653-4663.
- Gill, G.N. (2002). A pit stop at the ER. *Science* **295**, 1654-1655.
- Ginsberg, H.S., Lundholm-Beauchamp, U., Horswood, R.L., Pernis, B., Wold, W.S., Chanock, R.M., and Prince, G.A. (1989). Role of early region 3 (E3) in pathogenesis of adenovirus disease. *Proc. Natl. Acad. Sci. U. S. A* **86**, 3823-3827.
- Gonzalez, R.A. and Flint, S.J. (2002). Effects of mutations in the adenoviral E1B 55-kilodalton protein coding sequence on viral late mRNA metabolism. *J. Virol.* **76**, 4507-4519.
- Goodbourn, S., Didcock, L., and Randall, R.E. (2000). Interferons: cell signaling, immune modulation, antiviral response and virus countermeasures. *J. Gen. Virol.* **81**, 2341-2364.
- Gooding, L.R., Aquino, L., Duerksen-Hughes, P.J., Day, D., Horton, T.M., Yei, S.P., and Wold, W.S. (1991a). The E1B 19,000-molecular-weight protein of group C adenoviruses prevents tumor necrosis factor cytolysis of human cells but not of mouse cells. *J. Virol.* **65**, 3083-3094.
- Gooding, L.R., Elmore, L.W., Tollefson, A.E., Brady, H.A., and Wold, W.S. (1988). A 14,700 MW protein from the E3 region of adenovirus inhibits cytolysis by tumor necrosis factor. *Cell* **53**, 341-346.

References

- Gooding,L.R., Ranheim,T.S., Tollefson,A.E., Aquino,L., Duerksen-Hughes,P., Horton,T.M., and Wold,W.S. (1991b). The 10,400- and 14,500-dalton proteins encoded by region E3 of adenovirus function together to protect many but not all mouse cell lines against lysis by tumor necrosis factor. *J. Virol.* **65**, 4114-4123.
- Gooding,L.R., Sofola,I.O., Tollefson,A.E., Duerksen-Hughes,P., and Wold,W.S. (1990). The adenovirus E3-14.7K protein is a general inhibitor of tumor necrosis factor-mediated cytolysis. *J. Immunol.* **145**, 3080-3086.
- Graham,F.L., Smiley,J., Russell,W.C., and Nairn,R. (1977). Characteristics of a human cell line transformed by DNA from human adenovirus type 5. *J. Gen. Virol.* **36**, 59-74.
- Greenberg,M., DeTulleo,L., Rapoport,I., Skowronski,J., and Kirchhausen,T. (1998). A dileucine motif in HIV-1 Nef is essential for sorting into clathrin-coated pits and for downregulation of CD4. *Curr. Biol.* **8**, 1239-1242.
- Griffith,T.S., Wiley,S.R., Kubin,M.Z., Sedger,L.M., Maliszewski,C.R., and Fanger,N.A. (1999). Monocyte-mediated tumoricidal activity via the tumor necrosis factor-related cytokine, TRAIL. *J. Exp. Med.* **189**, 1343-1354.
- Gruber,W.C., Russell,D.J., and Tibbetts,C. (1993). Fiber gene and genomic origin of human adenovirus type 4. *Virology* **196**, 603-611.
- Hale,T.K. and Braithwaite,A.W. (1999). The adenovirus oncoprotein E1a stimulates binding of transcription factor ETF to transcriptionally activate the p53 gene. *J. Biol. Chem.* **274**, 23777-23786.
- Harty,J.T., Tvinnereim,A.R., and White,D.W. (2000). CD8+ T cell effector mechanisms in resistance to infection. *Annu. Rev. Immunol.* **18**, 275-308.
- Hauri,H.P., Kappeler,F., Andersson,H., and Appenzeller,C. (2000). ERGIC-53 and traffic in the secretory pathway. *J. Cell Sci.* **113 (Pt 4)**, 587-596.
- Hayashi,S. (2002). Latent adenovirus infection in COPD. *Chest* **121**, 183S-187S.
- Haynes,A.P., Daniels,I., Abhulayha,A.M., Carter,G.I., Metheringham,R., Gregory,C.D., and Thomson,B.J. (2002). CD95 (Fas) expression is regulated by sequestration in the Golgi complex in B-cell lymphoma. *Br. J. Haematol.* **118**, 488-494.
- Helgans,T. and Mannel,D.N. (2002). The TNF-TNF receptor system. *Biol. Chem.* **383**, 1581-1585.
- Heilker,R., Spiess,M., and Crottet,P. (1999). Recognition of sorting signals by clathrin adaptors. *Bioessays* **21**, 558-567.
- Herbst,J.J., Opresko,L.K., Walsh,B.J., Lauffenburger,D.A., and Wiley,H.S. (1994). Regulation of postendocytic trafficking of the epidermal growth factor receptor through endosomal retention. *J. Biol. Chem.* **269**, 12865-12873.
- Herrisse,J., Courtois,G., and Galibert,F. (1980). Nucleotide sequence of the EcoRI D fragment of adenovirus 2 genome. *Nucleic Acids Res.* **8**, 2173-2192.
- Herrisse,J. and Galibert,F. (1981). Nucleotide sequence of the EcoRI E fragment of adenovirus 2 genome. *Nucleic Acids Res.* **9**, 1229-1240.
- Hewitt,E.W., Duncan,L., Mufti,D., Baker,J., Stevenson,P.G., and Lehner,P.J. (2002). Ubiquitylation of MHC class I by the K3 viral protein signals internalization and TSG101-dependent degradation. *EMBO J.* **21**, 2418-2429.
- Hicke,L. (2001). A new ticket for entry into budding vesicles-ubiquitin. *Cell* **106**, 527-530.
- Higuchi,R., Krummel,B., and Saiki,R.K. (1988). A general method of in vitro preparation and specific mutagenesis of DNA fragments: study of protein and DNA interactions. *Nucleic Acids Res.* **16**, 7351-7367.
- Hirst,J., Lindsay,M.R., and Robinson,M.S. (2001). GGAs: roles of the different domains and comparison with AP-1 and clathrin. *Mol. Biol. Cell* **12**, 3573-3588.

- Hoffman,B.L., Ullrich,A., Wold,W.S., and Carlin,C.R. (1990). Retrovirus-mediated transfer of an adenovirus gene encoding an integral membrane protein is sufficient to down regulate the receptor for epidermal growth factor. *Mol. Cell Biol.* **10**, 5521-5524.
- Hoffman,P. and Carlin,C. (1994). Adenovirus E3 protein causes constitutively internalized epidermal growth factor receptors to accumulate in a prelysosomal compartment, resulting in enhanced degradation. *Mol. Cell Biol.* **14**, 3695-3706.
- Hoffman,P., Rajakumar,P., Hoffman,B., Heuertz,R., Wold,W.S., and Carlin,C.R. (1992a). Evidence for intracellular down-regulation of the epidermal growth factor (EGF) receptor during adenovirus infection by an EGF-independent mechanism. *J. Virol.* **66**, 197-203.
- Hoffman,P., Yaffe,M.B., Hoffman,B.L., Yei,S., Wold,W.S., and Carlin,C. (1992b). Characterization of the adenovirus E3 protein that down-regulates the epidermal growth factor receptor. Evidence for intermolecular disulfide bonding and plasma membrane localization. *J. Biol. Chem.* **267**, 13480-13487.
- Hofmann,M.W., Honing,S., Rodionov,D., Dobberstein,B., von Figura,K., and Bakke,O. (1999). The leucine-based sorting motifs in the cytoplasmic domain of the invariant chain are recognized by the clathrin adaptors AP1 and AP2 and their medium chains. *J. Biol. Chem.* **274**, 36153-36158.
- Hong,S.S., Karayan,L., Tournier,J., Curiel,D.T., and Boulanger,P.A. (1997). Adenovirus type 5 fiber knob binds to MHC class I alpha2 domain at the surface of human epithelial and B lymphoblastoid cells 2. *EMBO J.* **16**, 2294-2306.
- Honing,S. and Hunziker,W. (1995). Cytoplasmic determinants involved in direct lysosomal sorting, endocytosis, and basolateral targeting of rat lgp120 (lamp-I) in MDCK cells. *J. Cell Biol.* **128**, 321-332.
- Honing,S., Sosa,M., Hille-Rehfeld,A., and von Figura K. (1997). The 46-kDa mannose 6-phosphate receptor contains multiple binding sites for clathrin adaptors. *J. Biol. Chem.* **272**, 19884-19890.
- Honing,S., Sandoval,I.V., and von Figura,K. (1998). A di-leucine-based motif in the cytoplasmic tail of LIMP-II and tyrosinase mediates selective binding of AP-3. *EMBO J.* **17**, 1304-1314.
- Horton,T.M., Ranheim,T.S., Aquino,L., Kusher,D.I., Saha,S.K., Ware,C.F., Wold,W.S., and Gooding,L.R. (1991). Adenovirus E3 14.7K protein functions in the absence of other adenovirus proteins to protect transfected cells from tumor necrosis factor cytolysis. *J. Virol.* **65**, 2629-2639.
- Horwitz,M.S. (2001a). Adenoviruses. In *Fields Virology*. Fields, B.N., Knipe, D.M., and Howley, P.M. eds. Lippincott Williams&Wilkins Publishers, Philadelphia, New York, 2301-2326.
- Horwitz,M.S. (2001b). Adenovirus immunoregulatory genes and their cellular targets. *Virology* **279**, 1-8.
- Huang,X.L., Pawliczak,R., Cowan,M.J., Gladwin,M.T., Madara,P., Logun,C., and Shelhamer,J.H. (2002). Epidermal growth factor induces p11 gene and protein expression and down-regulates calcium ionophore-induced arachidonic acid release in human epithelial cells. *J. Biol. Chem.* **277**, 38431-38440.
- Ilan,Y., Droguett,G., Chowdhury,N.R., Li,Y., Sengupta,K., Thummala,N.R., Davidson,A., Chowdhury,J.R., and Horwitz,M.S. (1997). Insertion of the adenoviral E3 region into a recombinant viral vector prevents antiviral humoral and cellular immune responses and permits long-term gene expression. *Proc. Natl. Acad. Sci. U. S. A* **94**, 2587-2592.
- Imperiale,M.J., Akusjarvi,G., and Leppard,K.N. (1995). Post-transcriptional control of adenovirus gene expression. *Curr. Top. Microbiol. Immunol.* **199 (Pt 2)**, 139-171.
- Jarousse,N. and Kelly,R.B. (2000). Selective inhibition of adaptor complex-mediated vesiculation. *Traffic.* **1**, 378-384.
- Jiang,X., Huang,F., Marusyk,A., and Sorkin,A. (2003). Grb2 Regulates Internalization of EGF Receptors through Clathrin-coated Pits. *Mol. Biol. Cell* **14**, 858-870.
- Jones,N. (1995). Transcriptional modulation by the adenovirus E1A gene. *Curr. Top. Microbiol. Immunol.* **199 (Pt 3)**, 59-80.

References

- Jones,S.J., Ledgerwood,E.C., Prins,J.B., Galbraith,J., Johnson,D.R., Pober,J.S., and Bradley,J.R. (1999). TNF recruits TRADD to the plasma membrane but not the trans-Golgi network, the principal subcellular location of TNF-R1. *J. Immunol.* **162**, 1042-1048.
- Juang,Y.T., Lowther,W., Kellum,M., Au,W.C., Lin,R., Hiscott,J., and Pitha,P.M. (1998). Primary activation of interferon A and interferon B gene transcription by interferon regulatory factor 3. *Proc. Natl. Acad. Sci. U. S. A* **95**, 9837-9842.
- Kafri,T., Morgan,D., Krahl,T., Sarvetnick,N., Sherman,L., and Verma,I. (1998). Cellular immune response to adenoviral vector infected cells does not require de novo viral gene expression: implications for gene therapy. *Proc. Natl. Acad. Sci. U. S. A* **95**, 11377-11382.
- Kaplan,J.M., Armentano,D., Sparer,T.E., Wynn,S.G., Peterson,P.A., Wadsworth,S.C., Couture,K.K., Pennington,S.E., St George,J.A., Gooding,L.R., and Smith,A.E. (1997). Characterization of factors involved in modulating persistence of transgene expression from recombinant adenovirus in the mouse lung. *Hum. Gene Ther.* **8**, 45-56.
- Karin,M. and Lin,A. (2002). NF-kappaB at the crossroads of life and death. *Nat. Immunol.* **3**, 221-227.
- Kashii,Y., Giorda,R., Herberman,R.B., Whiteside,T.L., and Vujanovic,N.L. (1999). Constitutive expression and role of the TNF family ligands in apoptotic killing of tumor cells by human NK cells. *J. Immunol.* **163**, 5358-5366.
- Kassenbrock,C.K., Hunter,S., Garl,P., Johnson,G.L., and Anderson,S.M. (2002). Inhibition of Src family kinases blocks epidermal growth factor (EGF)- induced activation of Akt, phosphorylation of c-Cbl, and ubiquitination of the EGF receptor. *J. Biol. Chem.* **277**, 24967-24975.
- Katzmann,D.J., Babst,M., and Emr,S.D. (2001). Ubiquitin-dependent sorting into the multivesicular body pathway requires the function of a conserved endosomal protein sorting complex, ESCRT-I. *Cell* **106**, 145-155.
- Kawano,J., Ide,S., Oinuma,T., and Suganuma, T. (1994). A protein-specific monoclonal antibody to rat liver beta 1-4galactosyltransferase and its application to immunohistochemistry. *J. Histochem. Cytochem.* **42**, 363-369.
- Kay,M.A., Glorioso,J.C., and Naldini,L. (2001). Viral vectors for gene therapy: the art of turning infectious agents into vehicles of therapeutics. *Nat. Med.* **7**, 33-40.
- Kayagaki,N., Yamaguchi,N., Nakayama,M., Eto,H., Okumura,K., and Yagita,H. (1999a). Type I interferons (IFNs) regulate tumor necrosis factor-related apoptosis-inducing ligand (TRAIL) expression on human T cells: A novel mechanism for the antitumor effects of type I IFNs. *J. Exp. Med.* **189**, 1451-1460.
- Kayagaki,N., Yamaguchi,N., Nakayama,M., Kawasaki,A., Akiba,H., Okumura,K., and Yagita,H. (1999b). Involvement of TNF-related apoptosis-inducing ligand in human CD4+ T cell-mediated cytotoxicity. *J. Immunol.* **162**, 2639-2647.
- Kayagaki,N., Yamaguchi,N., Nakayama,M., Takeda,K., Akiba,H., Tsutsui,H., Okamura,H., Nakanishi,K., Okumura,K., and Yagita,H. (1999c). Expression and function of TNF-related apoptosis-inducing ligand on murine activated NK cells. *J. Immunol.* **163**, 1906-1913.
- Keller,P., Toomre,D., Diaz,E., White,J., and Simons,K. (2001). Multicolour imaging of post-Golgi sorting and trafficking in live cells. *Nat. Cell Biol.* **3**, 140-149.
- Kil,S.J. and Carlin,C. (2000). EGF receptor residues leu(679), leu(680) mediate selective sorting of ligand-receptor complexes in early endosomal compartments. *J. Cell Physiol* **185**, 47-60.
- Kil,S.J., Hobert,M., and Carlin,C. (1999). A leucine-based determinant in the epidermal growth factor receptor juxtamembrane domain is required for the efficient transport of ligand- receptor complexes to lysosomes. *J. Biol. Chem.* **274**, 3141-3150.
- Kim,S.Y., Lee,J.H., Shin,H.S., Kang,H.J., and Kim,Y.S. (2002). The human elongation factor 1 alpha (EF-1 alpha) first intron highly enhances expression of foreign genes from the murine cytomegalovirus promoter. *J. Biotechnol.* **93**, 183-187.

- Kirchhausen,T. (1999). Adaptors for clathrin-mediated traffic. *Annu. Rev. Cell Dev. Biol.* **15**, 705-732.
- Kirchhausen,T. (2000a). Clathrin. *Annu. Rev. Biochem.* **69**, 699-727.
- Kirchhausen,T. (2000b). Three ways to make a vesicle. *Nat. Rev. Mol. Cell Biol.* **1**, 187-198.
- Kirchhausen,T. (2002). Single-handed recognition of a sorting traffic motif by the GGA proteins. *Nat. Struct. Biol.* **9**, 241-244.
- Kobayashi,T., Stang,E., Fang,K.S., de Moerloose,P., Parton,R.G., and Gruenberg,J. (1998). A lipid associated with the antiphospholipid syndrome regulates endosome structure and function. *Nature* **392**, 193-197.
- Kongsvik,T.L., Honing,S., Bakke,O., and Rodionov,D.G. (2002). Mechanism of interaction between leucine-based sorting signals from the invariant chain and clathrin-associated adaptor protein complexes AP1 and AP2. *J. Biol. Chem.* **277**, 16484-16488.
- Konig,C., Roth,J., and Dobbelstein,M. (1999). Adenovirus type 5 E4orf3 protein relieves p53 inhibition by E1B-55- kilodalton protein. *J. Virol.* **73**, 2253-2262.
- Korner,H., Fritzsche,U., and Burgert,H.G. (1992). Tumor necrosis factor alpha stimulates expression of adenovirus early region 3 proteins: implications for viral persistence. *Proc. Natl. Acad. Sci. U. S. A* **89**, 11857-11861.
- Kornilova,E., Sorkina,T., Beguinot,L., and Sorkin,A. (1996). Lysosomal targeting of epidermal growth factor receptors via a kinase- dependent pathway is mediated by the receptor carboxyl-terminal residues 1022-1123. *J. Biol. Chem.* **271**, 30340-30346.
- Kozak,M. (1987). At least six nucleotides preceding the AUG initiator codon enhance translation in mammalian cells. *J. Mol. Biol.* **196**, 947-950.
- Kozak,M. (1999). Initiation of translation in prokaryotes and eukaryotes. *Gene* **234**, 187-208.
- Kozak,M. (2001). Constraints on reinitiation of translation in mammals. *Nucleic Acids Res.* **29**, 5226-5232.
- Krajcsi,P., Dimitrov,T., Hermiston,T.W., Tollefson,A.E., Ranheim,T.S., Vande Pol,S.B., Stephenson,A.H., and Wold,W.S. (1996). The adenovirus E3-14.7K protein and the E3-10.4K/14.5K complex of proteins, which independently inhibit tumor necrosis factor (TNF)- induced apoptosis, also independently inhibit TNF-induced release of arachidonic acid. *J. Virol.* **70**, 4904-4913.
- Krajcsi,P., Tollefson,A.E., Anderson,C.W., Stewart,A.R., Carlin,C.R., and Wold,W.S. (1992a). The E3-10.4K protein of adenovirus is an integral membrane protein that is partially cleaved between Ala22 and Ala23 and has a Cyt orientation. *Virology* **187**, 131-144.
- Krajcsi,P., Tollefson,A.E., Anderson,C.W., and Wold,W.S. (1992b). The adenovirus E3 14.5-kilodalton protein, which is required for down- regulation of the epidermal growth factor receptor and prevention of tumor necrosis factor cytolysis, is an integral membrane protein oriented with its C terminus in the cytoplasm. *J. Virol.* **66**, 1665-1673.
- Krajcsi,P., Tollefson,A.E., and Wold,W.S. (1992c). The E3-14.5K integral membrane protein of adenovirus that is required for down-regulation of the EGF receptor and for prevention of TNF cytolysis is O-glycosylated but not N-glycosylated. *Virology* **188**, 570-579.
- Krajcsi,P. and Wold,W.S. (1992). The adenovirus E3-14.5K protein which is required for prevention of TNF cytolysis and for down-regulation of the EGF receptor contains phosphoserine. *Virology* **187**, 492-498.
- Krajcsi,P. and Wold,W.S. (1998). Viral proteins that regulate cellular signaling. *J. Gen. Virol.* **79 (Pt 6)**, 1323-1335.
- Kuhnel,F., Zender,L., Paul,Y., Tietze,M.K., Trautwein,C., Manns,M., and Kubicka,S. (2000). NFkappaB mediates apoptosis through transcriptional activation of Fas (CD95) in adenoviral hepatitis. *J. Biol. Chem.* **275**, 6421-6427.
- Kuivinen,E., Hoffman,B.L., Hoffman,P.A., and Carlin,C.R. (1993). Structurally related class I and class II receptor protein tyrosine kinases are down-regulated by the same E3 protein coded for by human group C adenoviruses. *J. Cell Biol.* **120**, 1271-1279.

References

- Kurten,R.C., Cadena,D.L., and Gill,G.N. (1996). Enhanced degradation of EGF receptors by a sorting nexin, SNX1. *Science* **272**, 1008-1010.
- Laemmli,U.K. (1970). Cleavage of structural proteins during the assembly of the head of bacteriophage T4. *Nature* **227**, 680-685.
- Lavoie,J.N., Nguyen,M., Marcellus,R.C., Branton,P.E., and Shore,G.C. (1998). E4orf4, a novel adenovirus death factor that induces p53-independent apoptosis by a pathway that is not inhibited by zVAD-fmk. *J. Cell Biol.* **140**, 637-645.
- Le Borgne,R., Alconada,A., Bauer,U., and Hoflack,B. (1998). The mammalian AP-3 adaptor-like complex mediates the intracellular transport of lysosomal membrane glycoproteins. *J. Biol. Chem.* **273**, 29451-29461.
- Leppard,K.N. (1997). E4 gene function in adenovirus, adenovirus vector and adeno-associated virus infections. *J. Gen. Virol.* **78 (Pt 9)**, 2131-2138.
- Leslie,C.C. (1997). Properties and regulation of cytosolic phospholipase A2. *J. Biol. Chem.* **272**, 16709-16712.
- Letourneur,F. and Cosson,P. (1998). Targeting to the endoplasmic reticulum in yeast cells by determinants present in transmembrane domains. *J. Biol. Chem.* **273**, 33273-33278.
- Levkowitz,G., Waterman,H., Ettenberg,S.A., Katz,M., Tsygankov,A.Y., Alroy,I., Lavi,S., Iwai,K., Reiss,Y., Ciechanover,A., Lipkowitz,S., and Yarden,Y. (1999). Ubiquitin ligase activity and tyrosine phosphorylation underlie suppression of growth factor signaling by c-Cbl/Sli-1. *Mol. Cell* **4**, 1029-1040.
- Levkowitz,G., Waterman,H., Zamir,E., Kam,Z., Oved,S., Langdon,W.Y., Beguinot,L., Geiger,B., and Yarden,Y. (1998). c-Cbl/Sli-1 regulates endocytic sorting and ubiquitination of the epidermal growth factor receptor. *Genes Dev.* **12**, 3663-3674.
- Li,Y., Kang,J., Friedman,J., Tarassishin,L., Ye,J., Kovalenko,A., Wallach,D., and Horwitz,M.S. (1999). Identification of a cell protein (FIP-3) as a modulator of NF-kappaB activity and as a target of an adenovirus inhibitor of tumor necrosis factor alpha-induced apoptosis. *Proc. Natl. Acad. Sci. U. S. A* **96**, 1042-1047.
- Li,Y., Kang,J., and Horwitz,M.S. (1997). Interaction of an adenovirus 14.7-kilodalton protein inhibitor of tumor necrosis factor alpha cytolysis with a new member of the GTPase superfamily of signal transducers. *J. Virol.* **71**, 1576-1582.
- Li,Y., Kang,J., and Horwitz,M.S. (1998a). Interaction of an adenovirus E3 14.7-kilodalton protein with a novel tumor necrosis factor alpha-inducible cellular protein containing leucine zipper domains. *Mol. Cell Biol.* **18**, 1601-1610.
- Li,Z., Karakousis,G., Chiu,S.K., Reddy,G., and Radding,C.M. (1998b). The beta protein of phage lambda promotes strand exchange. *J. Mol. Biol.* **276**, 733-744.
- Lichtenstein,D.L., Krajcsi,P., Esteban,D.J., Tollefson,A.E., and Wold,W.S. (2002). Adenovirus RIDbeta subunit contains a tyrosine residue that is critical for RID-mediated receptor internalization and inhibition of Fas- and TRAIL-induced apoptosis. *J. Virol.* **76**, 11329-11342.
- Lill,N.L., Douillard,P., Awwad,R.A., Ota,S., Lupher,M.L., Jr., Miyake,S., Meissner-Lula,N., Hsu,V.W., and Band,H. (2000). The evolutionarily conserved N-terminal region of Cbl is sufficient to enhance down-regulation of the epidermal growth factor receptor. *J. Biol. Chem.* **275**, 367-377.
- Lloyd,T.E., Atkinson,R., Wu,M.N., Zhou,Y., Pennetta,G., and Bellen,H.J. (2002). Hrs regulates endosome membrane invagination and tyrosine kinase receptor signaling in *Drosophila*. *Cell* **108**, 261-269.
- Locksley,R.M., Killeen,N., and Lenardo,M.J. (2001). The TNF and TNF receptor superfamilies: integrating mammalian biology. *Cell* **104**, 487-501.
- Lomonosova,E., Subramanian,T., and Chinnadurai,G. (2002). Requirement of BAX for efficient adenovirus-induced apoptosis. *J. Virol.* **76**, 11283-11290.

- Longva,K.E., Blystad,F.D., Stang,E., Larsen,A.M., Johannessen,L.E., and Madshus,I.H. (2002). Ubiquitination and proteasomal activity is required for transport of the EGF receptor to inner membranes of multivesicular bodies. *J. Cell Biol.* **156**, 843-854.
- Lorenzo,M.E., Jung,J.U., and Ploegh,H.L. (2002). Kaposi's sarcoma-associated herpesvirus K3 utilizes the ubiquitin- proteasome system in routing class major histocompatibility complexes to late endocytic compartments. *J. Virol.* **76**, 5522-5531.
- Lukashok,S.A. and Horwitz,M.S. (1998). New perspectives in adenoviruses. *Curr. Clin. Top. Infect. Dis.* **18**, 286-305.
- Lukashok,S.A., Tarassishin,L., Li,Y., and Horwitz,M.S. (2000). An adenovirus inhibitor of tumor necrosis factor alpha-induced apoptosis complexes with dynein and a small GTPase. *J. Virol.* **74**, 4705-4709.
- Lutz,P. and Kedinger,C. (1996). Properties of the adenovirus IVa2 gene product, an effector of late- phase-dependent activation of the major late promoter. *J. Virol.* **70**, 1396-1405.
- Mahr,J.A. and Gooding,L.R. (1999). Immune evasion by adenoviruses. *Immunol. Rev.* **168**, 121-130.
- Marks,M.S., Woodruff,L., Ohno,H., and Bonifacino,J.S. (1996). Protein targeting by tyrosine- and di-leucine-based signals: evidence for distinct saturable components. *J. Cell Biol.* **135**, 341-354.
- Marsh,M. and McMahon,H.T. (1999). The structural era of endocytosis. *Science* **285**, 215-220.
- Martin,M.E. and Berk,A.J. (1998). Adenovirus E1B 55K represses p53 activation in vitro. *J. Virol.* **72**, 3146-3154.
- Mayer,B.J. (2001). SH3 domains: complexity in moderation. *J. Cell Sci.* **114**, 1253-1263.
- McNees,A.L., Garnett,C.T., and Gooding,L.R. (2002). The adenovirus E3 RID complex protects some cultured human T and B lymphocytes from Fas-induced apoptosis. *J. Virol.* **76**, 9716-9723.
- Mellman,I. and Warren,G. (2000). The road taken: past and future foundations of membrane traffic. *Cell* **100**, 99-112.
- Meyer,C., Eskelinen,E.L., Guruprasad,M.R., von Figura,K., and Schu,P. (2001). Mu 1A deficiency induces a profound increase in MPR300/IGF-II receptor internalization rate. *J. Cell Sci.* **114**, 4469-4476.
- Meyer,C., Zizioli,D., Lausmann,S., Eskelinen,E.L., Hamann,J., Saftig,P., von Figura,K., and Schu,P. (2000). mu1A-adaptin-deficient mice: lethality, loss of AP-1 binding and rerouting of mannose 6-phosphate receptors. *EMBO J.* **19**, 2193-2203.
- Mineo,C., Gill,G.N., and Anderson,R.G. (1999). Regulated migration of epidermal growth factor receptor from caveolae. *J. Biol. Chem.* **274**, 30636-30643.
- Mittereder,N., March,K.L., and Trapnell,B.C. (1996). Evaluation of the concentration and bioactivity of adenovirus vectors for gene therapy. *J. Virol.* **70**, 7498-7509.
- Moise,A.R., Grant,J.R., Vitalis,T.Z., and Jefferies,W.A. (2002). Adenovirus E3-6.7K maintains calcium homeostasis and prevents apoptosis and arachidonic acid release. *J. Virol.* **76**, 1578-1587.
- Molnar-Kimber,K.L., Serman,D.H., Chang,M., Kang,E.H., ElBash,M., Lanuti,M., Elshami,A., Gelfand,K., Wilson,J.M., Kaiser,L.R., and Albelda,S.M. (1998). Impact of preexisting and induced humoral and cellular immune responses in an adenovirus-based gene therapy phase I clinical trial for localized mesothelioma. *Hum. Gene Ther.* **9**, 2121-2133.
- Munro,S. (1998). Localization of proteins to the Golgi apparatus. *Trends Cell Biol.* **8**, 11-15.
- Murphy,K.C. (1991). Lambda Gam protein inhibits the helicase and chi-stimulated recombination activities of Escherichia coli RecBCD enzyme. *J. Bacteriol.* **173**, 5808-5821.
- Muruve,D.A., Barnes,M.J., Stillman,I.E., and Libermann,T.A. (1999). Adenoviral gene therapy leads to rapid induction of multiple chemokines and acute neutrophil-dependent hepatic injury in vivo. *Hum. Gene Ther.* **10**, 965-976.

References

- Musgrave,B.L., Phu,T., Butler,J.J., Makrigiannis,A.P., and Hoskin,D.W. (1999). Murine TRAIL (TNF-related apoptosis inducing ligand) expression induced by T cell activation is blocked by rapamycin, cyclosporin A, and inhibitors of phosphatidylinositol 3-kinase, protein kinase C, and protein tyrosine kinases: evidence for TRAIL induction via the T cell receptor signaling pathway. *Exp. Cell Res.* **252**, 96-103.
- Muyrers,J.P., Zhang,Y., Testa,G., and Stewart,A.F. (1999). Rapid modification of bacterial artificial chromosomes by ET⁻ recombination. *Nucleic Acids Res.* **27**, 1555-1557.
- Nagata,S. (1999). Fas ligand-induced apoptosis. *Annu. Rev. Genet.* **33**, 29-55.
- Nemerow,G.R. (2000). Cell receptors involved in adenovirus entry. *Virology* **274**, 1-4.
- Nemerow,G.R. and Stewart,P.L. (1999). Role of alpha(v) integrins in adenovirus cell entry and gene delivery. *Microbiol. Mol. Biol. Rev.* **63**, 725-734.
- Nesterov,A., Carter,R.E., Sorkina,T., Gill,G.N., and Sorkin,A. (1999). Inhibition of the receptor-binding function of clathrin adaptor protein AP-2 by dominant-negative mutant mu2 subunit and its effects on endocytosis. *EMBO J.* **18**, 2489-2499.
- Nesterov,A., Kurten,R.C., and Gill,G.N. (1995a). Association of epidermal growth factor receptors with coated pit adaptins via a tyrosine phosphorylation-regulated mechanism. *J. Biol. Chem.* **270**, 6320-6327.
- Nesterov,A., Wiley,H.S., and Gill,G.N. (1995b). Ligand-induced endocytosis of epidermal growth factor receptors that are defective in binding adaptor proteins. *Proc. Natl. Acad. Sci. U. S. A* **92**, 8719-8723.
- Nielsen,H., Engelbrecht,J., Brunak,S., and von Heijne,G. (1997). Identification of prokaryotic and eukaryotic signal peptides and prediction of their cleavage sites. *Protein Eng* **10**, 1-6.
- Nielsen,M.S., Madsen,P., Christensen,E.I., Nykjaer,A., Gliemann,J., Kasper,D., Pohlmann,R., and Petersen,C.M. (2001). The sortilin cytoplasmic tail conveys Golgi-endosome transport and binds the VHS domain of the GGA2 sorting protein. *EMBO J.* **20**, 2180-2190.
- O'Brien,V. (1998). Viruses and apoptosis. *J. Gen. Virol.* **79 (Pt 8)**, 1833-1845.
- O'Connor,R.J. and Hearing,P. (2000). The E4-6/7 protein functionally compensates for the loss of E1A expression in adenovirus infection. *J. Virol.* **74**, 5819-5824.
- O'Shea,J.J., Gadina,M., and Schreiber,R.D. (2002). Cytokine signaling in 2002: new surprises in the Jak/Stat pathway. *Cell* **109 Suppl**, S121-S131.
- Ohno,H., Aguilar,R.C., Yeh,D., Taura,D., Saito,T., and Bonifacino,J.S. (1998). The medium subunits of adaptor complexes recognize distinct but overlapping sets of tyrosine-based sorting signals. *J. Biol. Chem.* **273**, 25915-25921.
- Ohno,H., Fournier,M.C., Poy,G., and Bonifacino,J.S. (1996). Structural determinants of interaction of tyrosine-based sorting signals with the adaptor medium chains. *J. Biol. Chem.* **271**, 29009-29015.
- Ohno,H., Stewart,J., Fournier,M.C., Bosshart,H., Rhee,I., Miyatake,S., Saito,T., Gallusser,A., Kirchhausen,T., and Bonifacino,J.S. (1995). Interaction of tyrosine-based sorting signals with clathrin-associated proteins. *Science* **269**, 1872-1875.
- Oksvold,M.P., Skarpen,E., Wierod,L., Paulsen,R.E., and Huitfeldt,H.S. (2001). Re-localization of activated EGF receptor and its signal transducers to multivesicular compartments downstream of early endosomes in response to EGF. *Eur. J. Cell Biol.* **80**, 285-294.
- Ooi,C.E., Dell'Angelica,E.C., and Bonifacino,J.S. (1998). ADP-Ribosylation factor 1 (ARF1) regulates recruitment of the AP-3 adaptor complex to membranes. *J. Cell Biol.* **142**, 391-402.
- Opresko,L.K., Chang,C.P., Will,B.H., Burke,P.M., Gill,G.N., and Wiley,H.S. (1995). Endocytosis and lysosomal targeting of epidermal growth factor receptors are mediated by distinct sequences independent of the tyrosine kinase domain. *J. Biol. Chem.* **270**, 4325-4333.
- Owen,D.J. and Evans,P.R. (1998). A structural explanation for the recognition of tyrosine-based endocytotic signals. *Science* **282**, 1327-1332.

- Owen,D.J., Vallis,Y., Noble,M.E., Hunter,J.B., Dafforn,T.R., Evans,P.R., and McMahon,H.T. (1999). A structural explanation for the binding of multiple ligands by the alpha-adaptin appendage domain. *Cell* **97**, 805-815.
- Paabo,S., Bhat,B.M., Wold,W.S., and Peterson,P.A. (1987). A short sequence in the COOH-terminus makes an adenovirus membrane glycoprotein a resident of the endoplasmic reticulum. *Cell* **50**, 311-317.
- Padgett,R.A., Konarska,M.M., Grabowski,P.J., Hardy,S.F., and Sharp,P.A. (1984). Lariat RNA's as intermediates and products in the splicing of messenger RNA precursors. *Science* **225**, 898-903.
- Pahl,H.L. (1999). Activators and target genes of Rel/NF-kappaB transcription factors. *Oncogene* **18**, 6853-6866.
- Pelham,H.R. and Rothman,J.E. (2000). The debate about transport in the Golgi--two sides of the same coin? *Cell* **102**, 713-719.
- Perez,D. and White,E. (2003). E1A sensitizes cells to tumor necrosis factor alpha by downregulating c- FLIP. *S. J. Virol.* **77**, 2651-2662.
- Pfeffer,S.R. (1999). Transport-vesicle targeting: tethers before SNAREs. *Nat. Cell Biol.* **1**, E17-E22.
- Piguet,V., Wan,L., Borel,C., Mangasarian,A., Demaurex,N., Thomas,G., and Trono,D. (2000). HIV-1 Nef protein binds to the cellular protein PACS-1 to downregulate class I major histocompatibility complexes. *Nat. Cell Biol.* **2**, 163-167.
- Piper,R.C. and Luzio,J.P. (2001). Late endosomes: sorting and partitioning in multivesicular bodies. *Traffic.* **2**, 612-621.
- Pond,L., Kuhn,L.A., Teyton,L., Schutze,M.P., Tainer,J.A., Jackson,M.R., and Peterson,P.A. (1995). A role for acidic residues in di-leucine motif-based targeting to the endocytic pathway. *J. Biol. Chem.* **270**, 19989-19997.
- Posfai,G., Kolisnychenko,V., Berezcki,Z., and Blattner,F.R. (1999). Markerless gene replacement in *Escherichia coli* stimulated by a double- strand break in the chromosome. *Nucleic Acids Res.* **27**, 4409-4415.
- Posfai,G., Koob,M.D., Kirkpatrick,H.A., and Blattner,F.R. (1997). Versatile insertion plasmids for targeted genome manipulations in bacteria: isolation, deletion, and rescue of the pathogenicity island LEE of the *Escherichia coli* O157:H7 genome. *J. Bacteriol.* **179**, 4426-4428.
- Poteete,A.R. (2001). What makes the bacteriophage lambda Red system useful for genetic engineering: molecular mechanism and biological function. *FEMS Microbiol. Lett.* **201**, 9-14.
- Prudenziati,M., Siritto,M., van Dam,H., and Ravazzolo,R. (2000). Adenovirus E1A down-regulates the EGF receptor via repression of its promoter. *Int. J. Cancer* **88**, 943-948.
- Puertollano,R., Aguilar,R.C., Gorshkova,I., Crouch,R.J., and Bonifacino,J.S. (2001). Sorting of mannose 6-phosphate receptors mediated by the GGAs. *Science* **292**, 1712-1716.
- Putzer,B.M., Stiewe,T., Parssanedjad,K., Rega,S., and Esche,H. (2000). E1A is sufficient by itself to induce apoptosis independent of p53 and other adenoviral gene products. *Cell Death. Differ.* **7**, 177-188.
- Raiborg,C., Bache,K.G., Gillooly,D.J., Madshus,I.H., Stang,E., and Stenmark,H. (2002). Hrs sorts ubiquitinated proteins into clathrin-coated microdomains of early endosomes. *Nat. Cell Biol.* **4**, 394-398.
- Raiborg,C., Bache,K.G., Mehlum,A., Stang,E., and Stenmark,H. (2001). Hrs recruits clathrin to early endosomes. *EMBO J.* **20**, 5008-5021.
- Rapoport,I., Chen,Y.C., Cupers,P., Shoelson,S.E., and Kirchhausen,T. (1998). Dileucine-based sorting signals bind to the beta chain of AP-1 at a site distinct and regulated differently from the tyrosine-based motif-binding site. *EMBO J.* **17**, 2148-2155.
- Rathmell,J.C. and Thompson,C.B. (2002). Pathways of apoptosis in lymphocyte development, homeostasis, and disease. *Cell* **109 Suppl**, S97-107.

References

- Reggiori,F., Black,M.W., and Pelham,H.R. (2000). Polar transmembrane domains target proteins to the interior of the yeast vacuole. *Mol. Biol. Cell* **11**, 3737-3749.
- Reich,N., Pine,R., Levy,D., and Darnell,J.E., Jr. (1988). Transcription of interferon-stimulated genes is induced by adenovirus particles but is suppressed by E1A gene products. *J. Virol.* **62**, 114-119.
- Rensing-Ehl,A., Hess,S., Ziegler-Heitbrock,H.W., Riethmuller,G., and Engelmann,H. (1995). Fas/Apo-1 activates nuclear factor kappa B and induces interleukin-6 production. *J. Inflamm.* **45**, 161-174.
- Reusch,U., Muranyi,W., Lucin,P., Burgert,H.G., Hengel,H., and Koszinowski,U.H. (1999). A cytomegalovirus glycoprotein re-routes MHC class I complexes to lysosomes for degradation. *EMBO J.* **18**, 1081-1091.
- Robinson,M.S. and Bonifacino,J.S. (2001). Adaptor-related proteins. *Curr. Opin. Cell Biol.* **13**, 444-453.
- Rodionov,D.G. and Bakke,O. (1998). Medium chains of adaptor complexes AP-1 and AP-2 recognize leucine- based sorting signals from the invariant chain. *J. Biol. Chem.* **273**, 6005-6008.
- Rodionov,D.G., Honing,S., Silye,A., Kongsvik,T.L., von Figura,K., and Bakke,O. (2002). Structural requirements for interactions between leucine-sorting signals and clathrin-associated adaptor protein complex AP3. *J. Biol. Chem.* **277**, 47436-47443.
- Roelvink,P.W., Lizonova,A., Lee,J.G., Li,Y., Bergelson,J.M., Finberg,R.W., Brough,D.E., Kovesdi,I., and Wickham,T.J. (1998). The coxsackievirus-adenovirus receptor protein can function as a cellular attachment protein for adenovirus serotypes from subgroups A, C, D, E, and F. *J. Virol.* **72**, 7909-7915.
- Roelvink,P.W., Mi,L.G., Einfeld,D.A., Kovesdi,I., and Wickham,T.J. (1999). Identification of a conserved receptor-binding site on the fiber proteins of CAR-recognizing adenoviridae. *Science* **286**, 1568-1571.
- Rohn,W.M., Rouille,Y., Waguri,S., and Hoflack,B. (2000). Bi-directional trafficking between the trans-Golgi network and the endosomal/lysosomal system. *J. Cell Sci.* **113 (Pt 12)**, 2093-2101.
- Rohrer,J., Schweizer,A., Russell,D., and Kornfeld,S. (1996). The targeting of Lamp1 to lysosomes is dependent on the spacing of its cytoplasmic tail tyrosine sorting motif relative to the membrane. *J. Cell Biol.* **132**, 565-576.
- Routes,J.M. and Cook,J.L. (1995). E1A gene expression induces susceptibility to killing by NK cells following immortalization but not adenovirus infection of human cells. *Virology* **210**, 421-428.
- Routes,J.M., Ryan,S., Clase,A., Miura,T., Kuhl,A., Potter,T.A., and Cook,J.L. (2000). Adenovirus E1A oncogene expression in tumor cells enhances killing by TNF-related apoptosis-inducing ligand (TRAIL). *J. Immunol.* **165**, 4522-4527.
- Russell,W.C. (2000). Update on adenovirus and its vectors. *J. Gen. Virol.* **81**, 2573-2604.
- Sakaguchi,K., Okabayashi,Y., and Kasuga,M. (2001). Shc mediates ligand-induced internalization of epidermal growth factor receptors. *Biochem. Biophys. Res. Commun.* **282**, 1154-1160.
- Sandoval,I.V., Martinez-Arca,S., Valdueza,J., Palacios,S., and Holman,G.D. (2000). Distinct reading of different structural determinants modulates the dileucine-mediated transport steps of the lysosomal membrane protein LIMPII and the insulin-sensitive glucose transporter GLUT4. *J. Biol. Chem.* **275**, 39874-39885.
- Schweizer,A., Kornfeld,S., and Rohrer,J. (1997). Proper sorting of the cation-dependent mannose 6-phosphate receptor in endosomes depends on a pair of aromatic amino acids in its cytoplasmic tail. *Proc. Natl. Acad. Sci. U. S. A* **94**, 14471-14476.
- Sedger,L.M., Shows,D.M., Blanton,R.A., Peschon,J.J., Goodwin,R.G., Cosman,D., and Wiley,S.R. (1999). IFN-gamma mediates a novel antiviral activity through dynamic modulation of TRAIL and TRAIL receptor expression. *J. Immunol.* **163**, 920-926.
- Sester,M. and Burgert,H.G. (1994). Conserved cysteine residues within the E3/19K protein of adenovirus type 2 are essential for binding to major histocompatibility complex antigens. *J. Virol.* **68**, 5423-5432.

- Shao,R., Hu,M.C., Zhou,B.P., Lin,S.Y., Chiao,P.J., von Lindern,R.H., Spohn,B., and Hung,M.C. (1999). E1A sensitizes cells to tumor necrosis factor-induced apoptosis through inhibition of I κ B kinases and nuclear factor κ B activities. *J. Biol. Chem.* **274**, 21495-21498.
- Shaulian,E. and Karin,M. (2002). AP-1 as a regulator of cell life and death. *Nat. Cell Biol.* **4**, E131-E136.
- Shenk,T.E (2001). Adenoviridae: The viruses and their replication. In *Fields Virology*. Fields, B.N., Knipe, D.M., and Howley, P.M. eds. LippincottWilliams&Wilkins Publishers, Philadelphia, New York, 2265-2300.
- Shetty,S., Gladden,J.B., Henson,E.S., Hu,X., Villanueva,J., Haney,N., and Gibson,S.B. (2002). Tumor necrosis factor-related apoptosis inducing ligand (TRAIL) up-regulates death receptor 5 (DR5) mediated by NF κ B activation in epithelial derived cell lines. *Apoptosis.* **7**, 413-420.
- Shin,J., Dunbrack,R.L., Jr., Lee,S., and Strominger,J.L. (1991). Phosphorylation-dependent down-modulation of CD4 requires a specific structure within the cytoplasmic domain of CD4. *J. Biol. Chem.* **266**, 10658-10665.
- Shisler,J., Duerksen-Hughes,P., Hermiston,T.M., Wold,W.S., and Gooding,L.R. (1996). Induction of susceptibility to tumor necrosis factor by E1A is dependent on binding to either p300 or p105-Rb and induction of DNA synthesis. *J. Virol.* **70**, 68-77.
- Shisler,J., Yang,C., Walter,B., Ware,C.F., and Gooding,L.R. (1997). The adenovirus E3-10.4K/14.5K complex mediates loss of cell surface Fas (CD95) and resistance to Fas-induced apoptosis. *J. Virol.* **71**, 8299-8306.
- Shizuya,H., Birren,B., Kim,U.J., Mancino,V., Slepak,T., Tachiiri,Y., and Simon,M. (1992). Cloning and stable maintenance of 300-kilobase-pair fragments of human DNA in *Escherichia coli* using an F-factor-based vector. *Proc. Natl. Acad. Sci. U. S. A* **89**, 8794-8797.
- Signas,C., Akusjarvi,G., and Pettersson,U. (1986). Region E3 of human adenoviruses; differences between the oncogenic adenovirus-3 and the non-oncogenic adenovirus-2. *Gene* **50**, 173-184.
- Sorkin,A., Mazzotti,M., Sorkina,T., Scotto,L., and Beguinot,L. (1996). Epidermal growth factor receptor interaction with clathrin adaptors is mediated by the Tyr974-containing internalization motif. *J. Biol. Chem.* **271**, 13377-13384.
- Sorkin,A. and Waters,C.M. (1993). Endocytosis of growth factor receptors. *Bioessays* **15**, 375-382.
- Sorkina,T., Huang,F., Beguinot,L., and Sorkin,A. (2002). Effect of tyrosine kinase inhibitors on clathrin-coated pit recruitment and internalization of epidermal growth factor receptor. *J. Biol. Chem.* **277**, 27433-27441.
- Soubeyran,P., Kowanzet,K., Szymkiewicz,I., Langdon,W.Y., and Dikic,I. (2002). Cbl-CIN85-endophilin complex mediates ligand-induced downregulation of EGF receptors. *Nature* **416**, 183-187.
- Sparer,T.E., Tripp,R.A., Dillehay,D.L., Hermiston,T.W., Wold,W.S., and Gooding,L.R. (1996). The role of human adenovirus early region 3 proteins (gp19K, 10.4K, 14.5K, and 14.7K) in a murine pneumonia model. *J. Virol.* **70**, 2431-2439.
- Sprengel,J., Schmitz,B., Heuss-Neitzel,D., Zock,C., and Doerfler,W. (1994). Nucleotide sequence of human adenovirus type 12 DNA: comparative functional analysis. *J. Virol.* **68**, 379-389.
- Stang,E., Johannessen,L.E., Knardal,S.L., and Madshus,I.H. (2000). Polyubiquitination of the epidermal growth factor receptor occurs at the plasma membrane upon ligand-induced activation 1. *J. Biol. Chem.* **275**, 13940-13947.
- Stark,G.R., Kerr,I.M., Williams,B.R., Silverman,R.H., and Schreiber,R.D. (1998). How cells respond to interferons. *Annu. Rev. Biochem.* **67**, 227-264.
- Stellwagen,A.E. and Craig,N.L. (2001). Analysis of gain-of-function mutants of an ATP-dependent regulator of Tn7 transposition. *J. Mol. Biol.* **305**, 633-642.
- Stewart,A.R., Tollefson,A.E., Krajcsi,P., Yei,S.P., and Wold,W.S. (1995). The adenovirus E3 10.4K and 14.5K proteins, which function to prevent cytolysis by tumor necrosis factor and to down-regulate the epidermal growth factor receptor, are localized in the plasma membrane. *J. Virol.* **69**, 172-181.

References

- Stoorvogel,W., Oorschot,V., and Geuze,H.J. (1996). A novel class of clathrin-coated vesicles budding from endosomes. *J. Cell Biol.* **132**, 21-33.
- Storey,H., Stewart,A., Vandenabeele,P., and Luzio,J.P. (2002). The p55 tumour necrosis factor receptor TNFR1 contains a trans-Golgi network localization signal in the C-terminal region of its cytoplasmic tail. *Biochem. J.* **366**, 15-22.
- Strasser,A. and O'Connor,L. (1998). Fas ligand--caught between Scylla and Charybdis. *Nat. Med.* **4**, 21-22.
- Szymkiewicz,I., Kowanetz,K., Soubeyran,P., Dinarina,A., Lipkowitz,S., and Dikic,I. (2002). CIN85 participates in Cbl-b-mediated down-regulation of receptor tyrosine kinases. *J. Biol. Chem.* **277**, 39666-39672.
- Takei,K. and Haucke,V. (2001). Clathrin-mediated endocytosis: membrane factors pull the trigger. *Trends Cell Biol.* **11**, 385-391.
- Tauber,B. and Dobner,T. (2001). Adenovirus early E4 genes in viral oncogenesis. *Oncogene* **20**, 7847-7854.
- Teasdale,R.D. and Jackson,M.R. (1996). Signal-mediated sorting of membrane proteins between the endoplasmic reticulum and the golgi apparatus. *Annu. Rev. Cell Dev. Biol.* **12**, 27-54.
- Teodoro,J.G. and Branton,P.E. (1997). Regulation of apoptosis by viral gene products. *J. Virol.* **71**, 1739-1746.
- Teuchert,M., Berghofer,S., Klenk,H.D., and Garten,W. (1999). Recycling of furin from the plasma membrane. Functional importance of the cytoplasmic tail sorting signals and interaction with the AP-2 adaptor medium chain subunit. *J. Biol. Chem.* **274**, 36781-36789.
- Thorne,T.E., Voelkel-Johnson,C., Casey,W.M., Parks,L.W., and Laster,S.M. (1996). The activity of cytosolic phospholipase A2 is required for the lysis of adenovirus-infected cells by tumor necrosis factor. *J. Virol.* **70**, 8502-8507.
- Tikkanen,R., Obermuller,S., Denzer,K., Pungitore,R., Geuze,H.J., von Figura,K., and Honing,S. (2000). The dileucine motif within the tail of MPR46 is required for sorting of the receptor in endosomes. *Traffic.* **1**, 631-640.
- Tollefson,A.E., Hermiston,T.W., Lichtenstein,D.L., Colle,C.F., Tripp,R.A., Dimitrov,T., Toth,K., Wells,C.E., Doherty,P.C., and Wold,W.S. (1998). Forced degradation of Fas inhibits apoptosis in adenovirus-infected cells. *Nature* **392**, 726-730.
- Tollefson,A.E., Krajcsi,P., Pursley,M.H., Gooding,L.R., and Wold,W.S. (1990a). A 14,500 MW protein is coded by region E3 of group C human adenoviruses. *Virology* **175**, 19-29.
- Tollefson,A.E., Krajcsi,P., Yei,S.P., Carlin,C.R., and Wold,W.S. (1990b). A 10,400-molecular-weight membrane protein is coded by region E3 of adenovirus. *J. Virol.* **64**, 794-801.
- Tollefson,A.E., Ryerse,J.S., Scaria,A., Hermiston,T.W., and Wold,W.S. (1996a). The E3-11.6-kDa adenovirus death protein (ADP) is required for efficient cell death: characterization of cells infected with adp mutants. *Virology* **220**, 152-162.
- Tollefson,A.E., Scaria,A., Hermiston,T.W., Ryerse,J.S., Wold,L.J., and Wold,W.S. (1996b). The adenovirus death protein (E3-11.6K) is required at very late stages of infection for efficient cell lysis and release of adenovirus from infected cells. *J. Virol.* **70**, 2296-2306.
- Tollefson,A.E., Stewart,A.R., Yei,S.P., Saha,S.K., and Wold,W.S. (1991). The 10,400- and 14,500-dalton proteins encoded by region E3 of adenovirus form a complex and function together to down-regulate the epidermal growth factor receptor. *J. Virol.* **65**, 3095-3105.
- Tollefson,A.E., Toth,K., Doronin,K., Kuppaswamy,M., Doronina,O.A., Lichtenstein,D.L., Hermiston,T.W., Smith,C.A., and Wold,W.S. (2001). Inhibition of TRAIL-induced apoptosis and forced internalization of TRAIL receptor 1 by adenovirus proteins. *J. Virol.* **75**, 8875-8887.
- Tomko,R.P., Xu,R., and Philipson,L. (1997). HCAR and MCAR: the human and mouse cellular receptors for subgroup C adenoviruses and group B coxsackieviruses. *Proc. Natl. Acad. Sci. U. S. A* **94**, 3352-3356.

- Trapani, J.A., Davis, J., Sutton, V.R., and Smyth, M.J. (2000). Proapoptotic functions of cytotoxic lymphocyte granule constituents in vitro and in vivo. *Curr. Opin. Immunol.* **12**, 323-329.
- Traub, L.M., Downs, M.A., Westrich, J.L., and Fremont, D.H. (1999). Crystal structure of the alpha appendage of AP-2 reveals a recruitment platform for clathrin-coat assembly. *Proc. Natl. Acad. Sci. U. S. A* **96**, 8907-8912.
- Trotman, L.C., Mosberger, N., Fornerod, M., Stidwill, R.P., and Greber, U.F. (2001). Import of adenovirus DNA involves the nuclear pore complex receptor CAN/Nup214 and histone H1. *Nat. Cell Biol.* **3**, 1092-1100.
- Tufariello, J., Cho, S., and Horwitz, M.S. (1994). The adenovirus E3 14.7-kilodalton protein which inhibits cytolysis by tumor necrosis factor increases the virulence of vaccinia virus in a murine pneumonia model. *J. Virol.* **68**, 453-462.
- Urbanowski, J.L. and Piper, R.C. (2001). Ubiquitin sorts proteins into the intraluminal degradative compartment of the late-endosome/vacuole. *Traffic.* **2**, 622-630.
- van Weert, A.W., Dunn, K.W., Gueze, H.J., Maxfield, F.R., and Stoorvogel, W. (1995). Transport from late endosomes to lysosomes, but not sorting of integral membrane proteins in endosomes, depends on the vacuolar proton pump. *J. Cell Biol.* **130**, 821-834.
- Vidalain, P.O., Azocar, O., Lamouille, B., Astier, A., Rabourdin-Combe, C., and Servet-Delprat, C. (2000). Measles virus induces functional TRAIL production by human dendritic cells. *J. Virol.* **74**, 556-559.
- Walczak, H. and Krammer, P.H. (2000). The CD95 (APO-1/Fas) and the TRAIL (APO-2L) apoptosis systems. *Exp. Cell Res.* **256**, 58-66.
- Wallach, D., Varfolomeev, E.E., Malinin, N.L., Goltsev, Y.V., Kovalenko, A.V., and Boldin, M.P. (1999). Tumor necrosis factor receptor and Fas signaling mechanisms. *Annu. Rev. Immunol.* **17**, 331-367.
- Walters, R.W., Freimuth, P., Moninger, T.O., Ganske, I., Zabner, J., and Welsh, M.J. (2002). Adenovirus fiber disrupts CAR-mediated intercellular adhesion allowing virus escape. *Cell* **110**, 789-799.
- Wan, L., Molloy, S.S., Thomas, L., Liu, G., Xiang, Y., Rybak, S.L., and Thomas, G. (1998). PACS-1 defines a novel gene family of cytosolic sorting proteins required for trans-Golgi network localization. *Cell* **94**, 205-216.
- Wang, C.Y., Mayo, M.W., Korneluk, R.G., Goeddel, D.V., and Baldwin, A.S., Jr. (1998). NF-kappaB antiapoptosis: induction of TRAF1 and TRAF2 and c-IAP1 and c-IAP2 to suppress caspase-8 activation. *Science* **281**, 1680-1683.
- Wang, S.H., Hong, W. (1993). The SXYQRL sequence in the cytoplasmic domain of TGN38 plays a major role in Trans-Golgi Network Localization. *J Biol. Chem.* **268**, 22853-22862.
- Wang, X. and Bergelson, J.M. (1999). Coxsackievirus and adenovirus receptor cytoplasmic and transmembrane domains are not essential for coxsackievirus and adenovirus infection. *J. Virol.* **73**, 2559-2562.
- Wang, Z. and Moran, M.F. (1996). Requirement for the adapter protein GRB2 in EGF receptor endocytosis. *Science* **272**, 1935-1939.
- Waterman, H., Katz, M., Rubin, C., Shtiegman, K., Lavi, S., Elson, A., Jovin, T., and Yarden, Y. (2002). A mutant EGF-receptor defective in ubiquitylation and endocytosis unveils a role for Grb2 in negative signaling. *EMBO J.* **21**, 303-313.
- White, E. (2001). Regulation of the cell cycle and apoptosis by the oncogenes of adenovirus. *Oncogene* **20**, 7836-7846.
- White, E., Sabbatini, P., Debbas, M., Wold, W.S., Kusher, D.I., and Gooding, L.R. (1992). The 19-kilodalton adenovirus E1B transforming protein inhibits programmed cell death and prevents cytolysis by tumor necrosis factor alpha. *Mol. Cell Biol.* **12**, 2570-2580.

References

- Wilde,A., Beattie,E.C., Lem,L., Riethof,D.A., Liu,S.H., Mobley,W.C., Soriano,P., and Brodsky,F.M. (1999). EGF receptor signaling stimulates SRC kinase phosphorylation of clathrin, influencing clathrin redistribution and EGF uptake. *Cell* **96**, 677-687.
- Wilson-Rawls,J. and Wold,W.S. (1993). The E3-6.7K protein of adenovirus is an Asn-linked integral membrane glycoprotein localized in the endoplasmic reticulum. *Virology* **195**, 6-15.
- Windheim M., Hilgendorf A., Burgert,H.G., (2003). Immune evasion by adenovirus E3 proteins: Exploitation of intracellular trafficking pathways. *Curr. Top. Microbiol. Immunol.* *in press*.
- Wissing,D., Mouritzen,H., Egeblad,M., Poirier,G.G., and Jaattela,M. (1997). Involvement of caspase-dependent activation of cytosolic phospholipase A2 in tumor necrosis factor-induced apoptosis. *Proc. Natl. Acad. Sci. U. S. A* **94**, 5073-5077.
- Wold,W.S., Tollefson,A.E., and Hermiston,T.W. (1995). E3 transcription unit of adenovirus. *Curr. Top. Microbiol. Immunol.* **199 (Pt 1)**, 237-274.
- Worgall,S., Leopold,P.L., Wolff,G., Ferris,B., Van Roijen,N., and Crystal,R.G. (1997a). Role of alveolar macrophages in rapid elimination of adenovirus vectors administered to the epithelial surface of the respiratory tract. *Hum. Gene Ther.* **8**, 1675-1684.
- Worgall,S., Wolff,G., Falck-Pedersen,E., and Crystal,R.G. (1997b). Innate immune mechanisms dominate elimination of adenoviral vectors following in vivo administration. *Hum. Gene Ther.* **8**, 37-44.
- Wu,G.S., Burns,T.F., McDonald,E.R., III, Meng,R.D., Kao,G., Muschel,R., Yen,T., and el Deiry,W.S. (1999). Induction of the TRAIL receptor KILLER/DR5 in p53-dependent apoptosis but not growth arrest. *Oncogene* **18**, 6411-6418.
- Xu,X.N., Screaton,G.R., and McMichael,A.J. (2001). Virus infections: escape, resistance, and counterattack. *Immunity.* **15**, 867-870.
- Yang,Y., Su,Q., and Wilson,J.M. (1996). Role of viral antigens in destructive cellular immune responses to adenovirus vector-transduced cells in mouse lungs. *J. Virol.* **70**, 7209-7212.
- Yang,Y., Xiang,Z., Ertl,H.C., and Wilson,J.M. (1995). Upregulation of class I major histocompatibility complex antigens by interferon gamma is necessary for T-cell-mediated elimination of recombinant adenovirus-infected hepatocytes in vivo. *Proc. Natl. Acad. Sci. U. S. A* **92**, 7257-7261.
- Yarden,Y. and Sliwkowski,M.X. (2001). Untangling the ErbB signaling network. *Nat. Rev. Mol. Cell Biol.* **2**, 127-137.
- Yoshida,T., Maeda,A., Tani,N., and Sakai,T. (2001). Promoter structure and transcription initiation sites of the human death receptor 5/TRAIL-R2 gene. *FEBS Lett.* **507**, 381-385.
- Yoshimori,T., Yamamoto,A., Moriyama,Y., Futai,M., and Tashiro,Y. (1991). Bafilomycin A1, a specific inhibitor of vacuolar-type H(+)-ATPase, inhibits acidification and protein degradation in lysosomes of cultured cells. *J. Biol. Chem.* **266**, 17707-17712.
- Zalιαuskiene,L., Kang,S., Brouillette,C.G., Lebowitz,J., Arani,R.B., and Collawn,J.F. (2000). Down-regulation of cell surface receptors is modulated by polar residues within the transmembrane domain. *Mol. Biol. Cell* **11**, 2643-2655.
- Zerial,M. and McBride,H. (2001). Rab proteins as membrane organizers. *Nat. Rev. Mol. Cell Biol.* **2**, 107-117.
- Zhang,H.G., Zhou,T., Yang,P., Edwards,C.K., III, Curiel,D.T., and Mountz,J.D. (1998a). Inhibition of tumor necrosis factor alpha decreases inflammation and prolongs adenovirus gene expression in lung and liver. *Hum. Gene Ther.* **9**, 1875-1884.
- Zhang,X.D., Franco,A.V., Nguyen,T., Gray,C.P., and Hersey,P. (2000). Differential localization and regulation of death and decoy receptors for TNF-related apoptosis-inducing ligand (TRAIL) in human melanoma cells. *J. Immunol.* **164**, 3961-3970.

-
- Zhang, Y., Buchholz, F., Muirers, J.P., and Stewart, A.F. (1998b). A new logic for DNA engineering using recombination in *Escherichia coli*. *Nat. Genet.* **20**, 123-128.
- Zhu, Y., Doray, B., Poussu, A., Lehto, V.P., and Kornfeld, S. (2001). Binding of GGA2 to the lysosomal enzyme sorting motif of the mannose 6-phosphate receptor. *Science* **292**, 1716-1718.
- Zhu, Y., Traub, L.M., and Kornfeld, S. (1999). High-affinity binding of the AP-1 adaptor complex to trans-golgi network membranes devoid of mannose 6-phosphate receptors. *Mol. Biol. Cell* **10**, 537-549.
- Ziegler, H., Muranyi, W., Burgert, H.G., Kremmer, E., and Koszinowski, U.H. (2000). The luminal part of the murine cytomegalovirus glycoprotein gp40 catalyzes the retention of MHC class I molecules. *EMBO J.* **19**, 870-881.
- Zoltick, P.W., Chirmule, N., Schnell, M.A., Gao, G.P., Hughes, J.V., and Wilson, J.M. (2001). Biology of E1-deleted adenovirus vectors in nonhuman primate muscle. *J. Virol.* **75**, 5222-5229.
- Zuker, M. (1989). Computer prediction of RNA structure. *Methods Enzymol.* **180**, 262-288.

Abbreviations

In general, amino acids are given in single-letter code.

AA	arachidonic acid
Ad	adenovirus
ADP	adenovirus death protein
Ala	alanine
Ap	ampicillin
AP	adaptor protein
APS	ammonium persulfate
APS	ammonium persulfate
as	antisense orientation
BAC	bacterial artificial chromosome
bp	base-pairs
cAMP	cyclic adenosin-mono-phosphate
CAR	coxsackie/adenovirus receptor
CBP	CRE binding protein
cD MPR	MPR46, cation-dependent MPR
CDK	cyclin-dependent kinase
CDS	coding sequence, denotes genomic sequence from start to stop codon of translation
cI MPR	MPR 300, cation-independent MPR
Cm	chloramphenicol
cm	centimeter
cpe	cytopathic effect
cPLA ₂	cytosolic phospholipase A ₂
CR	conserved region
CRE	cAMP responsive element
C-tail	cytoplasmic tail
CTL	cytotoxic T lymphocytes
DBP	DNA binding protein
DD	death domain
DISC	death-inducing signaling complex
DMEM	Dulbecco's modified Eagle medium
DMSO	di-methyl-sulfoxid
DNA	desoxyribonucleic acid
dNTP	desoxynucleoside triphosphate
ds	double-stranded
DTT	dithiothreitol
E3	early region 3
EDTA	ethylenediamine-tetraacetic acid
EE	early endosome
EGF	epidermal growth factor
EGFR	epidermal growth factor receptor
ER	endoplasmic reticulum
ERGIC	ER-Golgi-intermediate compartment
EtOH	ethanol
FACS	fluorescence-activated cell sorter
Fas	CD95/APO-1: receptor for FasL
FADD/TRADD	Fas-associated/TNFR-associated death domain-containing protein
FasL	Fas ligand
FCS	fetal calf serum
Fig.	figure
FIP	14.7K interacting protein

FLIP	FLICE (caspase 8) inhibitory proteins
g	gravitation constant
GGA	golgi-associated gamma ear containing adaptor protein
GTPase	guanosine triphosphatase
h	hour
HCMV	human cytomegalovirus
HEPES	2-[4-(2-Hydroxyethyl)-1-piperazinyl]-ethane sulfonic acid
HHV8	human herpesvirus 8
HIV	human immunodeficiency virus
Hrs	hepatocyte growth factor tyrosine kinase substrate
IAP	inhibitor of apoptosis protein
IF	immunofluorescence
IFN	interferon
IKK	I κ B (inhibitor of NF- κ B)-kinase
IL	interleukin
IP/WB	immunoprecipitation/western blot
ITR	inverted terminal repeat
ISG	IFN-stimulated genes
JAK/STAT	janus kinase/signal transducers and activators of transcription
kb	kilobase(s)
kD	kilodaltons
K _D	equilibrium dissociation constant
KLH	keyhole limpet hemocyanin
Km	kanamycin
kV	kilo-Volt
l	liter
LAMP-2	lysosome-associated membrane protein 2
LE	late endosome
μ	micro (10^{-6})
μ g/ μ l	microgramm pro microliter
μ F	micro-Farad
M	Mol
MAPK	mitogen-activated protein kinase
MCMV	mouse cytomegalovirus
MCS	multiple cloning site
mdm 2	murine double minute 2
MHC	major histocompatibility complex
min	minutes
ml	milliliter
MLP	major late promoter
MOI	multiplicity of infection
MPR	mannose-6-phosphate receptor
mRNA	messenger RNA
mTn	mini-transposon (also referred to as Tn)
MVB	multivesicular body
MVF	mean value of fluorescence
nm	nano(10^{-9})meter
NEB	New England Biolabs
NF- κ B	nuclear factor kappa B
NK	natural killer cell
NGF	nerve growth factor
nm	nanometer

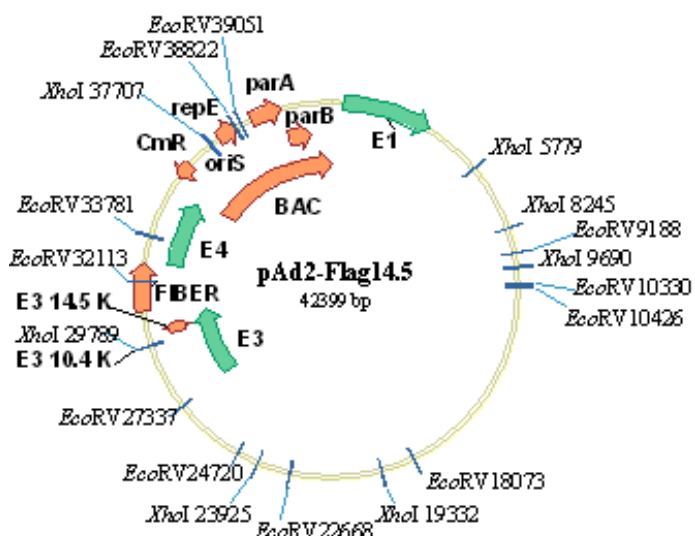
Abbreviations

NSF	N-ethylmaleimide-sensitive factor
OD	optical density
o/n	overnight
ORF	open reading frame
%	percent
PACS	phosphofurin acidic cluster binding protein
PBS	phosphate buffered saline
PCR	polymerase chain reaction
pfu	plaque forming units
p.i.	post infection
PI3K	phosphoinositide-3-OH kinase
PKR	ds RNA-dependent protein kinase
PM	plasma membrane
Pol	polymerase
Poly(A)	polyadenylation
PTB	Phosphotyrosine binding domain
RID	receptor internalization and degradation
RNA	ribonucleic acid
rpm	rounds per minute
RT	room temperature
RTK	receptor tyrosine kinase
s	sense orientation
SDS-PAGE	sodium dodecylsulfate polyacrylamide gel electrophoresis
sec	seconds
SEM	Standard error of the mean value
SH2	Src-homology domain type 2
SPR	Surface Plasmon Resonance
ss	single-stranded
SV40	simian virus 40
TAP	transporter associated with antigen processing
TBP	TATA-box binding protein
Tc	tetracycline
TGF	transforming growth factor
TGN	trans-Golgi-network
TIP 47	tail-interacting protein 47
TMD	transmembrane domain
TNF- α	tumor necrosis factor alpha, also referred to as TNF
TNFR	TNF-receptor
Tns	transposase
TP	terminal protein
TRAIL	TNF-related apoptosis inducing ligand
TRAIL-R	TRAIL-receptor
SAP	shrimp alkaline phosphatase
SEM	standard error of the mean
wt	wild-type
w/v	weight per volume
λ	wavelength lambda (in nm)

Annexe

Restriction fragment length pattern of newly generated mutant pAd2-BACs. Variations in fragment length and additional restriction sites in comparison to wt are highlighted in boldface. Restriction sites were determined using Vector NTI Suite software, Informax, and denote the position in the corresponding pAd2-BAC.

Fragment sizes are given in number of base-pairs. For reference, the circular map of pAd2/F14.5 is shown on the right.



1.) Annotation of Fig. 27

a) A new *Pad* site (position 30058) is generated by the mutation introduced in 14.5K to generate pAd2-H7/14.5ko

pAd2-H7/14.5ko		pAd2-H7		pAd2-H7/10.4ko-F14.5	
Fragment size	Restriction sites	Fragment size	Restriction sites	Fragment size	Restriction sites
28641	44060-28623	28641	44059-28623	28641	44079-28623
14002	30058 -44060	15436	28623-44059	15456	28623-44079
1435	28623- 30058				

b) A new *PvuI* site (position 30301) is introduced by the mutation of Y74 in FLAG-14.5K in construct pAd2-H7/FLAG-14.5Y74A

pAd2-H7/FLAG-14.5Y74A		pAd2-H7 (lacking the FLAG-sequence)	
Fragment size	Restriction sites	Fragment size	Restriction sites
10438	31831-42269	10438	31807-42245
		8255	23552-31807
8143	42269-6311	8143	42245-6311
6749	23552- 30301		
4555	7980-12535	4555	7980-12535
3945	14714-18659	3945	14714-18659
2828	18659-21487	2828	18659-21487
2179	12535-14714	2179	12535-14714
2065	21487-23552	2065	21487-23552
1669	6311-7980	1669	6311-7980
1530	30301 -31831		

c) *EcoRV* cleavage of mTn-containing mutant pAd2-BACs and wt pAd2 as compared to pAd2-H7

pAd2-H7/ FLAG-14.5Y74A pAd2-H7/10.4LL-F14.5		pAd2-H7/14.5ko no FLAG-sequence		pAd2-H7/10.4ko-F14.5		pAd2-H7 no FLAG-sequence	
Fragment size	Restriction sites	Fragment size	Restriction sites	Fragment size	Restriction sites	Fragment size	Restriction sites
12536	40753-9188	12536	40730-9188	12536	40749-9188	12536	40729-9188
7647	10426-18073	7647	10426-18073	7647	10426-18073	7647	10426-18073
5041	35483-40524	5041	35460-40501	5041	35479-40520	5041	35459-40500
4595	18073-22668	4595	18073-22668	4595	18073-22668	4595	18073-22668
3807	27337-31144	3784	27337-31121	3803	27337-31140	3783	27337-31120
2617	24720-27337	2617	24720-27337	2617	24720-27337	2617	24720-27337
2052	22668-24720	2052	22668-24720	2052	22668-24720	2052	22668-24720

1668	33815-35483	1668	33792-35460	1668	33811-35479	1668	33791-35459
1432	32383-33815	1432	32360-33792	1432	32379-33811	1432	32359-33791
1239	31144-32383	1239	31121-32360	1239	31140-32379	1239	31120-32359
1142	9188-10330	1142	9188-10330	1142	9188-10330	1142	9188-10330
229	40524-40753	229	40501-40730	229	40520-40749	229	40500-40729
96	10330-10426	96	10330-10426	96	10330-10426	96	10330-10426

pAd2 wt (clone B53)		pAd2-H7 (insertion of 1699 bp mTn sequence +3bp = duplication of CTA at Tn ends)	
Fragment size	Restriction sites	Fragment size	Restriction sites
12536	39027-9188	12536	40729-9188
7647	10426-18073	7647	10426-18073
5041	33757-38798	5041	35459-40500
4752	27337-32089		
4595	18073-22668	4595	18073-22668
		3783	27337-31120
2617	24720-27337	2617	24720-27337
2052	22668-24720	2052	22668-24720
1668	32089-33757	1668	33791-35459
		1432	32359-33791
		1239	31120-32359
1142	9188-10330	1142	9188-10330
229	38798-39027	229	40500-40729
96	10330-10426	96	10330-10426

d) *HindIII* and *XhoI* cleavage of pAd2-H7/10.4ko-F14.5 as compared to pAd2-H7

pAd2-H7 no FLAG-sequence		pAd2-H7/10.4ko-F14.5		pAd2-H7 no FLAG-sequence		pAd2-H7/10.4ko-F14.5 (lacking the site at 29789)	
<i>HindIII</i>				<i>XhoI</i>			
Fragment size		Restriction sites		Fragment size		Restriction sites	
9229	37647-2799	9229	37667-2799	10471	39385-5779	10471	39405-5779
8053	18317-26370	8053	18317-26370	9642	9690-19332	9642	9690-19332
5324	6232-11556	5324	6232-11556			8298	23925-32223
3433	2799-6232	3433	2799-6232	7182	32203-39385	7182	32223-39405
3284	15033-18317	3284	15033-18317	5864	23925-29789		
2761	33875-36636	2761	33895-36656	4593	19332-23925	4593	19332-23925
2720	28963-31683	2740	28963-31703	2466	5779-8245	2466	5779-8245
2284	26370-28654	2284	26370-28654	2414	29789-32203		
2192	31683-33875	2192	31703-33895	1445	8245-9690	1445	8245-9690
2081	11556-13637	2081	11556-13637				
1321	13712-15033	1321	13712-15033				
1011	36636-37647	1011	36636-37667				
309	28654-28963	309	28654-28963				
75	13637-13712	75	13637-13712				

For *PacI* cleavage sites of pAd2-H7/10.4ko-F14.5, refer to 1a).

2.) Annotation of Fig. 28

a) Restriction fragments obtained by *XhoI* cleavage of BAC clones after the Tn removal

pAd2/14.5ko no FLAG-sequence		pAd2/10.4ko-F14.5		pAd2/FLAG14.5 pAd2/FLAG-14.5Y74A pAd2/10.4LL-F14.5	
Fragment size	Restriction sites	Fragment size	Restriction sites	Fragment size	Restriction sites
		13778	23925-37703		
10471	37684-5779	10471	37703-5779	10471	37707-5779
9642	9690-19332	9642	9690-19332	9642	9690-19332
7895	29789-37684			7918	29789-37707
5864	23925-29789			5864	23925-29789
4593	19332-23925	4593	19332-23925	4593	19332-23925
2466	5779-8245	2466	5779-8245	2466	5779-8245

1445	8245-9690	1445	8245-9690	1445	8245-9690
------	-----------	------	-----------	------	-----------

b) *EcoRV*, *HindIII* cleavage of pAd2/10.4ko-F14.5 as compared to pAd2/FLAG14.5

pAd2/FLAG14.5		pAd2/10.4ko-F14.5		pAd2/FLAG14.5		pAd2/10.4ko-F14.5	
<i>EcoRV</i>				<i>HindIII</i>			
Fragment size	Restriction sites	Fragment size	Restriction sites	Fragment size	Restriction sites	Fragment size	Restriction sites
12536	39051-9188	12536	39047-9188	9229	35969-2799	9229	25965-2799
7647	10426-18073	7647	10426-18073	8053	18317-26370	8053	18317-26370
5041	33781-38822	5041	33777-38818	5324	6232-11556	5324	6232-11556
4776	27337-32113	4776	27337-32109	3433	2799-6232	3433	2799-6232
4595	18073-22668	4595	18073-22668	3284	15033-18317	3284	15033-18317
2617	24720-27337	2617	24720-27337	3234	28963-32197	3230	28963-32193
2052	22668-24720	2052	22668-24720	2761	32197-34958	2761	32193-34958
1668	32113-33781	1668	32109-33777	2284	26370-28654	2284	26370-28654
1142	9188-10330	1142	9188-10330	2081	11556-13637	2081	11556-13637
229	38822-39051	229	38818-39047	1321	13712-15033	1321	13712-15033
96	10330-10426	96	10330-10426	1011	34958-35969	1011	34954-35965
				309	28654-28963	309	28654-28963
				75	13637-13712	75	13637-13712

c) *Pad* cleavage of pAd2/F14.5, pAd2/14.5ko, pAd2/10.4ko-F14.5

pAd2/FLAG14.5		pAd2/14.5ko		pAd2/10.4ko-F14.5	
<i>Pad</i>		<i>Pad</i>		<i>Pad</i>	
Fragment size	Restriction sites	Fragment size	Restriction sites	Fragment size	Restriction sites
28641	42381-28623	28641	42358-28623	28641	42377-28623
13758	28623-42381	12300	30058-42358	13754	28623-42377
		1435	28623-30058		

d) A new *NheI* site is introduced by Tn removal from pAd2/H7-BAC

pB53s11-F14.5*		pAd2/FLAG14.5	
Fragment size	Restriction sites	Fragment size	Restriction sites
21677	31522-10800	21677	31522-10800
9902	10800-20702	9902	10800-20702
5156	25734-30890	5788	25734-31522
5032	20702-25734	5032	20702-25734
632	30890-31522		

* After Tn removal from pAd2-H7 BACs a new *NheI* site is introduced, and the restriction pattern of a pAd2-F14.5 sequence with the newly generated *NheI* site is shown here (clone pB53s11-F14.5) for comparison with pAd2/F14.5

3.) Annotation of Fig. 39
a) *EcoRV* cleavage of mTn-containing intermediate pAd2-BACs

pAd2/F14.5		pAd2/10.4Tn		pAd2/14.5Tn		pAd2/(10.4-14.5)Tn	
Fragment size	Restriction sites	Fragment size	Restriction sites	Fragment size	Restriction sites	Fragment size	Restriction sites
12536	39051-9188	12536	40448-9188	12536	40334-9188	12536	40058-9188
7647	10426-18073	7647	10426-18073	7647	10426-18073	7647	10426-18073
5041	33781-38822	5041	35178-40219	5041	35064-40105	5041	34788-39829
4803	27337-32113						
4595	18073-22668	4595	18073-22668	4595	18073-22668	4595	8073-22668
		2653	27337- 29990	2929	27337- 30266	2653	27337- 29990
2617	24720-27337	2617	24720-27337	2617	24720-27337	2617	24720-27337
		2281	31229 -33510				
2052	22668-24720	2052	22668-24720	2052	22668-24720	2052	22668-24720
				1891	31505 -33396	1891	31229 - 33120

1668	32113-33781	1668	33510-35178	1668	33396-35064	1668	33120-34788
		1239	29990-31229	1239	30266-31505	1239	29990-31229
1142	9188-10330	1142	9188-10330	1142	9188-10330	1142	9188-10330
229	38822-39051	229	40219-40448	229	40105-40334	229	39829-40058
96	10330-10426	96	10330-10426	96	10330-10426	96	10330-10426

b) *Hind*III cleavage of mTn-containing intermediate pAd2-BACs

pAd2/F14.5		pAd2/10.4Tn		pAd2/14.5Tn		pAd2/(10.4-14.5)Tn	
Fragment size	Restriction sites	Fragment size	Restriction sites	Fragment size	Restriction sites	Fragment size	Restriction sites
9229	35969-2799	9229	37366-2799	9229	37252-2799	9229	36976-2799
8053	18317-26370	8053	18317-26370	8053	18317-26370	8053	18317-26370
5324	6232-11556	5324	6232-11556	5324	6232-11556	5324	6232-11556
3433	2799-6232	3433	2799-6232	3433	2799-6232	3433	2799-6232
3284	15033-18317	3284	15033-18317	3284	15033-18317	3284	15033-18317
3234	28963-32197						
		2932	30662-33594				
2761	32197-34958	2761	33594-36355	2761	33480-36241	2761	33204-35965
				2542	30938-33480	2542	30662-33204
2284	26370-28654	2284	26370-28654	2284	26370-28654	2284	26370-28654
2081	11556-13637	2081	11556-13637	2081	11556-13637	2081	11556-13637
		1699	28963-30662			1699	28963-30662
1321	13712-15033	1321	13712-15033	1321	13712-15033	1321	13712-15033
1011	34958-35969	1011	36355-37366	1011	36241-37252	1011	35965-36976
309	28654-28963	309	28654-28963	309	28654-28963	309	28654-28963
75	13637-13712	75	13637-13712	75	13637-13712	75	13637-13712

c) *Xho*I cleavage of mTn-containing intermediate pAd2-BACs

pAd2/10.4Tn		pAd2/(10.4-14.5)Tn		pAd2/14.5Tn		pAd2/F14.5	
Fragment size	Restriction sites	Fragment size	Restriction sites	Fragment size	Restriction sites	Fragment size	Restriction sites
10471	39104-5779	10471	38714-5779	10471	38990-5779	10471	37707-5779
9642	9690-19332	9642	9690-19332	9642	9690-19332	9642	9690-19332
8962	30142-39104						
		8572	30142-38714	8572	30418-38990		
6217	23925-30142	6217	23925-30142			7918	29789-37707
				5864	23925-29789	5864	23925-29789
4593	19332-23925	4593	19332-23925	4593	19332-23925	4593	19332-23925
2466	5779-8245	2466	5779-8245	2466	5779-8245	2466	5779-8245
1445	8245-9690	1445	8245-9690	1445	8245-9690	1445	8245-9690
				629	29789-30418		

4.) Annotation of Fig. 41

a) *Eco*RV cleavage of chimeric pAd2/Ad4-BAC vectors

pAd2		pAd2/Ad410.4 (#12-1)		pAd2/Ad414.5 (#3-8) pAd2/Ad4(10.4-14.5) #(7-4)		pAd2/Ad414.5(#7-1) pAd2/Ad4(10.4-14.5) (#16-1)	
Fragment size	Restriction sites	Fragment size	Restriction sites	Fragment size	Restriction sites	Fragment size	Restriction sites
12536	39051-9188	12536	39030-9188	12536	39078-9188	12536	39075-9188
7647	10426-18073	7647	10426-18073	7647	10426-18073	7647	10426-18073
5041	33781-38822	5041	33760-38801	5041	33808-38849	5041	33805-38846
4752	27337-32089	4755	27337-32092	4803	27337-32140	4800	27337-32137
4595	18073-22668	4595	18073-22668	4595	18073-22668	4595	18073-22668
2617	24720-27337	2617	24720-27337	2617	24720-27337	2617	24720-27337
2052	22668-24720	2052	22668-24720	2052	22668-24720	2052	22668-24720
1668	32113-33781	1668	32092-33760	1668	32140-33808	1668	32137-33805

1142	9188-10330	1142	9188-10330	1142	9188-10330	1142	9188-10330
229	38822-39051	229	38801-39030	229	38849-39078	229	38846-39075
96	10330-10426	96	10330-10426	96	10330-10426	96	10330-10426

b) *Hind*III cleavage of chimeric pAd2/Ad4-BAC vectors (data not shown)

pAd2/F14.5		pAd2/Ad410.4 (#12-1)		pAd2/Ad414.5 (#3-8) pAd2/Ad4(10.4-14.5) (#7-4)		pAd2/Ad414.5 (#7-1) pAd2/Ad4(10.4-14.5) #16-1	
Fragment size	Restriction sites	Fragment size	Restriction sites	Fragment size	Restriction sites	Fragment size	Restriction sites
9229	35969-2799	9229	35948-2799	9229	35996-2799	9229	35993-2799
8053	18317-26370	8053	18317-26370	8053	18317-26370	8053	18317-26370
5324	6232-11556	5324	6232-11556	5324	6232-11556	5324	6232-11556
3433	2799-6232	3433	2799-6232	3433	2799-6232	3433	2799-6232
3284	15033-18317	3284	15033-18317	3284	15033-18317	3284	15033-18317
3234	28963-32197	3213	28963-32176	3261	28963-32224	3258	28963-32221
2761	32197-34958	2761	32176-34937	2761	32224-34985	2761	32221-34982
2284	26370-28654	2284	26370-28654	2284	26370-28654	2284	26370-28654
2081	11556-13637	2081	11556-13637	2081	11556-13637	2081	11556-13637
1321	13712-15033	1321	13712-15033	1321	13712-15033	1321	13712-15033
1011	34958-35969	1011	34937-35948	1011	34985-35996	1011	34982-35993
309	28654-28963	309	28654-28963	309	28654-28963	309	28654-28963
75	13637-13712	75	13637-13712	75	13637-13712	75	13637-13712

c) *Xho*I cleavage of chimeric pAd2/Ad4-BAC vectors

pAd2		pAd2/Ad410.4 (#12-1)		pAd2/Ad414.5 (#3-8)		pAd2/Ad414.5 (#7-1)	
Fragment size	Restriction sites	Fragment size	Restriction sites	Fragment size	Restriction sites	Fragment size	Restriction sites
		13758	23925-37683				
10471	37683-5779	10471	37683-5779	10471	37734-5779	10471	37731-5779
9642	9690-19332	9642	9690-19332	9642	9690-19332	9642	9690-19332
7894	29789 -37683			7945	29789 -37734	7942	29789 -37731
5864	23925- 29789			5864	23925- 29789	5864	23925- 29789
4593	19332-23925	4593	19332-23925	4593	19332-23925	4593	19332-23925
2466	5779-8245	2466	5779-8245	2466	5779-8245	2466	5779-8245
1445	8245-9690	1445	8245-9690	1445	8245-9690	1445	8245-9690

pAd2/Ad4(10.4-14.5) (#7-4)		pAd2/Ad4(10.4-14.5) (#16-1)	
Fragment size	Restriction sites	Fragment size	Restriction sites
13809	23925-37734	13806	23925-37731
10471	37734-5779	10471	37731-5779
9642	9690-19332	9642	9690-19332
4593	19332-23925	4593	19332-23925
2466	5779-8245	2466	5779-8245
1445	8245-9690	1445	8245-9690

5.) *Sna*B1 digest of pAd2-BACs

pAd2/F14.5 (mutant pAd2/F14.5 BACs are identical to pAd2/F14.5)		pAd2/Ad410.4 (#12-1)		pAd2/Ad414.5 (#3-8) pAd2/Ad4(10.4-14.5) (#7-4)		pAd2/Ad414.5 (#7-1) pAd2/Ad4(10.4-14.5) (#16-1)	
Fragment size	Restriction sites	Fragment size	Restriction sites	Fragment size	Restriction sites	Fragment size	Restriction sites
35967	42397-35965	35946	42376-35944	35994	42424-35992	35991	42421-35989
4360	35965-40325	4360	35944-40304	4360	35992-40352	4360	35989-40349
2072	40325-42397	2072	40304-42376	2072	40352-42424	2072	40349-42421

CURRICULUM VITAE

Name: Annette Hilgendorf
Geburtsdatum: 20.02.1974
Geburtsort: Ludwigshafen am Rhein
Familienstand: verheiratet
Nationalität: deutsch
Anschrift: Karl-Witthalm-Strasse 11
81375 München

AUSBILDUNG

06/1993 Abitur, Werner-Heisenberg-Gymnasium, Bad Dürkheim

10/1993--07/1996 Diplomstudiengang Chemie, Universität Karlsruhe (TH) und Ruprecht-Karls-Universität Heidelberg
Vordiplom Chemie, Ruprecht-Karls-Universität Heidelberg

09/1996-09/1999 Diplomstudiengang Biotechnologie der europäischen Konföderation der Universitäten Basel, Freiburg, Karlsruhe und Strasbourg, Ecole Supérieure de Biotechnologie de Strasbourg (esbs)

01/1999-09/1999 Diplomarbeit an der University of Michigan, Ann Arbor, USA
Abschluss: Diplôme d'Ingénieur en Biotechnologie/
Diplom in Biotechnologie,
DEA Biologie Moléculaire et Cellulaire

10/1999-12/2002 Doktorarbeit am Max-von-Pettenkofer-Institut und Genzentrum der Ludwig-Maximilians-Universität München (LMU)
PD Dr. H.-G. Burgert, Prof. R. Grosschedl
Titel der Arbeit:
Down-modulation of the apoptosis receptor Fas and the EGF receptor by the adenovirus E3/10.4-14.5K proteins requires the concerted action of two distinct transport signals

02/2003-03/2003 Praktikum bei Forum Venture Capital AG, München
Business Development von Biotechnologie-Unternehmen